Evidences for the non-redundant function of A-type proteins ISCA1 and ISCA2 in iron-sulfur cluster biogenesis

Lena Kristina Beilschmidt

UNIVERSITÉ DE STRASBOURG

Ecole doctorale des Sciences de la Vie et de la Santé

Institut de Génetique et de Biologie Moléculaire et Cellulaire

THÈSE présentée par :

Lena Kristina BEILSCHMIDT

soutenue le : **18 Novembre 2014**

pour obtenir le grade de : **Docteur de l'université de Strasbourg**

Discipline/ Spécialité : Aspects moléculaires et cellulaires de la biologie

Evidences for the non-redundant function of A-type proteins ISCA1 and ISCA2 in iron-sulfur cluster biogenesis

THÈSE dirigée par :
Dr. PUCCIO Hélène (IGBMC, Illkirch)

RAPPORTEURS :
Dr. BALK Janneke (University of East Anglia, Norwich UK)
Dr. BOUTON Cécile (Institut de Chimie des Substances Naturelles, Gif-sur-Yvette France)

AUTRES MEMBRES DU JURY :
Dr. OLLAGNIER-DE-CHOUDENS Sandrine (CEA, Grenoble France)
Dr. CHARLET BERGUERAND Nicolas (IGBMC, Illkirch France)

To Lavrans, Miron and Arja

Different people say different things at different times.

What matters is what stays – what stays is what matters.

I. Acknowledgements

First of all, I want to thank the members of my PhD jury for reading and evaluating my thesis. Thank you for the time and the effort.

I am indebted to Hélène Puccio for giving me the opportunity to do my PhD in her lab. Not only to be happy to “take me right away as a student” (as you said on the phone), but also for the stimulating surrounding for my research.

Alain Martelli, I am indebted to you as well in many ways. I learned to decide and not always ask for your advice. Thanks for making me do my own mistakes and successes. Thank you for giving me the opportunity to teach and gaining the experience the CV is asking for.

I am grateful for interacting with Marjorie Fournier for our collaboration concerning the MudPIT analysis, and thanks to Pascale Koebel who did all the AAV production. Further I want to thank all the common facilities that made scientific research possible.

I want to thank all present and former lab members, too many to mention everyone in person. You contributed to the development of my project and the daily environment.

I want to thank also many people from the department; especially Karim for being one of the few that showed scientific interest, gave support and honesty.

A particular big thanks to the few but outstanding people that helped in solving each and every problem occurring in the interface between Lena – the German and the French administration; in particular the University of Strasbourg (inventing new troubles each year). Mainly these thanks go to Morgane, who made many phone calls for me, and I missed you for my last year, but also others (like Leila) helped. Anyone claiming that French speaking is not required for (scientific) life in the IGBMC should try it for one week. So, big thanks to each and every one that made the effort to make communication in english-german-french possible.

I want to thank Ben and all present and former members of the SPB. The interactions, organizations and beers were lots of fun, success and an enriching experience. I want to thank Johann for all the interaction around teaching at the European school, and sharing beers over German football matches.

There are always a few special ones to thank and I am afraid I will forget more than one person and aspect. So I want to apologize to the ones I missed.

Leïla, you are one of the few that can discuss private life as a friend and still being critical and honest about science and a project over a coffee. I do hope for many future inter-actions! We share ideas about fundamental science. Floriana, I want to thank you for being a true scientific friend -always critical but motivating to go on – in life and in science. Both of you enriched my life so much.

Thanks to all friends that I found in the igbmc, many left the place before me. In particular Helena (the list, if it lay here, would be getting too long), Claire (always up for …), Nikolas (sarcastic from the beginning to the end), Serena (we will party together one day), Ana (thank you, seriously, thank you), Carlos (are you really from Sweden?), … and not to forget Mannu (the first coffee mate), Fred (sweetie always), Soumya (you know why) and Laurianne (Madeira, Paris, Berlin,…).

In addition, I would like to mention Lana (Svetlana) Sirko that supported me in the moment of a very difficult decision and made sure that I can go my way. You not just always offered profound scientific discussion, but in this step your help was neither obvious nor self-evident.

Special thanks to ”mes coeurs” Anaïs and Mike. You made my life in Strasbourg a life - a life outside of science, the institute and you provided family to me. Thanks for introducing me to your friends and your family, integrating the “silent-german only speaking english” of the beginning and keeping the “funny-sentence-creator” from the end. You started the running and dinners, showing how to speak and to cook the French way. This also accounts for “mes cheris” Anaïs and Jean-Christophe and Cyril – merci beaucoup. Jeanne, you became a special friend almost a granny.

Thanks to all my other friends for being friends and all supportive actions during these last years, also here too many to mention them all now. Thank you! Danke! Merci! Gracias! Obrigada og Tusen Takk!

Last but not least… will ich mich bei meiner Familie bedanken für all die Dinge, für die man eigentlich gar nicht danke sagen kann, weil sie wie selbstverständlich gegeben scheinen. Doch sie sind nicht selbstverständlich und trotzdem fällt es schwer, sie in Worte zu fassen. Danke für alles, jeden Moment, jede Hilfe und jeden Rat und jede Tat. Danke für die guten, aber auch die sprungfixen Gene, die ich mir wenigstens mit Arne teilen durfte. Danke Ihr drei!

II. Table of contents

List of Figures

List of Manuscript Figures

List of Tables

III. Preamble

Iron-sulfur (Fe-S) cluster biogenesis is essential for mammalian physiology. Current “hot topics” like mitochondria, physiology and metabolism are all linked directly to Fe-S cluster biogenesis. That seems not obvious at first, since Fe-S clusters are used for diverse functions in a variety of proteins and are thus involved in a number of different cellular functions. To fulfill their function, Fe-S clusters hence need to be supplied to a number of different proteins. This is ensured by the Fe-S cluster biogenesis machinery, which assembles and distributes Fe-S clusters within a cell.

The thesis will start by introducing the conserved principle of Fe-S biogenesis and then focus on the essential nature and the diverse aspects of Fe-S clusters and Fe-S cluster proteins. Attention will be drawn to a few examples to illustrate the diversity in requirements of Fe-S clusters and Fe-S proteins for mammalian physiology and life as such. The Fe-S cluster biogenesis machinery will be described. Subsequently, more details about the later-acting mitochondrial Fe-S biogenesis proteins will be provided with a focus on the A-type proteins. The review “Mammalian Fe-S biogenesis and its implication in disease” covers the current knowledge on the process in mammals and is included at the end of the introduction (Beilschmidt and Puccio 2014).

Results, including contributions of the other authors, are presented and discussed in a paper format. To explain the reasoning behind the approaches chosen, further information will be provided in the form of an introduction to the paper, and other additional results will be subsequently described. The thesis discussion will focus on the main results and the arising questions on the A-type proteins.

1. Introduction

Mitochondria have been long known as the organelles required for cellular energy metabolism, but are today widely recognized to be responsible for a plethora of additional important cellular functions including iron-sulfur (Fe-S) cluster biogenesis. Fe-S cluster are essential, inorganic protein cofactors (Lill 2009). Proteins harboring Fe-S cluster, termed Fe-S proteins, carry out tasks related to a large number of biological processes including electron transfer and DNA repair, and are therefore crucial for any cellular metabolism (Lill 2009; Beilschmidt and Puccio 2014). The reason why a large variety of unrelated proteins utilize Fe-S clusters as cofactors is best explained by both, the Fe-S clusters' chemical versatility and the fact that Fe and S were abundant elements in the early life's atmosphere and thus available for cofactor formation (Beinert, Holm et al. 1997; Johnson, Dean et al. 2005; Lill and Muhlenhoff 2006). Fe-S clusters as protein cofactors were discovered in the 1960s due to their characteristic paramagnetic resonance signal (Beinert and Lee 1961). Today, an increasing numbers of proteins, more than previously appreciated, have been shown to possess the ancient cofactor (Fontecave 2006; Lill 2009; Bailey 2012; Estellon, Ollagnier de Choudens et al. 2014). In humans, several diseases are associated to malfunction of different Fe-S proteins like Fanconi anemia caused by mutations in the Fe-S helicase *FANCJ* (Fregoso, Laine et al. 2007).

1.1 Fe-S cluster

Fe-S clusters in nature are mostly found as Fe_2S_2 or Fe_4S_4 clusters; however, more complex cluster types are known (Beinert 2000). The clusters redox-potential enables the cofactor to participate in redox-reactions like the electron transfer in the respiratory chain complexes I, II and III and the photosystem I (see 1.3). Other functions were uncovered for Fe-S cluster, likely due to their structural versatility. These include for instance direct binding of enzyme substrates or catalysis (see BOX (Beilschmidt and Puccio 2014)).

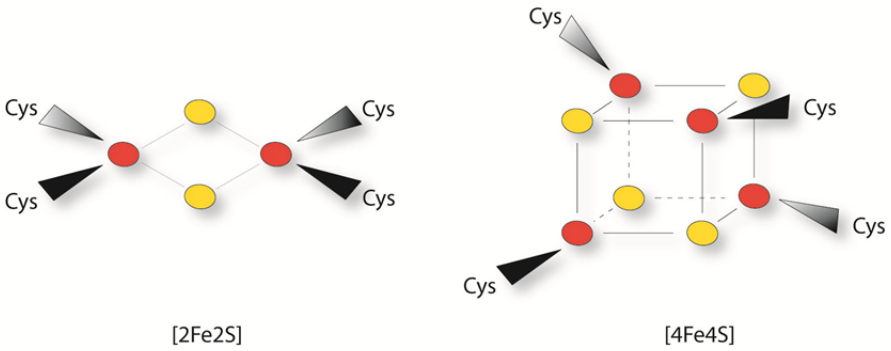

Figure 1: Fe-S cluster.

Structure of canonical Fe_2S_2 cluster (left) and Fe_4S_4 cluster (right) as they are most commonly found in mammalian proteins. Fe-S clusters are generally coordinated by cysteine (and histidine) residues of the proteins. Iron atoms are shown in red and sulfur atoms in yellow. Taken from Beilschmidt and Puccio, 2014.

BOX: Fe-S cluster – simple, almost magic

Fe-S clusters are common protein cofactors composed of iron and inorganic sulfur, most commonly found in the rhombic Fe_2S_2 and the cubic Fe_4S_4 cluster conformation (Kiley and Beinert 2003). The clusters are generally non-covalently ligated by cysteine or histidine residues of proteins (Figure 1). As most of the Fe-S clusters are labile to oxygen, many of the known Fe-S clusters are sheltered inside the respective protein conformation. It often requires strictly reducing conditions to manipulate Fe-S proteins, to purify or even crystallize them in presence of their prosthetic groups. Fe-S proteins lack a distinct amino acid motif that would make it fast forward to predict or identify new ones. However, there is increasing evidence that specific sequential arrangements or signatures of cluster-ligating amino acid residues, most often composed of cysteines and histidines, exist that can predict the likely presence of a cluster within a protein (unpublished results Colin and Puccio and (Fontecave 2006)). However, it is probable that the protein fold would be a better predictor.

Due to the chemical versatility of Fe-S clusters, Fe-S proteins are found to perform a variety of different reactions. Most prominent is their redox potential that can lead to a wide electrochemical range of the Fe-S cluster protein (+300 to -500mV). This is nicely illustrated in the mitochondrial respiratory chain complex I, where seven Fe-S clusters with stepwise increasing reduction potential form a path for the electrons to be transported (Beinert 2000; Sazanov and Hinchliffe 2006). Moreover, Fe-S clusters can be involved in the binding of enzymatic substrates as in aconitase in the citric acid cycle for the interconversion of citrate and isocitrate (Robbins and Stout 1989; Robbins and Stout 1989; Lauble, Kennedy et al. 1992; Rouault, Haile et al. 1992). Other important functions of Fe-S clusters for physiology are found in the regulatory function of the iron regulatory protein 1 (IRP1) (Rouault, Haile et al. 1992) and as redox catalysts in the radical S-adenosyl-L-methionine (SAM) enzymes. The mitochondrial SAM enzyme lipoate synthase catalyzes the last step of lipoate synthesis. Based on evidence from bacterial studies it is likely that its Fe-S cluster serves as a sulfur donor (Ollagnier-De Choudens, Sanakis et al. 2000; Cicchillo and Booker 2005). In the DNA helicase XPD, the Fe-S cluster stabilizes the distinct protein confirmation required for its proper function. The mitochondrial ferrochelatase is an Fe-S enzyme inserts iron into protoporphyrin in the last step of heme biosynthesis. Upon loss of the cluster, ferrochelatase function is strongly inhibited, most likely through a structural role of the cluster (Crouse, Sellers et al. 1996; Sellers, Johnson et al. 1996; Sellers, Wang et al. 1998).

Defects in Fe-S proteins are associated with numerous diseases, as mutation in the DNA repair enzyme XPD causes xeroderma pigmentosum, where patients develop severe skin malignancies after exposure to light (Suhasini and Brosh 2013; Suhasini and Brosh 2013). In Fanconi anemia, mutation in the DNA helicase *FANCJ* leads to cancer formation, most commonly acute myelogenous leukemia (Suhasini and Brosh 2013; Suhasini and Brosh 2013). Both are only two examples to underline the importance of Fe-S clusters for mammalian physiology and life. However, the role of Fe-S cluster within a protein, and whether the Fe-S cluster containing part of the protein is implicated in disease is not always clear. It is noteworthy that many newly discovered Fe-S cluster containing proteins have a long history of laboratory investigation under aerobic, thus probably cluster damaging, conditions. As an example, DNA polymerases were only recently discovered to contain Fe-S clusters. Their Fe-S clusters were shown to be required for the proper assembly of accessory subunits (Netz, Pierik et al. 2012; Netz, Stith et al. 2012), but the fact that they have been studied for many years *in vitro* without a Fe-S cluster, evokes questions about the role of the Fe-S cluster for the DNA polymerases. Could the clusters function as stress sensors or activity regulators? In case of oxidative stress, Fe-S cluster damage and subsequent dissociation of the DNA polymerase subunits would lead to reduction of replication rates. Likewise, could DNA repair mediated by the DNA repair enzymes XPD and FANCJ get tuned or shut down, when the stress impact on the cells gets too high?

BOX: Fe-S cluster – simple, almost magic. Summary on Fe-S cluster functions and roles in nature. Taken from Beilschmidt and Puccio, 2014.

1.2 Principle of Fe-S biogenesis

Although iron and inorganic sulfur form simple Fe-S cluster under reducing conditions *in vitro*, free iron and free sulfur are toxic for cells (Imlay 2006). Cellular iron and sulfur homeostasis is thus achieved by strictly controlled systems regulating iron uptake and storage as well as sulfur production (Komarnisky, Christopherson et al. 2003; Hentze, Muckenthaler et al. 2010). Accordingly, concentrations of free forms of iron and sulfur in cells are too low to allow acceptor-proteins to acquire Fe-S cofactors without accessory proteins. These accessory proteins were uncovered first in the early 1990s, starting with bacterial operons encoding for Fe-S biogenesis as described in Figure 2 (Dean and Brigle 1985; Zheng, Cash et al. 1998).

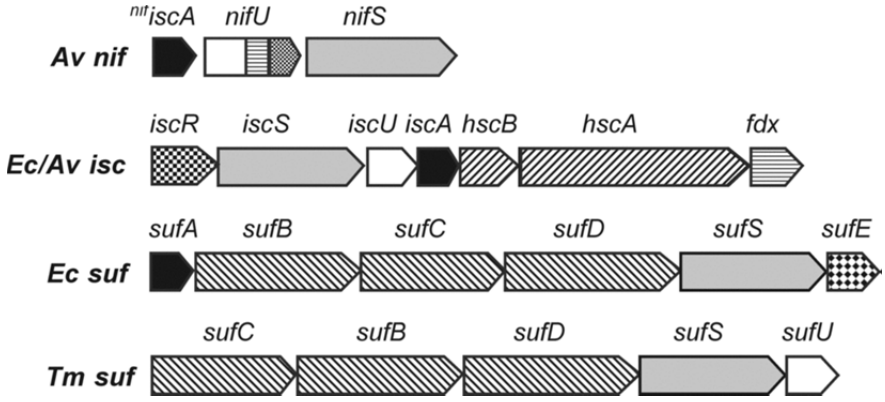

Figure 2: Organization of genes in bacterial *nif*, *isc* and *suf* operons.

In bacteria, Fe-S biogenesis genes are organized in operons. The *isc* operon encodes for proteins required for general biogenesis of Fe-S bluster. Homologues of these proteins are found in the mitochondria. Other bacterial machineries for Fe-S biogenesis exist; the *nif* operon, which was the first to be discovered, encodes for proteins involved Fe-S cluster formation on nitrogenase in nitrogen fixing bacteria; conserved homologues of the *suf* operon are found in plastids. *Av*, *Azotobacter vinelandii*; *Ec*, *Escherichia coli*; *Tm*, *Thermotoga maritima*. Taken from Bandyopadhyay *et al.,* 2008.

Each system involves a cysteine desulfurase for sulfur provision (in bacteria: IscS, SufSE and NifS) and a primary scaffold protein for initial cluster assembly (in bacteria: IscU, SufB and NifU) required to be followed by cluster transfer to acceptor proteins (Figure 3) (Johnson, Dean et al. 2005; Py and Barras 2010).

Homologues of the bacterial *isc* operon, coding for genes for general provision of Fe-S cluster in bacteria as *E. coli*, have been identified in yeast and higher eukaryotes mitochondria (Kispal, Csere et al. 1999; Schilke, Voisine et al. 1999) and it is known that a complex conserved protein machinery including over 20 proteins is involved in cellular Fe-S biogenesis (Frazzon, Fick et al. 2002; Lill 2009). According to the conservation of several Fe-S biogenesis proteins from bacteria to man, general aspects of Fe-S biogenesis were also found to be common to all kingdoms of life (Figure 3). In eukaryotes, nascent cluster assembly takes place in the mitochondria (Bekri, Kispal et al. 2000; Martelli, Wattenhofer-Donze et al. 2007; Ye, Jeong et al. 2010; Schmucker, Martelli et al. 2011). In brief, the cluster is then either inserted into mitochondrial acceptor proteins or a mitochondria-generated compound is exported to the cytoplasm where it is used for extra-mitochondrial Fe-S biogenesis (Lill 2009). The process is described in more details below (see 1.4.3).

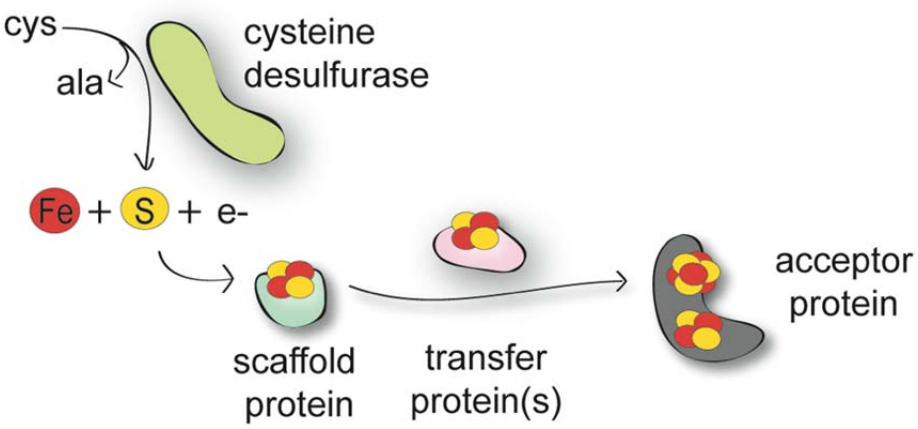

Figure 3: Conserved principle of Fe-S biogenesis.

Fe-S cluster biogenesis followed the same principle in different prokaryotic and eukaryotic organisms. Fe and sulfide, provided by a cysteine desulfurase, are assembled on a scaffold protein. With the help of so-called transfer proteins, assembled Fe-S cluster are provided to acceptor proteins.

Different mutations in Fe-S biogenesis genes have been linked to different but rare diseases underlining the importance of Fe-S biogenesis for mammalian physiology (reviewed in Beilschmidt and Puccio, 2014 (Beilschmidt and Puccio 2014)). Despite the fact that Fe-S biogenesis proteins are conserved and also certain aspects were shown to be in shared throughout phyla (i.e. the main principle of assembly and transfer), many aspects are still unknown to date. This includes the molecular function and the role of many mammalian Fe-S biogenesis proteins illustrating that a fundamental process in physiology only starts to be understood.

1.3 Essential nature of Fe-S cluster and proteins

It is remarkable that cultured human cells lacking mitochondrial DNA (ρ^0 cells) and thus lacking oxidative phosphorylation are viable as long as ATP production is ensured by glycolysis (Morais 1980; Hashiguchi and Zhang-Akiyama 2009). However, a eukaryotic cell is not viable without certain mitochondrial iron-sulfur cluster biogenesis proteins, demonstrating the essential character of mitochondria through iron-sulfur cluster biogenesis within a cell (Lill and Muhlenhoff 2008). The essential nature of Fe-S biogenesis is strongly supported by the characterization of mitosomes, double membrane-bound organelles, present for example in microsporidia and amoebozoa. Evolutionary related to mitochondria, they have lost quasi all functions of mitochondria but iron-sulfur cluster biogenesis (Tovar, Leon-Avila et al. 2003; Goldberg, Molik et al. 2008).

Although over 200 unique Fe-S proteins in diverse physiological processes have been described for bacteria up to now (Johnson, Dean et al. 2005; Fontecave 2006; Lill and Muhlenhoff 2006) a much

smaller number has been identified and characterized in the eukaryotic system. Still, a growing number of eukaryotic Fe-S proteins have been uncovered, as illustrated by the recently characterized Fe-S clusters in DNA polymerases (Netz, Stith et al. 2012).

Here, a selected number of Fe-S proteins and Fe-S-dependent proteins shall be described to emphasize the Fe-S clusters' importance for cellular and organism function. Comprising the nuclear DNA polymerases and primases (as extra-mitochondrial Fe-S proteins), the mitochondrial respiratory chain complexes I and II, as well as the cofactor lipoic acid (LA), the elaboration shall underline that Fe-S clusters are involved in distinct but important fundamental biological processes. It should be emphasized that even for the known Fe-S proteins, not all aspects of the clusters' properties and functions are characterized and understood yet.

1.3.1 Fe-S cluster in DNA metabolism

Numerous nuclear proteins involved in DNA replication and repair require Fe-S cluster, which are listed along with their function in Table 1: Fe-S proteins known to be involved in DNA maintenance in eukaryotes.

The DNA polymerases and primases, for instance, were only recently uncovered to possess the Fe-S cofactor (Prakash and Prakash 2002; Netz, Stith et al. 2012; Kilkenny, Longo et al. 2013). Most of the DNA synthesis throughout eukaryotes is performed by three conserved polymerases: Pol α, Pol δ and Pol ε (Miyabe, Kunkel et al. 2011). Here, Pol α and DNA primases tightly associate for the synthesis of short RNA primers that are subsequently used by Pol δ and Pol ε to synthesize both DNA strands (Schumacher, Stucki et al. 2000). All DNA polymerases, including Pol ζ that functions in translesion DNA synthesis, were then shown to require Fe-S cluster for the formation of the active holo-protein (Prakash and Prakash 2002; Netz, Pierik et al. 2012; Netz, Stith et al. 2012; White and Dillingham 2012; Jain, Vanamee et al. 2014). Eukaryotic primases generally contain a small (PriS) and a large (PriL) subunit. The large subunit contains a conserved Fe-S domain, which is necessary to initiate DNA replication (Prakash and Prakash 2002; Kilkenny, Longo et al. 2013)). Note that the question of the potentially regulatory role of these Fe-S clusters on DNA metabolism is not yet resolved as discussed above (see BOX in 1.1).

Table 1: Fe-S proteins known to be involved in DNA maintenance in eukaryotes.

Adapted from Netz *et al.*, 2013. (Note that most of them were identified in yeast and due to homology and conservation suggested to be Fe-S proteins also in mammals.)

Human Fe-S protein	Yeast homolog	Fe-S type	Proposed function
PRIM2	Pri2	Fe_4S_4	Primase, synthesis of RNA primers for DNA replication
POLA (POL α)	Pol1	Fe_4S_4	Catalytic subunit of polymerase α, DNA replication
POLE1 (POL ε1)	Pol2	Fe_4S_4	Catalytic subunit of polymerase ε, DNA replication
POLD1 (POL δ1)	Pol3	Fe_4S_4	Catalytic subunit of polymerase δ, DNA replication
REV3L	Rec3	Fe_4S_4	Catalytic subunit of polymerase ζ, DNA replication
FANCJ	Absent	Fe_4S_4	Helicase, DNA repair
NTHL1	Ntg2	Fe_4S_4	DNA glycosylase, DNA repair
XPD	Rad3	Fe_4S_4	Helicase, nucleotide excision repair
MUTYH	Absent	Fe_4S_4	DNA glycosylase, DNA repair
RTEL1	Absent	Fe_4S_4	Helicase, telomere stability, anti-recombinase
CHLR1	Chl1	Fe_4S_4	Helicase, chromosome segregation
DNA2	Dna2	Fe_4S_4	Helicase/nuclease, DNA repair

1.3.2 Fe-S cluster in the respiratory chain

The mitochondrial respiratory chain, the main energy producer in eukaryotic cells, requires Fe-S cluster for its function.

The respiratory chain complex I (complex I) is a NADH:ubiquinone reductase that couples the transfer of electrons from NADH to ubiquinone with the translocation of protons across the membrane (Figure 5). Its peripheral arm catalyzes the electron transfer reaction due to the redox-active cofactors; one flavin mononucleotide (FMN) and, depending on the species, up to ten Fe-S clusters (Friedrich 2014). The membrane arm catalyzes proton translocation by a yet unknown mechanism. Complex I couples the transfer of two electrons from NADH to ubiquinone to the translocation of four protons across the membrane (Friedrich 2014). Sazanov and Hinchliffe resolved the structure of the peripheral arm of *Thermus thermophilus* complex I localizing the Fe-S clusters within the protein, showing that electrons are transferred by a chain of seven Fe-S clusters with gradually increasing redox potential (Sazanov and Hinchliffe 2006). Cluster localized outside of this chain are suggested to have stabilizing and/or antioxidant effects on complex I (Sazanov, Baradaran et al. 2013; Friedrich 2014). Only very recently, Vinothkumar and colleagues published the architecture of the mammalian complex I resolved by single-particle electron cryo-microscopy (Vinothkumar, Zhu et al. 2014). The latter consists of 14 core subunits that contain all mechanistically critical cofactors and structural elements sufficient for catalysis. Due to high conservation of seven

core subunits of the hydrophilic arm (NDUFV1, NDUFS2, NDUFV2, NDUFS7, NDUFS8 and NDUFS1), the arrangements of eight Fe-S clusters forming a chain through the hydrophilic arm is very similar to the existing bacterial models. However, lower sequence and structural conservation of parts of NDUFS1, which in *T. thermophilus* contains an additional catalytically redundant cluster, and NDUFS3 were uncovered, likely because these core subunits are catalytically not critical.

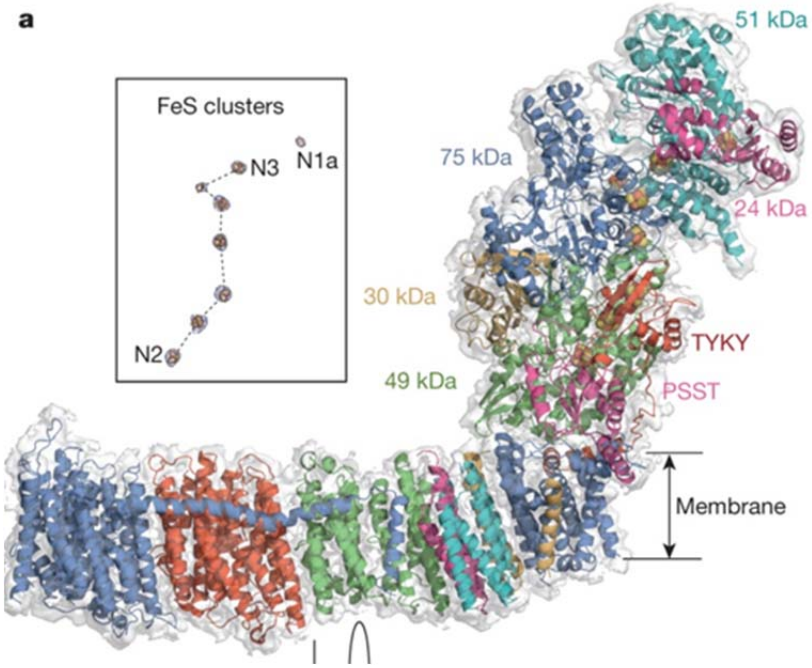

Figure 4: Structure of the core subunits of mammalian complex I.

A structural model of the 14 mammalian core subunits individually colored and labeled. The membrane domain consists of the core subunits ND1, ND2, ND3, ND4, ND5, ND6 and ND4L (not specified here). The hydrophilic domain comprises the following subunits: NDUFS1 (75 kDa), NDUFV1 (51 kDa), NDUFS2 (49 kDa), NDUFS3 (30 kDa), NDUFV2 (24 kDa), NDUFS7 (PSST) and NDUFS8 (TYKY). The modeled chain of Fe-S clusters is shown in the inset. Taken from Vinothkumar *et al.*, 2014.

In mammals, 30 additional subunits are known and may play important roles in the assembly, regulation, and the stability of complex I, or protection against oxidative stress. Most of the additional subunits are arranged around the membrane domains and the lower hydrophilic domain, and are thought to protect (certain Fe-S clusters) from oxidative damage. The recent study by Vinothkumar and colleagues could determine and localize 14 of these subunits: NDUFSA2, proposed to protect the core enzyme from oxidative damage, as well as NDUFS4 and NDUFS6, both thought to be important for complex I assembly (Mimaki, Wang et al. 2012), were assigned as part of the hydrophilic arm. Interestingly, two subunits, NDUFA6 and NDUFB9, contain a LYR motif, defined as an N-terminal leucine-tyrosine-arginine sequence. The LYR motif in NDUFA6 was shown to be required for the catalytic activity of complex I in *Y. lipolytica* (Angerer, Radermacher et al. 2014). LYR

motifs have recently been shown to be important for cluster targeting to complex II (Maio, Singh et al. 2014) (see 1.4.2.5). Three subunits, NDUFA8, NDUFS5 and NDUFB7, contain a sequence cysteine motif (precisely a twin C-X_9-C motif) that is assigned to the intermembrane surface of complex I. It should be mentioned that the mammalian nomenclature of complex I subunits is, first, not directly linked to the bacterial nomenclature and, second, not all subunits that are termed as Fe-S subunits (like NDUFS3) contain Fe-S cluster(s) and *vice versa*. Currently, based on the homology between core subunits and the seemingly conserved position of the Fe-S clusters within complex I, there is no experimental or bioinformatic evidence for NDUFS3, NDUFS4 or NDUFS5 to be Fe-S proteins, although it has been used as such in several publications in the field (Maio, Singh et al. 2014; Perdomini, Belbellaa et al. 2014).

A

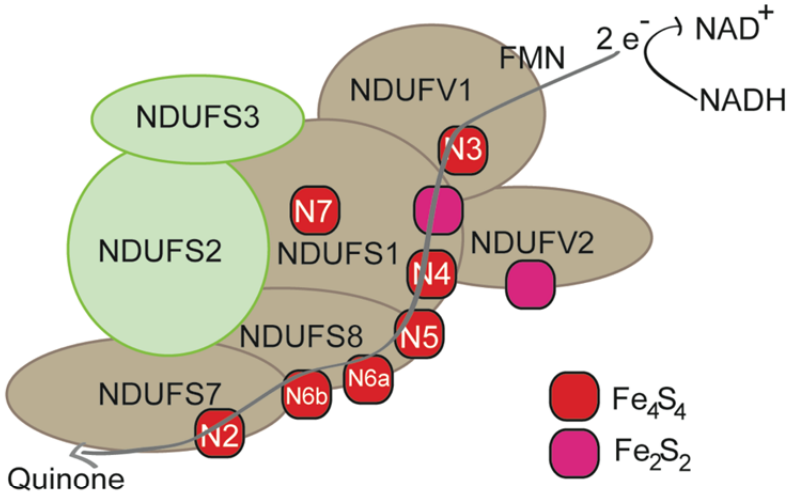

B

Mammals	Fe-S cluster	T. Thermophilus	E. coli
NDUFV1	N3, Flavin	Nqoi	NuoE
NDUFV2	N1a	Nqo2	NuoF
NDUFS1	N1b, N4, N5, N7	Nqo3	NuoG
NDUFS2	/	Nqo4	NuoD
NDUFS3	/	Nqo5	NuoC
NDUFS7	N2	Nqo6	NuoB
NDUFS8	N6a, N6b	Nqo9	NuoI

Figure 5: Characteristics of the hydrophilic domain of respiratory chain complex I.

Schematic representation of the hydrophilic domain of the human complex I based on sequence similarities (A). The table shows the human homologues compared to the *T. thermophilus* and *E. coli*

subunits. Based on homology, the Fe-S clusters for electron transfer can be localized in the different mammalian subunits (B). Adapted from the thesis of Florent Colin, Puccio laboratory 2013.

Despite knowledge that the correct sequential assembly of complex I is necessary for proper function, many, yet likely not all, assembly factors are known and studied. For instance the Fe-S biogenesis protein IND1 was shown to be involved in complex I formation (see 1.6, 1.4.2.2). When and how the Fe-S clusters are inserted into complex I remains unknown.

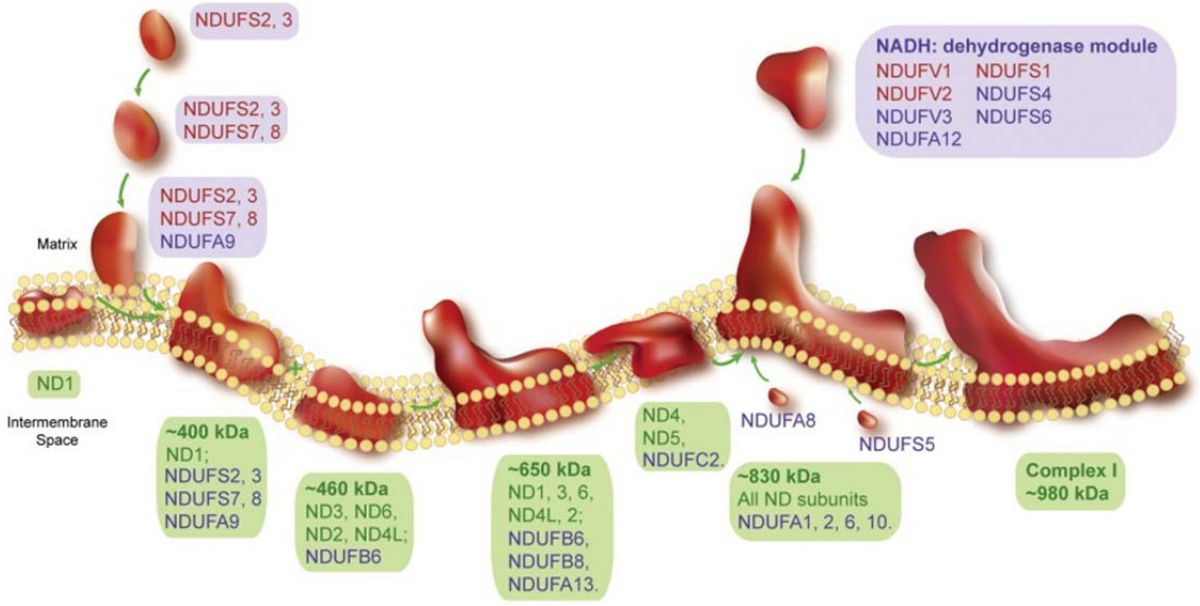

Figure 6: The assembly model of human complex I biogenesis.

In the early assembly stages, the core subunits NDUFS2 and NDUFS3 form a small hydrophilic assembly complex. This further expands by the incorporation of hydrophilic subunits such as NFUFS7, NDUFS8 and later NDUFS9. This peripheral complex, together with a small membrane complex containing mtDNA-encoded subunit ND1, forms an assembly intermediate of 400 kDA. This complex incorporates with a 460 kDa membrane complex containing ND3, ND6, ND2, ND4L and NDUFB6 to form a bigger complex of 650 kDa. Subsequently, with the association of another membrane complex of ND4, ND5 and probably NDUFC2, an assembly intermediate of 830 kDa is formed. Meanwhile, a hydrophilic complex, NADH: dehydrogenase module (N module) is assembled by some nuclear DNA encoded subunits. With the addition of the N module and remaining subunits (such as the intermembrane space subunits NDUFA8 and NDUFS5), mature complex I is assembled. All indicated complex sizes are approximations. The core subunits are colored in red, the rest of nuclear DNA-encoded subunits are colored in blue. The mtDNA-encoded subunits are in green. Taken from Mimaki *et al.*, 2012.

Importantly, malfunction of complex I is the most frequent mitochondrial disorder in childhood including Leigh syndrome and the NUBPL-linked mitochondrial encephalomyopathy (Mimaki, Wang et al. 2012; Beilschmidt and Puccio 2014). Mutations found in complex I itself include all subunits and

manifest with different neurological disorders, but also cardiomyopathy, missing yet a clear genotype-phenotype correlation (Mimaki, Wang et al. 2012).

Respiratory chain complex II (complex II), also termed succinate dehydrogenase (SDH) is involved in the citric acid cycle and the respiratory chain (Figure 7, Figure 8). While it catalyzes oxidation of succinate to fumarate in the citric acid cycle, it also transfers electrons from succinate to ubiquinone for respiration, but is less efficient than complex I (Liu, Chakraborty et al. 2014). Complex II harbors different cofactors. The catalytic domain is composed of a flavoprotein with a covalently bound FAD cofactor (SDH A) and an Fe-S protein (SDH B) containing three different Fe-S clusters (Fe_2S_2, Fe_3S_4, Fe_4S_4). The heme cofactor in SDH is not involved in respiration, but has been suggested to function as an electron sink to reduce ROS and thus to protect the FAD cofactor and Fe-S clusters of complex II (Yankovskaya, Horsefield et al. 2003; Liu, Chakraborty et al. 2014). The Fe_4S_4 cluster has usually a rather low reduction potential and is thought to function as an energy barrier during electron transfer to direct the electron flow and thus the reaction pathway.

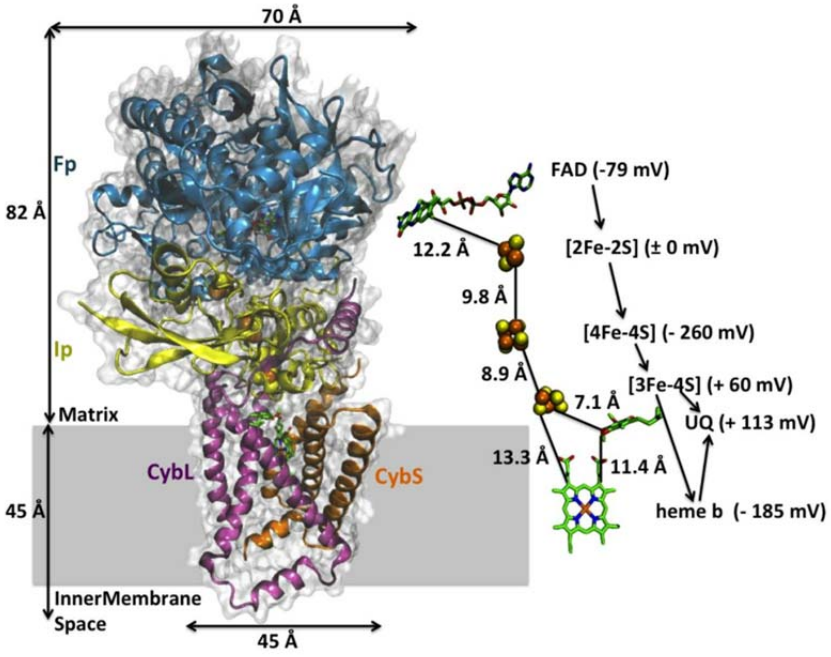

Figure 7: Crystal structure of mitochondrial respiratory chain complex II.

FAD binding protein (Fp) (also termed SDH A) is shown in blue, iron-sulfur protein (Ip) (also termed SDH B) is shown in yellow, hydrophobic domains are shown in pink and orange, and the putative membrane is shown in grey shading. Cofactors involved in the electron transfer pathway are shown on the right side, with distances, reduction potential, and directions denoted. Taken from Liu *et al.*, 2014.

1.3.3 Fe-S cluster in lipoic acid biosynthesis

The requirement of endogenous lipoic acid (LA) for development further highlights that Fe-S clusters are essential for mammalian physiology (Yi and Maeda 2005). LA is a protein cofactor required for the activity of multienzyme complexes such as pyruvate dehydrogenase complex (PDHc), α-ketoglutarate dehydrogenase complex (KGDHc), branched-chain α-ketoacid dehydrogenase complex (BCDHc) and the glycine cleavage system. It is covalently attached to lysine residues to specific subunits of these complexes (E2 or H protein) (Patel and Harris 1995; Hiltunen, Autio et al. 2010). Due to their central position in energy production, metabolism and biosynthesis processes, (genetic) defects in one of these complexes are associated with a variety of heterogeneous phenotypes: lactic acidosis and neuroanatomical manifestations due the brain dependence on glucose (for PDH deficiency); maple syrup urine disease and seizures; mental retardation and coma (for KGDH, BCDH deficiency) (Patel and Harris 1995; Hiltunen, Autio et al. 2010). Defects associated with the glycine cleavage generally lead to glycine encephalopathy (or non-ketonic hyperglycinemia), caused by elevated glycine levels in the body fluids (Yoshida and Kikuchi 1969).

LA biosynthesis requires Fe-S cluster and thus Fe-S biogenesis, since lipoic acid synthase (LIAS), the enzyme catalyzing the last step of lipoic acid synthesis, is a Fe_4S_4 radical S-adenosyl-L-methionine (SAM) enzyme (Miller, Busby et al. 2000; Marquet, Bui et al. 2001). Bacterial studies suggest that the Fe-S cluster of LIAS acts as a sulfur donor during this step (Ollagnier-De Choudens, Sanakis et al. 2000; Cicchillo and Booker 2005). Homozygous embryos lacking LIAS die at embryonic day 9.5 and cannot be rescued by LA supplementation of the mother (Yi and Maeda 2005), showing that endogenous LA production is essential. LIAS yeast homologue Lip5 mutants are also unable to utilize LA supplied in the growth medium (Sulo and Martin 1993). *Mayr et al.* described neonatal-onset epilepsy with defective mitochondrial energy metabolism and elevated glycine in a patient with a homozygous missense mutation in the *LIAS* gene that died at four years of age (Mayr, Zimmermann et al. 2011). Besides its attachment as cofactor to the protein complexes, lipoic acid is exclusively found in mitochondria and is one of the most potent natural antioxidants (Goraca, Huk-Kolega et al. 2011). Its negative redox potential enables reduction of other antioxidants, including vitamin C, vitamin E and glutathione. It can chelate redox metals and is a direct ROS quencher.

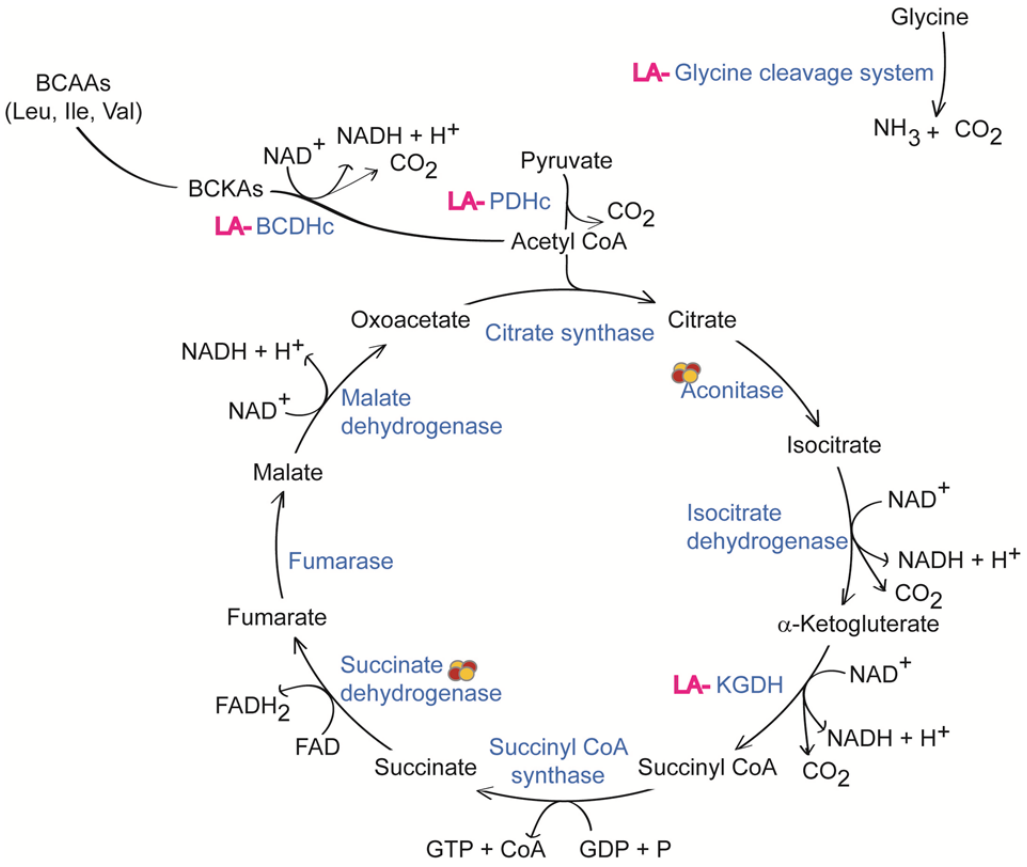

Figure 8: LA-dependent complexes in metabolism.

LA-dependent complexes are central in mitochondrial metabolism in the mitochondria. LA is highlighted in pink, enzymes in blue and Fe-S clusters in red-yellow. BCAAs stands for branched-chain amino acids (leucine, isoleucine and valine), BCKA for branched-chain keto-acids. Aadapted from Patel *et al.*, 1995 and Faseb and Wang, 2013 Amino Acids.

1.4 Fe- S biogenesis

The current knowledge on mammalian Fe-S biogenesis is reviewed in Beilschmidt and Puccio 2014 Biochimie (Beilschmidt and Puccio 2014). Here, the process will be illustrated, dividing the mechanism into nascent cluster formation, which is required for all cellular Fe-S cluster, the late-acting mitochondrial Fe-S biogenesis and subsequently extra-mitochondrial Fe-S biogenesis and, afterwards the focus will be on the A-type proteins (ISCA1 and ISCA2).

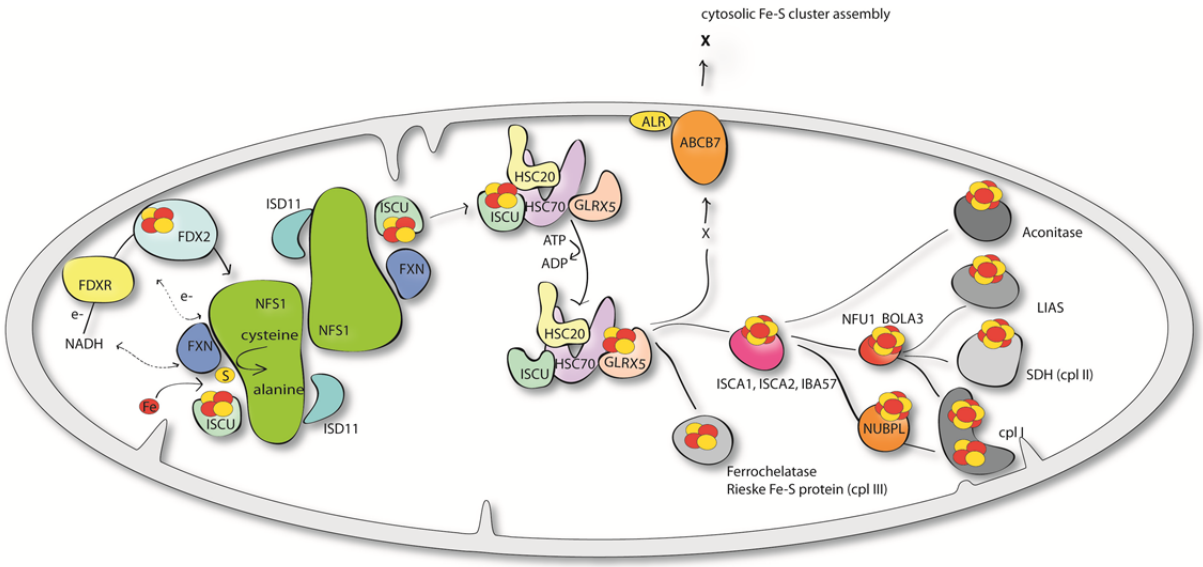

Figure 9: Mammalian Fe-S cluster biogenesis and genetic disorders caused by dysfunction of proteins in mitochondrial Fe-S cluster biogenesis.

Schematic representation of the current model of mammalian Fe-S cluster biogenesis. NFS1, the cysteine desulfurase subtracts sulfur from L-cysteine for nascent Fe-S cluster assembly. It forms a dimer and is bound by monomers of the primary scaffold protein ISCU, the regulator protein FXN and ISD11, that is required for NFS1 stability. Cysteine desulfurase activity and iron entry is controlled by FXN. Electrons are provided by a an electron transport chain consisting of NAD(P)H, ferredoxin reductase (FDXR) and ferredoxin (FDX2). The interaction of FDX2 with NFS1 seems to happen prior to binding of FXN/ISCU/ISD11. ISCU bound Fe-S clusters are subsequently transferred via a dedicated chaperone-co-chaperone system to GLRX5. The listed proteins are required for all cellular Fe-S clusters. Subsequently, for mitochondrial Fe-S proteins, Fe-S clusters are either directly inserted into mitochondrial $[Fe_2S_2]$ proteins or transferred via specific carrier systems such as the one composed of ISCA1, ISCA2 and IBA57 to mitochondrial $[Fe_4S_4]$ proteins. Some carrier proteins, such as NFU1, BOLA3 and NUBPL seem to be required for only a subset of mitochondrial $[Fe_4S_4]$ proteins. ISCU and GLRX5 proteins are represented with $[Fe_2S_2]$ clusters, whereas the carrier systems required for $[Fe_4S_4]$ proteins are represented as with $[Fe_4S_4]$ clusters. To date, he presence of another cluster type under physiological conditions cannot not be excluded. For extra-mitochondrial Fe-S cluster, a so far uncharacterized compound (X) is exported via the Fe-S cluster export machinery consisting of ALR, glutathione and ABCB7. In the cytoplasm the cytosolic Fe-S cluster assembly machinery (CIA) inserts Fe-S cluster into cytosolic and nuclear Fe-S proteins. Taken from Beilschmidt and Puccio, 2014.

Notably, the model described here is mainly based on data from studies in bacteria and yeast; however, the description of different phenotypes of patients with mutations in Fe-S biogenesis genes contributed to today's idea of different proteins' roles within Fe-S biogenesis.

1.4.1 Nascent cluster formation in mitochondria – the core machinery

The nascent Fe-S cluster is assembled *de novo* on the scaffold protein ISCU in a transient fashion providing a backbone structure of cysteine residues (Raulfs, O'Carroll et al. 2008; Lill 2009). Sulfur is provided by conversion of cysteine to alanine by the cysteine desulfurase complex NFS1 and ISD11, ISD11 being required for stability of NFS1 protein (Loiseau, Ollagnier-de-Choudens et al. 2003; Adam, Bornhovd et al. 2006; Wiedemann, Urzica et al. 2006; Pandey, Yoon et al. 2011). The sulfur has further to be reduced to sulfide in order to be assembled with ferrous Fe (Fe^{2+}). Electrons for sulfur reduction are probably provided by the electron transfer chain including NAD(P)H, ferredoxin reductase FDXR and ferredoxin (FDX2) (Shi, Ghosh et al. 2012). Bacterial ferredoxin was shown to enable reductive coupling for Fe-S formation on IscU (Chandramouli, Unciuleac et al. 2007) and to transfer electrons to the cysteine desulfurase in the presence of L-cysteine (Kim, Frederick et al. 2013; Yan, Konarev et al. 2013). (Please note that controversies on the role of FDX1 along with FDX2 in Fe-S biogenesis exist, which are discussed elsewhere (Sheftel, Stehling et al. 2010; Shi, Ghosh et al. 2012; Beilschmidt and Puccio 2014).) Fe availability for cluster assembly and cysteine desulfurase activity is regulated by frataxin (FXN) (Adinolfi, Iannuzzi et al. 2009; Tsai and Barondeau 2010; Bridwell-Rabb, Iannuzzi et al. 2012; Colin, Martelli et al. 2013). After assembly of the Fe-S cluster, it is thought to be transferred with the help of chaperone proteins HSCB and GRP75 (HSPA9). In bacteria and yeast, the co-chaperone HscB/Jac1 (HSCB-homologue) functions together with its chaperone HscA/Ssq1 (HSPA9 homologue) and the nucleotide exchange factor Mge1, which is suggested to mediate ATP-release in the interaction of yeast ISCU homologue Isu1 and Ssq1 (Craig and Marszalek 2002; Vickery and Cupp-Vickery 2007; Uhrigshardt, Singh et al. 2010). The interaction is highly specific and involved a LPPVK motif on Isu1, and induces conformational changes in Isu1 that lead to dislocation of the bound Fe-S cluster (Hoff, Cupp-Vickery et al. 2003; Dutkiewicz, Schilke et al. 2004). Yeast Grx5, a mitochondrial monothiol glutaredoxin, was shown to interact with Ssq1 on a binding site close to the one of Isu1 (Uzarska, Dutkiewicz et al. 2013). It was shown that this binding allows transfer of an Isu1 bound cluster to Grx5, although the role of GLRX5 is ambiguous (see 1.4.2.3).

Hitherto not mentioned, different diseases are known that were associated to mutations in *FXN, ISCU, FDX2* or *ISD11* genes. Of note, diseases caused by mutations in Fe-S biogenesis genes are rare. They have been reviewed previously (see 1.6) (Rouault 2012; Beilschmidt and Puccio 2014).

1.4.2 Targeting mitochondrial Fe-S proteins

For mitochondrial Fe-S proteins, the assembled cluster has to be specifically delivered to the mitochondrial acceptor proteins and integrated by coordination using specific ligands. The current working model is that A-type proteins ISCA1 and ISCA2 together with IBA57 ensure biogenesis of all mitochondrial Fe_4S_4 proteins, strongly suggested by knockdown studies is human HeLa cells (Sheftel, Stehling et al. 2010). Upon independent knockdown of each of the three proteins, the maturation of mitochondrial Fe_4S_4 proteins was affected. While data on IBA57 and its homologues are particularly sparse, few but controversial reports exist on the molecular function and the roles of the A-type proteins throughout phyla and will be elaborated below (see 1.5).

1.4.2.1 NFU1 and BOLA3 - specific mitochondrial targeting factors

Mammalian NFU1 is today accounted as one of the specialized mitochondrial Fe-S targeting factors, likely for a subset of Fe_4S_4 clusters (Beilschmidt and Puccio 2014). NFU1 was initially suggested to serve as an alternative scaffold protein that transiently binds a Fe_4S_4 cluster (Tong, Jameson et al. 2003), but it was also shown to enable sulfur delivery from NFS1 to ISCU by binding NFS1 *in vitro* (Liu and Cowan 2007; Liu and Cowan 2009; Liu, Qi et al. 2009). Sequence homology to the C-terminal part of bacterial NifU, which functions as scaffold protein during nitrogenase maturation (Jacobson, Cash et al. 1989), already suggested an implication of NFU1 in Fe-S biogenesis, but NFU1-homologues are neither present in the bacterial *isc* nor in the *suf* operons encoding Fe-S biogenesis proteins (Figure 2). Studies on *E. coli* NfuA has not only shown the presence of a Fe_4S_4 cluster, but also positioned NfuA upstream of the A-type proteins IscA and SufA (Angelini, Gerez et al. 2008; Py, Gerez et al. 2012). Although thorough biochemical data for mammalian NFU1 are sparse, yeast and bacterial data have shown that the role of NFU1 homologues is subsequent to the Fe-S cluster assembly complex involving ISCU (Navarro-Sastre, Tort et al. 2011; Py, Gerez et al. 2012). Taken these diverse data, the role of NFU-proteins remains unresolved.

Characterization of patients carrying mutations in *NFU1* strongly suggested the specific role for only a subset of Fe_4S_4 proteins namely complex II and LIAS (Cameron, Janer et al. 2011; Navarro-Sastre, Tort et al. 2011; Ferrer-Cortes, Font et al. 2012). However, NFU1 function has also not been well defined in mammals. Knockdown in cells resulted in decreased levels of LA-bound PDH and KGDH, whereas patient biochemical phenotypes span a spectrum from decreased LA only to phenotypes including the respiratory complexes. Six patients carrying a mutation in *BOLA3* presented a phenotype similar to NFU1-deficient patients (Cameron, Janer et al. 2011). Interestingly, BOLA proteins have previously been shown to form Fe-S containing complexes with monothiol redoxins. More precisely, yeast BOLA homologue Fra2 binds cytosolic Grx3/4 forming a stable Fe_2S_2-bridged heterodimer in *S. cerevisiae* regulating iron homeostasis through controlling nuclear translocation of the Aft1/Aft2 transcription

factor (Li, Mapolelo et al. 2009; Roret, Tsan et al. 2014). However, the biochemical function of BOLA3 as well as its' potential cooperation with other Fe-S biogenesis proteins remain to be established (Cameron, Janer et al. 2011; Haack, Rolinski et al. 2013; Baker, Friederich et al. 2014).

1.4.2.2 IND1 protein required for in complex I formation

IND1 or NUBPL has been proposed to be involved solely in complex I assembly (Bych, Kerscher et al. 2008; Sheftel, Stehling et al. 2009) and is thus the most specific Fe-S cluster targeting factor suggested so far. Maturation of complex I was strongly impaired upon decreased levels of IND1 protein in human cells and for the yeast homologue *IND1 Yarrowia lipolytica* (Bych, Kerscher et al. 2008; Sheftel, Stehling et al. 2009) although not all subunits were similarly affected. The yeast *Yarrowia lipolytica* and the human IND1 mitochondrial P-loop NTPase was shown to transiently assemble a Fe_4S_4 cluster, however, cluster transfer to complex I was not shown probably because of the intricate maturation process of complex I. Potential effects of IND1 knockdown on LA biogenesis that had not been tested previously were excluded recently (Stehling, Wilbrecht et al. 2014), further supporting the specific role of IND1 in complex I assembly.

1.4.2.3 GLRX5 protein, a specific or general targeting factor?

Glutaredoxins (Grx) are thioltransferases that reduce disulfide bonds or catalyse reversible (de-) glutathionylation of proteins (Herrero and de la Torre-Ruiz 2007). The precise function of the mitochondrial monothiol glutaredoxin GLRX5 in the process of Fe-S biogenesis is undefined (Ye and Rouault 2010; Beilschmidt and Puccio 2014), despite it's high conservation. Yeast Grx5 was shown to bind Ssq1, the homologue of HSCB, at a site close to the Isu-binding site (Uzarska, Dutkiewicz et al. 2013). The proximity of holo-Isu and apo-Grx5 was thought to enable cluster release to Grx5, which then mediates maturation of all cellular Fe-S proteins. Dimerization of GLRX5 (or GLRX5-homologues) thereby allows cluster coordination of a bridging Fe_2S_2 cluster (Picciocchi, Saguez et al. 2007; Bandyopadhyay, Chandramouli et al. 2008; Johansson, Roos et al. 2011). On the one hand, it was shown that deletion of the yeast homologue Grx5 affects all cellular Fe-S proteins, placing the protein just downstream of nascent cluster assembly and distribution of Fe-S cluster (Uzarska, Dutkiewicz et al. 2013). On the other hand, deletion of Grx5 is, in contrast to the chaperones and other proteins involved in nascent Fe-S assembly, not lethal in yeast (Rodriguez-Manzaneque, Ros et al. 1999; Rodriguez-Manzaneque, Tamarit et al. 2002), indicating that cluster targeting via Grx5 is not exclusive (see 1.4.2.5). Yeast Grx5 was further proposed to interact with the yeast homologues of the A-type proteins Isa1 and Isa2 (see 1.5.2.2) (Vilella, Alves et al. 2004; Kim, Chung et al. 2010; Banci, Brancaccio et al. 2014).

So far, four mutations of *GLRX5* in humans have been identified (Camaschella, Campanella et al. 2007; Baker, Friederich et al. 2014; Beilschmidt and Puccio 2014). One patient diagnosed with

sideroblastic anemia showed in particular defects in the maturation of ferrochelatase and decreased amounts of ALAS2. Both are required for heme biosynthesis, therefore contributing to the defect in hematopoiesis observed in the anemia patient, likely through increased IRP1 and IRP2 IRE-binding activity in erythrocytes (Wingert, Galloway et al. 2005; Ye, Jeong et al. 2010). In normal conditions, IRP1 harbors an Fe-S cluster and exhibits aconitase function. Under low iron conditions, the iron regulatory proteins IRP1 and IRP2 bind iron-responsive elements (IREs) on the mRNAs of genes involved in iron metabolism leading to increased or decreased translation, depending on whether the IRE lies within the 5'UTR (block of translation) or the 3'UTR (stabilization of mRNA) (Hentze, Muckenthaler et al. 2010; Anderson, Shen et al. 2012). Nevertheless, three other patients were recently described that, however, present nonketonic hyperglycinemia (Baker, Friederich et al. 2014) and decreased formation of LA. Defects in the glycine cleavage system and the other LA-depended complexes (PDH, KGDH and BCDH) are likely to cause neurotoxicity leading to neurodegeneration (Applegarth and Toone 2006) (see 1.6). The molecular causes for the differences in phenotypes between patients, the observed tissue specificity and the sole defect on LA-dependent complexes in the newly described patients need to be investigated in more detail. Based on the binding to yeast chaperone Ssq1, GLRX5 was first thought to be placed somewhere as the link between the early and the late-acting mitochondrial Fe-S biogenesis. The role for GLRX5 in Fe-S biogenesis remains ambiguous and potentially needs to be revised.

1.4.2.4 Conclusion on mitochondrial Fe-S targeting

Collectively, the requirement of all proteins thought to be involved in targeting mitochondrial Fe-S clusters are specific to all or a subset of mitochondrial Fe_4S_4 proteins only. No specific targeting factors have yet been identified for formation of mitochondrial Fe_2S_2 proteins, as ferrochelatase of the heme biogenesis and Rieske protein of the complex III.

Other aspects of the Fe-S biogenesis mechanism remain to be defined. For instance, it has been stated that for all mitochondrial Fe_4S_4 cluster proteins, cluster conversion of Fe_2S_2 to Fe_4S_4 clusters has to take place (Stehling and Lill 2013).

1.4.2.5 Cluster targeting from ISCU via HSCB to complex II: a new mechanism?

Maio and colleagues have shown cluster targeting from ISCU to the Fe-S subunit SDH B of complex II via a chaperone-co-chaperone system (Maio, Singh et al. 2014). This mechanism included the action of the chaperone HSPA9 together with its co-chaperone HSCB and the SDH accessory subunit SDHAF1 (for SDH assembly factor 1). Using a yeast two-hybrid screen for HSCB binding partners and complementary co-immunoprecipitations, they have shown direct binding of HSCB to SDH B via conserved motifs (LYR motifs); and subsequent formation of an assembly intermediate composed of ISCU, HSPA9, HSCB and SDH B in the mitochondrial matrix. SDHAF1 bound to both HSCB and SDH B

(on a non-LYR binding site), thereby seemed to enable initial docking of HSCB to SDH B. Binding of SDH B to the Fe-S biogenesis proteins without SDH A present suggests that SDH B acquires its Fe-S cluster before it associates with SDH A (Figure 7). Although open questions on when exactly and how Fe-S cluster transfer to SDH B takes place, this study attempts to answer one important question in the field on how are acceptor proteins identified for cluster targeting. Notably, although GLRX5 was previously shown in yeast to bind the chaperone Ssq1 (HSPA9 homologue), it was not shown to be involved in this cluster transfer to complex II.

1.4.3 Extra-mitochondrial Fe-S clusters: Export and cytosolic Fe-S assembly

A number of mitochondrial Fe-S biogenesis proteins were previously shown to be required for all cellular Fe-S clusters More precisely, mitochondrial localization of FXN, NFS1, ISD11 and ISCU as well as ABCB7 was required also for maturation of extra-mitochondrial Fe-S cluster in the mammalian system (Bekri, Kispal et al. 2000; Martelli, Wattenhofer-Donze et al. 2007; Ye, Jeong et al. 2010; Schmucker, Martelli et al. 2011), and the list was completed by ferredoxin and the chaperones based on yeast deletion phenotypes (Beinert, Holm et al. 1997; Kispal, Csere et al. 1999; Lange, Lisowsky et al. 2001; Sharma, Pallesen et al. 2010; Netz, Pierik et al. 2012; Netz, Stith et al. 2012). This suggested that the core machinery for nascent cluster assembly together with chaperone function acts prior not only to a transfer to mitochondrial Fe-S proteins but also to the export of a compound transported by the inner mitochondrial membrane transporter ABCB7. The ATP-binding transporter ABCB7, homologue of the yeast Atm1, is usually referred to as part of the termed Fe-S export machinery, together with the sulfhydryl oxidase ALR (GFER) and glutathione (Beilschmidt and Puccio 2014). Defects in ABCB7 (and similarly in yeast Atm1) cause impaired extra-mitochondrial Fe-S protein maturation and genetic mutations lead to X-linked sideroblastic anemia and ataxia (XLSA/A) (Allikmets, Raskind et al. 1999; Bekri, Kispal et al. 2000; Pondarre, Antiochos et al. 2006; Cavadini, Biasiotto et al. 2007; Pondarre, Campagna et al. 2007; D'Hooghe, Selleslag et al. 2012; Banci, Brancaccio et al. 2014). Recently, Schaedler and colleagues found glutathione polysulfide to be exported by the yeast Atm1 transporter (and by the plant homologue ATM3), opening the question whether this is also the case in mammals (Schaedler, Thornton et al. 2014).

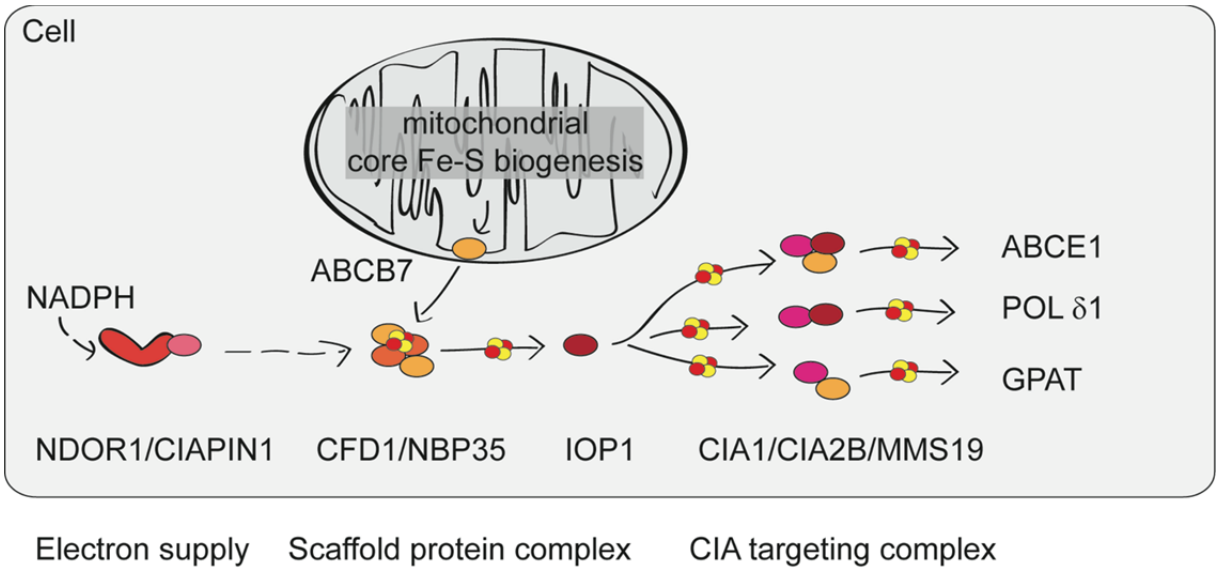

Figure 10: Schematic representation of cytosolic and nuclear Fe-S protein biogenesis.

Biogenesis of cytosolic and nuclear Fe-S proteins requires the mitochondrial core Fe-S biogenesis proteins and ABCB7 (see Beilschmidt and Puccio 2014). In a first step, a Fe_4S_4 cluster is assembled on the scaffold protein complex CFD1-NBP35. Electrons are provided by NADPH, NDOR1 and CIAPIN1. Biogenesis seems to further involve GLRX3 (not depicted here). Fe-S cluster transfer is accomplished by IOP1 and the CIA-targeting components CIA1, CIA2B and MMS19. Different sub complexes may deliver the Fe_4S_4 cluster in a target specific fashion to dedicated Fe-S proteins such as XPD, POL δ1 or others as represented. CIA: Cytosolic Fe-S protein assembly machinery. Adapted from Paul and Lill, 2014 and Netz *et al.,* 2013.

In the cytoplasm, a Fe-S cluster (Fe_4S_4) is assembled on a scaffold complex composed of two P-loop NTPases CFD1 and NBP35. As for the mitochondrial Fe-S cluster assembly, electrons need to be provided, here by an electron transport chain in the cytosol composed of NADPH, the diflavin reductase NDOR1 and the Fe-S protein CIAPIN1. Subsequently, the cluster is transferred to acceptor proteins by the iron-hydrogenase-like proteins IOP1 and a complex of the β-propeller protein CIA1, the HEAT repeat protein MMS19 and the small acidic protein CIA2 (Figure 10) (Netz, Mascarenhas et al. 2014; Stehling, Wilbrecht et al. 2014). MMS19 was very recently identified to be involved in extra-mitochondrial Fe-S biogenesis (Gari, Leon Ortiz et al. 2012; Stehling, Vashisht et al. 2012). Interestingly, MMS19 seems to be required for a subset of cytosolic and nuclear Fe-S proteins; the sulfide reductase in methionine synthesis, some DNA helicases, glycosylases and polymerases involved in DNA synthesis and repair as well as the helicase RTEL1 involved in telomere length regulation (Gari, Leon Ortiz et al. 2012; Stehling, Vashisht et al. 2012).

1.5 The A-type proteins and IBA57

A-type proteins comprise a group of small and highly conserved proteins from bacteria to plants and humans (Jensen and Culotta 2000; Kaut, Lange et al. 2000; Cozar-Castellano, del Valle Machargo et al. 2004; Abdel-Ghany, Ye et al. 2005; Johnson, Unciuleac et al. 2006), the mature proteins being rather small having a size about 110 amino acids (statement for bacterial proteins and counting the eukaryotic ones without the mitochondrial targeting sequence). Within their protein sequence, A-type proteins feature three highly conserved cysteine residues (C-X_n-CGC; n= 60-80) that were shown to be essential for function in yeast (Jensen and Culotta 2000; Kaut, Lange et al. 2000). Most bacteria possess several A-type proteins, whereas two are found in eukaryotic organisms.

Hereafter, facts and controversies published on A-type proteins will be stated, starting with the bacterial homologues to the human proteins. This will be followed by an introduction to IBA57 and its homologues, a protein mainly suggested to function along with A-type proteins.

1.5.1 Bacterial A-type proteins in Fe-S biogenesis

As mentioned above Fe-S biogenesis in bacteria involves three different machineries termed ISC (iron-sulfur cluster), SUF (mobilization of sulfur) and NIF (nitrogen fixation) system, with the components of each of these machineries organized in operons (*isc, suf and nif*) (Figure 2). While the roles for the cysteine desulfurases as well as the primary scaffold proteins are well established today, questions remain on the nature of the iron donor, and the role of the ubiquitous A-type proteins, which are present in all bacterial Fe-S biogenesis systems (IscA, SufA and ^{Nif}IscA).

E. coli harbors three A-type proteins: IscA, SufA and ErpA (ErpA for essential respiratory protein A, first described by Loiseau (Loiseau, Gerez et al. 2007)). While IscA and SufA are encoded by the *isc* and *suf* operons, respectively (Figure 2), the *ErpA* gene is located at distance to any other Fe-S biogenesis gene. Contrary to single mutants of IscA and SufA, ErpA single mutants show a severely impaired growth under aerobic conditions, a phenotype that was associated with impaired isoprenoid biosynthesis (Loiseau, Gerez et al. 2007). However, under anaerobic growth, all single mutants have only limited effect (Loiseau, Gerez et al. 2007), suggesting that multiple A-type proteins may exhibit functional redundancy in many bacterial organisms. In *Azotobacter vinelandii* single IscA mutants reveal impaired growth only under elevated oxygen levels (Johnson, Unciuleac et al. 2006). *E. coli* IscA SufA double mutants revealed an essential role for A-type proteins in the maturation of a subset of Fe_4S_4 clusters under aerobic growth conditions (Lu, Yang et al. 2008; Tan, Lu et al. 2009; Vinella, Brochier-Armanet et al. 2009); notably, IscA SufA double mutants lack an observable phenotype under anaerobic growth conditions (Lu, Yang et al. 2008; Vinella, Brochier-Armanet et al. 2009). In IscA ErpA double mutants, growth is strongly impaired (Loiseau, Gerez et al.

2007; Vinella, Brochier-Armanet et al. 2009) and it was subsequently shown that both, IscA and ErpA, are essential for the assembly of active hydrogen-oxidizing hydrogenases (Pinske and Sawers 2012). IscA and ErpA share only 40% amino acid sequence identity, which was previously suggested to be the basis for IscA and ErpA to target different acceptor proteins although evidence for that is missing (Pinske and Sawers 2012). IscA and ErpA were further proposed to act sequentially (Py and Barras 2010); however, overlapping roles for IscA and ErpA were also suggested based on partial compensation by IscA in ErpA mutants (Pinske and Sawers 2012).

1.5.1.1 Fe-S cluster binding versus Fe binding

Different bacterial purified A-type proteins (i.e. *A. vinelandii* ^{Nif}IscA, *E.coli* IscA, cyanobacterial IscA, *E. chrysanthemi* SufA) were shown to bind Fe-S cluster upon *in vitro* reconstitution with detection of both, Fe_2S_2 or Fe_4S_4 clusters, have been described (Krebs, Agar et al. 2001; Ollagnier-de-Choudens, Mattioli et al. 2001; Ollagnier-de Choudens, Nachin et al. 2003; Wollenberg, Berndt et al. 2003; Ollagnier-de-Choudens, Sanakis et al. 2004). Based on one study detecting a Fe_2S_2 intermediate prior to a labile Fe_4S_4 cluster per homo-dimer (Krebs, Agar et al. 2001), it was suggested that cluster conversion potentially take place on the A-type proteins. While all previous reports had required chemical reconstitution of the Fe-S cluster, two groups reported on direct purification of A-type proteins harboring an Fe-S cluster (*E.coli* SufA with a Fe_2S_2 cluster and *Acidithiobacillus ferrooxidans* IscA with a Fe_4S_4 cluster) (Zeng, Geng et al. 2007; Gupta, Sendra et al. 2009).

Although these studies showing (reconstitution of) Fe-S cluster bound to prokaryotic A-type proteins (Ollagnier-de-Choudens, Mattioli et al. 2001; Ollagnier-de Choudens, Nachin et al. 2003; Wollenberg, Berndt et al. 2003; Ollagnier-de-Choudens, Sanakis et al. 2004; Zeng, Geng et al. 2007; Gupta, Sendra et al. 2009), several, mostly experimentally consecutive studies reported and characterized iron binding properties for bacterial A-type proteins. After low-affinity iron binding was described at first (Krebs, Agar et al. 2001), Ding and co-workers have reported *E. coli* IscA and SufA as Fe-binding proteins with a relatively high affinity (K_{ass}, $3x\ 10^{19}\ M^{-1}$) (Ding and Clark 2004; Ding, Clark et al. 2004; Ding, Smith et al. 2005; Ding, Harrison et al. 2005; Ding, Yang et al. 2007; Wang, Huang et al. 2010). IscA was shown to recruit iron *in vitro* under limited free-iron conditions and *Azotobacter vinelandii* ^{Nif}IscA was subsequently also characterized as a high-affinity Fe-binding protein (Mapolelo, Zhang et al. 2012). A recent study reported *in vitro* data of a reconstituted Fe-bound *Acidithiobacillus ferrooxidans* IscA that can be converted into an Fe-S cluster-bound IscA in the presence of L-cysteine and the cysteine desulfurase (Qian, Zheng et al. 2013) and IscA was thus suggested to potentially possess a dual role during Fe-S biogenesis including both Fe-binding and Fe-S cluster binding.

1.5.1.2 A-type protein oligomers

Bacterial A-type proteins have been purified as oligomeric structures, mainly as dimers but also as tetramers (Krebs, Agar et al. 2001; Ollagnier-de Choudens, Nachin et al. 2003; Ollagnier-de-Choudens, Sanakis et al. 2004; Wada, Hasegawa et al. 2005; Gupta, Sendra et al. 2009), suggesting A-type proteins to function in an oligomeric state rather than as a monomer.

Crystal and NMR structures have been reported for the apo- and reconstituted forms of dimeric or tetrameric IscA and SufA of different bacterial species (Bilder, Ding et al. 2004; Cupp-Vickery, Silberg et al. 2004; Wada, Hasegawa et al. 2005; Morimoto, Yamashita et al. 2006). All structures show a novel protein fold, but most of them did not observe the C-terminally located C-G-C motif, most likely due to conformational flexibility. Thus, potential Fe or Fe-S binding could not be resolved, but at least two out of the three conserved cysteines were suggested to be exposed at the surface of each dimer. Subsequently, Morimoto and colleagues showed the structure of an asymmetric tetramer with two bridging Fe_2S_2 clusters for the *Thermosynechoccus elongatus* IscA. Since at physiological salt conditions, holo-IscA was predominantly found as a dimer, models were generated for dimeric structures. Their model suggests that the asymmetric cluster ligation provides an attractive mechanism for cluster incorporation and release due to distinct conformational stabilities (Morimoto, Yamashita et al. 2006).

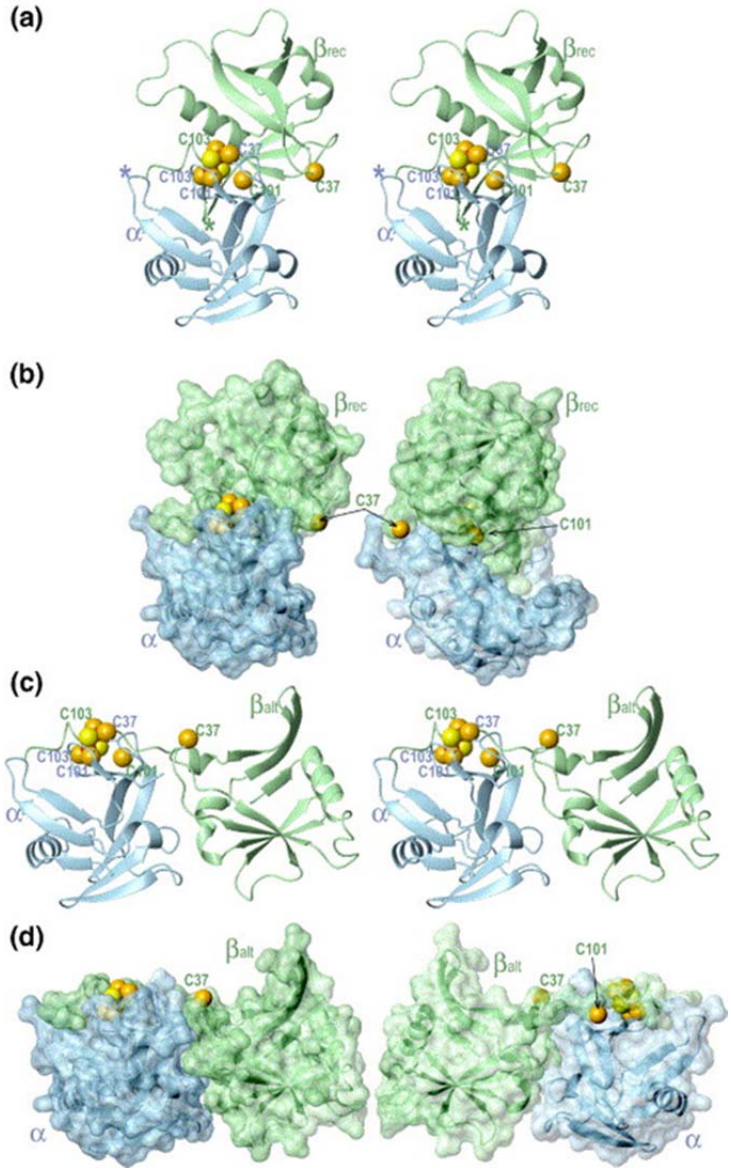

Figure 11: The most plausible model structures of asymmetric holo-IscA dimer in solution.

A non-domain swapped model (a) and (b) and an alternative model (c) and (d). At physiological salt concentrations holo-IscA was found to exist predominantly as a dimer in solution. (a) Stereo view of a non-domain swapped dimeric model is shown as a ribbon diagram. (b) A surface representation of the protein and its 120° rotation is shown. Fe-S clusters are shown as spheres: S, yellow and Fe, red. Sulfur atoms of invariant cysteine residues are shown in orange. In this model, two cysteines are non-ligating (C37 and C101 of *T. elongates* IscA), with C37 being exposed to the solvent and C101 deeply embedded within the protein. (c) Stereo view of an alternative model of the reconstructed dimer. (d) Front and back view of the alternative model, with both non-ligating cysteines being exposed to the solvent. Taken from Morimoto *et al.,* 2006.

1.5.1.3 Transfer of Fe-S cluster or function as an Fe-donor

Fe-binding properties reported above were tested along with the ability to provide Fe for Fe-S assembly on scaffold proteins. *E. coli* IscA and SufA were shown to effectively provide iron in the presence of L-cysteine for *in vitro* cluster assembly on IscU under aerobic conditions (Ding and Clark

2004; Ding, Clark et al. 2004; Ding, Smith et al. 2005; Ding, Harrison et al. 2005; Ding, Yang et al. 2007; Wang, Huang et al. 2010). ^{Nif}IscA from *Azotobacter vinelandii* was albeit characterized as high-affinity Fe-binding protein, described to be an effective but non-specific iron donor for cluster assembly NifU under aerobic conditions; non-specific since iron transfer occurred not direct but via cysteine-mediated release of iron (Mapolelo, Zhang et al. 2012).

Combined with characterization of Fe-S clusters on A-type proteins, the different possibilities of receiving a preformed cluster from a U-type scaffold protein, transferring a cluster to U-type proteins or transferring a cluster to acceptor proteins was tested. Cluster transfer from *E. coli* IscU to IscA was observed, while cluster transfer from IscA to IscU was not detected (Ollagnier-de-Choudens, Sanakis et al. 2004). Different studies further showed transfer of a chemically reconstituted Fe-S cluster from *E. coli* IscA, SufA and cyanobacterial IscA to Fe_2S_2 and Fe_4S_4 acceptor proteins, like for instance ferredoxin and BioB (Ollagnier-de-Choudens, Mattioli et al. 2001; Ollagnier-de Choudens, Nachin et al. 2003; Wollenberg, Berndt et al. 2003; Ollagnier-de-Choudens, Sanakis et al. 2004). In addition, also as-purified holo-SufA was shown to transfer its cluster to both, Fe_2S_2 and Fe_4S_4, acceptor proteins (Gupta, Sendra et al. 2009), which strongly suggested the native A-type proteins to be competent to function as Fe-S transfer proteins. This was further supported by a study assessing cluster transfer between *A. vinelandii* ^{Nif}Grx, a monothiol glutaredoxin homologue (see 1.4.2.3) and ^{Nif}IscA (Mapolelo 2012 Dalton transactions). Cluster transfer was shown from ^{Nif}Grx to ^{Nif}IscA, and could also be observed from ^{Nif}IscA to a heterodimer of ^{Nif}Grx and Fra2, the homologue of the yeast Fra2 and mammalian BOLA protein (see 1.4.2.1). Collectively, these data suggested that A-type proteins are able of receiving and transferring Fe-S clusters.

1.5.1.4 Conclusion on bacterial A-type proteins

Taken together, different lines of evidence have suggested prokaryotic A-type proteins as Fe-S proteins that are able to transfer the cluster to acceptor proteins. To our knowledge only two studies managed to purify holo-IscA directly with its Fe-S cluster (Zeng, Geng et al. 2007; Gupta, Sendra et al. 2009). As the most urgent question remains whether or not A-type proteins can provide iron for nascent cluster assembly *in vivo*. Although purified with bound iron after high-iron, aerobic growth conditions (Wang, Huang et al. 2010), there is currently no *in vivo* evidence supporting a role for A-type proteins as Fe-donors to primary scaffold proteins. Moreover, if bacterial A-type proteins function as Fe-S scaffolds *in vivo*, the question remains whether or not their role is in nascent cluster assembly as alternative scaffolds and thus overlapping with the one of IscU or in the late acting distribution of clusters as a carrier protein.

1.5.2 Eukaryotic A-type proteins

A-type proteins are found in all multicellular (model) organisms, but are less conserved or missing in protists with reduced mitochondria or mitosomes as in *Encephalitozoon cuniculi*, *Cryptosporidium parvum*, *Entamoeba histolytica* and *Trichomonas vaginalis* (Lill and Muhlenhoff 2006; Vinella, Brochier-Armanet et al. 2009).

The requirement for these proteins in yeast and cells for mitochondrial Fe_4S_4 cluster proteins in cultured human cells and *S. cerevisiae* will be described, but conflicting properties were also described for the eukaryotic A-type proteins.

1.5.2.1 A-type proteins in blastocystis (*Trypanosoma brucei*)

Trypanosoma brucei is a eukaryotic kinetoplastid flagellate and the causative agent of the highly pathogenic African sleeping sickness in humans. This early-branching model protist is known for a broad range of unique features and was also used to study Fe-S protein biogenesis. In the organism, physiological processes can be dissected in the procyclic stage with one active mitochondrion and its pathogenic bloodstream stage with a metabolically repressed organelle (Lukes, Hashimi et al. 2005). Lukes and others have previously investigated several key component of the Fe-S biogenesis pathway in *T. brucei* and their function seemed to be conserved with respect to the knowledge on the eukaryotic model systems as *S. cerevisiae* (Smid, Horakova et al. 2006; Long, Jirku et al. 2008; Long, Jirku et al. 2008; Long, Vavrova et al. 2008; Paris, Changmai et al. 2010).

Two A-type proteins are found in the *T. brucei*, *T. cruzi*, *Leishmania major*, *Leishmania braziliensis* and *Leishmania infantum* genomes. They possess highly conserved amino acid sequences including the three cysteine residues predicted to bind iron or Fe-S cluster in prokaryotes (see 1.5). *T. brucei* A-type proteins, TbIsa1 and TbIsa2, are solely mitochondrion-localized. Analyzing clones with inducible RNAi ablation of TbIsa1 and/or TbIsa2 showed reduced growth starting 4 days post induction (dpi), where the double-knockdown virtually stopped dividing without the potential for recovery. Only mitochondrial Fe-S proteins like the mitochondrial aconitase or SDH were affected upon TbIsa-depletion and reactive oxygen species (ROS) levels were reported to be elevated, likely due to the disruption of the respiratory chain. Iron accumulation was not observed. While the effect of TbIsa-knockdown was prominent in the procyclic *T. brucei* stage, both TbIsa-proteins are non-essential in the bloodstream stage. Furthermore, TbIsa1 could partially rescue TbIsa2 knockdown and both human A-type proteins could partially compensate for any of the TbIsa deficiencies. This partial compensation was based on the observed recovery of enzymatic activities whereas cell growth was not rescued, thus suggesting partial redundancy between the two A-type proteins. Interestingly, enzymatic activities and the growth phenotype of the double knockdown TbaIsa1/2 was rescued by

the only A-type homologue present in *Blastocystis hominis* BhIsa2. Collectively, these results suggest a requirement for both A-type proteins only during the procyclic stage, thus likely to be restricted to mitochondrial Fe-S clusters.

1.5.2.2 Yeast A-type proteins

S. cerevisiae harbors two A-type proteins named Isa1 and Isa2. Isa1 and/or Isa2 deletion strains are viable and exhibit delayed growth on non-fermentable carbon sources, accumulating iron in mitochondria with a marked decrease in the activity of mitochondrial and cytosolic Fe-S enzymes (Garland, Hoff et al. 1999; Jensen and Culotta 2000; Kaut, Lange et al. 2000; Pelzer, Muhlenhoff et al. 2000). After description of this rather imprecise role of Isa1 and Isa2 in iron metabolism (Jensen and Culotta 2000) and Fe-S biogenesis (Kaut, Lange et al. 2000; Pelzer, Muhlenhoff et al. 2000), Isa1 and Isa2 were described to be required for the catalytic activity of biotin synthesis (Muhlenhoff, Gerl et al. 2007). More recently, *S. cerevisiae* Isa1 and Isa2 were shown to interact and to be required for the maturation of mitochondrial Fe_4S_4 cluster proteins (Muhlenhoff, Richter et al. 2011). Isa1 and Isa2 were shown to co-immunoprecipitate the tetrahydrofolate-depending protein Iba57 suggesting that a complex of these is necessary for function (Gelling, Dawes et al. 2008) (see 1.5.3). Although reported to bind iron *in vivo*, Isa-bound iron was not needed for *de novo* Fe-S assembly on the yeast U-type proteins Isu1/Isu2 (Muhlenhoff, Richter et al. 2011). This was shown by ^{55}Fe-immunoprecipitation experiments under Isa1 and Isa2 depletion, which resulted in a minor increase of Fe associated with Isu1, arguing that Fe-bound Isa1-Isa2 complex could not be the only Fe donor for initial cluster assembly on Isu1 (Muhlenhoff, Richter et al. 2011). Taken together, yeast Isa-proteins were accordingly localized in the late-acting mitochondrial Fe-S biogenesis. Of note, Isa1, but not Isa2 depletion, was functionally replaced by the bacterial IscA, SufA or ErpA, indicating non-redundant roles for yeast A-type proteins.

The only biophysical characterization of an A-type protein in yeast is available for *Schizosaccharomyces pombe* Isa1 (Wu, Mansy et al. 2002). Isa1 was purified and reconstituted as multimeric Fe_2S_2 cluster containing protein. Degradation of the reconstituted Isa1 was not accelerated under aerobic conditions, suggesting that the holo-Isa1 is not oxygen sensitive. Crosslinking experiments have further shown complex formation of Isa1 with a redox-active ferredoxin. In *Schizarromyces pombe* Isa1 and Isa2 were further shown to bind Grx5, the yeast mitochondria monothiol redoxin GLRX5 homologue, by bimolecular fluorescence complementation as previously proposed by a phylogenetic profiling study (Vilella, Alves et al. 2004; Kim, Chung et al. 2010). Interestingly, Grx5 deletion growth phenotype was partly complemented by overproducing Isa1 or Isa2 by restoring tested Fe-S enzyme activity.

1.5.2.3 A-type proteins of higher eukaryotes

The first description of a mammalian A-type protein was for human ISCA1 (Cozar-Castellano, del Valle Machargo et al. 2004) shown to be ubiquitously expressed, localized to mitochondria and displaying high sequence homology to yeast Isa1 and Isa2. It was accordingly suggested to be involved in Fe-S biogenesis. Functional homology of human ISCA1 to yeast Isa1 was proposed based on complementation of the growth phenotype in yeast Isa1 null mutant.

In vivo evidence for an important function of mammalian A-type proteins in physiology came from a screen to discover genes essential for heme biogenesis, heme being a prosthetic group involved in important processes like oxygen transport (Nilsson, Schultz et al. 2009). The large-scale computational analysis uncovered strong co-expression between ISCA1 and ISCA2 proteins and the synthesis of heme. ISCA1 and IBA57 were among the selected candidates to be tested for their expression pattern and tested to see if their specific knockdown interfered with heme biogenesis. ISCA2, although detected in the screen, was not investigated further. While iba57 mRNA showed clear localization to the intermediate cell mass in the developing zebra-fish embryo, isca1 mRNA did not show clear tissue-restricted expression and was instead highly expressed throughout the embryo. Using a morpholino approach, isca1 and iba57 knockdown resulted both in profound anemia. Despite this implication in heme biosynthesis, detailed molecular mechanisms for the role of A-type proteins and IBA57 in this process remain to be uncovered.

One paper reported that UV-visible absorption and EPR (electron paramagnetic resonance) of human ISCA1 provided evidence of an iron-binding activity of the recombinant protein (Lu, Bitoun et al. 2010). Using the same assays as applied for *E. coli* IscA (Ding and Clark 2004; Ding, Clark et al. 2004; Ding, Smith et al. 2005; Ding, Harrison et al. 2005; Wang, Huang et al. 2010), effective Fe transfer from human ISCA1 for Fe-S assembly on *E. coli* IscU was shown *in vitro*. By restoring cell growth, ISCA1 was further shown to partially complement for IscA/SufA double-deletion in *E. coli* under aerobic conditions.

A dual role for ISCA1 in mitochondrial and extra-mitochondrial Fe-S biogenesis was subsequently proposed based on the finding that ISCA1 was also localized in the cytoplasm and interaction with the cytoplasmic Fe-S biogenesis protein IOP1 (Song, Tu et al. 2009). Upon ISCA1 knockdown cell viability was reduced, and mitochondrial and cytosolic aconitase (and thus IRP1) as well as SDH showed decreased activity. On the contrary, EGFP-ISCA1 transgene expression in HEK 293 cells also leads to decreased cytosolic aconitase activity, suggesting a dominant-negative effect of cytosolic ISCA1.

Characterization of HeLa cells depleted for A-type proteins (ISCA1 and ISCA2) was provided by Sheftel and co-workers (Sheftel, Wilbrecht et al. 2012). First, human overexpressed proteins were localized to mitochondria and subsequently shown by knockdown to be required for maturation of all mitochondrial Fe_4S_4 proteins tested. Affected proteins include respiratory chain complex I and II and the Fe_4S_4 –dependent LA bound to PDH and KGDH. Notably, other proteins of the respiratory chain namely the Fe_2S_2 RIESKE protein and the non-Fe-S COX2 protein were also affected, proposed as a secondary consequence of the specific knockdown. Upon sequential RNAi treatment mitochondria showed considerable physiological and morphological alterations including acidification of culture media and massively enlarged mitochondria with swollen cristae structure. The role for ISCA-proteins in the cytosol proposed by Song *et al.* was questioned. Although cytosolic aconitase activity was found to be decreased along with an increase in IRP1-IRE binding upon RNAi treatment, only mitochondria localized ISCA-proteins compensated for it, while truncated ISCA1 or ISCA2 were probably efficiently degraded. Other tested extra-mitochondrial Fe-S proteins were not affected, therefore suggesting an indirect effect on cytosolic aconitase. Heme biogenesis seemed generally not affected.

Recently, transfer of a Fe_2S_2 cluster from recombinant human GLRX5 to both human ISCA-proteins was shown following UV-visible spectra *in vitro* (Banci, Brancaccio et al. 2014). Different combinations of apo- and holo-proteins suggested a non-specific cluster transfer with a unique direction from GLRX5 to ISCA-proteins. The data suggest a direct interaction between these proteins with the cluster itself promoting the transient protein-protein interaction.

1.5.2.4 Conclusion on eukaryotic A-type proteins

In summary, different aspects of mammalian A-type proteins have been investigated so far. As for bacterial A-type proteins, diverging findings were reported for eukaryotic A-type proteins. Accordingly, a distinct model on their function including all data is difficult to draw. Yet, a rigorous characterization of the mammalian A-type proteins using complementary *in vitro* and *in vivo* approaches is missing. Moreover, the question of why two seemingly functionally redundant both essential proteins with high sequence similarity exist throughout phyla has yet to be uncovered.

A phylogenetic study has defined three subfamilies for the A-type proteins based on evolutionary considerations mainly for sequence conservation (ATC for A-type Carrier: ATC-I, ATC-II and ATC-III). IscA and SufA were placed in the same subfamily as eukaryotic Isa1/ISCA1 (ATC-II), while ErpA was placed together with Isa2/ISCA2 (Vinella, Brochier-Armanet et al. 2009). Of note, experimental evidence for this classification in terms of functions is still required.

1.5.3 The A-type protein interacting protein IBA57

The first insight in favor of an implication of IBA57 in Fe-S biogenesis came from studies in the yeast *Saccharomyces cerevisiae* Iba57. By screening for mutants defective for Fe-S biogenesis, Iba57 was found to be required for the maturation of mitochondrial aconitase and the radical SAM Fe-S proteins biotin and LA synthase (Gelling, Dawes et al. 2008). Iba57 was localized to the mitochondrial matrix and co-immunoprecipitated both Isa1 and Isa2 and *vice versa*. Complementation of the growth defect of Iba57 deletion by the human IBA57 (C1orf69) homologue suggested conserved function of Iba57. This was further supported by IBA57 knockdown in HeLa cells exhibiting a phenotype similar to ISCA1 and ISCA2 knockdown cells (Sheftel, Wilbrecht et al. 2012). Although IBA57 protein knockdown was not as effective as the one for ISCA1 or ISCA2, the same subset of mitochondrial Fe-S proteins was affected, with the exception of mitochondrial aconitase. Of note, consecutive RNAi treatment for Iba57 mRNA also resulted in severely affected proteins of the respiratory chain, the mitochondria ultrastructure and acidification of the culture medium. Lately, two siblings with a mutation in *IBA57* gene were described with a fatal mitochondrial phenotype (Ajit Bolar, Vanlander et al. 2013; Beilschmidt and Puccio 2014). The mutation was found to affect IBA57 stability. The patients showed severe myopathy and encephalopathy. Isolated skeletal muscle proteins exhibited decreased levels of complex I, II and IV along with decreased LA-depend enzyme levels. Contrary to the siRNA reported previously (Sheftel, Wilbrecht et al. 2012), IBA57 knockdown published with the patient data resulted in a decrease of complex II, complex IV and the LA-dependent complexes (Ajit Bolar, Vanlander et al. 2013).

IBA57 homologues occur in all domains of life and are also functionally conserved since bacterial IBA57-homologue YgfZ deletion growth phenotype can be restored by other prokaryotic IBA57 homologues, termed COG0354 proteins, from phylogenetically distant *E. coli, Bartonella henselae*, mice, plants (Arabidopsis from plastids and mitochondrial) and Leishmania (Waller, Alvarez et al. 2010). Phylogenetic studies showed that genes encoding IBA57 homologues are only found in prokaryotic organisms that also encode A-type proteins (IscA and/or SufA) or are absent altogether. The biochemical function of IBA57 or its homologues is yet unknown and the genomic context does not associate with any particular operon or other genomic organisation. Three dimensional structures of *E. coli* YgfZ predicted a folate-binding site (Teplyakov, Obmolova et al. 2004). Folate binding was confirmed by NMR analysis of purified *E.coli* IBA57 homologue YgfZ (Waller, Alvarez et al. 2010) and its relevance was further shown by folate synthesis mutations that mimicked the effect of ablating YgfZ namely on the Fe-S enzymes succinate dehydrogenase, fumarase and dimethylsulfoxide reductase as well as MiaB, a radiacal SAM enzyme. Folate binding on YgfZ was eventually suggested to function as anelectron donor, since tetrahydrofolate was previously shown

to act as electron donor in bacterial phenylalanine hydroxylase (Fujisawa and Nakata 1987) and in thymidylate synthesis (Matthews 1982).

1.6 Mammalian Fe-S cluster biogenesis and its implication in disease

Lena K. Beilschmidt, Hélène L. Puccio

Biochimie 100 (2014) 48–60

Contents lists available at ScienceDirect

Biochimie

journal homepage: www.elsevier.com/locate/biochi

Review

Mammalian Fe–S cluster biogenesis and its implication in disease

Lena K. Beilschmidt [a,b,c,d,e], Hélène M. Puccio [a,b,c,d,e,*]

[a] Translational Medicine and Neurogenetics, IGBMC (Institut de Génétique et de Biologie Moléculaire et Cellulaire), Illkirch, France
[b] Inserm, U596, Illkirch, France
[c] CNRS, UMR7104, Illkirch, France
[d] Université de Strasbourg, Strasbourg, France
[e] Collège de France, Chaire de génétique humaine, Illkirch, France

ARTICLE INFO

Article history:
Received 30 July 2013
Accepted 7 January 2014
Available online 17 January 2014

Keywords:
Mitochondria
Iron–sulfur cluster
Genetic disease
Mutation

ABSTRACT

Iron–sulfur (Fe–S) clusters are inorganic cofactors that are ubiquitous and essential. Due to their chemical versatility, Fe–S clusters are implicated in a wide range of protein functions including mitochondrial respiration and DNA repair. Composed of iron and sulfur, they are sensible to oxygen and their biogenesis requires a highly conserved protein machinery that facilitates assembly of the cluster as well as its insertion into apoproteins. Mitochondria are the central cellular compartment for Fe–S cluster biogenesis in eukaryotic cells and the importance of proper function of this biogenesis for life is highlighted by a constantly increasing number of human genetic diseases that are associated with dysfunction of this Fe–S cluster biogenesis pathway. Although these disorders are rare and appear dissimilar, common aspects are found among them. This review will give an overview on what is known on mammalian Fe–S cluster biogenesis today, by putting it into the context of what is known from studies from lower model organisms, and focuses on the associated diseases, by drawing attention to the respective mutations. Finally, it outlines the importance of adequate cellular and murine models to uncover not only each protein function, but to resolve their role and requirement throughout the mammalian organism.

1. Iron–sulfur clusters: versatile co-factors

Iron–sulfur (Fe–S) clusters are widespread inorganic cofactors composed of iron and sulfur. Harboring versatile chemical properties, Fe–S clusters are involved in a variety of different protein functions in a plethora of pathways, ranging from DNA repair to metabolism [1]. Fe–S clusters are essential protein cofactors that can accept and donate electrons, stabilize specific protein conformations, bind and activate substrates or regulate the enzymatic activity. Evolutionary ancient and highly conserved, Fe–S clusters are present in virtually all organisms and most probably had a high impact on the development of early life forms due to their functional and structural versatility [2,3].

Ferrous iron and sulfide can spontaneously assemble simple Fe–S clusters under reducing conditions, however, free iron and sulfur are toxic for the cell, and most of the clusters are labile to oxygen [4]. Thus, a tightly regulated, complex and highly conserved machinery for the biogenesis of Fe–S clusters evolved [5]. Fe–S clusters themselves were discovered in the 1960s by Beinert and colleagues by their characteristic paramagnetic resonance signal [6], followed by the discovery of the bacterial Fe–S cluster biosynthesis machinery in the mid-1980s (Fig. 1) [7,8] and the subsequent discovery of the homologues in yeast [9,10]. It has to be pointed out that mammalian Fe–S cluster biogenesis was only recently started to be uncovered and is still rather poorly characterized. The general principle of the biosynthesis and the implicated proteins are highly conserved; however, the process increased in complexity with increasing cellular differentiation and multicellularity.

A steadily increasing number of rare and seemingly distinct diseases (Table 1, Fig. 3) are associated with dysfunction in different steps of Fe–S cluster biogenesis, underlining the importance of Fe–S clusters for mammalian physiology. Together, they affect virtually all organs, and often have linked underlying mechanisms. However, the respective phenotypes can be quite different and tissue specificity appears. Insight into the different pathophysiologies provided important knowledge on mammalian Fe–S cluster biogenesis, but there is still a multitude of open questions that need to be addressed in the following years. This review will summarize the current knowledge on mammalian Fe–S biogenesis and focus on the genetic causes of the associated diseases.

* Corresponding author. Translational Medicine and Neurogenetics, IGBMC (Institut de Génétique et de Biologie Moléculaire et Cellulaire), Illkirch, France. Tel.: +33 388653264; fax: +33 388653246.
E-mail address: hpuccio@igbmc.fr (H.M. Puccio).

0300-9084/$ – see front matter © 2014 Elsevier Masson SAS. All rights reserved.
http://dx.doi.org/10.1016/j.biochi.2014.01.009

BOX: Iron–sulfur cluster – simple, almost magic

Fe–S clusters are common protein cofactors composed of iron and inorganic sulfur, most commonly found in the rhombic [Fe_2S_2] and the cubic [Fe_4S_4] cluster conformation [11]. The clusters are generally non-covalently coordinated by cysteine or histidine residues of proteins (Fig. 2). As most of the Fe–S clusters are labile to oxygen, many of the known Fe–S clusters are sheltered inside the respective protein conformation. It often requires strictly reducing conditions to manipulate Fe–S proteins, to purify or crystallize them in presence of their prosthetic groups. Fe–S proteins lack a distinct amino acid motif that would make it fast forward to predict or identify new ones. However, there is increasing evidence that specific sequential arrangements or signatures of cluster-coordinating amino acid residues, most often composed of cysteines and histidines, exist that can predict the likely presence of a clusters within a protein (unpublished results Colin and Puccio and [12]). However, it is probable that the protein fold would be a better predictor.

Due to the chemical versatility of Fe–S clusters, Fe–S proteins are found in a variety of different reactions. Most prominent is the redox potential of Fe–S clusters that can lead to a wide electrochemical range of the Fe–S cluster protein (+300 to −500 mV). It is nicely illustrated in the mitochondrial respiratory chain complex I, where seven Fe–S clusters with stepwise increasing reduction potential form a path for the electrons to be transported [13,14]. Moreover, Fe–S clusters can be involved in binding of enzymatic substrates as aconitase in the citric acid cycle for the interconversion of citrate and isocitrate [15,16]. Other important functions of Fe–S clusters for physiology are found in the regulatory function of the iron regulatory protein 1 (IRP1) (see below and [17]) and as redox catalysts in the radical S-adenosyl-L-methionine (SAM) enzymes. The mitochondrial SAM enzyme lipoate synthase catalyzes the last step of lipoate synthesis. Based on evidence from bacterial studies, it is likely that its Fe–S cluster serves as a sulfur donor [18,19]. In the DNA helicase XPD, the Fe–S cluster stabilizes the distinct protein conformation required for its proper function. The mitochondrial ferrochelatase is a Fe–S enzyme that inserts iron into protoporphyrin in the last step of heme biosynthesis. Upon loss of the cluster, ferrochelatase function gets strongly inhibited, most likely through a structural role of the cluster [20–22].

Defects in Fe–S proteins are associated with numerous diseases. Mutation in the DNA repair enzyme XPD causes xeroderma pigmentosum, a disease in which patients develop severe skin malignancies after exposure to light [23]. In Fanconi anemia, mutation in the DNA helicase FANCJ leads to cancer formation, most commonly acute myelogenous leukemia [23]. Both are only two examples to underline the importance of Fe–S clusters for mammalian physiology and life. However, the role of Fe–S cluster within a protein, and whether the Fe–S cluster containing part of the protein is implicated in disease is not always clear. It is worth to note that many newly discovered Fe–S cluster containing proteins have a long history of laboratory investigation under aerobic, thus probably cluster damaging, conditions. As an example, DNA polymerases were only recently discovered to contain Fe–S clusters. Their Fe–S clusters were shown to be required for proper assembly of accessory subunits [24], but the fact that they have been studied for many years *in vitro* without a Fe–S cluster, evokes questions about the role of the Fe–S cluster for the DNA polymerases. Could the clusters function as some kind of stress sensors or activity regulators? In case of oxidative stress, Fe–S cluster damage and subsequent dissociation of the DNA polymerase subunits would lead to reduction of replication rates. Likewise, could DNA repair mediated by the DNA repair enzymes XPD and FANCJ get tuned or shut down, when the stress impact on the cells gets too high?

2. Iron sulfur cluster biogenesis: conserved machinery under regulation

The general aspects of the Fe–S clusters biogenesis are common to all kingdoms of life, and many proteins involved are highly conserved. In bacteria, the *Isc* operon (Fig. 2) encodes for proteins required for the general biogenesis of Fe–S clusters [8]. Homologues of these proteins are found in the eukaryotic mitochondria and are highly conserved. Thus, the ancient ability to form Fe–S clusters and their use in different cellular contexts was most certainly an advantage for eukaryotic cells leading to the maintenance of the endosymbiont as an organelle [13]. Other bacterial machineries for Fe–S cluster biogenesis exist, such as the SUF system, whose conserved homologues can be found in plastids (for a detailed review, please refer to Py and Barras 2010 [25]). This review will focus on what is known for the mammalian Fe–S cluster biogenesis, taking into account that many aspects have only been well understood for the bacterial or yeast system (for terminology of the homologues please refer to Table 2).

Throughout organisms, nascent Fe–S cluster biogenesis consists of two basic steps, the cluster assembly and its subsequent transfer into apoproteins, while the cluster is harbored and protected by chaperones, scaffold or carrier proteins. In eukaryotes, Fe–S proteins are found in all different cellular compartments. While the assembly step takes place in the mitochondria, the clusters are subsequently either inserted into mitochondrial apoproteins or a so far uncharacterized compound is exported to the cytosol to the cytosolic Fe–S cluster assembly machinery (CIA), where the insertion into cytosolic and nuclear apoproteins takes place (Fig. 3) [1]. Although the exact nature of the exported compound is yet unknown, the core step of Fe–S biogenesis in the mitochondria is essential to all extra-mitochondrial Fe–S proteins [26,27].

The assembly of iron and sulfur constitutes the initial step of nascent Fe–S cluster biogenesis. It is accomplished by a multimeric protein complex with the cluster transiently bound on a scaffold protein termed ISCU, providing the backbone structure for cluster assembly with cysteine residues required for cluster coordination. Sulfur is provided by the cysteine desulfurase NFS1 that subtracts elemental sulfur from L-cysteine through a persulfide intermediate by a pyridoxal-phosphate dependent mechanism [28]. In eukaryotes, NFS1 binds the ISD11 protein that is probably required for NFS1 stability [29–31]. The source of iron for nascent cluster assembly has not yet been clearly identified. Frataxin (FXN) was long suggested to serve as the iron donor due to the presence of an acidic ridge that can bind iron [32,33]. Even though, the exact role of FXN has long been unresolved, it is evident today that, throughout phyla, it functions as a regulatory protein controlling Fe–S cluster formation. Mammalian FXN was first shown to be an allosteric regulator of the cysteine desulfurase activity of NFS1 [34]. Recently, FXN function got refined and shown to function as a regulatory partner in the complex of NFS1/ISD11/ISCU controlling not only sulfur production, but also iron entry during [Fe_4S_4] assembly, thereby accelerating the rate of Fe–S cluster biogenesis [35]. Thus, *in vitro* [Fe_4S_4] can be formed on ISCU, nevertheless, the physiological presence of [Fe_2S_2] and/or [Fe_4S_4] formation on ISCU and the relevance for subsequent steps is not determined up to date. Interestingly, contrary to the accelerating effect of mammalian FXN, the bacterial FXN homologue CyaY seems to inhibit nascent Fe–S

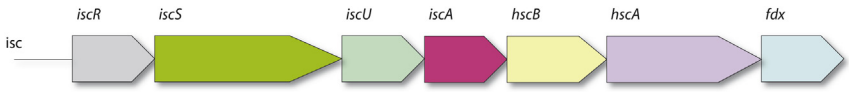

Fig. 1. Isc operon from *E. coli*. The *isc* operon is the general provider of Fe–S clusters in bacteria such as *E. coli*. Homologues of the isc genes have been identified in mammals and encode for mitochondrial proteins (please refer to Table 2).

cluster formation. This negative regulatory effect can be attributed to the higher basal activity of the bacterial cysteine desulfurase IscS compared to the mammalian NFS1 [36,37], leaving FXN as a highly conserved regulator of Fe–S cluster biogenesis.

Formation of Fe–S clusters requires electrons for reduction of sulfur to sulfide (S^{2-}). Increasing evidences suggest FDX2 (ferredoxin or FDX1L) as the electron source, functioning in an electron transfer chain with NAD(P)H and ferredoxin reductase (FDXR) [38]. The bacterial FDX2 homologue Fdx is found in the *Isc* operon, already suggesting an important function for nascent cluster formation. After Fdx was originally shown to enable reductive coupling for the formation of a [Fe_4S_4] on bacterial IscU [39], two recent papers have demonstrated for the first time a direct interaction between bacterial Fdx and the cysteine desulfurase as well as electron transfer from reduced Fdx to the cysteine desulfurase in the presence of L-cysteine [40,41]. Interestingly, the interaction was found to be competing with IscU and CyaY binding sites on the cysteine desulfurase, suggesting that electron transfer takes place before or independently of the assembly of the core complex composed of the cysteine desulfurase, scaffold protein and CyaY. For mammalian FDX2, the evidence is less strong, but it was shown to be required for Fe–S clusters in human cells [42]. However, mammalian genomes contain two homologous ferredoxins, FDX1 and FDX2, and controversies exist whether both proteins are important for Fe–S cluster biogenesis, or whether only FDX2 plays an important role [38,42]. This controversy was recently taken further by the discovery of a patient with a seemingly fatal mutation in the *FDX1L* gene causing severely decreased protein levels of FDX2, but a relatively mild phenotype [43]. Taken together, this raises the question, whether the mammalian FDX2 solely accounts for the electron provision as well as how this process takes place, that is whether the sequential action of FDX2 and FXN and ISCU on the cysteine desulfurase, as recently discovered for the bacterial proteins, is conserved up to mammals.

After formation of the nascent Fe–S cluster by the core complex of NFU1/ISD11/ISCU/FXN, the cluster needs to be transferred to apoproteins. Here, very little is known for the mammalian counterparts. Evidences, based on bacteria and yeast data, suggest that the co-chaperone HSC20 (mammalian homolog of HscB/Jac1) binds ISCU [44–46]. In bacteria and yeast, HscB/Jac1 functions together with its chaperone partner HscA/Ssq1, but the mammalian homologue (probably GRP75/HSP70) remains to be identified. This equally accounts for the yeast nucleotide exchange factor Mge1 that seems to be required for ATP-release in the ATP-hydrolysis-dependent and the highly specific interaction between the LPPVK motif of Isu1 and the HSP70 homologue Ssq1 [47,48]. This interaction induces conformational changes in Isu1, which enables dislocation of the Isu1-bound Fe–S cluster either to selected target proteins or to specific Fe–S cluster carrier proteins. It still remains unclear how these target proteins are identified, but probably involves a dimer of GLRX5, which is bridged by the cluster. A recent study narrows down the role of GLRX5 in Fe–S cluster biogenesis, by showing direct binding between the yeast HSP70 homologue Ssq1 with Grx5 at an Ssq1 binding site that is close to the one of Isu1, thereby allowing a rapid transfer of an Isu1 bound cluster to Grx5 [49]. Thus, mammalian GLRX5 probably acts early in targeting preformed Fe–S cluster from ISCU via a chaperone mediated mechanisms to recipient proteins. This was already proposed as deficiency in GLRX5 affects all cellular Fe–S proteins, placing it early in the Fe–S cluster biogenesis pathway [50,51].

A number of other proteins are known to be further involved in Fe–S biogenesis. Their involvement into genetic diseases (NUBPL, NFU1, BOLA3 and IBA57), their high conservation as well as studies in cell models and lower model organisms (ISCA1 and ISCA2) led to a common scheme that specific carrier proteins exist to transfer preformed Fe–S cluster to specific subsets of recipient proteins [52–56]. However, direct interactions between subsequent Fe–S cluster carrier proteins with GLRX5 or among each other to show sequential action remain to be shown.

Recent knockdown studies in human HeLa cells confirmed an important role of the two highly conserved proteins, ISCA1 and ISCA2, for only a subset of mitochondrial Fe–S clusters. Upon knockdown of the respective protein, respiratory chain complex I and II, aconitase and lipoic acid-bound pyruvate dehydrogenase (PDH) and α-ketogluterate dehydrogenase complex (KGDH) were affected. All either contain a [Fe_4S_4] cluster or in case of lipoic acid-bound proteins are dependent on the [Fe_4S_4] enzyme lipoic acid synthase (LIAS) that facilitates the last step of lipoic acid biosynthesis [55]. Although a thorough biochemical characterization of the mammalian proteins is yet missing, ISCA1 and ISCA2 are highly similar in sequence and both possess conserved cysteine residues for cluster coordination [57,58], already suggesting a function as Fe–S cluster alternative scaffold or carrier proteins. However, human ISCA1 and bacterial IscA were previously described to have strong iron binding properties and were also suggested to function as the iron donor for nascent Fe–S cluster formation [59,60]. However, phylogenetic studies provided evidence that A-type proteins function as carriers involved in Fe–S cluster transfer [61], so it remains controversial whether or not the iron binding properties observed on recombinant proteins *in vitro* solely account for coordination of Fe–S clusters as suggested for bacterial IscA [62–64]. Moreover, it is unknown whether ISCA1 and ISCA2 function in a redundant manner, as it is suggested from knockdown studies [55]. Complementation experiments of A-type protein *Escherichia coli* mutants using yeast Isa1 and Isa2 suggested partial redundancy that depends on the environmental or physiological conditions [61]. The conserved role of the A-type proteins in mitochondrial [Fe_4S_4] biogenesis is further supported by previously published yeast strains deficient for the homologues Isa1, Isa2 or Iba57 affecting mitochondrial [Fe_4S_4] proteins [65,66]. A similar phenotype is observed upon knockdown of IBA57 (or C1orf69) in HeLa cells [55], a protein of yet unknown biochemical function. The yeast homologue Iba57 was shown to interact with Isa1 and Isa2. It seems not to harbor a Fe–S cluster itself, but could be required to facilitate the cluster transfer through Isa1 and Isa2 [65]. The recent discovery of two patients with mutations in IBA57, that died perinatally of multiorgan mitochondrial disease caused by malfunction of mitochondrial [Fe_4S_4] proteins [56], support its suggested role in mitochondrial [Fe_4S_4] biogenesis.

The finding that deficiency in the mitochondrial P-loop NTPase NUBPL or IND1 in human HeLa cells affects specifically the respiratory chain complex I [52], got strongly supported by the subsequent discovery that mutations in NUBPL cause severe mitochondrial encephalomyopathy in infants with strongly

Table 1
Diseases caused by defects in Fe–S cluster biogenesis.

Gene Protein	Disease	Mutation	No of patients or incidence	Residual amount of protein Functional impairment of proteins	Tissue specificity Underlying cause	Age of onset	Death and cause of death	Gene function or mechanism proposed Subset of cellular Fe–S clusters	References
FXN FXN	Friedreich's Ataxia	Homozygous GAA expansion in first intro or compound heterozygous with point mutation	1/50 000	Yes Point mutations can functionally impair protein function	Yes, in DRG, Cerebellum, spinal cord, heart, β-cells Cause unknown	<25	60% heart failure	Regulatory function in initial Fe–S cluster assembly All cellular Fe–S cluster	Campunzano 1996, Martelli 2012, Koeppen 2011
ISCU ISCU	Myopathy	Homozygous for intronic mutation g.7044G > C or compound heterozygous with a missense mutation c.149G > A	Approx. 25	Yes, but decreased expression due to altered C-terminus of the protein specifically in muscle Yes, but functionally impaired for c.149G > A	Skeletal muscle And also heart in compound heterozygous state with missense mutation	Childhood	x	Main scaffold protein for assembly of Fe–S cluster All cellular ISC	Mochel et al., 2008, Olsson et al., 2008, Kollberg et al., 2009
FDX1L FDX2/FDX1L	Myopathy	Homozygous c. 1A > T (p.0?)	1	?	Not reported, but only muscle phenotype	Adolescence	x	Strongly suggested as electron donor for Fe–S cluster formation All cellular Fe–S clusters	Spiegel et al., 2013
ISD11/*LYRM4* ISD11	Deficiency of multiple respiratory chain complexes	Homozygous c.203G > T p.R68L	2	Not detected	x	Perinatally	1 died at 2 month of age	Stabilization of NFS1, All cellular Fe–S clusters	Lim et al., 2013
GLRX5 GLRX5	Sideroblastic –like microcytic anemia	Homozygous c.294A > G Affects splicing	1	Yes, but strongly decreased expression	Blood (bone marrow), spleen and liver	Middle age	x	Precise function unknown, Fe–S protein and suggested to functions in the targeting of preformed clusters Aall cellular Fe–S clusters	Camaschella et al., 2007 Ye et al., 2010
GFER ALR/GFER	Mitochondrial myopathy with cataract and combined respiratory chain deficiency	c.G581A p.R194H	3	Not shown for patient samples	x	Childhood	x	Precise molecular function for Fe–S cluster biogenesis unknown, suggested export of a mitochondria-derived compound Potentially extra-mitochondrial Fe–S cluster	Di Fonzo 2009, Lange 2001, Hell 2007
ABCB7 ABCB7	X-linked sideroblastic anemia and ataxia	Hemizygous c.T1200G p. Ile400Met c.G1299C p.Val411Leu c.1305G > A p.Glu433Lys c.627A > T p.Glu209Asp	At least 14	Yes, but functionally impaired	Yes, developing blood system and cerebellum	Childhood	x	Transporter in the inner mitochondrial membrane for export of an unknown compound Extra-mitochondrial Fe–S cluster	Bekri 2000, Allikmets 1999, Maguire 2001, D'Hooghe 2012; Pondarré 2008
NUBPL NUBPL/IND1	Mitochondrial encephalomyopathy	mostly compound heterozygous with c.166G > A p.Gly56Arg c.815-27T > C (intronic) and missense, frameshift, del/dup or	8	Severely decreased levels	Neurons and skeletal muscle primarily affected	Infancy	1 died at 9 years due to respiratory complications	Fe–S cluster protein Involved in Fe–S cluster transfer to respirator chain complex I	Kevelan et al., 2013; Calvo et al., 2010 Tenisch 2012

(*continued on next page*)

Table 1 (*continued*)

Gene Protein	Disease	Mutation	No of patients or incidence	Residual amount of protein Functional impairment of proteins	Tissue specificity Underlying cause	Age of onset	Death and cause of death	Gene function or mechanism proposed Subset of cellular Fe–S clusters	References
		exon skipping one patient: c.205_206delGT p.Val69Tyrfs[a]80 c.815-217T > C p.Asp273Glnfs[a]32							
NFU1 NFU1	NFU1-type multiple mitochondrial dysfunction syndrome	Homozygous c.545+5G > A p.Arg182Gln Homozygous c.622G > T p.Gly208Cys or compound heterozygous with both	15	Residual amounts only in c.545+5G > A p.Arg182Gln normal levels for c.622G > T p.Gly208Cys but exon 6 is spliced out	x	Perinatally	Perinatally, between 1 and 15 month of age	Fe–S cluster protein Mitochondria [4Fe–4S], (LIAS and potentially others)	Cameron 2011, Navarro Sastre 2011, Seyda 2001
BOLA3 BOLA3	BOLA3-type multiple mitochondrial dysfunction syndrome	Homozygous c.123dupA p.Glu42Argfe[a]13 Frameshift with predicted premature stop Homozygous c.200T > A p.Ile67Asn	3	x	Not observed, but mainly CNS and heart	Perinatally	Perinatally, max 11 month of age	Molecular function unknown Mitochondrial Fe–S cluster, probably [4Fe–4S]	Cameron et al. 2011 Haack 2012
IBA57 IBA57	Severe myopathy and encephalopathy	Homozygous c.914A > C p.Gln314Pro	2	No	x	Perinatally	Perinatally from systemic mitochondrial defect	Molecular function unknown Mitochondrial [4Fe–4S]	Bolar et al., 2013 Hum Mol. Genetics

[a] Unknown or not reported.

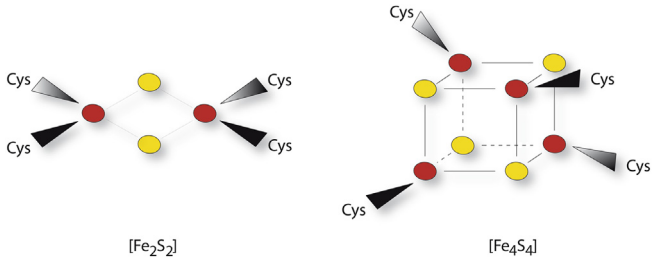

Fig. 2. Fe–S cluster. Structure of canonical $[Fe_2S_2]$ (left) and $[Fe_4S_4]$ (right) as they are most commonly found in mammalian proteins. Fe–S clusters are generally coordinated by cysteine (or histidine) residues of the proteins. Iron atoms are shown in red and sulfur atoms in yellow.

reduced activity of respiratory chain complex I [67–70]. The protein binds an Fe–S cluster via conserved cysteine residues in a labile fashion, suggesting a possible role in the delivery of Fe–S clusters towards complex I [52], the UV visible spectra being indicative of a $[Fe_4S_4]$. However, IND1 was previously suggested to perform a scaffold role in general Fe–S cluster assembly, because the protein shows sequence similarities to two Fe–S scaffold proteins in the CIA machinery, CFD1/NUBP2 and NPB35/NUBP1. This was revised by the finding that the yeast homologue Ind1, depends on Nfs1 and Isu1 [71], thus placing it in a subsequent and not a parallel step to nascent cluster assembly. Taken together, NUBPL rather acts in the specific targeting of a preformed cluster to complex I.

The NFU1 protein was long thought to be involved in Fe–S cluster biogenesis due to its sequence similarity to the C-terminus of the bacterial multi-domain protein NifU functioning as scaffold during nitrogenase maturation [72]. In addition, biochemical and spectroscopic investigations suggest that NFU1 can assemble a $[Fe_4S_4]$ [73]. However, reports on NFU1 function remained controversial, as it was described to mediate sulfur delivery to ISCU in the final step of $[Fe_2S_2]$ assembly [74], but a recent phylogenetic study and biochemical characterization of the *E. coli* homologue NufA showed the presence of a $[Fe_4S_4]$. In addition, it refined the subsequent action of IscU, NfuA and an A-type carrier in Fe–S cluster transfer [75]. As for NUBPL, clear insight into

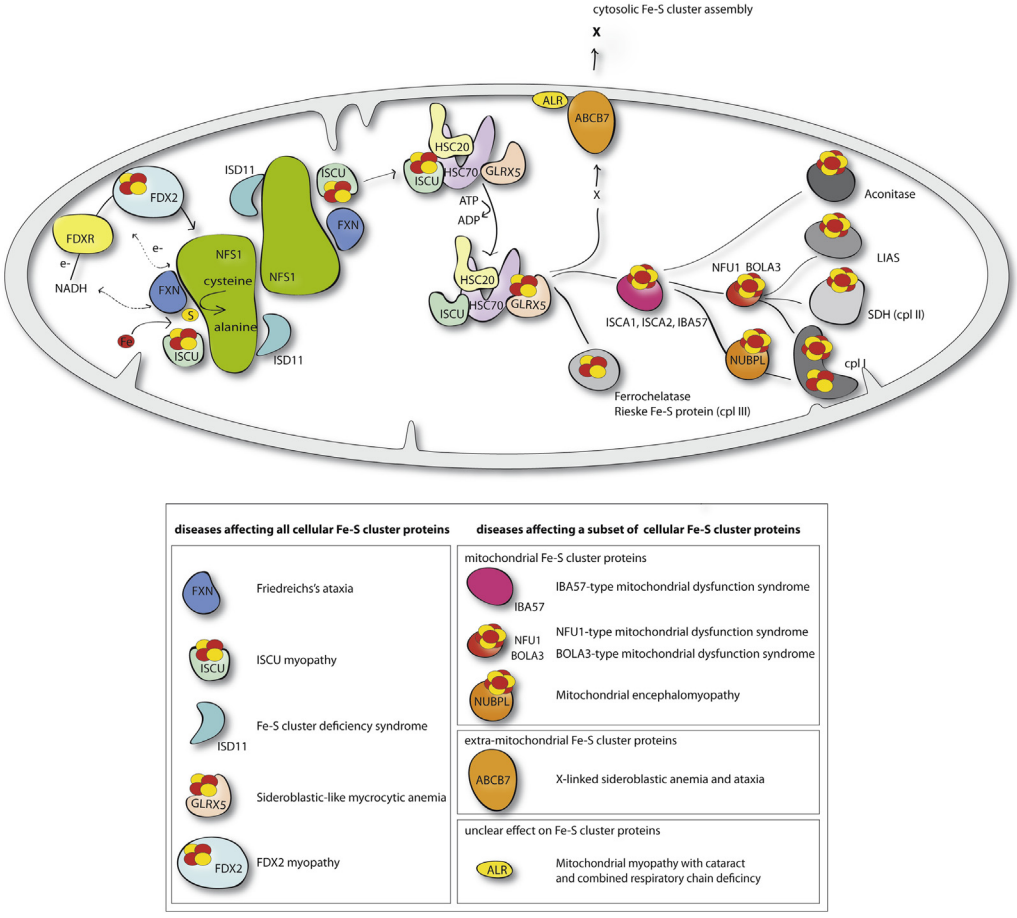

Fig. 3. Mammalian Fe–S cluster biogenesis and genetic disorders caused by dysfunction of proteins in mitochondrial Fe–S cluster biogenesis. Schematic representation of the current model of mammalian Fe–S cluster biogenesis. NFS1, the cysteine desulfurase subtracts sulfur from L-cysteine for nascent Fe–S cluster assembly. It forms a dimer and is bound by monomers of the primary scaffold protein ISCU, the regulator protein FXN and ISD11, that is required for NFS1 stability. Cysteine desulfurase activity and iron entry is controlled by FXN. Electrons are provided by an electron transport chain consisting of NAD(P)H, ferredoxin reductase (FDXR) and ferredoxin (FDX2). The interaction of FDX2 with NFS1 was reported to be early, prior to binding of FXN/ISCU/ISD11. ISCU bound Fe–S clusters are subsequently transferred via a dedicated chaperone-co-chaperone system to GLRX5. The listed proteins are required for all cellular Fe–S clusters. Subsequently, for mitochondrial Fe–S proteins, Fe–S clusters are either directly inserted into mitochondrial $[Fe_2S_2]$ proteins or transferred via specific carrier systems such as the one composed of ISCA1, ISCA2 and IBA57 to mitochondrial $[Fe_4S_4]$ proteins. Some carrier proteins, such as NFU1, BOLA3 and NUBPL seem to be required for only a subset of mitochondrial $[Fe_4S_4]$ proteins. ISCU and GLRX5 proteins are represented with $[Fe_2S_2]$ clusters, whereas the carrier systems required for $[Fe_4S_4]$ proteins are represented as with $[Fe_4S_4]$ clusters. To date, the presence of another cluster type under physiological conditions cannot not be excluded. For extra-mitochondrial Fe–S cluster, a so far uncharacterized compound (X) is exported via the Fe–S cluster export machinery consisting of ALR, glutathione and ABCB7. In the cytoplasm the cytosolic Fe–S cluster assembly machinery (CIA) inserts Fe–S cluster into cytosolic and nuclear Fe–S proteins. A constantly increasing number of diseases caused by perturbation of Fe–S cluster biogenesis proteins are known (see also Table 1). The diseases can be notably distinguished since they either affect all cellular Fe–S cluster proteins (FXN, ISCU, ISD11, GLRX5, FDX2) or only a subset of cellular Fe–S cluster proteins (IBA57, NFU1, BOLA3, NUBPL, ABCB7). It remains to be determined whether ALR participates in mammalian Fe–S cluster biogenesis.

Table 2
Mammalian mitochondrial Fe–S protein assembly components.

Mammalian name	Yeast homologue	Bacterial relative	Function
NFS1	Nfs1	IscS	Cysteine desulfurase: Sulfur donor
ISD11	Isd11	–	NFS1 stability
ISCU	Isu1, Isu2	IscU	Fe–S scaffold protein
Frataxin/FXN	Yfh1	CyaY	Regulation of NFS1 activity and iron entry
Ferredoxin/ FDX2/FDX1L	Yah1	Fdx	Electron donor
Ferredoxin reductase/ FDXR	Arh1	–	Ferredoxin-NADP + reductase
GRP75	Ssq1, Ssc1	Hsc66	Fe–S cluster transfer
HSC20	Jac1	Hsc20	Fe–S cluster transfer
Glutaredoxin5/ GLRX5	Grx5	GrxD	Fe–S cluster transfer
ISCA1	Isa1	IscA	Specific targeting of Fe–S cluster
ISCA2	Isa2	ErpA[a]	Specific targeting of Fe–S cluster
IBA57 (or C1orf69)	Iba57	–	Specific targeting of Fe–S cluster
NFU1	Nfu1	NifU (C-terminus), NfuA	Specific targeting of Fe–S cluster
NUBPL/IND1	Ind1	–	Specific targeting of Fe–S cluster
BOLA3	Aim1?	BolA?	Specific targeting of Fe–S cluster

[a] Based on phylogenetic studies.

mammalian NFU1 function and its role in the Fe–S cluster biogenesis pathway came from patients with mutations in the *NFU1* gene [53,54]. Based on the biochemical phenotype in patients as well as the phenotype upon knockdown of NFU1 in HeLa cells [54], it was concluded that NFU1 functions in the targeting of preformed clusters for a subset of proteins, namely LIAS and complex II [76]. In addition, a role of BOLA3, a protein of unknown function that is related to glutaredoxin binding proteins, in Fe–S cluster biogenesis was recently discovered by the identification of patient mutations [53,77] presenting overlapping features to the NFU1 phenotype. Whether the proteins interact together or with other proteins involved in Fe–S cluster biogenesis remains to be investigated.

In conclusion, several proteins have been demonstrated to function in the specific targeting of preformed Fe–S clusters to mitochondrial recipient proteins. It seems so far to be specific for $[Fe_4S_4]$ or complex of proteins like complex I. Whether there is a specific transfer path for mitochondrial $[Fe_2S_2]$ remains to be investigated.

3. Extra-mitochondrial Fe–S cluster: a mitochondria-dependent system

Evidence from patient phenotypes and mouse work proved the dependence of cytosolic and nuclear Fe–S proteins on the first step of the mitochondrial Fe–S cluster assembly machinery, precisely on the mitochondrial localization and activity of FXN/NFS1/ISD11/ISCU, GLRX5 as well as the mitochondrial ATP-binding cassette transporter ABCB7 [26,27,50,78]. This is strongly supported by yeast depletion phenotypes of Nfs1-Isd11, ferredoxin or the chaperones that also affected cytosolic and nuclear Fe–S cluster target proteins as Leu1, Ntg2, Rli1 and Rad3 [10,24,79,80]. The current accepted model is that biogenesis of extra-mitochondrial Fe–S proteins crucially depends on a functional mitochondrial *de novo* cluster assembly, the Fe–S cluster export machinery and the cytosolic Fe–S protein assembly machinery (often referred to as CIA), the two latter being specific for eukaryotic systems [79].

The Fe–S export machinery is composed of at least three major components, the ATP-binding transporter ABCB7, the sulfhydryl oxidase ALR (or GFER) and the tripeptide glutathione (GSH) (Table 3). The nature of the exported compound is still unknown, but was suggested to contain sulfur, as the mitochondrial localization of the sulfur donor NFS1 was essentially required for extra-mitochondrial Fe–S cluster biogenesis [81]. The implication of the inner mitochondrial transporter ABCB7 is clearly illustrated by the identification of patients carrying mutations in ABCB7 leading to X-linked sideroblastic anemia and ataxia (XLSA/A) [78,82–85]. Disruption of the protein function in mice leads to a Fe–S cluster defect in cytosolic and nuclear Fe–S proteins only, mitochondrial Fe–S proteins are primarily not affected [86,87]. This is supported by yeast data, showing a corresponding phenotype upon deletion of the yeast ABCB7-homologue Atm1 [10]. The export probably further requires ALR (Erv1 in yeast), a sulfhydryl oxidase and glutathione, even though precise molecular evidence for the mammalian counterparts is still lacking [80,88].

Studies in yeast and mammalian cells led to the characterization of a cytosolic Fe–S protein assembly machinery (CIA) for the maturation of cytosolic and nuclear ISC proteins (for detailed reviews please refer to [1,89]). As in the mitochondria, the principle of ISC protein formation consists of two main steps: the formation of a cluster on a scaffold, composed by the two P-loop NTPases CFD1 and NBP35 [90,91] and then the transfer to apoproteins involving IOP1 [92,93] and CIAO1 [94,95]. Other proteins seem to play a role in the cytosolic pathway such as DRE2 [96], but its exact function need yet to be clarified. Regarding the steadily increasing number of Fe–S proteins identified also in the nucleus and cytoplasm, and the growing evidence of increasing complexity of the mitochondrial pathway, it seems likely that other proteins involved in the cytosolic assembly machinery will be discovered.

4. A controversy in the field

Many proteins of the mitochondrial Fe–S cluster biogenesis machinery have been described to be additionally localized in the cytosol: for example NFS1 and ISD11 [97,98], ISCU and NFU1 [73,99]. Yet, if confirmed, the functional relevance remains to be clarified. In yeast, they were shown not to participate in extra-mitochondrial Fe–S cluster biogenesis [81]. This is further supported by the fact that mammalian FXN is not localized in the cytosol and the mitochondrial localization is essentially required for its function [26]. A recent paper reported cytosolic Nfs1 to function as the sulfur donor in molybdenum cofactor (Moco) biogenesis [100], opening to the discussion whether other functions for these proteins exists.

5. Diseases caused by mutations in genes coding for iron–sulfur cluster biogenesis proteins: rare but informative

A number of diseases with different symptoms are linked to mutation in genes coding for proteins involved in the

Table 3
Mammalian mitochondrial Fe–S cluster export machinery components.

Mammalian name	Yeast homologue	Bacterial relative	Function
ABCB7	Atm1	–	Translocation of a compound to the cytoplasm
ALR/GFER	Erv1	–	?
Glutathion/GSH	Isu1, Isu2	–	?

mitochondrial Fe–S cluster biogenesis, a number that increases steadily due to the increasing availability of genetic sequencing methods. Characterization of these diseases enormously contributed to the identification and clarification of different aspects of the mammalian Fe–S cluster biogenesis pathway and underlined the importance for mammalian physiology. The different types of mutations will be presented together with the pathologies and common clinical and biochemical features (Table 1, Fig. 3).

5.1. Friedreich's ataxia (FXN)

By far the most common of the diseases linked to malfunction of Fe–S cluster biosynthesis is Friedreich's ataxia (FRDA) caused by mutations in the *FXN* gene with an incidence of 1 in 50 000 in the caucasian population [101]. FRDA is a neurodegenerative disease characterized by progressive spinocerebellar and sensory ataxia with most of the symptoms resulting from degeneration of the dorsal root ganglia (DRG), in particular the large sensory neurons, the posterior column, the spinocerebellar and corticospinal tracts as well as the dentate nucleus of the cerebellum [102]. Non-neurological symptoms include hypertrophic cardiomyopathy and increased incidence of diabetes [103]. Three prominent biochemical features characterize the pathophysiology of FRDA, namely a deficit in mitochondrial Fe–S cluster enzymes, in particular aconitase and the respiratory chain complexes [104], intracellular iron deposits [105] and the presence of oxidative stress markers in blood samples [106,107]. All FRDA patients carry a GAA-triplet repeat expansion mutation in the first intron of the *FXN* gene, most of them being homozygous for the expansion. The expansion leads to transcriptional silencing of *FXN* through heterochromatinization of the locus, resulting in severely decreased levels of FXN protein [108,109]. Around 7% of the individuals with FRDA are compound heterozygous with a different mutation in the *FXN* gene, including nonsense, missense, deletions and insertions, which mainly lead to the loss of FXN function. A few point mutations are described to cause atypical or milder clinical presentation, although there is no clear genotype phenotype correlation [110–112]. All patients have around 5–30% estimated residual FXN levels, and together with the fact that constitutive deletion of the *FXN* gene in mice leads to embryonic lethality, lead to conclude that complete loss of FXN is not compatible with life [113]. Since the discovery of the underlying gene for FRDA in 1996, an increase in interest in the mammalian Fe–S cluster biogenesis pathway was noted. Thus, the *FXN* gene and the protein function were extensively studied (reviewed in detail by Martelli 2012 [114]). Today, FXN is known to function as a regulator of the cysteine desulfurase activity and the entry of iron for the first step of Fe–S cluster assembly [26,34,35]. No therapy for FRDA exists today, despite lots of efforts at trying to increase frataxin levels or mitochondrial function, or alleviating secondary symptoms by antioxidants or iron chelator strategies [115] (please refer as well to the FARA web site: http://www.curefa.org/). Still, many open questions remain on why certain tissues as the heart and even neuronal subtypes are more susceptible to the decreased FXN levels than others, although this might be partly linked to the dynamic nature of the mutation.

5.2. ISCU myopathy

ISCU myopathy was originally described in families from northern Sweden, and is characterized by lifelong severe exercise intolerance in which minor exertion causes shortness of breath, tachycardia, fatigue and pain of active muscles [116]. Blood lactate and pyruvate concentrations increase steeply at low levels of exercise, with higher pyruvate to lactate concentrations than found in patients with mitochondrial defects restricted to the respiratory chain. Besides decreased activities of mitochondrial Fe–S cluster enzymes in muscle samples from patients, iron deposits are commonly found as well [117,118]. Most affected individuals known to date are homozygous for a splice site mutation in intron 4 of the *ISCU* gene, originating from a founder haplotype in northern Sweden. The intronic mutation affects mRNA splicing of *ISCU* and results in inclusion of a pseudo-exon in most of the transcripts in muscle. The pseudo-exon inclusion results in a premature stop codon and thus severely diminished ISCU protein levels in muscle [118,119]. The tissue specificity seems to be a direct consequence of a muscle specific splice factor, as higher levels of normally spliced *ISCU* mRNA were found in fibroblasts, heart and other tissues [120,121]. Two brothers from Finnish origin were recently described as compound heterozygous for the deep intronic mutation and a missense mutation in exon 3, changing a highly conserved glycine residue to glutamate [122]. They were characterized by early onset of a slowly progressive severe muscle weakness, severe exercise intolerance and cardiomyopathy, features that are more severe that in the original patients. The fact that constitutive knockout of *ISCU* gene in mice is embryonically lethal, underlines the essential nature of ISCU for Fe–S cluster biogenesis [121]. A promising therapeutic approach was suggested with the use of antisense oligonucleotides to induce skipping of the aberrant splice site to restored normal mRNA splicing in fibroblasts from affected individuals [120,123].

5.3. FDX2 myopathy

The recent discovery of one patient exhibiting recurrent myoglobinuria and slowly progressive muscle weakness augmented the number of diseases associated to Fe–S cluster biogenesis [43]. The adolescent onset myopathy in a daughter from a consanguineous family is caused by a homozygous missense mutation in the first codon of the *FDX1L* gene encoding the mitochondrial ferredoxin 2 (FDX2) protein. The mutation disrupts the ATG translation initiation site, resulting in undetectable protein levels of FDX2 proteins in muscle and fibroblasts. The patient displayed severely decreased activity levels of the Fe–S cluster containing respiratory chain complexes I, II and III as well as aconitase and PDH complex. The myoglobinuria points in addition to a problem with heme biogenesis which requires mitochondrial Fe–S clusters. Since FDX2 is thought to serve as the electron donor for nascent Fe–S cluster formation and therefore being essential [42]), the rather mild phenotype of the patient caused by a seemingly drastic mutation raises several questions about FDX2 function. First, are FDX2 and FDX1 redundant and could FDX1 compensate for the FDX2 mutation [38,42]. Second, whether FDX2 is solely required for reduction during nascent Fe–S clusters assembly and/or at later points during Fe–S cluster biogenesis. Third, does the *FDX2* mutation affect also extra-mitochondrial Fe–S clusters as it would be suggested by its primary role in *de novo* Fe–S cluster biosynthesis and whether the muscle specific phenotype is a result of a tissue specificity effect.

5.4. Deficiency of multiple respiratory chain complexes (ISD11)

MitoExome sequencing recently discovered the cause of deficiency of multiple respiratory chain complexes in two affected cousins from a consanguineous family [124]. A homozygous mutation was found in a highly conserved residue of the ISD11 protein, leading to undetectable protein levels and notably a severely decreased activity of the cysteine desulfurase NFS1, when tested *in vitro*. Both patients suffered from neonatal lactic acidosis, but whereas one of them died during neonate period, the other is currently healthy at 20 years of age, despite defects in numerous Fe–S cluster proteins, such as the respiratory chain complexes, aconitase and ferrochelatase. The crucial difference between the

two patients seemed to be in the availability of L-cysteine for Fe–S cluster biosynthesis during the neonatal period. Even though this is the only study on patient samples with a mutation in *ISD11*, it nicely fits with the current model of the role of ISD11 for NFS1 stability and thus its requirement for all cellular Fe–S clusters. However, it leads to the urgent question of how much residual activity the cysteine desulfurase NFS1 is needed for *de novo* Fe–S cluster biogenesis and why the neonatal period seems to be particularly critical.

5.5. Sideroblastic-like microcytic anemia and iron overload (GLRX5)

One middle-aged man was diagnosed with moderate anemia, low numbers of ringed sideroblasts, hepatosplenomegaly and iron overload, and was found to carry a homozygous mutation in the penultimate nucleotide of the last codon of exon 1 of the *GLRX5* gene. This mutation interferes with intron 1 splicing and leads to strong decrease of normal mRNA but an incomplete loss of GLRX5 protein function [50,125]. GLRX5 is highly expressed in murine bone marrow, spleen and liver [126] with low ubiquitous levels in adult. This expression pattern is in line with non-hematopoetic tissues being less affected by GLRX5 deficiency. Although the precise molecular function of the mitochondrial protein GLRX5 in Fe–S cluster biogenesis is yet to be uncovered, there is increasing evidence from studies in cell models or in lower model organisms that supports a role for GLRX5 in the early step of transfer of preformed Fe–S clusters [49,50,125,126]. Several studies point to a link between loss of GLRX5 function and activation of the cytosolic iron regulatory protein (IRP1). Upon activation, IRP1 binds iron responsive elements (IREs) on different mRNAs of genes involved in iron homeostasis. The position of the IREs in the 5′ or 3′ UTR thereby determines whether the respective mRNA translation gets blocked (5′UTR) or the mRNA is stabilized (3′UTR). The underlying mechanism for the specific effect on hematopoiesis could arise from the difference between the heme biogenesis enzymes ALAS1 and ALAS2. Indeed, ALAS2 is specific for the erythroid cell line and containing an IRE in its 5′UTR, whereas ALAS1 does not contain an IRE [126].

5.6. Mitochondrial myopathy with cataract and combined respiratory chain deficiency (ALR)

A mutation in the *ALR* gene (also known as *GFER*) was described to lead to a progressive myopathy with congenital cataract, sensorineural hearing loss and developmental delay in three children from consanguineous parents [127]. The homozygous mutation leads to change of a highly conserved amino acid that was not detected in controls, suggesting it to be disease-causing. The consequences of the mutation were a reduction in complex I, II, and IV activities, a lower cysteine-rich protein content, abnormal ultrastructural morphology of the mitochondria, with enlargement of the inter membrane space (IMS), and accelerated time-dependent accumulation of multiple mtDNA deletions. The yeast homologue Erv1, a sulfhydryl oxidase essential for import of sulfhydryl-bond containing mitochondrial inter membrane proteins, has been proposed to be involved in Fe–S cluster export machinery [80,128]. Whether ALR participates in Fe–S cluster biogenesis remains to be determined.

5.7. X-linked sideroblastic anemia and ataxia (ABCB7)

X-linked sideroblastic anemia and ataxia (XLSA/A) is characterized by early-onset non-progressive ataxia and usually mild sideroblastic anemia with neither hepatic nor systemic iron overload. Cerebellar hypoplasia and atrophy are observed in the pathology, whereas the anemia is often asymptomatic, even though elevated free protoporphyrin levels are observed in erythrocytes [78,129,130]. Iron overload, but notably only in the affected tissues [82,129] and strong dysregulation of iron homeostasis are observed in cellular and murine disease models [85–87,131,132]. ABCB7 was shown to be essential for hematopoiesis, supported by the finding that excess of iron found in the mitochondria seem not to be available for proper ferrochelatase function in heme biogenesis [85,133]. Besides its requirement during blood development, ABCB7 was shown to be expressed in the developing cerebellum [82]. Unfortunately, neuron-specific Abcb7 knockout in mice show no gross developmental abnormalities of the brain at birth, but die immediately after birth [86]. As the cerebellum develops primarily after birth in mice, the nature of the cerebellar phenotype observed in patients could not be evaluated. The thorough studies of tissue-specific knockouts and knockdown in human cellular models were able to validate the role of ABCB7 for extra-mitochondrial Fe–S clusters and the link to iron metabolism through IRP1 activity [85,87]. All mutations described for XLSA/A lie within or adjacent to a putative transmembrane domain of the transporter [78,82–84], but are not full loss of function mutations. Thus, it seems that only slight structural changes in the transmembrane domain can underlie the disease phenotype. Still, many questions concerning ABCB7 function and the disease pathology remain, such as the tissue specificity.

5.8. Mitochondrial encephalomyopathy (NUBPL)

Different clinical features including developmental delay, myopathy, brain abnormalities and often ataxia, compose the phenotype of the mitochondrial encephalomyopathy caused by mutated NUBPL or IND1 [67,69]. In all cases described, a strong respiratory chain complex I deficiency is observed. Most patients are compound heterozygous with an allele carrying two mutations (a missense mutation and an intronic mutation) and a different mutation (missense, intronic or deletion/duplication) on the second allele [67,69]. Although the missense mutation affects a highly conserved amino acid, the expression of the mutant protein was shown to restore complex I activity in patient fibroblasts. Thus, it is most likely that the intronic mutation that causes aberrant splicing and thus reduced mRNA and protein expression, is the causative mutation [68]. Since all patients are compound heterozygous a synergy effect of the mutations cannot be excluded, but detailed investigations are not yet published. One patient was described with a different compound heterozygous genotype composed of a deletion leading to a premature stop codon and a missense mutation, creating an aberrant splice site leading to frameshift [70]. Surprisingly, there seem to be no correlation between the remaining activity levels of NUBPL and the severity of the phenotype.

5.9. NFU1-type multiple mitochondrial dysfunction syndrome

Two papers described a total of 14 patients with a fatal mitochondrial disease caused by mutations in NFU1, the symptoms ranging from failure to thrive to metabolic acidosis with hyperglycinemia [53,54]. Five patients were described with a homozygous mutation in NFU1 (c.545+5G > A p.Arg182Gln), where the mutation is close to a splice site, resulting in skipping of exon 6 and no detectable protein levels [53]. Most of the other patients were described with an homozygous mutation (c.622G > T, p.Gly208-Cys), affecting an amino acid close to a highly conserved Fe–S cluster binding cysteine of the NFU1 protein. Here, normal NFU1 protein levels were detected, but the position is likely to affect Fe–S

cluster binding [54]. One patient was compound heterozygous for the two mutations described in both papers [54]. Even though, both mutations resulted in early postnatal lethality of the patients, the patients without residual protein levels described by Cameron and colleagues died during the first month of age, whereas the patients with a normal level of mutated NFU1 protein survived a couple of months longer, suggesting a minimal residual activity of the mutated NFU1 in the latter. Both mutations had a strong effect on lipoic acid biogenesis as the complex-bound lipoid acid to pyruvate dehydrogenase (PDH) and α-ketogluterate dehydrogenase (KGDH) were strongly affected. Lipoate biogenesis relies on the mitochondrial [Fe_4S_4] enzyme lipoate synthase (LIAS). Due to the important involvement of lipoate-bound complexes into mitochondrial metabolism, loss of lipoic acid has a detrimental effect for patients (for further details please refer to [134–136]). However, besides the role of NFU1 for targeting Fe–S cluster to lipoate synthase, it may be required also for cluster transfer to the mitochondrial respiratory chain complexes I and II, as these were affected in a subgroup of the patients tested [53]. Further detailed analysis will be required to conclude precisely on the requirement of NFU1 in the targeting of mitochondrial Fe–S cluster.

5.10. BOLA3-type multiple mitochondrial dysfunction syndrome

Several patients with mutations in the *BOLA3* gene were identified with similar clinical and biochemical features as the NFU1 patients [53,77]. Although not previously studied, BOLA3 most probably functions in a similar context as NFU1, for the distribution of a subset of mitochondrial Fe–S clusters.

5.11. IBA57-type multiple mitochondrial dysfunction syndrome

Two siblings from consanguineous parents died shortly after birth of a novel metabolic syndrome with myopathy and encephalopathy caused by multiple Fe–S protein defects [56]. Symptoms of generalized hypotonia, respiratory insufficiency, congenital brain malformations and hyperglycemia pointed to a systemic mitochondrial defect. The underlying cause was found to be a homozygous mutation in the *IBA57* gene. The mutation results in subsequent degradation of the mutated protein by the proteasome. Tissue specificity was not observed. Defects detected in mitochondrial respiratory chain complex I and II, PDH and KGDH complex-bound lipoate as well as mitochondrial aconitase, support the idea that IBA57 is involved in targeting mitochondrial [Fe_4S_4] to their apoproteins, being perfectly in line with what is reported for knockdown of IBA57 in HeLa cells [55].

6. Seemingly dissimilar: common features of ISC biogenesis-related diseases

Although these diseases appear diverse, there are common features among many of them. Due to the essential nature of the proteins involved in Fe–S cluster biogenesis, the disease-causing mutations are either complete loss-of-function (as for NFU1, BOLA3, IBA57) leading to very severe phenotypes and neonatal death or partial loss-of-function mutations (as in FXN, ABCB7 or ISCU) causing relatively less severe disease with tissue specificity. Individually, and as a group, these diseases are rare, and all manifest with a prominent mitochondrial phenotype.

Diseases linked to mitochondria dysfunction can notably manifest at any age with virtually any symptom or manifestation ranging from neurodegeneration to cancer. Although mitochondrial disorders are in total quite common, individual subgroups caused by the same specific defect are rare diseases [137]. This seems particularly true for diseases linked to the Fe–S cluster biogenesis pathway, probably due to the wide use and essential requirement of the clusters for proper protein function in a multitude of pathways. Two prominent questions arise from that by having a closer look. First, it often remains to be elucidated why these diseases affect in certain cases just a specific subset of tissues. Although tissues that are high in mitochondrial content, seem in part primarily affected, in many cases that does not completely explain the phenotype. It appears that a tissue specific requirement such as for GLRX5 or a tissue specific mutation such as for ISCU might be the underlying mechanisms of tissue-specificity. Detailed molecular investigations of the pathologies and appropriate mouse models might help to resolve these questions in the future. Second, the primary description of the Fe–S cluster biogenesis-linked diseases almost exclusively focuses on the deficiency of mitochondrial Fe–S proteins. However, in the case of mutations in the proteins involved in nascent cluster formation as FXN and ISCU also extra-mitochondrial Fe–S clusters are affected, but analysis of these extra-mitochondrial Fe–S cluster proteins in patient samples have not been explored. It would be important to know whether the neurological phenotype observed in Friedreich's Ataxia, for example, is strictly a mitochondrial phenotype, or whether Fe–S cluster DNA repair enzyme or helicases are also involved. Indeed, other recessive ataxias are known to be linked to nucleotide metabolism [138].

The common hallmark of many of the diseases is the appearance of deregulation of iron homeostasis and/or iron deposits in the affected cells or tissues. Today, we know that iron deregulation often appears as a secondary feature of these pathologies, due to disruption of Fe–S cluster biogenesis. The first evident link between iron and Fe–S clusters is the need for iron for Fe–S cluster biogenesis. The second link arises through the iron regulatory protein 1 (IRP1) that gets activated upon sensing iron deplete conditions and binding of IREs on mRNAs of different iron metabolism genes. For detailed reviews about the current knowledge on iron homeostasis please refer to [139,140].

7. Conclusion: the urgent need for *in vivo* models

Different laboratories have investigated the function of mammalian Fe–S cluster biogenesis proteins by knockdown of the respective protein in cellular models. This is a valid and fast method. However, many studies show drastic morphological changes to the mitochondria. Detailed analysis of the models, but in parts also of the pathophysiology in patients and mice, often shows mitochondria that are not functional anymore and show affected ultrastructure and/or decreased functions of the respiratory chain complex IV, which does not harbor any Fe–S cluster. Therefore, these effects are secondary to the pathology. However, it is still a matter of uncertainty to distinguish between primary and secondary events of the respective pathology, because cell models cannot completely recapitulate the *in vivo* situation.

On the other hand, *in vivo* models are often not yet available to an adequate extent. Not surprisingly, constitutive knockouts of the essential proteins are usually embryonic lethal (as for FXN, ABCB7, ISCU). Still, with increasing cellular differentiation in mammals, an increase in complexity of the Fe–S cluster biogenesis pathway is likely to be present and might show tissue specificity, in a similar manner to the different biosynthesis machineries found and required in bacteria for Fe–S cluster biogenesis depending on the environmental confrontation (for review on isc and suf systems please see Roche et al., 2013 [141]). Thus, there is a big interest to resolve not only the precise molecular and biochemical function of each protein implicated, but also its spatial and temporal requirement. Accordingly, tissue specific knockouts and especially temporal progression of a phenotype is needed to be analyzed in the

future. However, creating knockout models and the thorough analysis of their phenotype is very time consuming and costly.

Competing interests

We declare that there are no competing commercial interests in relation to the submitted work.

Acknowledgments

This work was supported by the European Community under the European Research Council [206634/ISCATAXIA] and the 7th Framework Program [242193/EFACTS].

References

[1] R. Lill, Function and biogenesis of iron–sulphur proteins, Nature 460 (2009) 831–838.
[2] H. Beinert, R.H. Holm, E. Munck, Iron–sulfur clusters: nature's modular, multipurpose structures, Science 277 (1997) 653–659.
[3] D.C. Rees, J.B. Howard, The interface between the biological and inorganic worlds: iron–sulfur metalloclusters, Science 300 (2003) 929–931.
[4] J.A. Imlay, Iron–sulphur clusters and the problem with oxygen, Mol. Microbiol. 59 (2006) 1073–1082.
[5] J. Frazzon, J.R. Fick, D.R. Dean, Biosynthesis of iron–sulphur clusters is a complex and highly conserved process, Biochem. Soc. Trans. 30 (2002) 680–685.
[6] H. Beinert, W. Lee, Evidence for a new type of iron containing electron carrier in mitochondria, Biochem. Biophys. Res. Commun. 5 (1961) 40–45.
[7] D.R. Dean, K.E. Brigle, Azotobacter vinelandii nifD- and nifE-encoded polypeptides share structural homology, Proc. Natl. Acad. Sci. U. S. A. 82 (1985) 5720–5723.
[8] L. Zheng, V.L. Cash, D.H. Flint, D.R. Dean, Assembly of iron–sulfur clusters. Identification of an iscSUA-hscBA-fdx gene cluster from *Azotobacter vinelandii*, J. Biol. Chem. 273 (1998) 13264–13272.
[9] B. Schilke, C. Voisine, H. Beinert, E. Craig, Evidence for a conserved system for iron metabolism in the mitochondria of *Saccharomyces cerevisiae*, Proc. Natl. Acad. Sci. U. S. A. 96 (1999) 10206–10211.
[10] G. Kispal, P. Csere, C. Prohl, R. Lill, The mitochondrial proteins Atm1p and Nfs1p are essential for biogenesis of cytosolic Fe/S proteins, EMBO J. 18 (1999) 3981–3989.
[11] P.J. Kiley, H. Beinert, The role of Fe–S proteins in sensing and regulation in bacteria, Curr. Opin. Microbiol. 6 (2003) 181–185.
[12] M. Fontecave, Iron–sulfur clusters: ever-expanding roles, Nat. Chem. Biol. 2 (2006) 171–174.
[13] H. Beinert, Iron–sulfur proteins: ancient structures, still full of surprises, J. Biol. Inorg. Chem. 5 (2000) 2–15.
[14] L.A. Sazanov, P. Hinchliffe, Structure of the hydrophilic domain of respiratory complex I from *Thermus thermophilus*, Science 311 (2006) 1430–1436.
[15] A.H. Robbins, C.D. Stout, The structure of aconitase, Proteins 5 (1989) 289–312.
[16] H. Lauble, M.C. Kennedy, H. Beinert, C.D. Stout, Crystal structures of aconitase with isocitrate and nitroisocitrate bound, Biochemistry 31 (1992) 2735–2748.
[17] T.A. Rouault, D.J. Haile, W.E. Downey, C.C. Philpott, C. Tang, F. Samaniego, J. Chin, I. Paul, D. Orloff, J.B. Harford, et al., An iron–sulfur cluster plays a novel regulatory role in the iron-responsive element binding protein, Biometals 5 (1992) 131–140.
[18] S. Ollagnier-De Choudens, Y. Sanakis, K.S. Hewitson, P. Roach, J.E. Baldwin, E. Munck, M. Fontecave, Iron–sulfur center of biotin synthase and lipoate synthase, Biochemistry 39 (2000) 4165–4173.
[19] R.M. Cicchillo, S.J. Booker, Mechanistic investigations of lipoic acid biosynthesis in *Escherichia coli*: both sulfur atoms in lipoic acid are contributed by the same lipoyl synthase polypeptide, J. Am. Chem. Soc. 127 (2005) 2860–2861.
[20] V.M. Sellers, M.K. Johnson, H.A. Dailey, Function of the [2FE-2S] cluster in mammalian ferrochelatase: a possible role as a nitric oxide sensor, Biochemistry 35 (1996) 2699–2704.
[21] V.M. Sellers, K.F. Wang, M.K. Johnson, H.A. Dailey, Evidence that the fourth ligand to the [2Fe–2S] cluster in animal ferrochelatase is a cysteine. Characterization of the enzyme from *Drosophila melanogaster*, J. Biol. Chem. 273 (1998) 22311–22316.
[22] B.R. Crouse, V.M. Sellers, M.G. Finnegan, H.A. Dailey, M.K. Johnson, Site-directed mutagenesis and spectroscopic characterization of human ferrochelatase: identification of residues coordinating the [2Fe–2S] cluster, Biochemistry 35 (1996) 16222–16229.
[23] A.N. Suhasini, R.M. Brosh Jr., Disease-causing missense mutations in human DNA helicase disorders, Mutat. Res. 752 (2013) 138–152.
[24] D.J. Netz, C.M. Stith, M. Stumpfig, G. Kopf, D. Vogel, H.M. Genau, J.L. Stodola, R. Lill, P.M. Burgers, A.J. Pierik, Eukaryotic DNA polymerases require an iron–sulfur cluster for the formation of active complexes, Nat. Chem. Biol. 8 (2012) 125–132.
[25] B. Py, F. Barras, Building Fe–S proteins: bacterial strategies, Nat. Rev. Microbiol. 8 (2010) 436–446.
[26] S. Schmucker, A. Martelli, F. Colin, A. Page, M. Wattenhofer-Donze, L. Reutenauer, H. Puccio, Mammalian frataxin: an essential function for cellular viability through an interaction with a preformed ISCU/NFS1/ISD11 iron–sulfur assembly complex, PLoS One 6 (2011) e16199.
[27] A. Martelli, M. Wattenhofer-Donze, S. Schmucker, S. Bouvet, L. Reutenauer, H. Puccio, Frataxin is essential for extramitochondrial Fe–S cluster proteins in mammalian tissues, Hum. Mol. Genet. 16 (2007) 2651–2658.
[28] L. Loiseau, S. Ollagnier-de-Choudens, L. Nachin, M. Fontecave, F. Barras, Biogenesis of Fe–S cluster by the bacterial Suf system: SufS and SufE form a new type of cysteine desulfurase, J. Biol. Chem. 278 (2003) 38352–38359.
[29] N. Wiedemann, E. Urzica, B. Guiard, H. Muller, C. Lohaus, H.E. Meyer, M.T. Ryan, C. Meisinger, U. Muhlenhoff, R. Lill, N. Pfanner, Essential role of Isd11 in mitochondrial iron–sulfur cluster synthesis on Isu scaffold proteins, EMBO J. 25 (2006) 184–195.
[30] A. Pandey, H. Yoon, E.R. Lyver, A. Dancis, D. Pain, Isd11p protein activates the mitochondrial cysteine desulfurase Nfs1p protein, J. Biol. Chem. 286 (2011) 38242–38252.
[31] A.C. Adam, C. Bornhovd, H. Prokisch, W. Neupert, K. Hell, The Nfs1 interacting protein Isd11 has an essential role in Fe/S cluster biogenesis in mitochondria, EMBO J. 25 (2006) 174–183.
[32] G. Isaya, H.A. O'Neill, O. Gakh, S. Park, R. Mantcheva, S.M. Mooney, Functional studies of frataxin, Acta Paediatr. (Suppl. 93) (2004) 68–71 discussion 72–63.
[33] M. Nair, S. Adinolfi, C. Pastore, G. Kelly, P. Temussi, A. Pastore, Solution structure of the bacterial frataxin ortholog, CyaY: mapping the iron binding sites, Structure 12 (2004) 2037–2048.
[34] C.L. Tsai, D.P. Barondeau, Human frataxin is an allosteric switch that activates the Fe–S cluster biosynthetic complex, Biochemistry 49 (2010) 9132–9139.
[35] F. Colin, A. Martelli, M. Clemancey, J.M. Latour, S. Gambarelli, L. Zeppieri, C. Birck, A. Page, H. Puccio, S. Ollagnier de Choudens, Mammalian frataxin controls sulfur production and iron entry during de novo Fe4S4 cluster assembly, J. Am. Chem. Soc. 135 (2013) 733–740.
[36] S. Adinolfi, C. Iannuzzi, F. Prischi, C. Pastore, S. Iametti, S.R. Martin, F. Bonomi, A. Pastore, Bacterial frataxin CyaY is the gatekeeper of iron–sulfur cluster formation catalyzed by IscS, Nat. Struct. Mol. Biol. 16 (2009) 390–396.
[37] J. Bridwell-Rabb, C. Iannuzzi, A. Pastore, D.P. Barondeau, Effector role reversal during evolution: the case of frataxin in Fe–S cluster biosynthesis, Biochemistry 51 (2012) 2506–2514.
[38] Y. Shi, M. Ghosh, G. Kovtunovych, D.R. Crooks, T.A. Rouault, Both human ferredoxins 1 and 2 and ferredoxin reductase are important for iron–sulfur cluster biogenesis, Biochim. Biophys. Acta 1823 (2012) 484–492.
[39] K. Chandramouli, M.C. Unciuleac, S. Naik, D.R. Dean, B.H. Huynh, M.K. Johnson, Formation and properties of [4Fe–4S] clusters on the IscU scaffold protein, Biochemistry 46 (2007) 6804–6811.
[40] J.H. Kim, R.O. Frederick, N.M. Reinen, A.T. Troupis, J.L. Markley, [2Fe–2S]-Ferredoxin binds directly to cysteine desulfurase and supplies an electron for iron–sulfur cluster assembly but is displaced by the scaffold protein or bacterial frataxin, J. Am. Chem. Soc. 135 (22) (2013) 8117–8120. Epub ahead of print.
[41] R. Yan, P.V. Konarev, C. Iannuzzi, S. Adinolfi, B. Roche, G. Kelly, L. Simon, S.R. Martin, B. Py, F. Barras, D.I. Svergun, A. Pastore, Ferredoxin competes with bacterial frataxin in binding to the desulfurase IscS, J. Biol. Chem. 288 (34) (2013) 24777–24787.
[42] A.D. Sheftel, O. Stehling, A.J. Pierik, H.P. Elsasser, U. Muhlenhoff, H. Webert, A. Hobler, F. Hannemann, R. Bernhardt, R. Lill, Humans possess two mitochondrial ferredoxins, Fdx1 and Fdx2, with distinct roles in steroidogenesis, heme, and Fe/S cluster biosynthesis, Proc. Natl. Acad. Sci. U. S. A. 107 (2010) 11775–11780.
[43] R. Spiegel, A. Saada, J. Halvardson, D. Soiferman, A. Shaag, S. Edvardson, Y. Horovitz, M. Khayat, S.A. Shalev, L. Feuk, O. Elpeleg, Deleterious mutation in FDX1L gene is associated with a novel mitochondrial muscle myopathy, Eur. J. Hum. Genet. (27 November 2013), http://dx.doi.org/10.1038/ejhg.2013.269.
[44] L.E. Vickery, J.R. Cupp-Vickery, Molecular chaperones HscA/Ssq1 and HscB/Jac1 and their roles in iron–sulfur protein maturation, Crit. Rev. Biochem. Mol. Biol. 42 (2007) 95–111.
[45] H. Uhrigshardt, A. Singh, G. Kovtunovych, M. Ghosh, T.A. Rouault, Characterization of the human HSC20, an unusual DnaJ type III protein, involved in iron–sulfur cluster biogenesis, Hum. Mol. Genet. 19 (2010) 3816–3834.
[46] E.A. Craig, J. Marszalek, A specialized mitochondrial molecular chaperone system: a role in formation of Fe/S centers, Cell. Mol. Life Sci. 59 (2002) 1658–1665.
[47] R. Dutkiewicz, B. Schilke, S. Cheng, H. Knieszner, E.A. Craig, J. Marszalek, Sequence-specific interaction between mitochondrial Fe–S scaffold protein Isu and Hsp70 Ssq1 is essential for their *in vivo* function, J. Biol. Chem. 279 (2004) 29167–29174.
[48] K.G. Hoff, J.R. Cupp-Vickery, L.E. Vickery, Contributions of the LPPVK motif of the iron–sulfur template protein IscU to interactions with the Hsc66–Hsc20 chaperone system, J. Biol. Chem. 278 (2003) 37582–37589.

[49] M.A. Uzarska, R. Dutkiewicz, S.A. Freibert, R. Lill, U. Muhlenhoff, The mitochondrial Hsp70 chaperone Ssq1 facilitates Fe/S cluster transfer from Isu1 to Grx5 by complex formation, Mol. Biol. Cell. 24 (2013) 1830–1841.
[50] H. Ye, S.Y. Jeong, M.C. Ghosh, G. Kovtunovych, L. Silvestri, D. Ortillo, N. Uchida, J. Tisdale, C. Camaschella, T.A. Rouault, Glutaredoxin 5 deficiency causes sideroblastic anemia by specifically impairing heme biosynthesis and depleting cytosolic iron in human erythroblasts, J. Clin. Invest. 120 (2010) 1749–1761.
[51] C.H. Lillig, C. Berndt, A. Holmgren, Glutaredoxin systems, Biochim. Biophys. Acta 1780 (2008) 1304–1317.
[52] A.D. Sheftel, O. Stehling, A.J. Pierik, D.J. Netz, S. Kerscher, H.P. Elsasser, I. Wittig, J. Balk, U. Brandt, R. Lill, Human ind1, an iron–sulfur cluster assembly factor for respiratory complex I, Mol. Cell. Biol. 29 (2009) 6059–6073.
[53] J.M. Cameron, A. Janer, V. Levandovskiy, N. Mackay, T.A. Rouault, W.H. Tong, I. Ogilvie, E.A. Shoubridge, B.H. Robinson, Mutations in iron–sulfur cluster scaffold genes NFU1 and BOLA3 cause a fatal deficiency of multiple respiratory chain and 2-oxoacid dehydrogenase enzymes, Am. J. Hum. Genet. 89 (2011) 486–495.
[54] A. Navarro-Sastre, F. Tort, O. Stehling, M.A. Uzarska, J.A. Arranz, M. Del Toro, M.T. Labayru, J. Landa, A. Font, J. Garcia-Villoria, B. Merinero, M. Ugarte, L.G. Gutierrez-Solana, J. Campistol, A. Garcia-Cazorla, J. Vaquerizo, E. Riudor, P. Briones, O. Elpeleg, A. Ribes, R. Lill, A fatal mitochondrial disease is associated with defective NFU1 function in the maturation of a subset of mitochondrial Fe–S proteins, Am. J. Hum. Genet. 89 (2011) 656–667.
[55] A.D. Sheftel, C. Wilbrecht, O. Stehling, B. Niggemeyer, H.P. Elsasser, U. Muhlenhoff, R. Lill, The human mitochondrial ISCA1, ISCA2, and IBA57 proteins are required for [4Fe-4S] protein maturation, Mol. Biol. Cell. 23 (2012) 1157–1166.
[56] N. Ajit Bolar, A.V. Vanlander, C. Wilbrecht, N. Van der Aa, J. Smet, B. De Paepe, G. Vandeweyer, F. Kooy, F. Eyskens, E. De Latter, G. Delanghe, P. Govaert, J.G. Leroy, B. Loeys, R. Lill, L. Van Laer, R. Van Coster, Mutation of the iron–sulfur cluster assembly gene IBA57 causes severe myopathy and encephalopathy, Hum. Mol. Genet. 22 (2013) 2590–2602.
[57] L.T. Jensen, V.C. Culotta, Role of *Saccharomyces cerevisiae* ISA1 and ISA2 in iron homeostasis, Mol. Cell. Biol. 20 (2000) 3918–3927.
[58] A. Kaut, H. Lange, K. Diekert, G. Kispal, R. Lill, Isa1p is a component of the mitochondrial machinery for maturation of cellular iron–sulfur proteins and requires conserved cysteine residues for function, J. Biol. Chem. 275 (2000) 15955–15961.
[59] J. Lu, J.P. Bitoun, G. Tan, W. Wang, W. Min, H. Ding, Iron-binding activity of human iron–sulfur cluster assembly protein hIscA1, Biochem. J. 428 (2010) 125–131.
[60] H. Ding, J. Yang, L.C. Coleman, S. Yeung, Distinct iron binding property of two putative iron donors for the iron–sulfur cluster assembly: IscA and the bacterial frataxin ortholog CyaY under physiological and oxidative stress conditions, J. Biol. Chem. 282 (2007) 7997–8004.
[61] D. Vinella, C. Brochier-Armanet, L. Loiseau, E. Talla, F. Barras, Iron–sulfur (Fe/S) protein biogenesis: phylogenomic and genetic studies of A-type carriers, PLoS Genet. 5 (2009) e1000497.
[62] A.P. Landry, Z. Cheng, H. Ding, Iron binding activity is essential for the function of IscA in iron–sulphur cluster biogenesis, Dalton Trans. 42 (2013) 3100–3106.
[63] D.T. Mapolelo, B. Zhang, S.G. Naik, B.H. Huynh, M.K. Johnson, Spectroscopic and functional characterization of iron–sulfur cluster-bound forms of *Azotobacter vinelandii* (Nif)IscA, Biochemistry 51 (2012) 8071–8084.
[64] L. Qian, C. Zheng, J. Liu, Characterization of iron–sulfur cluster assembly protein IscA from *Acidithiobacillus ferrooxidans*, Biochem. (Moscow) 78 (2013) 244–251.
[65] U. Muhlenhoff, N. Richter, O. Pines, A.J. Pierik, R. Lill, Specialized function of yeast Isa1 and Isa2 proteins in the maturation of mitochondrial [4Fe–4S] proteins, J. Biol. Chem. 286 (2011) 41205–41216.
[66] C. Gelling, I.W. Dawes, N. Richhardt, R. Lill, U. Muhlenhoff, Mitochondrial Iba57p is required for Fe/S cluster formation on aconitase and activation of radical SAM enzymes, Mol. Cell. Biol. 28 (2008) 1851–1861.
[67] S.E. Calvo, E.J. Tucker, A.G. Compton, D.M. Kirby, G. Crawford, N.P. Burtt, M. Rivas, C. Guiducci, D.L. Bruno, O.A. Goldberger, M.C. Redman, E. Wiltshire, C.J. Wilson, D. Altshuler, S.B. Gabriel, M.J. Daly, D.R. Thorburn, V.K. Mootha, High-throughput, pooled sequencing identifies mutations in NUBPL and FOXRED1 in human complex I deficiency, Nat. Genet. 42 (2010) 851–858.
[68] E.J. Tucker, A.G. Compton, S.E. Calvo, D.R. Thorburn, The molecular basis of human complex I deficiency, IUBMB Life 63 (2011) 669–677.
[69] S.H. Kevelam, R.J. Rodenburg, N.I. Wolf, P. Ferreira, R.J. Lunsing, L.G. Nijtmans, A. Mitchell, H.A. Arroyo, D. Rating, A. Vanderver, C.G. van Berkel, T.E. Abbink, P. Heutink, M.S. van der Knaap, NUBPL mutations in patients with complex I deficiency and a distinct MRI pattern, Neurology 80 (17) (2013) 1577–1583.
[70] E.V. Tenisch, A.S. Lebre, D. Grevent, P. de Lonlay, M. Rio, M. Zilbovicius, B. Funalot, I. Desguerre, F. Brunelle, A. Rotig, A. Munnich, N. Boddaert, Massive and exclusive pontocerebellar damage in mitochondrial disease and NUBPL mutations, Neurology 79 (2012) 391.
[71] K. Bych, S. Kerscher, D.J. Netz, A.J. Pierik, K. Zwicker, M.A. Huynen, R. Lill, U. Brandt, J. Balk, The iron–sulphur protein Ind1 is required for effective complex I assembly, EMBO J. 27 (2008) 1736–1746.
[72] Y. Liu, J.A. Cowan, Iron–sulfur cluster biosynthesis: characterization of a molten globule domain in human NFU, Biochemistry 48 (2009) 7512–7518.
[73] W.H. Tong, G.N. Jameson, B.H. Huynh, T.A. Rouault, Subcellular compartmentalization of human Nfu, an iron–sulfur cluster scaffold protein, and its ability to assemble a [4Fe-4S] cluster, Proc. Natl. Acad. Sci. U. S. A. 100 (2003) 9762–9767.
[74] Y. Liu, J.A. Cowan, Iron sulfur cluster biosynthesis. Human NFU mediates sulfide delivery to ISU in the final step of [2Fe-2S] cluster assembly, Chem. Commun. (Cambridge) (2007) 3192–3194.
[75] B. Py, C. Gerez, S. Angelini, R. Planel, D. Vinella, L. Loiseau, E. Talla, C. Brochier-Armanet, R. Garcia Serres, J.M. Latour, S. Ollagnier-de Choudens, M. Fontecave, F. Barras, Molecular organization, biochemical function, cellular role and evolution of NfuA, an atypical Fe–S carrier, Mol. Microbiol. 86 (2012) 155–171.
[76] X. Ferrer-Cortes, A. Font, N. Bujan, A. Navarro-Sastre, L. Matalonga, J.A. Arranz, E. Riudor, M. Del Toro, A. Garcia-Cazorla, J. Campistol, P. Briones, A. Ribes, F. Tort, Protein expression profiles in patients carrying NFU1 mutations. Contribution to the pathophysiology of the disease, J. Inherit. Metab. Dis. 36 (2013) 841–847.
[77] T.B. Haack, B. Rolinski, B. Haberberger, F. Zimmermann, J. Schum, V. Strecker, E. Graf, U. Athing, T. Hoppen, I. Wittig, W. Sperl, P. Freisinger, J.A. Mayr, T.M. Strom, T. Meitinger, H. Prokisch, Homozygous missense mutation in BOLA3 causes multiple mitochondrial dysfunctions syndrome in two siblings, J. Inherit. Metab. Dis. 36 (2013) 55–62.
[78] S. Bekri, G. Kispal, H. Lange, E. Fitzsimons, J. Tolmie, R. Lill, D.F. Bishop, Human ABC7 transporter: gene structure and mutation causing X-linked sideroblastic anemia with ataxia with disruption of cytosolic iron–sulfur protein maturation, Blood 96 (2000) 3256–3264.
[79] A.K. Sharma, L.J. Pallesen, R.J. Spang, W.E. Walden, Cytosolic iron–sulfur cluster assembly (CIA) system: factors, mechanism, and relevance to cellular iron regulation, J. Biol. Chem. 285 (2010) 26745–26751.
[80] H. Lange, T. Lisowsky, J. Gerber, U. Muhlenhoff, G. Kispal, R. Lill, An essential function of the mitochondrial sulfhydryl oxidase Erv1p/ALR in the maturation of cytosolic Fe/S proteins, EMBO Rep. 2 (2001) 715–720.
[81] A. Biederbick, O. Stehling, R. Rosser, B. Niggemeyer, Y. Nakai, H.P. Elsasser, R. Lill, Role of human mitochondrial Nfs1 in cytosolic iron–sulfur protein biogenesis and iron regulation, Mol. Cell. Biol. 26 (2006) 5675–5687.
[82] R. Allikmets, W.H. Raskind, A. Hutchinson, N.D. Schueck, M. Dean, D.M. Koeller, Mutation of a putative mitochondrial iron transporter gene (ABC7) in X-linked sideroblastic anemia and ataxia (XLSA/A), Hum. Mol. Genet. 8 (1999) 743–749.
[83] A. Maguire, K. Hellier, S. Hammans, A. May, X-linked cerebellar ataxia and sideroblastic anaemia associated with a missense mutation in the ABC7 gene predicting V411L, Br. J. Haematol. 115 (2001) 910–917.
[84] M. D'Hooghe, D. Selleslag, G. Mortier, R. Van Coster, P. Vermeersch, J. Billiet, S. Bekri, X-linked sideroblastic anemia and ataxia: a new family with identification of a fourth ABCB7 gene mutation, Eur. J. Paediatr. Neurol. 16 (2012) 730–735.
[85] C. Pondarre, D.R. Campagna, B. Antiochos, L. Sikorski, H. Mulhern, M.D. Fleming, Abcb7, the gene responsible for X-linked sideroblastic anemia with ataxia, is essential for hematopoiesis, Blood 109 (2007) 3567–3569.
[86] C. Pondarre, B.B. Antiochos, D.R. Campagna, S.L. Clarke, E.L. Greer, K.M. Deck, A. McDonald, A.P. Han, A. Medlock, J.L. Kutok, S.A. Anderson, R.S. Eisenstein, M.D. Fleming, The mitochondrial ATP-binding cassette transporter Abcb7 is essential in mice and participates in cytosolic iron–sulfur cluster biogenesis, Hum. Mol. Genet. 15 (2006) 953–964.
[87] P. Cavadini, G. Biasiotto, M. Poli, S. Levi, R. Verardi, I. Zanella, M. Derosas, R. Ingrassia, M. Corrado, P. Arosio, RNA silencing of the mitochondrial ABCB7 transporter in HeLa cells causes an iron-deficient phenotype with mitochondrial iron overload, Blood 109 (2007) 3552–3559.
[88] K. Sipos, H. Lange, Z. Fekete, P. Ullmann, R. Lill, G. Kispal, Maturation of cytosolic iron–sulfur proteins requires glutathione, J. Biol. Chem. 277 (2002) 26944–26949.
[89] D.J. Netz, J. Mascarenhas, O. Stehling, A.J. Pierik, R. Lill, Maturation of cytosolic and nuclear iron–sulfur proteins, Trends Cell. Biol. (2013 Dec 3), http://dx.doi.org/10.1016/j.tcb.2013.11.005.
[90] O. Stehling, D.J. Netz, B. Niggemeyer, R. Rosser, R.S. Eisenstein, H. Puccio, A.J. Pierik, R. Lill, Human Nbp35 is essential for both cytosolic iron–sulfur protein assembly and iron homeostasis, Mol. Cell. Biol. 28 (2008) 5517–5528.
[91] D.J. Netz, A.J. Pierik, M. Stumpfig, U. Muhlenhoff, R. Lill, The Cfd1-Nbp35 complex acts as a scaffold for iron–sulfur protein assembly in the yeast cytosol, Nat. Chem. Biol. 3 (2007) 278–286.
[92] D. Song, F.S. Lee, A role for IOP1 in mammalian cytosolic iron–sulfur protein biogenesis, J. Biol. Chem. 283 (2008) 9231–9238.
[93] J. Balk, A.J. Pierik, D.J. Netz, U. Muhlenhoff, R. Lill, The hydrogenase-like Nar1p is essential for maturation of cytosolic and nuclear iron–sulphur proteins, EMBO J. 23 (2004) 2105–2115.
[94] V. Srinivasan, D.J. Netz, H. Webert, J. Mascarenhas, A.J. Pierik, H. Michel, R. Lill, Structure of the yeast WD40 domain protein Cia1, a component acting late in iron–sulfur protein biogenesis, Structure 15 (2007) 1246–1257.
[95] J. Balk, D.J. Aguilar Netz, K. Tepper, A.J. Pierik, R. Lill, The essential WD40 protein Cia1 is involved in a late step of cytosolic and nuclear iron–sulfur protein assembly, Mol. Cell. Biol. 25 (2005) 10833–10841.
[96] Y. Zhang, E.R. Lyver, E. Nakamaru-Ogiso, H. Yoon, B. Amutha, D.W. Lee, E. Bi, T. Ohnishi, F. Daldal, D. Pain, A. Dancis, Dre2, a conserved eukaryotic Fe/S

cluster protein, functions in cytosolic Fe/S protein biogenesis, Mol. Cell. Biol. 28 (2008) 5569–5582.
[97] T. Land, T.A. Rouault, Targeting of a human iron–sulfur cluster assembly enzyme, nifs, to different subcellular compartments is regulated through alternative AUG utilization, Mol. Cell. 2 (1998) 807–815.
[98] Y. Shi, M.C. Ghosh, W.H. Tong, T.A. Rouault, Human ISD11 is essential for both iron–sulfur cluster assembly and maintenance of normal cellular iron homeostasis, Hum. Mol. Genet. 18 (2009) 3014–3025.
[99] W.H. Tong, T.A. Rouault, Functions of mitochondrial ISCU and cytosolic ISCU in mammalian iron–sulfur cluster biogenesis and iron homeostasis, Cell. Metab. 3 (2006) 199–210.
[100] Z. Marelja, M. Mullick Chowdhury, C. Dosche, C. Hille, O. Baumann, H.G. Lohmannsroben, S. Leimkuhler, The L-cysteine desulfurase NFS1 is localized in the cytosol where it provides the sulfur for molybdenum cofactor biosynthesis in humans, PLoS One 8 (2013) e60869.
[101] M. Cossee, M. Schmitt, V. Campuzano, L. Reutenauer, C. Moutou, J.L. Mandel, M. Koenig, Evolution of the Friedreich's ataxia trinucleotide repeat expansion: founder effect and premutations, Proc. Natl. Acad. Sci. U. S. A. 94 (1997) 7452–7457.
[102] A.H. Koeppen, Friedreich's ataxia: pathology, pathogenesis, and molecular genetics, J. Neurol. Sci. 303 (2011) 1–12.
[103] A.E. Harding, R.L. Hewer, The heart disease of Friedreich's ataxia: a clinical and electrocardiographic study of 115 patients, with an analysis of serial electrocardiographic changes in 30 cases, Q. J. Med. 52 (1983) 489–502.
[104] A. Rotig, P. de Lonlay, D. Chretien, F. Foury, M. Koenig, D. Sidi, A. Munnich, P. Rustin, Aconitase and mitochondrial iron–sulphur protein deficiency in Friedreich ataxia, Nat. Genet. 17 (1997) 215–217.
[105] J.B. Lamarche, M. Cote, B. Lemieux, The cardiomyopathy of Friedreich's ataxia morphological observations in 3 cases, Can. J. Neurol. Sci. 7 (1980) 389–396.
[106] M. Emond, G. Lepage, M. Vanasse, M. Pandolfo, Increased levels of plasma malondialdehyde in Friedreich ataxia, Neurology 55 (2000) 1752–1753.
[107] J.B. Schulz, T. Dehmer, L. Schols, H. Mende, C. Hardt, M. Vorgerd, K. Burk, W. Matson, J. Dichgans, M.F. Beal, M.B. Bogdanov, Oxidative stress in patients with Friedreich ataxia, Neurology 55 (2000) 1719–1721.
[108] A. Saveliev, C. Everett, T. Sharpe, Z. Webster, R. Festenstein, DNA triplet repeats mediate heterochromatin-protein-1-sensitive variegated gene silencing, Nature 422 (2003) 909–913.
[109] S. Schmucker, H. Puccio, Understanding the molecular mechanisms of Friedreich's ataxia to develop therapeutic approaches, Hum. Mol. Genet. 19 (2010) R103–R110.
[110] V. Campuzano, L. Montermini, M.D. Molto, L. Pianese, M. Cossee, F. Cavalcanti, E. Monros, F. Rodius, F. Duclos, A. Monticelli, et al., Friedreich's ataxia: autosomal recessive disease caused by an intronic GAA triplet repeat expansion, Science 271 (1996) 1423–1427.
[111] M. Cossee, A. Durr, M. Schmitt, N. Dahl, P. Trouillas, P. Allinson, M. Kostrzewa, A. Nivelon-Chevallier, K.H. Gustavson, A. Kohlschutter, U. Muller, J.L. Mandel, A. Brice, M. Koenig, F. Cavalcanti, A. Tammaro, G. De Michele, A. Filla, S. Cocozza, M. Labuda, L. Montermini, J. Poirier, M. Pandolfo, Friedreich's ataxia: point mutations and clinical presentation of compound heterozygotes, Ann. Neurol. 45 (1999) 200–206.
[112] C. Gellera, B. Castellotti, C. Mariotti, R. Mineri, V. Seveso, S. Didonato, F. Taroni, Frataxin gene point mutations in Italian Friedreich ataxia patients, Neurogenetics 8 (2007) 289–299.
[113] M. Cossee, H. Puccio, A. Gansmuller, H. Koutnikova, A. Dierich, M. LeMeur, K. Fischbeck, P. Dolle, M. Koenig, Inactivation of the Friedreich ataxia mouse gene leads to early embryonic lethality without iron accumulation, Hum. Mol. Genet. 9 (2000) 1219–1226.
[114] A. Martelli, M. Napierala, H. Puccio, Understanding the genetic and molecular pathogenesis of Friedreich's ataxia through animal and cellular models, Dis. Model. Mech. 5 (2012) 165–176.
[115] M.G. Cotticelli, L. Rasmussen, N.L. Kushner, S. McKellip, M.I. Sosa, A. Manouvakhova, S. Feng, E.L. White, J.A. Maddry, J. Heemskerk, R.J. Oldt, L.F. Surrey, R. Ochs, R.B. Wilson, Primary and secondary drug screening assays for Friedreich ataxia, J. Biomol. Screen 17 (2012) 303–313.
[116] L.E. Larsson, H. Linderholm, R. Mueller, T. Ringqvist, R. Soernaes, Hereditary metabolic myopathy with *Paroxysmal myoglobinuria* due to abnormal glycolysis, J. Neurol. Neurosurg. Psychiatry 27 (1964) 361–380.
[117] R.E. Hall, K.G. Henriksson, S.F. Lewis, R.G. Haller, N.G. Kennaway, Mitochondrial myopathy with succinate dehydrogenase and aconitase deficiency. Abnormalities of several iron–sulfur proteins, J. Clin. Invest. 92 (1993) 2660–2666.
[118] F. Mochel, M.A. Knight, W.H. Tong, D. Hernandez, K. Ayyad, T. Taivassalo, P.M. Andersen, A. Singleton, T.A. Rouault, K.H. Fischbeck, R.G. Haller, Splice mutation in the iron–sulfur cluster scaffold protein ISCU causes myopathy with exercise intolerance, Am. J. Hum. Genet. 82 (2008) 652–660.
[119] A. Olsson, L. Lind, L.E. Thornell, M. Holmberg, Myopathy with lactic acidosis is linked to chromosome 12q23.3-24.11 and caused by an intron mutation in the ISCU gene resulting in a splicing defect, Hum. Mol. Genet. 17 (2008) 1666–1672.
[120] P.S. Sanaker, M. Toompuu, V.E. Hogan, L. He, C. Tzoulis, Z.M. Chrzanowska-Lightowlers, R.W. Taylor, L.A. Bindoff, Differences in RNA processing underlie the tissue specific phenotype of ISCU myopathy, Biochim. Biophys. Acta 1802 (2010) 539–544.
[121] A. Nordin, E. Larsson, L.E. Thornell, M. Holmberg, Tissue-specific splicing of ISCU results in a skeletal muscle phenotype in myopathy with lactic acidosis, while complete loss of ISCU results in early embryonic death in mice, Hum. Genet. 129 (2011) 371–378.
[122] G. Kollberg, M. Tulinius, A. Melberg, N. Darin, O. Andersen, D. Holmgren, A. Oldfors, E. Holme, Clinical manifestation and a new ISCU mutation in iron–sulphur cluster deficiency myopathy, Brain 132 (2009) 2170–2179.
[123] G. Kollberg, E. Holme, Antisense oligonucleotide therapeutics for iron–sulphur cluster deficiency myopathy, Neuromuscul. Disord. 19 (2009) 833–836.
[124] S.C. Lim, M. Friemel, J.E. Marum, E.J. Tucker, D.L. Bruno, L.G. Riley, J. Christodoulou, E.P. Kirk, A. Boneh, C. Degennaro, M. Springer, V.K. Mootha, T.A. Rouault, S. Leimkuhler, D.R. Thorburn, A.G. Compton, Mutations in LYRM4, encoding iron–sulfur cluster biogenesis factor ISD11, cause deficiency of multiple respiratory chain complexes, Hum. Mol. Genet. 22 (22) (2013) 4460–4473.
[125] C. Camaschella, A. Campanella, L. De Falco, L. Boschetto, R. Merlini, L. Silvestri, S. Levi, A. Iolascon, The human counterpart of zebrafish shiraz shows sideroblastic-like microcytic anemia and iron overload, Blood 110 (2007) 1353–1358.
[126] R.A. Wingert, J.L. Galloway, B. Barut, H. Foott, P. Fraenkel, J.L. Axe, G.J. Weber, K. Dooley, A.J. Davidson, B. Schmid, B.H. Paw, G.C. Shaw, P. Kingsley, J. Palis, H. Schubert, O. Chen, J. Kaplan, L.I. Zon, Deficiency of glutaredoxin 5 reveals Fe–S clusters are required for vertebrate haem synthesis, Nature 436 (2005) 1035–1039.
[127] A. Di Fonzo, D. Ronchi, T. Lodi, E. Fassone, M. Tigano, C. Lamperti, S. Corti, A. Bordoni, F. Fortunato, M. Nizzardo, L. Napoli, C. Donadoni, S. Salani, F. Saladino, M. Moggio, N. Bresolin, I. Ferrero, G.P. Comi, The mitochondrial disulfide relay system protein GFER is mutated in autosomal-recessive myopathy with cataract and combined respiratory-chain deficiency, Am. J. Hum. Genet. 84 (2009) 594–604.
[128] K. Hell, The Erv1-Mia40 disulfide relay system in the intermembrane space of mitochondria, Biochim. Biophys. Acta 1783 (2008) 601–609.
[129] R.A. Pagon, T.D. Bird, J.C. Detter, I. Pierce, Hereditary sideroblastic anaemia and ataxia: an X linked recessive disorder, J. Med. Genet. 22 (1985) 267–273.
[130] K.D. Hellier, E. Hatchwell, A.S. Duncombe, J. Kew, S.R. Hammans, X-linked sideroblastic anaemia with ataxia: another mitochondrial disease? J. Neurol. Neurosurg. Psychiatr. 70 (2001) 65–69.
[131] J. Boultwood, A. Pellagatti, M. Nikpour, B. Pushkaran, C. Fidler, H. Cattan, T.J. Littlewood, L. Malcovati, M.G. Della Porta, M. Jadersten, S. Killick, A. Giagounidis, D. Bowen, E. Hellstrom-Lindberg, M. Cazzola, J.S. Wainscoat, The role of the iron transporter ABCB7 in refractory anemia with ring sideroblasts, PLoS One 3 (2008) e1970.
[132] M. Nikpour, C. Scharenberg, A. Liu, S. Conte, M. Karimi, T. Mortera-Blanco, V. Giai, M. Fernandez-Mercado, E. Papaemmanuil, K. Hogstrand, M. Jansson, I. Vedin, J. Stephen Wainscoat, P. Campbell, M. Cazzola, J. Boultwood, A. Grandien, E. Hellstrom-Lindberg, The transporter ABCB7 is a mediator of the phenotype of acquired refractory anemia with ring sideroblasts, Leukemia 27 (2013) 889–896.
[133] C. Camaschella, Recent advances in the understanding of inherited sideroblastic anaemia, Br. J. Haematol. 143 (2008) 27–38.
[134] A. Goraca, H. Huk-Kolega, A. Piechota, P. Kleniewska, E. Ciejka, B. Skibska, Lipoic acid - biological activity and therapeutic potential, Pharmacol. Rep. 63 (2011) 849–858.
[135] J.A. Mayr, F.A. Zimmermann, C. Fauth, C. Bergheim, D. Meierhofer, D. Radmayr, J. Zschocke, J. Koch, W. Sperl, Lipoic acid synthetase deficiency causes neonatal-onset epilepsy, defective mitochondrial energy metabolism, and glycine elevation, Am. J. Hum. Genet. 89 (2011) 792–797.
[136] K.P. Shay, R.F. Moreau, E.J. Smith, A.R. Smith, T.M. Hagen, Alpha-lipoic acid as a dietary supplement: molecular mechanisms and therapeutic potential, Biochim. Biophys. Acta 1790 (2009) 1149–1160.
[137] A. Suomalainen, Therapy for mitochondrial disorders: little proof, high research activity, some promise, Semin. Fetal Neonatal. Med. 16 (2011) 236–240.
[138] Y. Shiloh, Y. Ziv, The ATM protein kinase: regulating the cellular response to genotoxic stress, and more, Nat. Rev. Mol. Cell. Biol. 14 (2013) 197–210.
[139] B. Galy, D. Ferring-Appel, S.W. Sauer, S. Kaden, S. Lyoumi, H. Puy, S. Kolker, H.J. Grone, M.W. Hentze, Iron regulatory proteins secure mitochondrial iron sufficiency and function, Cell. Metab. 12 (2010) 194–201.
[140] M.W. Hentze, M.U. Muckenthaler, B. Galy, C. Camaschella, Two to tango: regulation of mammalian iron metabolism, Cell 142 (2010) 24–38.
[141] B. Roche, L. Aussel, B. Ezraty, P. Mandin, B. Py, F. Barras, Iron/sulfur proteins biogenesis in prokaryotes: formation, regulation and diversity, Biochim. Biophys. Acta 1827 (2013) 455–469.

1.6.1 Conclusion from the review work

The present review on mammalian Fe-S cluster biogenesis and its implication in disease concludes with Fe-S clusters being versatile cofactors found in a variety of different proteins. Fe-S cluster biogenesis requires a conserved protein machinery and rare diseases are linked to Fe-S cluster biogenesis. These dysfunctions manifest mostly with a mitochondrial phenotype and provided information as to the role of the mutated proteins during Fe-S biogenesis. Still, many aspects of mammalian Fe-S biogenesis and the molecular functions of different proteins involved remain to be investigated. Eventually, *in vivo* models will help to refine our knowledge on mammalian physiology.

1.6.2 Newly described diseases linked to mutations in Fe-S proteins and biogenesis

Since the publication of the review, a few additional mutations linked to Fe-S biogenesis have been discovered lately, which will be briefly described here.

An infantile mitochondrial complex II/complex III deficiency was described to be caused by missense mutations in *NFS1* (c.215G>A, p.R72Q (Farhan, Wang et al. 2014). This autosomal recessive disease affected three children of a consangenious family and was characterized by lactic acidosis, hypotonia, complex II and complex III deficiency with multi-organ failure and abnormal mitochondria. The mutation leads to markedly reduced mRNA and protein levels of NFS1, consequently proposed to result in reduced complex II/ complex III activities in muscle and liver tissue. In line with current models of NFS1 function, ISD11 could not be co-immunoprecipitated with the mutated NFS1 from patient cells suggesting a disruption of the NFS1-ISD11 interaction known to be required for NFS1 stability (Wiedemann, Urzica et al. 2006; Pandey, Yoon et al. 2011).

Cases of 'variant nonketonic hyperglycemia' were uncovered to be caused by novel mutations in *LIAS, BOLA3* and *GLRX5* (Baker, Friederich et al. 2014). 'Variant nonketonic hyperglycemia' includes all patients with nonketonic hyperglycemia and deficient glycine cleavage enzyme activity without mutations in AMT, GLDC or GCSH, three key proteins of the glycine cleavage system. Novel mutations in *BOLA3* (c.136C>T, p.R46X) and *GLRX5* (c.151_153delAAG, p.K51del, and in one patient combined with c.82_83insGCGTGCGG, p.G28Gfs*25) were identified as likely causative mutations. The *BOLA3* patients showed slightly reduced levels of lipoic acid (LA) on the PDH and KGDH complexes in patient fibroblasts, but further analysis is missing for these patients. Although GLRX5 proteins levels seemed unaffected in three other patients, the mutation in the highly conserved glutaredoxin domain lies in proximity to the Fe-S cluster binding site. Strongly decreased levels of LA on PDH and KGDH complexes in patient fibroblasts were restored after transfection with full length GLRX5. This is the

first mutation described for *GLRX5* that leads to a neurological phenotype raising the question of tissue specificity, since previously *GLRX5* mutation was reported to be restricted to the hematopoetic system (Ye, Jeong et al. 2010).

Wydro and Balk had specified on *IND1* mutations, precisely on the effect of one of the compound heterozygous alleles (c.815-27T>C) in a yeast *Yarrowia lipolytica* model. The mutation results in decreased Ind1 protein levels leading to severely decreased complex I activity. A potential dominant-negative effect of the mutation was also excluded (Wydro, Sharma et al. 2013).

1.7 Aims of the PhD project

At my arrival in the laboratory in 2011, Alain Martelli and our collaborator Sandrine Ollagnier de Choudens in Grenoble had characterized mouse ISCA1 and ISCA2 using different biochemical and biophysical techniques to investigate whether ISCA1 and potentially ISCA2 could function as iron donors during Fe-S cluster assembly. Up to that point, a thorough characterization of any eukaryotic A-type protein was still missing. They showed that ISCA1 and ISCA2 are directly purified as Fe-S-containing homo-dimers when expressed in bacteria. Both proteins share high sequence homology and can harbor a Fe_2S_2 cluster, which can be transferred to classical Fe_2S_2 and Fe_4S_4 acceptor proteins *in vitro*. However, the respective clusters show different sensitivity to oxidation and, while holo-ISCA1 is purified under aerobic conditions, holo-ISCA2 required anaerobic conditions.

That being said, together with the importance of A-type proteins throughout phyla, the discrepancies on molecular functions and roles as well as the lack of knowledge for the mammalian A-type, lead to my thesis project.

The goal of my PhD project was thus to elucidate the *in vivo* role of mouse ISCA1 and ISCA2, by characterizing their interactions as well as the effect of knocking down the proteins *in vivo*. The main question I address in my work is: Why is it that the mouse possesses two A-type proteins that show different properties albeit high sequence similarities? In other words, are ISCA1 and ISCA2 functionally redundant *in vivo*?

Please note that at the time my thesis project was initiated, neither the latest data on yeast A-type proteins (Muhlenhoff, Richter et al. 2011) nor on ISCA-knockdown in HeLa cells (Sheftel, Wilbrecht et al. 2012) were yet published.

To address ISCA1 and ISCA2 role(s) *in vivo*, I have used co-immunoprecipiations coupled to large-scale proteomics as well as AAV (Adeno-associated virus) -delivered shRNA-mediated knockdown *in vivo*. Since knockdown *in vivo* lead to a phenotype for ISCA1 only, different approaches were tested to elucidate the role for ISCA2. Eventually, I addressed whether ISCA1 and ISCA2 are functionally redundant proteins.

1.8 Biological questions

In order to further our understanding of the mammalian A-type proteins, I used different approaches to answer the following questions:

1.8.1 What are the interacting proteins of ISCA1 and ISCA2 *in vivo*?

Heterologous co-expression experiments in bacteria in the lab had provided an interaction network for the ISCA-proteins suggesting a function for the ISCAs in mitochondrial Fe-S distribution. Based on that, I addressed whether these and other interaction take place in cells by co-immunoprecipitations combined with mass spectrometry analysis.

1.8.2 What is the phenotype upon knockdown of ISCA1 or ISCA2 *in vivo?*

Knockdown or knockout models for the A-type proteins had not been published when this project started. I established a novel mouse model using a viral-induced knockdown approach to address the role of ISCA1 and ISCA2. It further examined whether functional redundancy between ISCA1 and ISCA2 mitigates the phenotype observed upon deletion of single A-type proteins in other model systems.

2. Introduction to the paper

This part shall allow integration of the approaches taken in the thesis work into the context of the literature and previous work performed in this project. It will thus provide the reasoning behind my thesis work and outline the methods.

2.1 Interaction study

To our knowledge, few protein interactions with prokaryotic A-type proteins were described in the literature: Ollagnier-de-Choudens and colleagues showed that recombinant *E. coli* IscA could interact with Fdx *in vitro* (Ollagnier-de-Choudens, Mattioli et al. 2001), whereas Chahal and colleagues provided evidence that SufA can bind the SufBCD complex during the transfer of the nascent Fe-S cluster to SufA (Chahal, Dai et al. 2009). In yeast, Isa1 bound Isa2 and both were co-immunoprecipitated by Iba57 and the interaction was confirmed by reverse immunoprecipitation (Gelling, Dawes et al. 2008; Muhlenhoff, Richter et al. 2011). Both Isa proteins were also described to interact with Grx5 (Vilella, Alves et al. 2004; Kim, Chung et al. 2010). Finally, recent evidence for a cluster transfer from human GLRX5 to human ISCA1 and ISCA2 *in vitro* suggests that ISCAs and GLRX5 may interact in mammalian cells (Banci, Brancaccio et al. 2014). Thus, the global interactome has not been addressed and interactions reported so far are poorly characterized.

Previous interaction studies on the mammalian A-type proteins in the lab had used heterologous co-expression of recombinant mouse ISCA1 and ISCA2 to determine possible direct protein partners. Combinations of ISCA1 or ISCA2 with the different components of mammalian Fe-S biogenesis had shown direct interaction of ISCA1 with ISCA2 and each of them with IBA57, GLRX5 and NFU1. In parallel, direct interaction of ISCA1 and ISCA2 with other proteins of nascent Fe-S cluster assembly, NFS1 and ISCU as well as the chaperone HSCB, was not observed.

One main aim was to address the interaction network for mammalian ISCA1 and ISCA2 in cells in order to decipher the role and mechanistic involvement of ISCA proteins within Fe-S cluster biogenesis.

2.1.1 The approach

I choose to develop an unbiased approach based on immunoprecipitation coupled to mass spectrometry analysis (multidimensional protein identification technology, MudPIT) from HeLa cells overexpressing the Flag-tagged mouse proteins. In addition to address potential interactions by using ISCA1 and ISCA2 as baits, I also overexpressed and analyzed the interaction of Flag-tagged IBA57,

NFU1 and GLRX5 as well as FDX2. All steps concerning mass spectrometry analysis were performed at the IGBMC proteomic platform and in close collaboration with Marjorie Fournier (IGBMC).

2.1.1.1 Workflow

The workflow (Figure 12) employed (1) transient expression of murine C-terminally Flag-tagged protein, (2) mitochondrial enrichment and cell lysis, (3) immunoprecipitation via Flag antibody-coupled beads, (4) MudPIT (5) proteomic-bioinformatic analyses to filter and identify co-isolated proteins and (6) biological validation.

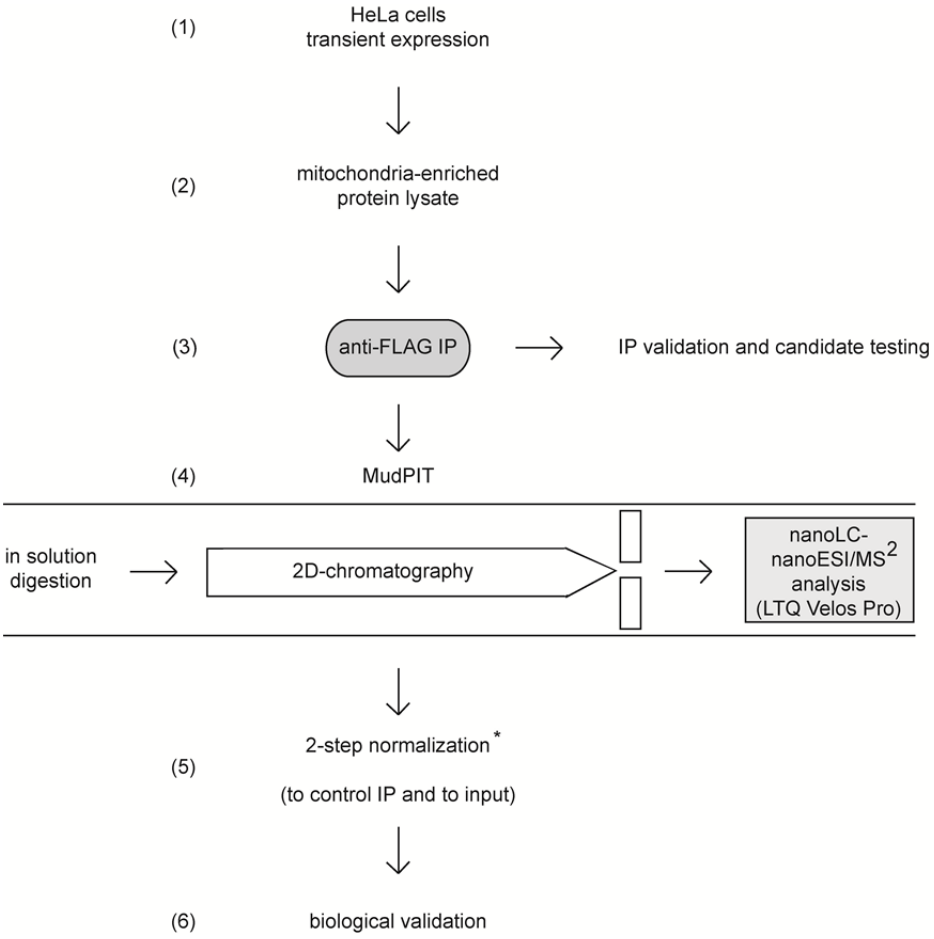

Figure 12: Scheme illustrating the workflow employed to uncover ISCA1 and ISCA2 interactions in cells.

Mitochondria-enriched protein lysates of HeLa cells transiently expressing Flag-tagged bait proteins were used for immunoprecipitations (1-3). IP procedure was validated by western blot analysis prior to MudPIT. For MudPIT analysis, samples were digested in solution before separation by 2D-chromatography and tandem mass spectromerty by nanoLC-nanoESI/MS^2 analysis using the LTQ Velos (Pro) (4). Data mining included a two-step normalization, which is specified below (5). Interactions were validated by western blot (6).

2.1.1.2 Cells and transfections

Fe-S biogenesis proteins are ubiquitously expressed, although prominent expression differences amongst tissues are reported for several Fe-S biogenesis proteins (i.e. for GLRX5 and ABCB7 (Allikmets, Raskind et al. 1999; Wingert, Galloway et al. 2005; Pondarre, Antiochos et al. 2006; Beilschmidt and Puccio 2014)) and also found for the A-type proteins (manuscript Figure S4). However, specific expression differences of all Fe-S biogenesis proteins between tissues or cell types were not systematically investigated yet. I sought to address ISCA1 and ISCA2 interaction in mammalian cultured HeLa cells, given the fact that this cervical cancer cells express mitochondrial Fe-S biogenesis proteins in a level that is detectable by mass spectrometry (Schmucker, Martelli et al. 2011). In addition, HeLa cells can easily be transfected.

Transient transfections were used to generate cells expressing C-terminally Flag-tagged murine ISCA1, ISCA2 or one of the other baits selected from the previous *in vitro* interaction studies (IBA57, GLRX5, NFU1 and FDX2). Immunoprecipitations of overexpressed proteins was chosen over immunoprecipitation of endogenous proteins for several reasons: first, specific antibodies for immunoprecipitations were not available for all proteins of interest and second, the increased risk that the antibody could mask an interaction site, in particular for smaller proteins. All bait proteins are nuclear encoded and thus need to be imported into the mitochondria. Although not studied in detail for all the proteins of interest, most of the reported mitochondrial targeting sequences are N-terminal amino acid stretches rich in acidic residues that are processed upon import into the mitochondria (Chacinska, Koehler et al. 2009) (see 87.1). Accordingly, C-terminal tags were used throughout the study. Expression of murine homologues in a human cell line was performed, based on the assumption that protein-protein interactions are conserved between mammalian homologues due to the high degree of conservation. For instance, comparing the mouse and human protein sequence alignment of ISCA1 and ISCA2 with the respective homologues shows a difference of only 2 amino acids for ISCA1 and 1 amino acid for ISCA2 (see 87.1). Transient expression durations were kept between 24 and 48 h.

2.1.1.3 Cell lysates

Mitochondrial enrichment (using digitonin 0,001%) prior to protein extraction was performed to increase the chance of detection of relevant interactions and decreased putative unspecific binding and transport-related interactions of a cytoplasmic precursor, since enrichment of the subcellular localization of interest is strongly advised to decrease complexity of the sample (Liu, Qian et al. 2004). Although protein spectral counts (PSM) were shown as reliable semi-quantitative measure of protein abundance, it was also shown that the detection of small proteins is underrepresented in the presence of high abundance or large proteins. Still, in the approach taken here the relatively non-

stringent treatment could not exclude the presence of cytoplasmic or nuclear proteins. During the entire experiment the samples were processed quickly and strictly at 4°C to avoid disruption of mitochondria prior to the protein extraction and potential protein degradation.

2.1.1.4 Immunoprecipitation

Based on previous observations that protein stability and therefore also the interaction stability of overexpressed ISCA1 and ISCA2 may be low, incubation of the protein extract with Flag antibody coupled beads was kept relatively short (two hours) and always performed directly subsequent to the extraction. By adjusting the ratio of tagged protein to beads towards a slight excess of tagged protein, saturation of the beads with bait protein was ensured and unspecific binding likely decreased. Samples were washed twice with PBS, before elution using acidic conditions.

2.1.1.5 MudPIT

As the mass spectrometry approach of choice I sought to uncover interactions using multidimensional protein identification technology (MudPIT), also termed “shotgun” proteomics that combines liquid chromatography (LC) with tandem mass spectrometry (ESI-MS^2). This gel-free approach resolves complex peptide mixtures by high-pressure liquid chromatography prior to the MS, therefore improving detection coverage and sensitivity. Prior to MudPIT, protein samples were digested by trypsin, which cleaves C-terminally to lysine and arginine residues, therefore generating smaller peptides. Resulting spectra are mapped to peptide sequences and IDs in the human Swissprot database (version from *2012-10)*. Human protein sequence of the respective bait protein was replaced by the Flag-tagged murine protein sequence to avoid double counting afterwards. This part of the analysis was performed by the Proteomics platform of the IGBMC. During normalization and analysis exclusively the human protein sequences and annotations were used to enable merging of the datasets.

2.1.1.6 Data mining

The total spectral counts (or PSM) in the samples were used to determine protein abundance and to normalize for the relative enrichment over controls (Figure 13). Using spectral counts for relative protein quantification was proven to be reliable (Liu, Qian et al. 2004) and that the total cumulative spectral count (PSM) in a MudPIT experiment is directly correlated to the relative protein abundance (Liu, Qian et al. 2004; Kislinger and Emili 2005).

For accurate and reliable detection of protein-protein interaction, datasets of spectral counts were filtered and analyzed as follows (Figure 13). Analyses were performed for three biological IP replicates per bait to normalize for run-to-run differences. Further normalization was performed to reduce number of false-positives. Each replicate was normalized first against one control-IP (CTL-IP)

(Step 1) and second against two mitochondria-enriched non-transfected input replicates (Step 2). For normalization two different stringency criteria were applied in parallel to allow comparison of abundance or strength of interactions, and proteins were filtered to be enriched 2x (low stringency) and 10x (high stringency) over controls, respectively.

Subsequently, the two step normalized datasets of each bait replicate were merged to get the Sum PSM dataset (merging all PSM of all IPs of one bait for all different proteins after filtering) (Step 3).

To allow relative comparison of protein-protein interactions for each bait files were subsequently merged and normalized for protein size (Step 4) as follows. Since sample digestion creates a higher number of peptides for larger proteins than for smaller, the chance of detecting large proteins in increased. Accordingly, the total PSM of three bait replicates were normalized against the respective protein length (PSM/L). The normalized spectral abundance factor (NSAF) is then calculated the value PSM/L, divided by the sum of PSM/L for all proteins in the experiment (Zybailov, Mosley et al. 2006). Concomitantly, the filtered and merged bait datasets were analyzed for proteins that were detected at least in two out of the three replicates.

All datasets were further filtered to select for hits that are annotated as mitochondrial proteins in Uniprot.

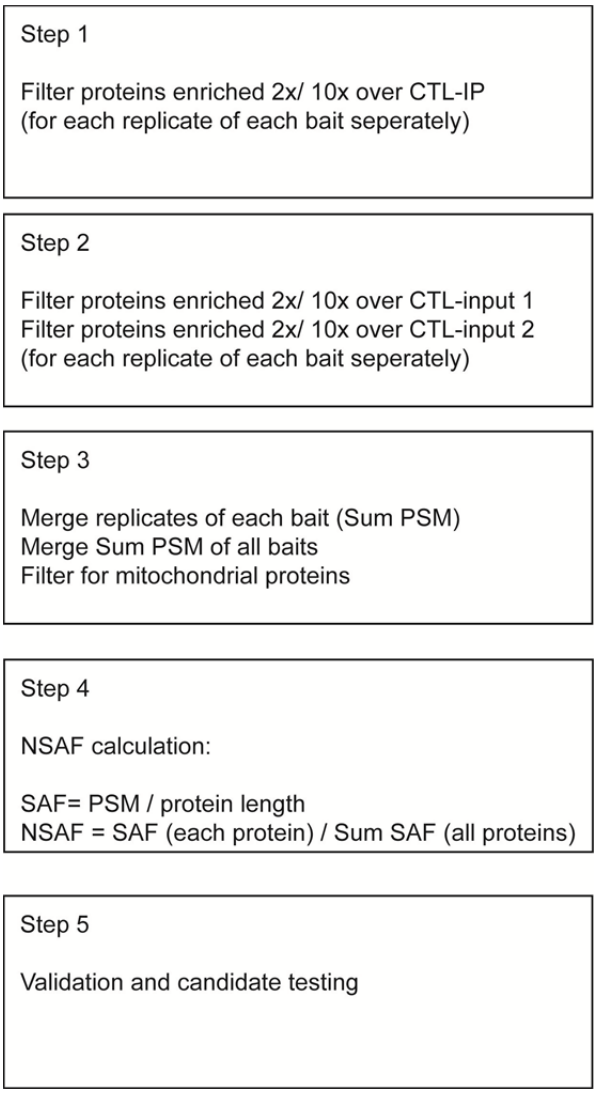

Figure 13: Representation of the Data mining process performed for the MudPIT analysis.

Each replicate of each bait was first filtered and normalized separately (Step 1 and Step 2). Data were then merged and selected for mitochondrial proteins (Step 3). Then, data were normalized for protein size, abundance and coverage of the whole IP set (Step 4) before validation and candidate testing (Step 5).

2.1.1.7 Validation and candidate testing

After these normalization steps, selection of interesting candidates was done on the following basis. First, enrichment specifically for mitochondrial Fe-S biogenesis proteins was tested. Second, known mitochondrial Fe-S proteins were checked. Third, the different subsets of proteins were analyzed by unbiased approaches (see 4.1.4).

2.2 *In vivo* model for ISCA1 and ISCA2

Aim of this part of the study was to generate a model for investigation of direct consequences of loss-of ISCA1 or ISCA2 function *in vivo*. We choose to perform a knockdown of A-type proteins for several reasons: First, constitutive knockout models of different Fe-S biogenesis proteins were shown to be embryonically lethal (as for FXN and ABCB7 (Puccio, Simon et al. 2001; Pondarre, Antiochos et al. 2006)) and thus possibility of ISCA-protein knockout being lethal could not be excluded. Second, tissue specific knockouts would have been valid to model loss of ISCA protein function, but creation of knockout models (including tissue specific knockouts) is very time consuming and costly.
For the present study, it was attempted to target early phenotypic consequences. I targeted ISCA1 and ISCA2 function by local knockdown in the mouse. To deliver specific shRNA to the targeted tissue, injection of adeno-associated virus (AAV) was used.

2.2.1 Biology of AAV

AAVs belong to the group of parvoviruses. The non-enveloped, single strand DNA virus is non-integrative and non-pathogenic. Its wild type genome spans 4,7 kb with open reading frames encoding for replication (*rep*) and capsid proteins (*cap*). AAVs were described to have low immune- and genotoxicity *in vivo* compared to other recombinant vectors derived from adenovirus or retrovirus (Berns 1990; Mays and Wilson 2011; Grieger and Samulski 2012). The first recombinant AAV (rAAV) vector was generated in 1982 by Samulski and colleagues (Samulski, Berns et al. 1982). Subsequent developments enabled the total absence of the wild type genome, and the safety for handling and production of rAAV was highly increased by encoding different genes for encapsidation and the transgene on different plasmids for production by co-transfection (Ferrari, Xiao et al. 1997). Today, the transgene of rAAVs is flanked only by the inverted terminal repeats (ITRs) of AAV2 (AAV serotype 2), as requirement for packaging the DNA into capsids (Rabinowitz, Rolling et al. 2002; Schultz and Chamberlain 2008; Mays and Wilson 2011). Different serotypes are known, which are distinguished by different capsid motifs mainly found in the surface regions of the capsids. The serotypes or capsid variants determine cell tropism and the susceptibility to neutralizing antibodies. 2012 more than 12 different serotypes and 120 capsid variants were known (Mays and Wilson 2011; Weinberg, Samulski et al. 2013).

For (trans-) gene expression, the virus needs to transduce the cells and the single-stranded genome needs to be converted to double-stranded DNA (Figure 14). Notably, for transduction different pathways can be utilized seemingly depending on the serotype, the dose and the targeted cell type. Here, a model of the potentially common principle is described. The AAV attaches to the cell at certain surface receptors and is subsequently internalized mainly via endocytosis (Ortolano, Spuch et

al. 2012). Endosomal processing and trafficking of the virions are critical for transduction and described to be rate-limiting steps. For both, the cellular surface receptors for AAV binding and the intracellular trafficking pathways, different mechanisms and pathways were reported (Xiao, Lentz et al. 2012). The virus escapes the endosomal compartment in the cytoplasm, before it enters the nucleus, where the virus is uncoated (Buning, Perabo et al. 2008). To enable transcription of the genome, free ends of the ITRs are used as primers for generation of double-stranded DNA; this step is described to be most rate-limiting (Wang, Ma et al. 2003; Grieger and Samulski 2012). The AAV genome resides as episomes in the nucleus (Schultz and Chamberlain 2008). Of note, most studies on wild type AAV to understand its biology are performed on AAV2; thus the described features are mostly for AAV2 and differences between serotypes and engineered vectors are likely.

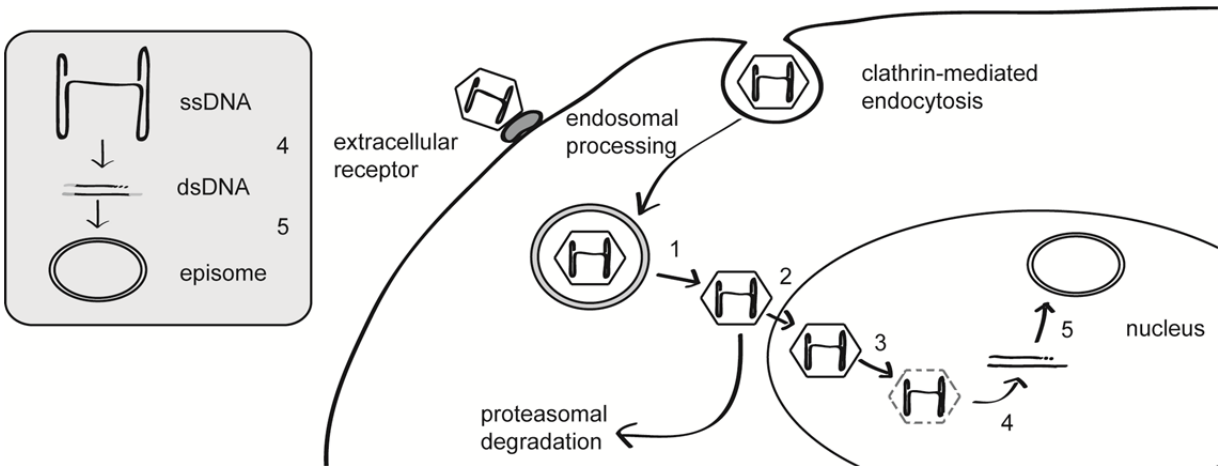

Figure 14: Schematic representation of cell transduced by AAV.

AAVs bind receptors on the cell surface and are internalized by endocytosis (mostly clathrin-mediated), AAVs exit the endosomal pathway (1) and get either degraded by the proteasome or enter the nucleus (2). After uncoating of the virus (3), dsDNA is buils from the ssDNA (4) and resides in the cell mostly as non-integrated eposime (5). Generation of episomes (4, 5) is shown in the inset; this is a rate-limiting step of successful transduction. ssDNA: single stranded DNA, dsDNA: double stranded DNA. Adapted from Buning *et al.* 2008.

2.2.2 Choice of route of administration, serotype and vector

Different routes of rAAV administration have been previously used for different scientific purposes. While local administration of rAAV is advantageous to target a very specific region of interest, the serotype further determines the tropism.

It was previously determined in the lab, that ISCA proteins are highly expressed in skeletal muscle and heart, both mitochondria-rich tissues. While the skeletal muscle can be easily accessible for local administration by injection, direct targeting the heart would require surgical procedures. Therefore,

in the present study rAAV was injected locally in the tibialis anterior (TA), which is accessible by removing the fur from the hindlimbs. Prior to this study, local administration of rAAV serotype 2/1 into the TA has proven useful in house for transgene expression (Amoasii, Bertazzi et al. 2012). The vector of choice encodes specific shRNA under the mU6 promoter and eGFP under the CMV promoter.

3. Manuscript

ISCA1 is the required A-type protein
for the maturation of mitochondrial Fe_4S_4 proteins in mouse skeletal muscle

Lena Kristina Beilschmidt, Sandrine Ollagnier de Choudens, Marjorie Fournier, Stéphane Schmucker, Ioannis Sanakis, Nadia Messaddeq, Alain Martelli and Hélène Puccio

ISCA1 is the required A-type protein for the maturation of mitochondrial Fe_4S_4 proteins in mouse skeletal muscle

Lena Kristina Beilschmidt[1,3,4,5,6], Sandrine Ollagnier de Choudens[7], Marjorie Fournier[2,3,4,5,6], Stéphane Schmucker[1,3,4,5,6], Ioannis Sanakis[8], Nadia Messaddeq, Alain Martelli[1,3,4,5,6] and Hélène Puccio[1,3,4,5,6]

1 Translational Medicine and Neurogenetics, IGBMC (Institut de Génétique et de Biologie Moléculaire et Cellulaire, Illkirch, France
2 Functional Genomics and Cancer, IGBMC (Institut de Génétique et de Biologie Moléculaire et Cellulaire, Illkirch, France
3 Inserm U596, Illkirch, France
4 CNRS, UMR7104, Illkirch, France
5 Université de Strasbourg, Strasbourg, France
6 Collège de France, Chaire de Génétique Humaine, Illkirch, France
7 DSV/iRTSV/LCBM, UMR 5248 CEA (Commissariat à l'Energie Atomique) Université Grenoble I-CNRS/ Equipe Biocatalyse, CEA-Grenoble, 17 Rue des Martyrs, 38054 Grenoble Cedex 09, France
8 NCSR, Demokritos, Institut of Materials Science, 15310 Ag. Paraskevi, Attiki, Greece.

Correspondence to:
Alain Martelli: martelli@igbmc.fr
Hélène Puccio: hpuccio@igbmc.fr

Abstract

Iron-sulfur clusters (Fe-S) are cofactors that participate in a plethora of essential cellular processes. Mammalian A-type proteins, ISCA1 and ISCA2, are evolutionary conserved proteins involved in Fe-S biogenesis, but their respective role remains unclear. In the present work, we show that native ISCA1 and ISCA2 are unambiguously purified as Fe_2S_2-containing proteins and that both proteins are capable to function as Fe-S transfer proteins. Interestingly, we demonstrate that the Fe_2S_2 of each protein exhibit different sensibility to oxygen. Furthermore, we show that ISCAs interact predominantly with proteins of the late-acting mitochondrial Fe-S biogenesis, and although they can form a complex together, specific interactions suggest that each ISCA may also have a role in different protein complexes. Finally, *in vivo* knockdown experiments provide evidence that ISCA1, but not ISCA2, is required for mitochondrial Fe_4S_4 proteins in skeletal muscle, therefore suggesting that ISCA1 and ISCA2 may function in different pathways.

Key words: A-type proteins; ISCA1; ISCA2; iron-sulfur cluster; interaction; in vivo knockdown; skeletal muscle

Introduction

Iron-sulfur clusters (Fe-S) are ancient and essential cofactors that participate in a number of cellular processes ranging from DNA metabolism to mitochondrial respiration (Lill 2009; Beilschmidt and Puccio 2014). In eukaryotes, *de novo* Fe-S biogenesis takes place within mitochondria and relies on proteins that are mostly highly conserved, since homologues can be found in yeast and bacteria. During *de novo* Fe-S biogenesis, the cluster is assembled from inorganic iron and sulfur on a scaffold protein named ISCU. Sulfur is provided by a cysteine desulfurase consisting of NFS1 bound by ISD11 that form a complex with ISCU during cluster assembly (Wiedemann, Urzica et al. 2006; Raulfs, O'Carroll et al. 2008; Pandey, Yoon et al. 2011). Frataxin (FXN), the protein deficient in Friedreich ataxia, was shown to bind the ternary ISCU-NFS1-ISD11 complex and regulate the cysteine desulfurase activity and the iron entry (Tsai and Barondeau 2010; Colin, Martelli et al. 2013). Finally, electrons that are needed during the process are most likely provided by the ferredoxin FDX2 (Kim, Frederick et al. 2013). Once Fe-S is assembled on ISCU, additional proteins are then required to transfer the cluster to mitochondrial acceptor proteins. In parallel, a sulfur compound, most likely derived from glutathione, is provided by the *de novo* mitochondrial Fe-S machinery and is exported to the cytosol by the ABCB7 transporter where it is used as substrate to elaborate Fe-S for extra-mitochondrial acceptor proteins (Schaedler, Thornton et al. 2014).

A-type proteins are evolutionary conserved proteins involved in Fe-S biogenesis. In bacteria, several A-type proteins can co-exist. For instance, *E.coli* encodes three A-type proteins: IscA encoded by the *isc* operon, SufA encoded by the *suf* operon and ErpA (Loiseau, Gerez et al. 2007). In yeast *S. cerevisiae* and in mammals, two A-type proteins, ISCA1 (yeast Isa1) and ISCA2 (yeast Isa2), are nuclear-encoded and addressed to mitochondria. Despite their presence throughout phyla, the role of A-type proteins remains poorly understood.

Bacterial A-type proteins were reported to bind either iron (Ding and Clark 2004; Ding, Clark et al. 2004; Mapolelo, Zhang et al. 2013) or Fe-S (Krebs, Agar et al. 2001; Ollagnier-de-Choudens, Sanakis et al. 2004; Zeng, Geng et al. 2007; Gupta, Sendra et al. 2009), and accordingly to display a role either as iron donor (Ding and Clark 2004; Ding, Clark et al. 2004; Mapolelo, Zhang et al. 2013), in particular during Fe-S cluster assembly on IscU (Mapolelo 2012 Biochem, Ding 2004 Biochem, Ding 2004 J Biol Chem), or as Fe-S carrier/scaffold proteins that can provide Fe-S to acceptor proteins (Krebs, Agar et al. 2001; Ollagnier-de-Choudens, Sanakis et al. 2004; Zeng, Geng et al. 2007; Gupta, Sendra et al. 2009). Furthermore, in *E. coli*, only the double *IscA;SufA* deletion leads to a severe

phenotype, suggesting bacterial A-type proteins might be functionally redundant (Lu, Yang et al. 2008; Tan, Lu et al. 2009; Vinella, Brochier-Armanet et al. 2009).

In *S. cerevisiae*, isa1 and/or isa2 deletion strains are viable and were initially reported to present both mitochondrial and cytosolic Fe-S defects, thus further supporting their role in Fe-S biogenesis (Garland, Hoff et al. 1999; Jensen and Culotta 2000; Kaut, Lange et al. 2000; Pelzer, Muhlenhoff et al. 2000). However, Isa1 and Isa2, together with their binding partner Iba57, were recently shown to be specifically required in the maturation of mitochondrial Fe_4S_4 proteins (Gelling, Dawes et al. 2008; Muhlenhoff, Richter et al. 2011). Furthermore, similar data were obtained with human ISCA1 and ISCA2 through knockdown experiments in HeLa cells (Sheftel, Wilbrecht et al. 2012). Although these data provide a better understanding of the implication of A-type proteins in mammalian Fe-S biogenesis, the question of functional redundancy remains unclear since no phenotypic differences between ISCA1 and ISCA2 knockdown experiments could be observed.

To further elucidate the role of mammalian A-type proteins in Fe-S biogenesis and to address their specific roles, we characterized mouse ISCA1 and ISCA2 using multiple approaches. Both ISCA proteins were biochemically and spectroscopically characterized as Fe_2S_2-containing homodimers when expressed in bacteria, although presenting different sensitivity to oxygen. Clusters on ISCA1 and ISCA2 could be transferred *in vitro* to classical acceptor proteins, showing that native A-type proteins can function as carrier proteins. By screening for potential interaction partners, we identified direct binding of ISCA1 and ISCA2 as well as differential interactions with other proteins of the late-acting mitochondrial Fe-S machinery. Interestingly, preferential interaction of ISCA1 with subunits of the respiratory chain complex I was also observed. Finally, *in vivo* knockdown in mouse provided clear evidence that only ISCA1 is required for mitochondrial Fe_4S_4 proteins in skeletal muscle under normal physiological conditions. Collectively, our study unravels that ISCA1 and ISCA2 are two related Fe-S-containing proteins that have different roles in Fe-S biogenesis *in vivo*.

Results

Recombinant ISCA1 and ISCA2 are purified as Fe_2S_2 cluster-containing proteins

To determine the role of ISCA1 and ISCA2 in Fe-S biogenesis, we first biochemically and functionally characterized the recombinant proteins as-isolated from bacterial expression. His-tag proteins were overexpressed in *E. coli* BL21(DE3) under aerobic conditions at 37°C for ISCA2 and 19°C for ISCA1 to prevent inclusion bodies formation. In both cases, harvested

cells display a red-brown color suggesting the presence of an Fe-S. Purification using Ni-NTA column was performed under anaerobic conditions in order to avoid potential oxidation of the metallic center purification of each protein. Under these conditions, ISCA2 was obtained with a good purity (between 70% and 90%) as checked by SDS-PAGE (not shown) with a yield of 80 mg/5L culture. On an analytical Superdex-75 column ISCA2 eluted as a single symmetric peak corresponding to a dimeric form (theoretical mass of the monomer: 13 554 Da). Purified ISCA2 displayed a red color suggesting the presence of a Fe_2S_2 center. Analysis of iron and sulfide content revealed stoichiometric amounts of iron and sulfide with an average of 0.9 iron and sulfur atom/monomer. The UV-visible spectrum of the as-isolated protein displayed an absorption band at 420 nm and 320 nm and shoulders at 460 nm and 550 nm (Figure 1A), indicating the presence of a Fe_2S_2 cluster rather than a Fe_4S_4 cluster. Upon exposure to air, the UV-visible spectrum changed with a decrease of the 420 nm, 460 nm absorption bands ($t_{1/2}$=60 min) (data not shown). We used Mössbauer spectroscopy to further characterize the iron sites in the anaerobically purified ISCA2. Purified ISCA2 expressed in ^{57}Fe-enriched M9 medium contained 0.7 iron and 0.65 sulfide/polypeptide chain and displayed a similar UV-visible absorption properties than the ^{56}Fe-S-ISCA2 (data not shown). The 4.2K Mössbauer spectrum consisted of one symmetric quadrupole doublet whose parameters, δ=0.27(±0.01) mm/s and ΔE_Q=0.53(±0.03), are typical for a $[Fe_2S_2]^{2+}$(S=0) cluster and represented almost 100% of the iron (Figure 1B). Reduction of the purified protein with dithionite under anaerobic conditions led to a rapid bleaching of the solution with disappearance of the 420 nm and 460 nm bands and apparition of a band at 550 nm in the UV-visible spectrum (Figure 1A). During this reaction the initial EPR-silent protein was converted to a S=1/2 species, characterized by a rhombic EPR signal with *g* values at g_1= 1.99, g_2= 1.96 and g_3=1.91 (Figure 1C). Temperature dependence and microwave power saturation properties of the signal were in agreement with a $[Fe_2S_2]^{+1}$ center (data not shown). The signal integrated to 20% of total iron. As dithionite is known to be a strong reducing agent that can lead to degradation of Fe-S clusters, we tested another reducing agent, dithiothreitol (DTT) already shown to reduce labile Fe-S cluster contained in SufA (Gupta, Sendra et al. 2009). Using 5 mM DTT, a similar EPR signal was obtained integrating for 15% of total iron, showing that the low yield of the Fe-S under the +1 oxidation state was not due to dithionite treatment. All these data show that ISCA2 binds a Fe_2S_2 cluster, presumably at the interface of two monomers. This cluster is relatively unstable in the presence of oxygen as a purification of the protein under air leads to an apo-protein (data not shown).

Surprisingly, upon anaerobic purification of ISCA1, the brown ring present during the first hours of the Ni-NTA loading disappeared during column washing and no protein could be eluted after imidazole treatment. Interestingly, when ISCA1 was purified aerobically, it remained colored during all purification procedure. Analysis of iron and sulfide content revealed significant amount of iron and sulfide (0.9 iron and 0.8 sulfur atom/monomer). The pure protein (4 mg/5L de culture) behaved as a mixture of dimeric (main) and tetrameric (minor) forms on Superdex-75 (theoretical mass of the monomer: 13 898.8 Da). The presence of an Fe-S was confirmed by UV-visible absorption and Mössbauer spectroscopy (Figure 2 A,B) on a 1.1 mM ISCA1 preparation obtained after expression in ^{57}Fe-enriched M9 medium and aerobic purification. This preparation containing 1 iron and 0.9 sulfide/polypeptide chain displayed similar UV-visible absorption properties than the Fe_2S_2-ISCA2 (Figure 2A). The Mössbauer spectrum recorded at 78K (Inset Figure 2B) consisted of one symmetric quadrupole doublet, whose parameters δ=0.27(±0.01) mm/s and ΔE_Q=0.49(±0.03) exclude the presence of a Fe_4S_4 or Fe_3S_4, and that are consistent with Fe^{III} (S=5/2) in tetrahedral environment consisting of sulphur ligands. The liquid helium measurement clarified the issue. The spectrum at 4.2K in the presence of an external field of 0.83 kG applied perpendicular to the γ rays consisted of a narrow doublet with δ=0.28(1) mm/s and ΔE_Q=0.50(2) parameters that unambiguously demonstrated the presence of a $[Fe_2S_2]^{2+}$(S=0) cluster representing almost 100% of the iron (Figure 2B). After reduction with dithionite, the protein displayed an EPR signal whose temperature dependence and microwave properties were characteristic of a $[Fe_2S_2]^{+1}$ cluster (Figure 2C). All these data suggest that ISCA1, like ISCA2, binds a Fe_2S_2 cluster.

ISCA1 and ISCA2 transfer their Fe-S cluster to apo-ferredoxin and apo-aconitase *in vitro*

Cluster transfer to apo-ferredoxin- To investigate whether native ISCA proteins have the ability to transfer their cluster to target proteins (as it was previously demonstrated *in vitro* with bacterial A-type proteins (Ollagnier-de-Choudens, Mattioli et al. 2001; Gupta, Sendra et al. 2009), apo ferredoxin (Fdx) from *E. coli* was used as a cluster acceptor protein. The holo-protein of Fdx contains a Fe_2S_2 cluster that exhibits unique spectroscopic properties, allowing easy monitoring of the cluster transfer reaction. Apo-Fdx was incubated anaerobically with sufficient Fe_2S_2-ISCA2 to provide a 2 fold-molar excess of Fe and S with respect to apo-Fdx. The UV-visible spectrum of the ISCA2-Fdx mixture after 60 min incubation indicates the formation of holo-Fdx with λ_{max} at 415 and 460 nm (Figure 3A). Subsequent reduction of the

ISCA2-Fdx mixture with an excess of dithionite unambiguously demonstrated the formation of holo-Fdx, as indicated by the characteristic S=1/2 EPR signal of reduced $[Fe_2S_2]^+$ Fdx (Gupta, Sendra et al. 2009), whose shape and *g* values were distinct from those of ISCA2 and matched those of holo-Fdx (Ta and Vickery 1992) (Figure 3B). Assuming complete reduction, EPR quantification indicates that 75% of the Fe_2S_2 clusters present in ISCA2 were transferred to Fdx. Similar results were obtained with ISCA1 used as an Fe-S donor protein (data not shown).

Cluster transfer to aconitase- To investigate whether ISCA proteins could provide Fe-S clusters also to Fe_4S_4 target enzymes, native ISCA proteins were anaerobically incubated with the apo-form of mammalian mitochondrial aconitase (ACO2) a well-characterized Fe_4S_4 protein (Emptage, Dreyers et al. 1983). Apo-ACO2 was first pre-treated with DTT and desalted and then incubated anaerobically with a 3.5 fold molar excess of either native ISCA1 or ISCA2 in order to provide a sufficient amount to build a Fe_4S_4 in ACO2. ACO2 was activated with incubation time by ISCA2 and reached 90% of activity compared to a reconstituted ACO2 after 30 min incubation (Figure 3C). A plateau is observed beyond 20 min incubation time and Fe-S transfer specifically requires a reducing agent such as DTT (Figure 3C, black bar with white dots at 30 min), as already observed (Gupta, Sendra et al. 2009). Similar results were obtained with ISCA1 as an Fe-S donor (data not shown). These studies clearly show that native ISCA proteins have the ability to transfer their Fe-S to both Fe_2S_2 and Fe_4S_4 apo-proteins, a function expected for Fe-S scaffolds or Fe-S carrier proteins.

In vitro Fe-S transfer between mammalian ISCU and ISCA proteins.

To investigate the Fe-S transfer between ISCU and ISCAs, His-tagged holoISCA1 or holo ISCA2 were incubated, under anaerobic conditions, with one equivalent of His-tagged apo-ISCU. After desalting and separation onto a Superdex-75 column, holoISCA2 (initially with 0.6 Fe and S/monomer) was still containing 0.4 Fe and 0.45 S/monomer and the general shape of its UV-visible spectrum (absorption bands at 320 nm, 420 nm and 460 nm) was very similar to that before incubation with ISCU, showing that no cluster transfer occurred (data not shown). Accordingly, no iron and sulfur could be detected on ISCU (data not shown). A similar result was obtained using holo-ISCA1 as an Fe-S donor (data not shown). When holo-ISCU was used as Fe-S donor and incubated with apo-ISCA2, cluster transfer was observed, with a loss of 98% of the iron on ISCU (Figure 4A,B) and 0.7 Fe/monomer and 0.6 S/monomer on ISCA2 after separation (Figure 4C). Due to the instability of apo-ISCA1, the transfer between holo-ISCU and apo-ISCA1 could not be conclusively assessed.

ISCA1 and ISCA2 can form a complex but also display different interacting partners *in vivo*.

To search for interacting partners of the ISCA proteins *in vivo*, we performed immunoprecipitation (IP) coupled to multidimensional protein identification technology (MudPIT). In the absence of immunoprecipitating antibodies for each protein, the IP were performed from HeLa mitochondrial extracts expressing mouse ISCA1, ISCA2, IBA57, FDX2 or GLRX5 with a C-terminal Flag epitope, respectively (Figure S1A). MudPIT analysis was performed on crude IP elutions. The MudPIT data were filtered to be enriched 10x (high stringency) over both control-IP and non-IP mitochondria-enriched inputs. Absolute numbers of spectral counts for mitochondrial hits were normalized to the respective protein size and represented as normalized spectral abundance factor (NSAF) (Florens, Carozza et al. 2006) (Figure 5A). As previously described for the yeast homologs (Muhlenhoff, Richter et al. 2011), a prominent reciprocal interaction between ISCA1 and ISCA2 in MudPIT analysis was found (Figure 5A, left panel). We confirmed the interaction in an independent ISCA1-Flag IP followed by western blot analysis with an ISCA2 antibody (Figure 5B). Due to the absence of a reliable ISCA1 antibody, we could not perform the reciprocal experiment. Although the co-chaperone HSCB was also found with low abundance (low NSAF values) with ISCA1 and ISCA2 in the MudPit analysis (Figure 5A), no direct interaction between the ISCA-proteins and HSCB was observed in heterologous co-expression experiments (Figure S1B).

Interestingly, ISCA2 and IBA57 reciprocally co-purified with high NSAF values, respectively (Figure 5A, left panel), whereas no interaction was detected between IBA57 and ISCA1. The specific interaction between endogenous ISCA2 and IBA57-Flag was confirmed independently by western blot analysis (Figure S1C). The absence of antibody recognizing endogenous IBA57 in HeLa cells prevented the reciprocal confirmation. These results suggest ISCA2 might be the main IBA57 protein partner *in vivo*, contrasting with published results for the yeast proteins (Gelling, Dawes et al. 2008; Muhlenhoff, Richter et al. 2011). Similarly, GLRX5 and ISCA2 reciprocally co-purified, but with rather low NSAF values (Figure 5A, left panel). Independent IP followed by western blot analysis confirmed that GLRX5 interacts specifically with ISCA2-Flag (Figure 5C) and not with ISCA1-Flag (Figure 5B). Finally, while an interaction with FDX2 was observed in the ISCA2-Flag IP (Figure 5A, left panel), the interaction was not detected in reverse IP, suggesting that FDX2 may be an indirect and rather weak binding partner of ISCA2. In contrast, the *de novo* Fe-S biosynthesis complex

components, NFS1, ISCU and ISD11 were found in high abundance in the FDX2-Flag IP (Figure 5A, left panel) supporting the current model of FDX2 as an electron donor for *de novo* Fe-S assembly (Kim, Frederick et al. 2013).

NFU1 was detected in the ISCA1-Flag IP (Figure 5A, left panel), which was confirmed by independent IP followed by western blot (Figure 5B). Of note, the interaction between ISCA1 and NFU1 is rather weak and probably transient as NFU1 is detected in the supernatant and washes of the ISCA1-Flag IP (Figure S1D). However, the interaction is specific to ISCA1 as no NFU1 is co-immunoprecipitated with ISCA2-Flag or IBA57-Flag, respectively (Figures 5C and S1C). Interestingly, a clear enrichment of several subunits of the hydrophilica arm of respiratory chain complex I, in particular with ISCA1, was observed in the MudPIT analysis (Figure 5A, right panel). Respiratory chain complex I in mammals consists of 14 highly conserved core subunits sufficient for activity with an additional 30 supernumerary subunits acquired over the evolution and at least eight Fe_4S_4 involved in electron transfer (Vinothkumar, Zhu et al. 2014). Assembly of complex I is thought to occur in a sequential manner with a growing number of known assembly factors (Mimaki, Wang et al. 2012). Interestingly, a relatively abundant co-immunoprecipitation of the complex I core subunit NDUFS3 was observed with ISCA1-Flag (Figure 5A, right panel), and confirmed by immunoblot on independent IP (Figure 5B). No direct interaction between NDUFS3 and ISCA2-Flag was observed (Figure 5C).

Collectively, these results demonstrate a direct and robust interaction between ISCA1 and ISCA2, as well as between ISCA2 and IBA57, while NFU1 and GLRX5 are lower abundance partners of ISCA1 and ISCA2, respectively. Our results suggest that despite the existence of a prominent (or strong) ISCA1/ISCA2 complex *in vivo*, specific complexes containing either ISCA1 or ISCA2 *in vivo* might exist (Figure 5D). Furthermore, we uncovered a novel interaction between ISCA1 and NDUFS3, suggesting that ISCA1 may participate directly in complex I assembly, potentially to provide Fe-S. We cannot exclude a role of ISCA2 and IBA57 as several complex I components were identified in the MudPIT analysis.

Under normal physiological conditions in muscle, ISCA1 is required for maturation of mitochondrial Fe_4S_4 proteins whereas ISCA2 and IBA57 are not required

Knockdown experiments in HeLa cell of the human ISCA1, ISCA2 and IBA57 pointed to a role of all three proteins in the maturation of mitochondrial Fe_4S_4 proteins (Sheftel, Wilbrecht et al. 2012). To examine the physiological consequences of ISCA1 or ISCA2 knockdowns in mouse tissues, we injected recombinant Adeno-associated virus (AAVs) encoding for specific

shRNAs against *Isca1* or *Isca2* into the tibialis anterior (TA), a mixed type I and II skeletal muscle, of wild type mice at 4 weeks of age. Strong knockdown of *Isca1* mRNA expression was confirmed by qRT-PCR 3 weeks post injection (wpi) and at the protein level for ISCA2 (Figure 6A). At dissection, the muscle to body weight ratio was unaffected by the viral injection and the knockdown (Figure S2A). Histological analysis confirmed an overall preserved muscle organization in both ISCA1 and ISCA2 knockdown TA (Figure 6B). Furthermore, while the ultrastructure of the muscle fibers and the mitochondria by electron microscopy was completely normal in ISCA2 knockdown (Figure 6C), the ultrastructure of the muscle fibers in ISCA1 knockdown animals was normal but presented rare slightly enlarged mitochondria along with rare changes in mitochondrial cristae organization (data not shown), suggesting a mild mitochondrial phenotype.

To further narrow the function of ISCA1 and ISCA2 in muscle, we specifically analyzed Fe-S-dependent proteins in the TA muscle, as both proteins have been previously demonstrated to be essential for mitochondrial Fe_4S_4 protein biogenesis in HeLa cells and in yeast (Gelling, Dawes et al. 2008; Muhlenhoff, Richter et al. 2011). The activity of succinate dehydrogenase (SDH), containing Fe_2S_2 and Fe_4S_4, was strongly decreased on muscle sections after *Isca1* knockdown, while COX activity remains unchanged (Figure 6C). Furthermore, a substantial decrease of mitochondrial Fe_4S_4 containing proteins, including aconitase (ACO2), complex II (SDH B) and several subunits of complex I (NDUFS3, NDUFS4, NDUFS5, NDUFS6) was observed by western blot after ISCA1 knockdown (Figure 6D), as a result of the instability of the respective apo-proteins or the whole complex. In addition, a decrease in the LA cofactor bound to pyruvate dehydrogenase (PDH) and α-ketogluterate dehydrogenase (KGDH) complexes was also observed after ISCA1 knockdown (Figure 6D). As PDC-E2 (the PDH subunit to which LA is bound) levels remained unchanged between the different injected animals (Figure 6D), the decrease in LA-bound complexes indirectly demonstrates a defect in the Fe_4S_4 enzyme lipoic acid synthase (LIAS). In contrast, we did not observe any decrease in the tested mitochondrial Fe_2S_2 enzymes (FECH and RIESKE) nor in the non-Fe-S containing enzyme COX IV after ISCA1 knockdown (Figure 6D). Furthermore, extra-mitochondrial Fe-S enzymes (ABCE1, GPAT, mNT) protein levels were not affected by ISCA1 knockdown (Figure 6D). While no effect was seen 1 wpi, most likely because the ISCA1 knockdown is not efficient, the deleterious effect on mitochondrial Fe_4S_4 enzymes was already observed 2 wpi (Figure S2B) and did not appear to progress further at 6 wpi (Figure S2C, left panel).

To control for the specificity of the observed effects, we generated a rescue construct that expresses an shRNA-resistant version of ISCA1, by introducing a silent mutation into the

region targeted by the shRNA (ISCA1^R). The combination of ISCA1 knockdown with overexpression of the ISCA1R was validated by qRT-PCR using primers pairs within the coding region as well as in the 3'UTR to specifically detect the endogenous *Isca1* mRNA (Figure 7A). All alterations in maturation of mitochondrial Fe_4S_4 enzymes were fully reversed by the expression of the resistant ISCA1^R (Figure 7B), demonstrating the specificity of the effects. As validation of our AAV-based approach, knockdown of the main scaffold protein ISCU was found to compromise all tested cellular Fe-S proteins, both mitochondrial and extra-mitochondrial Fe_4-S_4 and Fe_2S_2 enzymes (Figure S2D). Together, these results confirm a deleterious effect of ISCA1 knockdown specifically on mitochondrial Fe_4S_4 enzymes. It is interesting to note that ISCA2 protein levels remain unchanged upon ISCA1 knockdown (Figure 6D, left panel), despite the existence of an ISCA1/ISCA2 complex *in vivo*.

In contrast, knockdown of ISCA2, as confirmed by western blot (Figure 6D, right panel) had no effect on any of the tested Fe-S proteins in muscle 3 wpi under normal physiological conditions (Figure 6B,D right panel). Normal SDH activity as well as normal levels of all tested mitochondrial and extra-mitochondrial Fe_4S_4 and Fe_2S_2 enzymes was observed even 6 wpi (Figure S2C, right panel). In agreement with a specific interaction between ISCA2 and IBA57, no effect on any Fe-S proteins tested was observed after IBA57 knockdown (Figure S3). Note again that ISCA2 was not destabilized by IBA57 knockdown (Figure S3B,C).

The expression of the *Isca1* and *Isca2* genes is ubiquitous, with high expression in skeletal muscle and heart, following the expression pattern of other proteins involved in Fe-S biogenesis such as *Nfs1*, *Iscu* and *Fxn* (Figure S4). In all tissues tested, *Isca1* mRNA level was systematically higher than *Isca2* mRNA level, suggesting that ISCA2 levels are not sufficient to compensate ISCA1 knockdown. To test this hypothesis, we combined knockdown of endogenous *Isca1* with overexpression of ISCA2^R (the plasmid used was a silent mutation resistant to the shRNA against *Isca2*, a construct not specifically needed for this experiment, but that expresses a wild-type ISCA2 protein). Simultaneous knockdown of *Isca1* and overexpression of ISCA2^R was validated by qRT-PCR and western blot, respectively (Figure 7A,B). In contrast to the full rescue that is obtained with ISCA1^R, as previously discussed, ISCA2^R overexpression had no effect on the maturation of mitochondrial Fe_4S_4 enzymes after ISCA1 knockdown (Figure 7B), demonstrating that ISCA2 cannot compensate for the loss of ISCA1 function *in vivo*.

Discussion

In the present manuscript, we demonstrate that mouse A-type proteins, ISCA1 and ISCA2, are Fe_2S_2 containing proteins with different biophysical characteristics. Native ISCA proteins have the ability to transfer their Fe-S cluster to both Fe_2-S_2 and Fe_4-S_4 apo-proteins, but not to the apo-ISCU scaffold protein, and ISCA2 could receive its cluster from holo-ISCU, providing strong evidence of a role of ISCA as carrier proteins, downstream of ISCU. Through interaction studies, we provide evidence of the existence of a prominent ISCA1/ISCA2 complex *in vivo*, as well as specific complexes containing either ISCA1 or ISCA2 *in vivo*. Finally, we demonstrate that, contrary to previously published data, only ISCA1 is required for mitochondrial Fe_4S_4 biogenesis whereas ISCA2 and IBA57 appear to be dispensable under normal physiological conditions.

The difference in stability toward oxygen for ISCA1 and ISCA2 proteins could be explained as follow: ISCA2 protein is rather devoted to maturation of Fe_2S_2 containing proteins and therefore has to be transferred to target either directly or through other Fe-S shuttle proteins (for instance GLRX5) which implies that the cluster has to be "labile". In contrast, ISCA1 is devoted specifically to the maturation of Fe_4S_4 proteins. One possibility to explain that ISCA1 cluster is more stable than ISCA2 cluster would be that its Fe_2S_2 cluster has to be converted to Fe_4S_4 form before being transferred to target Fe_4S_4 protein. If it is too labile it would not resist to reductive coupling and conversion in Fe_4S_4 cluster.

Characterization of recombinant ISCA1 and ISCA2

Early controversy on the roles of A-type proteins was based on Fe-binding versus Fe-S cluster binding both described for the bacterial A-type proteins (Mapolelo, Zhang et al. 2012). This resulted in suggestion of two different roles either as Fe-donor for nascent cluster assembly or as alternative scaffold protein or Fe-S carrier protein. Apart from Fe-binding properties described for human ISCA1 (Lu, Bitoun et al. 2010), no detailed biochemical and biophysical characterization was yet available for any eukaryotic A-type protein. Herein, we purified both A-type proteins directly as Fe_2S_2 proteins, without chemical reconstitution. During purification, each A-type protein was predominantly eluted in a dimeric state, while minor parts of ISCA1 also elute as a tetramer. Since all A-type proteins harbor 3 cysteine residues per monomer, we can suggest that the cluster is at the dimer interface, in agreement with structural studies and previous reports on bacterial A-type proteins (Wada, Hasegawa et al. 2005; Morimoto, Yamashita et al. 2006; Gupta, Sendra et al. 2009). Although most clusters on proteins of the Fe-S biogenesis are labile in the presence of oxygen, our data uncover

different properties for the ISCA proteins. Indeed, from our biochemical and spectroscopic studies, we can conclude that ISCA1 contains a Fe_2S_2 cluster which is rather stable under aerobic conditions in contrast to ISCA2 cluster which is sensitive to oxygen and can be maintained within the protein only under anaerobic conditions. Properties of ISCA2 cluster are reminiscent to those of both bacterial and eukaryote scaffold Fe-S proteins such as ISCU, SufBCD. Our biochemical results demonstrate that both native ISCA1 and ISCA2 can transfer Fe-S to classical acceptor proteins. Transfer takes place to both Fe_2S_2 and Fe_4S_4 apo-proteins *in vitro*, as shown for *E. coli* ferredoxin and mitochondrial aconitase (ACO2). As previously shown, assembly of the Fe_4S_4 holo-ACO2 requires a reducing agent (DTT) to provide electrons necessary during formation of a Fe_4S_4 cluster from two Fe_2S_2 cluster (Gupta, Sendra et al. 2009). Whether reductive coupling of clusters occurs on the A-type or the acceptor protein remains to be shown. Although both mouse A-type proteins were characterized as Fe_2S_2 proteins, the striking difference in the clusters' sensitivity to oxygen suggests that they might exert different roles during Fe-S biogenesis/transfer or exert a similar function under different physiological conditions.

In vivo interaction network of ISCA1 and ISCA2

Immunoprecipitation experiments coupled to MudPIT enabled us to analyze the ISCA-protein interacting network, uncovering the presence of complexes with different abundance within the cell. As previously demonstrated (Muhlenhoff, Richter et al. 2011), the complex formed by ISCA1 and ISCA2 is robust and relatively abundant in cells. However, the physiological role and the possibility of Fe-S transfer or cluster conversion upon binding of the two remains to be investigated in the future. Despite the prominent and robust interaction between ISCA1 and ISCA2, we uncovered several differential interactions between ISCA1 and ISCA2.

One striking result is the absence of interaction between ISCA1 and IBA57. Indeed, based on the literature, we expected to find a complex composed of ISCA1, ISCA2 and IBA57 (Gelling, Dawes et al. 2008; Muhlenhoff, Richter et al. 2011). Our data clearly demonstrated that only ISCA2 binds IBA57 with high abundance *in vivo*, suggesting that ISCA1 is not part of the core complex. While the role of IBA57 is not known, both yeast studies and knockdown in HeLa cells have shown a role for IBA57 homologues in Fe-S biogenesis (Gelling, Dawes et al. 2008; Sheftel, Wilbrecht et al. 2012). In bacteria, the phylogenic studies demonstrate the co-evolution of A-type proteins (IscA or SufA) and IBA57 homologs (Waller, Alvarez et al. 2010). Interestingly, in *E. Coli*, YgfZ (the IBA57 homolog) was shown to bind folate, and thus proposed to function as electron donors (Teplyakov, Obmolova et al.

2004). Together, these results have led to the suggestion that IBA57 might be the electron donor for conversion of Fe_2S_2 into Fe_4S_4 cluster on ISCA proteins or during the transfer to Fe_4S_4 acceptor proteins. Uncovering the biochemical function of mammalian IBA57 will refine the knowledge on its molecular function and may lead to an understanding of ISCA2 function.

We uncovered a specific interaction between ISCA2 and GLRX5, although quite weak in comparison to the interaction with IBA57. These results suggest that GLRX5 binding to ISCA2 is most likely transient. The precise functions of GLRX5 in Fe-S biogenesis is unknown and mainly based on a disease phenotype. Several studies in cell models and lower eukaryotes have supported a role for GLRX5 in the early step of Fe-S transfer, based on the fact that mitochondrial and also extra-mitochondrial Fe-S proteins were (Wingert, Galloway et al. 2005; Camaschella, Campanella et al. 2007; Ye, Jeong et al. 2010; Uzarska, Dutkiewicz et al. 2013). However, newly reported phenotypes from patients with mutations in GLRX5 displaying variant nonketonic hyperglycemia with strongly decreased levels of LA on PDH and KGDH rather suggest a role of GLRX5 specifically in the maturation of the mitochondrial Fe_4S_4 protein LIAS. The fact that we see direct binding of GLRX5 with ISCA2 and that we do not detect ISCU or HSCB in the MudPIT analysis for the GLRX5 IP, further support a role for GLRX5 towards the late-acting mitochondrial Fe-S biogenesis. In addition, Fe-S transfer was previously shown between human holo-GLRX5 and both A-type proteins *in vitro*, but interestingly also from holo-ISCA proteins to apo-GLRX5 (Banci, Brancaccio et al. 2014). Whether GLRX5 functions upstream or downstream of ISCA2 remains to be defined.

We uncovered a novel interaction between ISCA1 and NFU1, a protein suggested as specific carrier protein in targeting Fe-S to LIAS and complex II based on data from patients and knockdown studies in HeLa cells (Cameron, Janer et al. 2011; Navarro-Sastre, Tort et al. 2011). As for the interaction between ISCA2 and GLRX5, the interaction is most likely transient. However, this interaction may suggest that ISCA1 act upstream of NFU1 in the distribution of Fe_4S_4 to mitochondrial acceptor proteins.

Our unbiased proteomics approach also unraveled potential novel interaction of ISCA1 with several complex I subunits located in the hydrophilic domain. In particular, we confirmed the interaction between ISCA1 and NDUFS3. NDUFS3 is one of the core subunits of complex I involved in the first assembly step (Mimaki 2012). We can therefore hypothesize that ISCA1 may be involved in complex I assembly, most likely by providing Fe-S during the process. Complex I assembly requires a number of assembly factors, including the Fe-S binding protein NUBPL (Bych, Kerscher et al. 2008; Sheftel, Stehling et al. 2009). Whether NUBPL

and ISCA1 function in coordination to target Fe-S to complex I would need further investigation.

We note two other potential protein interactions that might be of interest. IBA57 was found to strongly co-immunoprecipitate PRDX3, the thioredoxin-dependent peroxide reductase suggested to be involved in redox regulation of the cell (Angeles, Gan et al. 2011; Whitaker, Patel et al. 2013). A putative interaction between GLRX5 and ALAS1, the enzyme of the first step of heme biogenesis, was also uncovered. Since a patient carrying a mutation in GLRX5 exhibits sideroblastic-like microcytic anemia (Camaschella, Campanella et al. 2007), our data may provide valuable information to understand the pathophysiology.

In vivo differential role of ISCA1 and ISCA2

In accordance with recent studies on ISCA proteins in cells (Sheftel, Wilbrecht et al. 2012), ISCA1 was seen to be involved in maturation of mitochondrial Fe_4S_4 proteins in muscle. Although major mitochondrial components comprising LA-bound complexes PDH and KGDH as well as complex I and complex II levels were found to be severely decreased, mitochondria were predominantly not affected by EM, confirming that our approach allows characterization of the primary phenotype of ISCA1 deficiency. Contrary to ISCA1, ISCA2 knockdown did not recapitulate the previously documented cellular phenotype, in which maturation of mitochondrial Fe_4S_4 and Fe_4S_4-dependent proteins was also affected (Sheftel, Wilbrecht et al. 2012). Indeed, none of the tested Fe-S proteins was affected even by prolonging knockdown up to 6 wpi. By addressing potential functional redundancy using overexpression of ISCA2 in muscle with *Isca1* knockdown, we further showed that ISCA1 and ISCA2 are not performing similar functions in normal physiological conditions.

In line with a prominent interaction between IBA57 and ISCA2, IBA57 knockdown did not show any overt Fe-S phenotype. However, although *Iba57* mRNA knockdown was confirmed 3 wpi, the protein level was only decreased 6 wpi, suggesting high stability of IBA57.

Taken together, our data thus suggest that ISCA2 and IBA57 may function together *in vivo*. Their role needs however to be further investigated. The discrepancy between our results and the ones obtained with HeLa cells (Sheftel, Wilbrecht et al. 2012) may provide indication of the conditions in which ISCA2 and IBA57 may be required. Indeed, cellular models and tissues have different metabolic requirements and Fe-S requirements are likely substantially different. It is therefore tempting to speculate that ISCA2 and IBA57 may function to provide Fe-S only under certain cellular context. Whether this relies on cell division or different metabolic requirements would have to be defined.

In conclusion, our complementary results establish that mouse ISCA1 and ISCA2 are Fe_2S_2 proteins that most likely function as Fe-S transport proteins with different roles *in vivo*. Moreover, our data underline the elaborated nature of Fe-S biogenesis from cluster assembly to the acceptor proteins that involves interactions between different proteins of the Fe-S biogenesis.

FIGURE LEGENDS

Figure 1. Spectroscopic characterization of ISCA2. (A) UV-visible spectrum of the as-isolated ISCA2 in 0.1 Tris-HCl pH 8, 50 mM NaCl before (bold line) and after reduction with 1 mM dithionite (dotted line). (B) Mössbauer spectrum of the ^{57}Fe/S-ISCA2 (380 µM, 0.7 Fe and 0.65 S/ protein). The Mössbauer spectrum was recorded at 4.2 K in a magnetic field of 60 mT applied to the γ beam. The solid line corresponds to simulation of the experimental spectrum; (C) X-band EPR spectrum of as-isolated ISCA2 (500 µM) reduced with 1 mM dithionite for 10 min.

Figure 2. Spectroscopic characterization of ISCA1. (A) UV-visible spectrum of the as-isolated ISCA1 in 0.1 Tris-HCl pH 8, 50 mM NaCl. (B) Mössbauer spectrum of the ^{57}Fe/S-ISCA1 (1.1 mM, 1 Fe and 0.9 S/ protein). The Mössbauer spectrum was recorded at 4.2 K in an external magnetic field of 83 mT applied to the γ beam. Mössbauer spectrum recorded at 78K is presented in the Inset; (C) X-band EPR spectrum of as-isolated ISA1 (250 µM) reduced with 1 mM dithionite for 10 min.

Figure 3. Maturation of ferredoxin and aconitase using holo-ISCA proteins as Fe-S donors. (A) Monitoring of the apo-ferredoxin (thin line, 100 µM) and as-isolated ISCA2 (bold line, 200 µM) mixture after 15 min (dotted line) and 30 min (dashed line) incubation. The inset shows the UV-visible spectrum of the holo-ferredoxin (20 µM) obtained after separation onto a NiNTA column; (B) X-band EPR spectrum of the dithionite (1 mM) reduced ferredoxin (100 µM) after incubation with Fe-S ISCA2 for 30 min and separation. Temp: 10 K, microwave power: 25 µW, gain: 2.10^4, modulation: 10 gauss. (C) ACO2 (0.2 nmole) activity after incubation with as-isolated ISCA2 (1.5 nmoles, 0.7 Fe/protein) (hatched bars) or 4 molar excess of Fe^{2+} and S^{2-} (black bars) at 5, 10, 15, 20 and 30 min. Reconstituted

ACO2 (0.2 nmole, 3.8 iron/protein) was used as positive control (gray bar). ACO2 activity obtained without DTT is also shown at 30 min (black bars with white dots).

Figure 4. Fe-S transfer from ISCU to ISCA2. (A) UV-visible spectrum of holo-ISCU (200 μM) before incubation with apo-ISCA2; (B) UV-visible spectrum of ISCU (60 μM) after incubation with apo-ISCA2 and separation onto Superdex-75; (C) UV-visible spectrum of ISCA2 (300 μM) after incubation with holo-ISCU and separation on Superdex-75.

Figure 5. Interaction screening using immunoprecipitations. (A) Co-immunoprecipitated proteins and their relative abundance (NSAF) determined by MudPiT analysis. Data represent proteins enriched 10x over controls. The color intensity reflects the NSAF values multiplied by 100. Left panel represents NSAF values obtained for subunits of respiratory chain complex I in ISCA1, ISCA2 and IBA57 IPs. (B) Western blot analysis of ISCA1-IP versus control-IP (CTL) using different antibodies as indicated. (C) Western blot analysis of ISCA2-IP versus control-IP (CTL) using different antibodies as indicated. (D) Interaction network for ISCA1 and ISCA2 based on western blot (blue line) or MudPIT (green line) of IPs. Thickness of lines and spatial distances represent high, medium and low relative abundance, respectively. cplx I: complex I

Figure 6. ISCA1 and ISCA2 knockdown in skeletal muscle. (A) *Isca1* mRNA expression in TA muscle injected with rAAV-shISCA1 or rAAV-scramble shRNA (CTL). Results are given as the mean (n=9) ± SD. ***$p<0.0001$ (B) Histological analysis on cryosections from TA muscle injected with rAAV-shISCA1 or rAAV-shISCA2 and their respective controls (CTL). (C) Muscle structure observed by EM on TA muscle injected with rAAV-shISCA1 or rAAV-shISCA2 and respective controls (CTL). Scale bar 10 μm (upper row) and 5 μm (lower row). (D) Representative western blots of the indicated proteins using extracts from TA muscle at 3 wpi, injected with rAAV-shISCA1 or rAAV-shISCA2 and their respective controls (CTL).

Figure 7. Evaluation of compensation of ISCA1 knockdown. (A) Relative mRNA expression of endogenous *Isca1* and total *Isca1* in TA muscle simultaneously injected with rAAV-shISCA1 or rAAV-scramble shRNA (CTL) and rAAV-ISCA1^R or rAAV-ISCA2^R. Results are given as the mean (n=3) ± SD.* $p<0.05$.(B) Representative western blots of the indicated proteins using extracts from TA muscle at 3 wpi, simultaneously injected with

rAAV-shISCA1 or rAAV-scramble shRNA (CTL) and rAAV-ISCA1^{R} or rAAV-ISCA2^{R}. GAPDH was used as loading control.

Figure S1. Interaction screening using immunoprecipitations. (A) Western blot analysis using FLAG antibody of the IP fractions obtained with ISCA1, ISCA2, FDX2, IBA57, NFU1 and GLRX5. (B) SDS-PAGE analysis followed by coomassie blue staining of GST purified elutions after co-expression of GST-HSCB with ISCA1 and ISCA2 or with ISCU in bacteria. Western blot analysis (IB) of the input fractions using ISCA1, ISCA2 or ISCU antibodies are shown. (C) Western blot analysis of IBA57-IP versus control-IP (CTL) using different antibodies as indicated. SN: Supernatant. (D) Western blot analysis of ISCA1-IP versus control-IP (CTL) using different antibodies as indicated. SN: Supernatant.

Figure S2. Evaluation of different aspects of knockdown phenotypes. (A) Weight of TA muscles 3wpi, injected with rAAV-shISCA1, rAAV-shISCA2 or their respective controls (CTL). Results were normalized to the body weight and are given as the mean (n=8) ± SD. (B) Representative western blots of the indicated proteins using extracts from TA muscle at 1 and 2 wpi, injected with rAAV-shISCA1 or rAAV-shISCA2 and their respective controls (CTL). GAPDH and βTUB were used as loading controls. (C) Representative western blots of the indicated proteins using extracts from TA muscle at 6 wpi, injected with rAAV-shISCA1 or rAAV-shISCA2 and their respective controls (CTL). GAPDH was used as loading control. (D) Representative western blots of the indicated proteins using extracts from TA and EDL muscles at 3 wpi, injected with rAAV-shISCU or rAAV-scramble shRNA (CTL). GAPDH and βTUB were used as loading controls.

Figure S3. IBA57 knockdown in skeletal muscle. (A) Relative *Iba57* mRNA expression in TA muscle at 3 wpi, injected with rAAV-shIBA57 or saline injection (CTL). Results are given as the mean (n=3) ± SD. **p<0.001 (B) Representative western blots of the indicated proteins using extracts from TA muscle at 3 wpi, injected with rAAV-shIBA57 or saline injection (CTL). GAPDH and βTUB were used as loading controls. (C) Representative western blots of the indicated proteins using extracts from TA muscle at 6 wpi, injected with rAAV-shIBA57 or saline injection (CTL). GAPDH and βTUB were used as loading controls.

Figure S4. Expression of mouse ISCA1 and ISCA2. Relative mRNA expression of *Isca1*, *Isca2*, *Iscu*, *Nfs1* and *Fxn* genes in different mouse tissues, as indicated. *Hprt* was used as a

housekeeping gene. The results are given as the mean of two 10 weeks old C57Bl/6J males ± SD.

MATERIALS AND METHODS

Plasmid constructs and site-directed mutagenesis

cDNAs were PCR-amplified from a bank of mouse heart cDNAs using specific primers and cloning into expression vectors was performed using restriction enzymes. For GST-fusion expression in bacteria or mammalian expression, full length *Isca1*, *Isca2*, *Glrx5*, *Fdx2* and *Iba57* (*C1orf69* homolog) cDNAs were cloned into pGEX-4T1 (GE Healthcare) or pcDNA3.1/zeo(+) (Invitrogen), respectively. Mature forms of ISCA1 and ISCA2 were cloned into pET-11a (Novagen) for the bacterial expression of the HIS-tagged proteins, and in pACYCDuet-1 (Novagen) for co-expression experiments. Cloning of *Iscu*, *Nfs1* and *Isd11* cDNAs was previously described (Martelli, Wattenhofer-Donze et al. 2007; Schmucker, Argentini et al. 2008).

Specific shRNA against mouse *Isca1*, *Isca2*, *Iba57* or *Iscu* and scramble shRNAs were designed and cloned into modified pENTR1A (Invitrogen Life Technologies) vector containing the U6 promoter and a CMV-eGFP cassette (sequences of shRNA are listed in Table S1). Scrambled shRNAs were designed using Wizard v3.0 http://www.sirnawizard.com. ShRNAs were then subcloned into pAAV vector using Gateway® techonology for AAV production. Mouse ISCA1 or ISCA2 sequences resistant to their respective shRNAs ($ISCA1^R$ and $ISCA2^R$, respectively) were obtained by directed mutagenesis and cloned into pAAV-CMV (Stratagene) for AAV production. Site-directed mutagenesis was carried out using specific primers (primer sequences are listed in Table S2) and the Phusion® high-fidelity DNA polymerase (Finnzymes) with the provided GC-Buffer. PCR amplifications were carried out following the manufacturer's recommendations. All sequences were verified by sequencing.

Cell culture, transfection and protein extracts

HeLa cells were cultured in DMEM medium supplemented with 1g/L glucose, 5% fetal calf serum (FCS) and 40 μg/mL gentamycine at 37% with 5% CO_2. Cells were transfected with the different constructs (*Isca1*, *Isca2, Iba57, Glrx5, Fdx2*) using Fugene® 6 transfection reagent (Roche) as recommended by the manufacturer and as previously described (Schmucker, Argentini et al. 2008). Transfected cells were harvested 24h to 48h after

transfection. Mitochondrial-enriched protein extracts from HeLa cells were obtained as described (Schmucker, Argentini et al. 2008). Briefly, cell pellets were resuspended in 50 mM Tris pH 7.5, 10 % glycerol, 100 mM KCl, 0.014 % digitonin supplemented with Complete protease inhibitor cocktail (Roche) and incubated for 10 min at 4°C. Suspensions were then centrifuged for 10 min at 13,000 g to obtain mitochondria-enriched pellets. Pellets were resuspended in Tris-HCl 10mM pH7.4, 10% Glycerol, 100mM NaCl, 50mM KCl, Complete® protease inhibitor cocktail (Roche). The suspension was kept on ice for 20 min and then centrifuged at 12,000 g, 10 min, 4°C to eliminate cellular debris. Protein concentrations were determined by Bradford (Bio Rad Protein assay).

Immunoprecipitations

Mitochondria-enriched protein extracts (0.3-8 μg) of HeLa cells overexpressing Flag-tagged proteins were used for immunoprecipitation (Tris-HCl 10mM pH7.4, 10% Glycerol, 100mM NaCl, 50mM KCl, Complete® protease inhibitor cocktail (Roche)) using 25-100 μl Flag M2 coupled resin (SIGMA) (50 % slurry, prepared as recommended by the manufacturer) in the presence of Complete protease inhibitor (Roche). Mix was incubated 2 hours at 4°C, centrifuged 10 min at 12,000 g and beads were washed twice with 1 ml PBS. Elution was performed by incubating resin 5 min in glycine buffer (0.1M glycine pH 2.8) and centrifugation for 10 min at 12,000 g.

SDS-PAGE and Western blot

SDS-PAGE and Western blot were carried out as previously described. Unless otherwise indicated, protein extracts were denaturated in loading buffer and loaded on Tris-glycine polyacrylamide gel. Antibodies were incubated overnight in PBS-Tween (0.05%) (antibodies and dilutions in Table S3).

Quantitative Real Time PCR

Total RNA was obtained from mice tissues using Tri Reagent (Molecular Research Centre, Inc.) according to the manufacturer's protocol. Reverse transcription was carried out using Superscript II kit (Invitrogen). Quantitative RT-PCR was performed on a LightCycler® 480 apparatus (Roche) using specific oligonucleotides as listed in Table S4 or as previously described ((Martelli, Wattenhofer-Donze et al. 2007)). *Hprt* expression was used as control.

Production of recombinant proteins

ISCA1 and ISCA2 were obtained by growing *E. coli* BL21(DE3)/pET-ISCA1 or pET-ISCA2 in LB medium containing 100 µg/ml ampicillin, at 37°C. ISCA2 expression was induced for 4h by adding 0.5 mM isopropyl b-D-thiogalactoside (IPTG) to an exponentially growing culture. ISCA1 protein induction was performed at 20°C over-night. Bacterial pellets were resuspended in buffer A (50 mM Tris-HCl pH 8, 50 mM NaCl, 0.1% TritonX100, 5 mM DTT, 1 mM PMSF) and sonicated before ultracentrifugation (90min, 45,000 rpm, 4°C). Supernatants were treated with DNAse I and 10 mM $MgCl_2$ at 4°C for 45min, and after centrifugation (30min, 15000 rpm, 4°C), soluble proteins were loaded onto a 5 ml Ni-NTA affinity column (Qiagen) equilibrated with buffer B (50 mM Tris-HCl pH 8, 50 mM NaCl, 0.1% TritonX100). Fractionc containing ISCA proteins were pooled after elution with buffer B containing 0.2 M imidazole. This protocol allowed the purification of approximately 5 mg and 40 mg of ISCA1 and ISCA2, respectively. For Mossbauer experiments, bacteria expressing ISCA1 or ISCA2 were grown aerobically in minimal M9 ^{57}Fe-enriched medium (35 µM) supplemented with 2 mM $MgSO_4$, 0.4% glucose, 2 µg/ml thiamine, 1 mM $CaCl_2$. ^{57}Fe (Cambridge Isotopes) was prepared by resuspended ^{57}Fe powder in concentrated HCl:HNO3 (1:1 ratio) in order to get a 500 mM solution. Proteins expressions as well as purifications were performed as described above.

Mouse aconitase (ACO2) was purified from an *E. coli* BL21(DE3) strain containing pRARE2 plasmid (encoding seldom tRNAs) and pGEX-ACO2 that were grown in LB at 37°C for 3 hours after addition of 0.5 mM IPTG. The bacterial pellet was resuspended in buffer E (PBS supplemented with 0.1% TritonX100 and 1 mM PMSF) and sonicated before ultracentrifugation (90min, 45000 rpm, 4°C). The supernatant was treated with DNAse I and 10 mM $MgCl_2$ at 4°C for 45min, and after centrifugation (30min, 15000 rpm, 4°C), soluble proteins were loaded onto a 5 ml GST-trap affinity column (Qiagen) equilibrated with buffer E without PMSF. The GST-fused ACO2 protein was eluted with buffer E containing 30 mM glutathione and pooled fractions were stored at -80°C. ISCU was obtained from purification of the NfS1-Isd11-IscU complex (Schmucker, Martelli et al. 2011) and a further gel filtration step onto a Superdex-75 (Pharmacia) equilibrated with buffer F (100 mM Tris-HCl pH 7.5, 100 mM NaCl). *E. coli* apo-ferredoxin (Fdx) was purified as previously described (Ollagnier-de-Choudens, Mattioli et al. 2001). Protein concentrations were measured by Bradford assay using bovine serum albumin as a standard.

Heterologous co-expression experiments were carried out in 100 mL 2xYT medium, and by inducing protein productions with 0.5 mM IPTG at 22°C for 16 hrs. Cells were lysed by sonication in PBS, 10 mM DTT, 0.5% Triton X-100, Complete®, EDTA-free (Roche), and

the suspension was centrifuged 15,000g, 4°C for 30 min to eliminate unsoluble material. One hundred microliters of glutathione (GSH)-sepharose beads (GE Healthcare) were added to the supernatant and incubated 1 hr at 4°C. The suspension was then poured into a Poly-Prep® chromatography column (Bio Rad), and beads were washed with 10 mL Tris-HCl 100 mM, pH 8, 100 mM NaCl before elution with Tris-HCl 100 mM, pH 8, 100 mM NaCl, 30 mM GSH. Elutions were then analysed on SDS-PAGE.

Determination of the oligomerization state of ISCA proteins

FPLC gel filtration with an analytical Superdex-200 (Pharmacia Amersham Biotech) at a flow rate of 0.5 ml/min equilibrated with buffer G (100 mM Tris-HCl pH 7.5, 100 mM NaCl, 5 mM DTT) was used for size determination of oligomerization state of ISCA1/2 proteins. A gel filtration calibration kit (calibration protein II, Boehringer Inc) was used as molecular weight standards.

Fe-S cluster transfer experiments

E. coli apo-Fdx was expressed and purified in our laboratory as already described. Apo-Fdx (180 µM) was incubated anaerobically in 200 µL buffer H (0.1 M Tris-HCl pH: 8; 50 mM KCl) with native ISCA1 (0.9 iron and sulfur atom/monomer) or ISCA2 (1:1 Fe/monomer) in order to provide 2 iron and sulfur atoms/ferredoxin. Fe-S transfer was followed by monitoring the UV-visible absorption in the 300-600 nm region and by EPR analysis of the ISCA-Fdx protein mixture after reduction with 2 mM dithionite.

To assess mouse aconitase activation, DTT pretreated apo-ACO2 (0.2 nmol) was incubated anaerobically in a glove box at 18 °C in buffer I (50 mM Tris-HCl pH: 7.6) with a 10-fold molar excess of the native ISCA1 (0.9 iron and sulfur atom/monomer) or ISCA2 (0.6 Fe/monomer) in order to provide 4 iron and 4 sulfur atoms/ACO2. After 5, 10, 15, 20 and 30 min incubation, aconitase activity was assessed as described by Gardner, P.R., and Fridovitch, I.(Gardner and Fridovich 1992). Briefly, ACO2-ISCA1/2 mixtures were added to 0.6 mM $MnCl_2$, 25 mM citrate, 0.5 U isocitric dehydrogenase, 0.25 mM $NADP^+$, 50 mM Tris-HCl, pH 7.6, in a 100-µL final volume and NADPH formation was monitored at 340 nm. The 100 % activity corresponds to the activity of the chemically reconstituted ACO2 prepared by incubating apo-ACO2 with 4 molar excess of ferrous iron and sulfur for 30 min in the presence of 5 mM DTT (4 µmol/min/mg).

Spectroscopic analyses

UV-visible absorption spectra were recorded with an Uvikon XL spectrophotometer (BioTek Instruments). ^{57}Fe-Mössbauer spectra were recorded using 400 µl cuvettes containing 170-560 µM protein. Spectra were recorded on a spectrometer operating in constant acceleration mode using an Oxford cryostat that allowed temperatures from 1.5 to 300 K and a ^{57}Co source in rhodium. Isomer shifts are reported relative to metallic iron at room temperature.

EPR spectra were recorded on a Bruker EMX (9.5 GHz) or ER200D EPR spectrometers equipped with an ESR 900 helium flow cryostat (Oxford Instruments). Double integrals of the EPR signals and spin concentration were obtained through the Win-EPR software using the spectrum of a 200 µM Cu(EDTA) standard recorded under non saturating conditions.

Antibody production and purification

Polyclonal antibodies against mouse ISCA1, ISCA2 or IBA57 protein were produced asfollows. The peptides (epitopes are listed in Table S3) were coupled to activated KLH using Imject Maleimide Actovated Carrier Protein Spin Kits (Thermo Scientific) in Tris-EDTA buffer (50 mM Tris pH 8.5; 5 mM EDTA). Rabbits were injected with 1:1 solution of the respective antigen and Freunds Complet adjuvant. Sera were purified by SulfoLink Coupling Resin (Thermo Scientific) according to manufacturer's protocol. Antibodies were purified against GST-ISCA2 or their respective antigens/epitope-peptides, respectively. Antibodies were eluted in acidic conditions (0.1 M glycine, pH 2.8) and antibody containing fractions (pH 7.5) were dialyzed against PBSx1 and stored in glycerol 29 % with NaN_3.

Mice

100% C57BL/6J were maintained in a temperature- and humidity-controlled animal facility, with a 12-h light-dark cycle and free access to water and a standard rodent chow (D03, SAFE). Both male and female mice were used in all experiments. All animal procedures and experiments were approved by the local ethical committee (Comité d'Ethique en Expérimentation Animale IGBMC-ICS) for Animal Care and Use (Com'Eth 2012-149, 2012-150, 2014-010), and were performed in accordance with the Guide for the Care and Use of Laboratory Animals (US National Institutes of Health). For local knockdown 4 weeks old C57BL/6J wild-type mice were anesthetized by intraperitoneal injection of ketamine-xylazine (75 and 10 mg per kg body weight, respectively) to allow intramuscular administration of rAAV at a dose of 2.5×10^{10} vg in a volume of 25ml per tibialis anterior. For knockdown studies, rAAV2/1-CMV-eGFP-mU6-shRNA (as indicated) and rAAV2/1-CMV-eGFP-mU6-scrambled shRNA were injected at contralateral sides respectively. Mice were anesthetized by

intraperitoneal injection of ketamine-xylazine, dissected and killed 3 or 6 weeks after injection as indicated. For molecular analysis, tissue samples were directly snap-frozen in isopentane chilled in liquid nitrogen. For histology, skeletal muscle were embedded in OCT Tissue Tek (Sakura Finetechnical, Torrance, California) and snap-frozen in isopentane chilled in liquid nitrogen.

Tissue lysates

Lysates of whole tissue were prepared from frozen mouse skeletal muscle. Tissue was manually homogenized using the ULTRA-TURRAX T25 basic (IKA-WERKE) in SDS-buffer (10 µl/1mg tissue; 280 mM Tris, 43 % glycerol, 10 % SDS, pH 6.8).

Histology and electron microscopy

For histological analysis, muscles were dissected under profound anesthesia and frozen in cold isopentane. Ten µm cryostat sections were stained with hematoxilin and eosin (H&E), or for the activity of succinate dehydrogenase (SDH) and cytochrome *c* oxidase (COX) as previously described (Puccio, Simon et al. 2001). An incubation time of 10 min for SDH and overnight for COX at 37°C was needed before mounting. For electron microscopy, ultrathin sections (70 nm) of skeletal muscle were contrasted with uranyl acetate and lead citrate and examined with a Morgagni 268D electron microscope, as described previously (Puccio, Simon et al. 2001).

AAV production and purification

AAV2/1 vectors were generated by a triple transfection of AAV-293 cell line with pAAV2 insert containing the shRNA transgene under the mU6 promoter and eGFP under the CMV promoter both flanked by serotype 2 inverted terminal repeats, PXR1 containing rep and cap genes of AAV serotype 1, and pHelper enconding the adenovirus helper function. Cell lysates were subjected to 3 freeze/thaw cycles, then treated with 50 U/mL of Benzonase (Sigma) for 30 minutes at 37°C, and clarified by centrifugation. Viral vectors were purified by Iodixanol gradient ultracentrifugation followed by dialysis and concentration against Dulbecco's Phosphate Buffered Saline using centrifugal filters (Amicon Ultra-15 Centrifugal Filter Devices 30K, Millipore, Bedford). Physical particles were quantified by real-time PCR using a plasmid standard pAAV-eGFP, and titers are expressed as viral genomes per milliliter (vg/mL). rAAV titers in Table S1.

Mass spectrometry analysis

Immunoprecipitats were analyzed by NanoLC-nanoESI/MS^2 (Dual linear ion trap LTQ Velos Pro; Thermo Scientific). Native mass determination was carried out by ESI-MS analysis. Steps were performed as described before (Schmucker, Martelli et al. 2011). For normalization, MudPIT data were filtered to be enriched 2x and 10x over negative controls. Remaining proteins were selected for mitochondrial localization using SWISSprot library. SAF and NSAF values were calculated as previously described (Florens, Carozza et al. 2006). In brief, spectral counts of three IP replicates were merged, normalized for protein length and for IP set differences. The normalized spectral abundance factor (NSAF) is calculated as the number of spectral counts (PSM) that identify a protein, divided by the protein length (L), the PSM/L value represents the spectral abundance factor (SAF), which is then divided by the sum of PSM/L for all proteins in the experiment. Values were multiplied by 100 (NSAF*100). NSAF*100 values were used for representation and clustering.

References:

Angeles, D. C., B. H. Gan, et al. (2011). "Mutations in LRRK2 increase phosphorylation of peroxiredoxin 3 exacerbating oxidative stress-induced neuronal death." Hum Mutat **32**(12): 1390-1397.

Banci, L., D. Brancaccio, et al. (2014). "[2Fe-2S] cluster transfer in iron-sulfur protein biogenesis." Proc Natl Acad Sci U S A **111**(17): 6203-6208.

Beilschmidt, L. K. and H. M. Puccio (2014). "Mammalian Fe-S cluster biogenesis and its implication in disease." Biochimie **100**: 48-60.

Bych, K., S. Kerscher, et al. (2008). "The iron-sulphur protein Ind1 is required for effective complex I assembly." EMBO J **27**(12): 1736-1746.

Camaschella, C., A. Campanella, et al. (2007). "The human counterpart of zebrafish shiraz shows sideroblastic-like microcytic anemia and iron overload." Blood **110**(4): 1353-1358.

Cameron, J. M., A. Janer, et al. (2011). "Mutations in iron-sulfur cluster scaffold genes NFU1 and BOLA3 cause a fatal deficiency of multiple respiratory chain and 2-oxoacid dehydrogenase enzymes." Am J Hum Genet **89**(4): 486-495.

Colin, F., A. Martelli, et al. (2013). "Mammalian frataxin controls sulfur production and iron entry during de novo Fe4S4 cluster assembly." J Am Chem Soc **135**(2): 733-740.

Ding, H. and R. J. Clark (2004). "Characterization of iron binding in IscA, an ancient iron-sulphur cluster assembly protein." Biochem J **379**(Pt 2): 433-440.

Ding, H., R. J. Clark, et al. (2004). "IscA mediates iron delivery for assembly of iron-sulfur clusters in IscU under the limited accessible free iron conditions." J Biol Chem **279**(36): 37499-37504.

Emptage, M. H., J. L. Dreyers, et al. (1983). "Optical and EPR characterization of different species of active and inactive aconitase." J Biol Chem **258**(18): 11106-11111.

Florens, L., M. J. Carozza, et al. (2006). "Analyzing chromatin remodeling complexes using shotgun proteomics and normalized spectral abundance factors." Methods **40**(4): 303-311.

Gardner, P. R. and I. Fridovich (1992). "Inactivation-reactivation of aconitase in Escherichia coli. A sensitive measure of superoxide radical." J Biol Chem **267**(13): 8757-8763.

Garland, S. A., K. Hoff, et al. (1999). "Saccharomyces cerevisiae ISU1 and ISU2: members of a well-conserved gene family for iron-sulfur cluster assembly." J Mol Biol **294**(4): 897-907.

Gelling, C., I. W. Dawes, et al. (2008). "Mitochondrial Iba57p is required for Fe/S cluster formation on aconitase and activation of radical SAM enzymes." Mol Cell Biol **28**(5): 1851-1861.

Gupta, V., M. Sendra, et al. (2009). "Native Escherichia coli SufA, coexpressed with SufBCDSE, purifies as a [2Fe-2S] protein and acts as an Fe-S transporter to Fe-S target enzymes." J Am Chem Soc **131**(17): 6149-6153.

Jensen, L. T. and V. C. Culotta (2000). "Role of Saccharomyces cerevisiae ISA1 and ISA2 in iron homeostasis." Mol Cell Biol **20**(11): 3918-3927.

Kaut, A., H. Lange, et al. (2000). "Isa1p is a component of the mitochondrial machinery for maturation of cellular iron-sulfur proteins and requires conserved cysteine residues for function." J Biol Chem **275**(21): 15955-15961.

Kim, J. H., R. O. Frederick, et al. (2013). "[2Fe-2S]-Ferredoxin binds directly to cysteine desulfurase and supplies an electron for iron-sulfur cluster assembly but is displaced by the scaffold protein or bacterial frataxin." J Am Chem Soc.

Krebs, C., J. N. Agar, et al. (2001). "IscA, an alternate scaffold for Fe-S cluster biosynthesis." Biochemistry **40**(46): 14069-14080.

Lill, R. (2009). "Function and biogenesis of iron-sulphur proteins." Nature **460**(7257): 831-838.

Loiseau, L., C. Gerez, et al. (2007). "ErpA, an iron sulfur (Fe S) protein of the A-type essential for respiratory metabolism in Escherichia coli." Proc Natl Acad Sci U S A **104**(34): 13626-13631.

Lu, J., J. P. Bitoun, et al. (2010). "Iron-binding activity of human iron-sulfur cluster assembly protein hIscA1." Biochem J **428**(1): 125-131.

Lu, J., J. Yang, et al. (2008). "Complementary roles of SufA and IscA in the biogenesis of iron-sulfur clusters in Escherichia coli." Biochem J **409**(2): 535-543.

Mapolelo, D. T., B. Zhang, et al. (2012). "Spectroscopic and functional characterization of iron-bound forms of Azotobacter vinelandii (Nif)IscA." Biochemistry **51**(41): 8056-8070.

Mapolelo, D. T., B. Zhang, et al. (2013). "Monothiol glutaredoxins and A-type proteins: partners in Fe-S cluster trafficking." Dalton Trans **42**(9): 3107-3115.

Martelli, A., M. Wattenhofer-Donze, et al. (2007). "Frataxin is essential for extramitochondrial Fe-S cluster proteins in mammalian tissues." Hum Mol Genet **16**(22): 2651-2658.

Mimaki, M., X. Wang, et al. (2012). "Understanding mitochondrial complex I assembly in health and disease." Biochim Biophys Acta **1817**(6): 851-862.

Morimoto, K., E. Yamashita, et al. (2006). "The asymmetric IscA homodimer with an exposed [2Fe-2S] cluster suggests the structural basis of the Fe-S cluster biosynthetic scaffold." J Mol Biol **360**(1): 117-132.

Muhlenhoff, U., N. Richter, et al. (2011). "Specialized function of yeast Isa1 and Isa2 proteins in the maturation of mitochondrial [4Fe-4S] proteins." J Biol Chem **286**(48): 41205-41216.

Navarro-Sastre, A., F. Tort, et al. (2011). "A fatal mitochondrial disease is associated with defective NFU1 function in the maturation of a subset of mitochondrial Fe-S proteins." Am J Hum Genet **89**(5): 656-667.

Ollagnier-de-Choudens, S., T. Mattioli, et al. (2001). "Iron-sulfur cluster assembly: characterization of IscA and evidence for a specific and functional complex with ferredoxin." J Biol Chem **276**(25): 22604-22607.

Ollagnier-de-Choudens, S., Y. Sanakis, et al. (2004). "SufA/IscA: reactivity studies of a class of scaffold proteins involved in [Fe-S] cluster assembly." J Biol Inorg Chem **9**(7): 828-838.

Pandey, A., H. Yoon, et al. (2011). "Isd11p protein activates the mitochondrial cysteine desulfurase Nfs1p protein." J Biol Chem **286**(44): 38242-38252.

Pelzer, W., U. Muhlenhoff, et al. (2000). "Mitochondrial Isa2p plays a crucial role in the maturation of cellular iron-sulfur proteins." FEBS Lett **476**(3): 134-139.

Puccio, H., D. Simon, et al. (2001). "Mouse models for Friedreich ataxia exhibit cardiomyopathy, sensory nerve defect and Fe-S enzyme deficiency followed by intramitochondrial iron deposits." Nat Genet **27**(2): 181-186.

Raulfs, E. C., I. P. O'Carroll, et al. (2008). "In vivo iron-sulfur cluster formation." Proc Natl Acad Sci U S A **105**(25): 8591-8596.

Schaedler, T. A., J. D. Thornton, et al. (2014). "A conserved mitochondrial ATP-binding cassette transporter exports glutathione polysulfide for cytosolic metal cofactor assembly." J Biol Chem **289**(34): 23264-23274.

Schmucker, S., M. Argentini, et al. (2008). "The in vivo mitochondrial two-step maturation of human frataxin." Hum Mol Genet **17**(22): 3521-3531.

Schmucker, S., A. Martelli, et al. (2011). "Mammalian frataxin: an essential function for cellular viability through an interaction with a preformed ISCU/NFS1/ISD11 iron-sulfur assembly complex." PLoS One **6**(1): e16199.

Sheftel, A. D., O. Stehling, et al. (2009). "Human ind1, an iron-sulfur cluster assembly factor for respiratory complex I." Mol Cell Biol **29**(22): 6059-6073.

Sheftel, A. D., C. Wilbrecht, et al. (2012). "The human mitochondrial ISCA1, ISCA2, and IBA57 proteins are required for [4Fe-4S] protein maturation." Mol Biol Cell **23**(7): 1157-1166.

Ta, D. T. and L. E. Vickery (1992). "Cloning, sequencing, and overexpression of a [2Fe-2S] ferredoxin gene from Escherichia coli." J Biol Chem **267**(16): 11120-11125.

Tan, G., J. Lu, et al. (2009). "IscA/SufA paralogues are required for the [4Fe-4S] cluster assembly in enzymes of multiple physiological pathways in Escherichia coli under aerobic growth conditions." Biochem J **420**(3): 463-472.

Teplyakov, A., G. Obmolova, et al. (2004). "Crystal structure of the YgfZ protein from Escherichia coli suggests a folate-dependent regulatory role in one-carbon metabolism." J Bacteriol **186**(21): 7134-7140.

Tsai, C. L. and D. P. Barondeau (2010). "Human frataxin is an allosteric switch that activates the Fe-S cluster biosynthetic complex." Biochemistry **49**(43): 9132-9139.

Uzarska, M. A., R. Dutkiewicz, et al. (2013). "The mitochondrial Hsp70 chaperone Ssq1 facilitates Fe/S cluster transfer from Isu1 to Grx5 by complex formation." Mol Biol Cell **24**(12): 1830-1841.

Vinella, D., C. Brochier-Armanet, et al. (2009). "Iron-sulfur (Fe/S) protein biogenesis: phylogenomic and genetic studies of A-type carriers." PLoS Genet **5**(5): e1000497.

Vinothkumar, K. R., J. Zhu, et al. (2014). "Architecture of mammalian respiratory complex I." Nature.

Wada, K., Y. Hasegawa, et al. (2005). "Crystal structure of Escherichia coli SufA involved in biosynthesis of iron-sulfur clusters: implications for a functional dimer." FEBS Lett **579**(29): 6543-6548.

Waller, J. C., S. Alvarez, et al. (2010). "A role for tetrahydrofolates in the metabolism of iron-sulfur clusters in all domains of life." Proc Natl Acad Sci U S A **107**(23): 10412-10417.

Whitaker, H. C., D. Patel, et al. (2013). "Peroxiredoxin-3 is overexpressed in prostate cancer and promotes cancer cell survival by protecting cells from oxidative stress." Br J Cancer **109**(4): 983-993.

Wiedemann, N., E. Urzica, et al. (2006). "Essential role of Isd11 in mitochondrial iron-sulfur cluster synthesis on Isu scaffold proteins." EMBO J **25**(1): 184-195.

Wingert, R. A., J. L. Galloway, et al. (2005). "Deficiency of glutaredoxin 5 reveals Fe-S clusters are required for vertebrate haem synthesis." Nature **436**(7053): 1035-1039.

Ye, H., S. Y. Jeong, et al. (2010). "Glutaredoxin 5 deficiency causes sideroblastic anemia by specifically impairing heme biosynthesis and depleting cytosolic iron in human erythroblasts." J Clin Invest **120**(5): 1749-1761.

Zeng, J., M. Geng, et al. (2007). "The IscA from Acidithiobacillus ferrooxidans is an iron-sulfur protein which assemble the [Fe4S4] cluster with intracellular iron and sulfur." Arch Biochem Biophys **463**(2): 237-244.

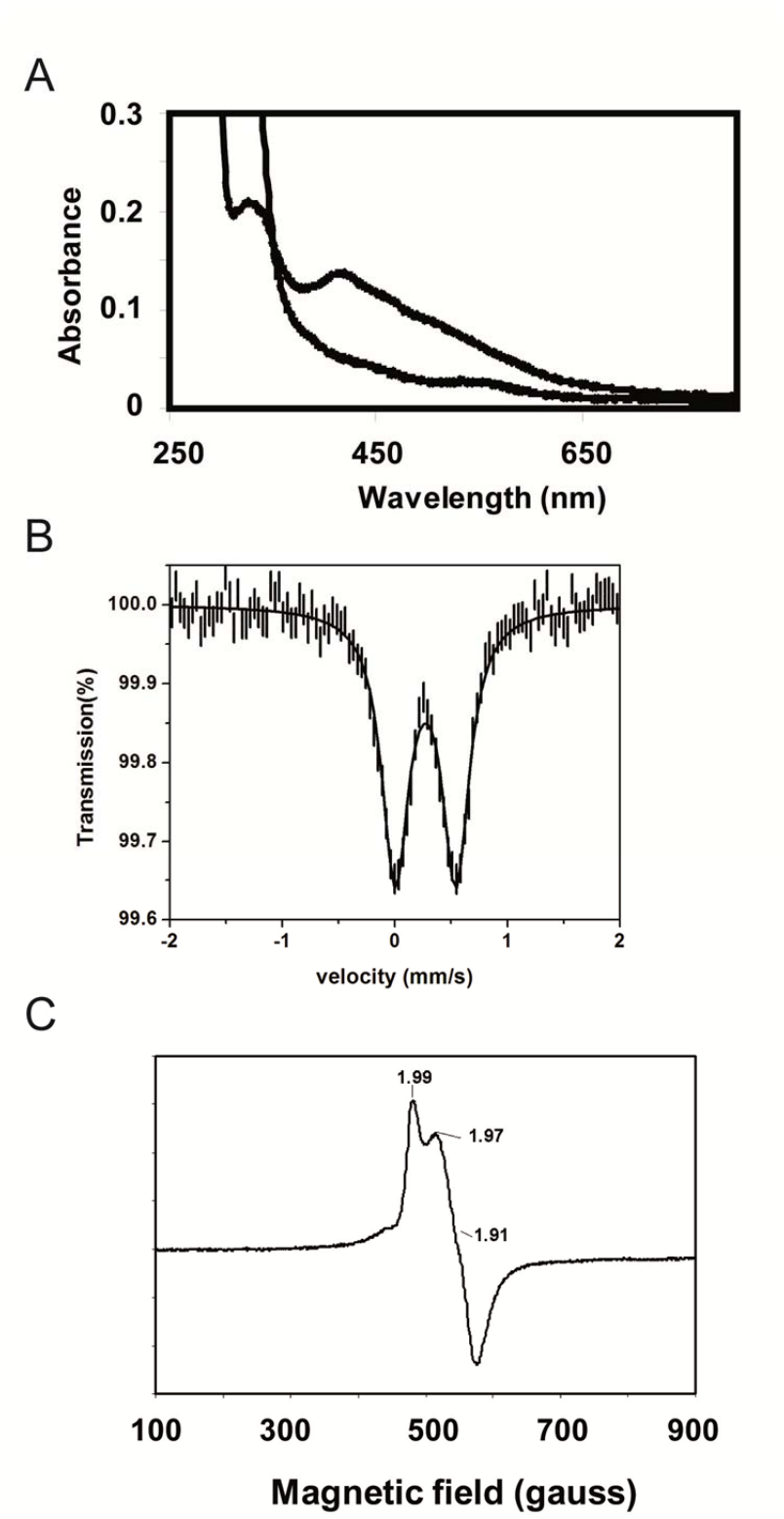
A
0.3
0.2
0.1
0
Absorbance
250
450
650
Wavelength (nm)
B
100.0
99.9
99.8
99.7
99.6
Transmission(%)
-2
-1
0
1
2
velocity (mm/s)
C
1.99
1.97
1.91
100
300
500
700
900
Magnetic field (gauss)

Figure 1

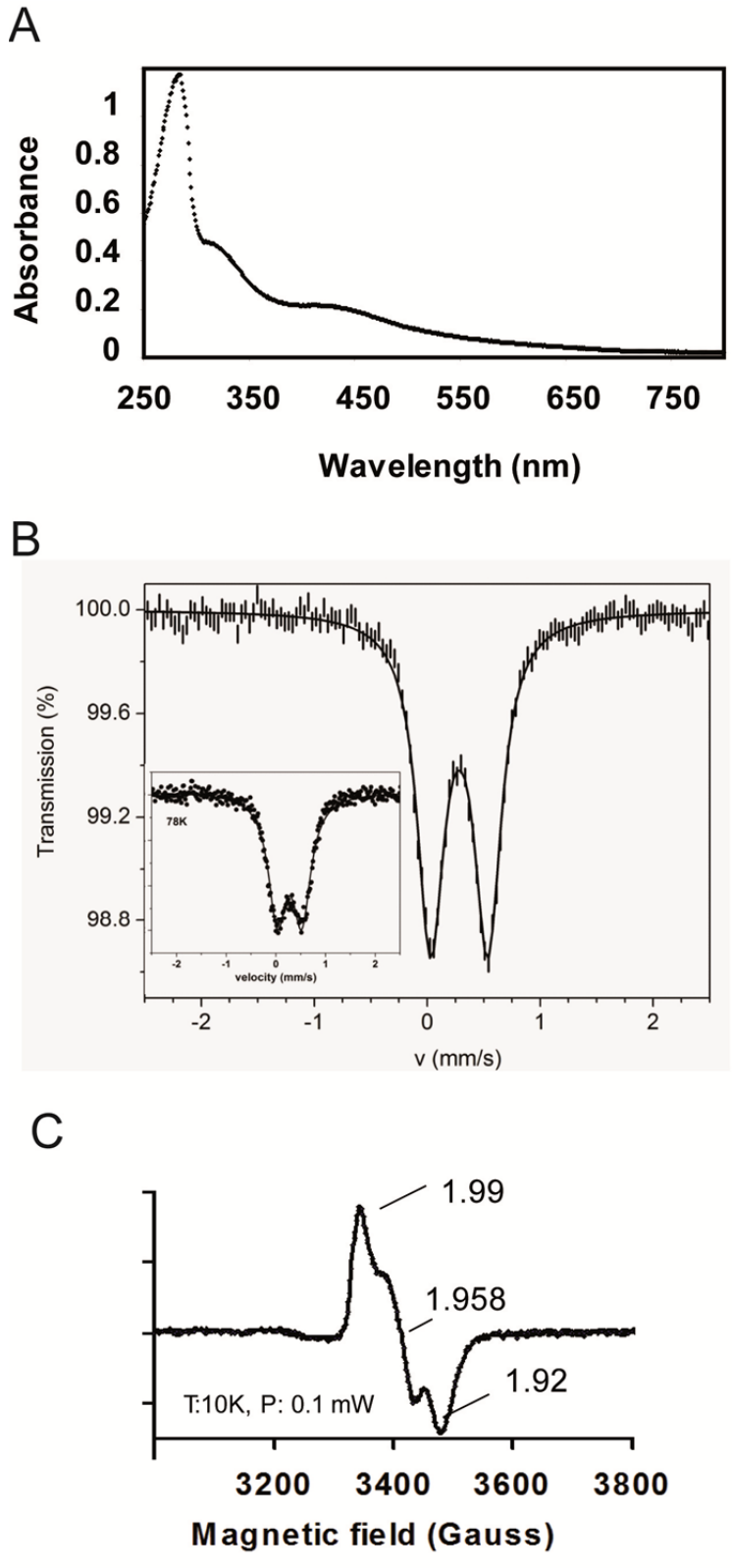
A
Absorbance
1
0.8
0.6
0.4
0.2
0
250
350
450
550
650
750
Wavelength (nm)
B
Transmission (%)
100.0
99.6
99.2
98.8
78K
velocity (mm/s)
-2
-1
0
1
2
v (mm/s)
C
1.99
1.958
1.92
T:10K, P: 0.1 mW
3200
3400
3600
3800
Magnetic field (Gauss)

Figure 2

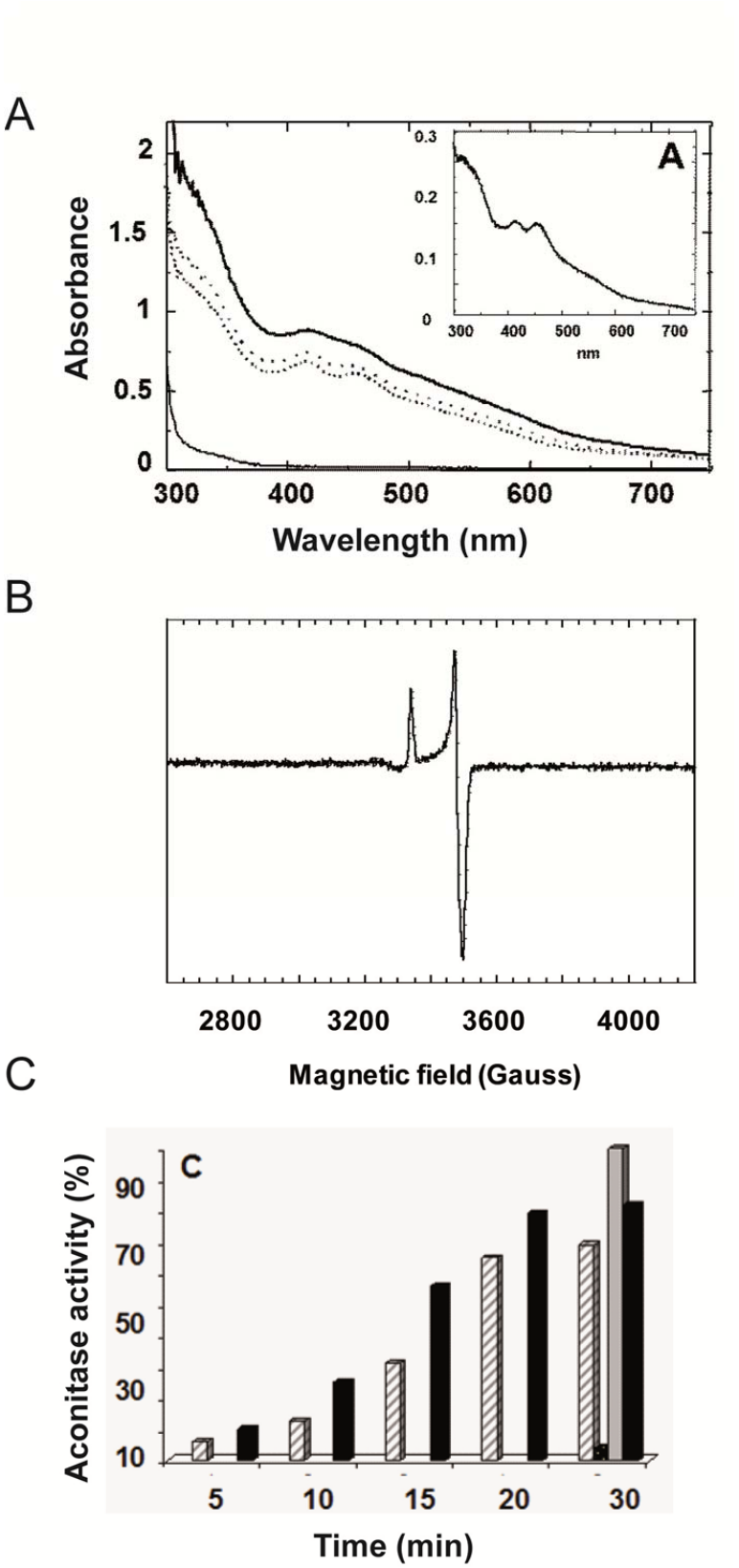
A
Absorbance
2
1.5
1
0.5
0
300
400
500
600
700
Wavelength (nm)
0.3
0.2
0.1
0
A
300
400
500
600
700
nm
B
2800
3200
3600
4000
Magnetic field (Gauss)
C
Aconitase activity (%)
90
70
50
30
10
C
5
10
15
20
30
Time (min)

Figure 3

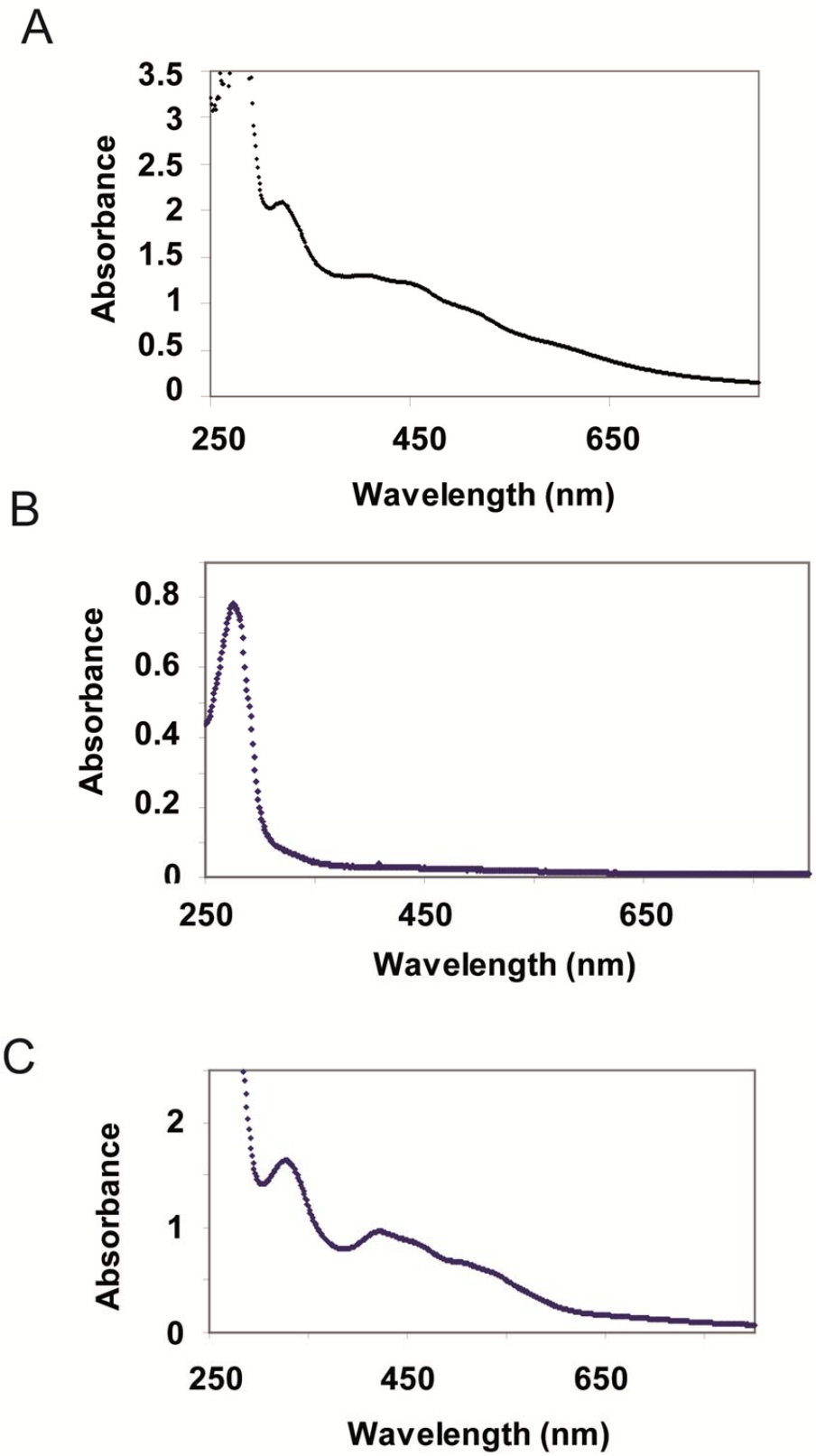
A
Absorbance
3.5
3
2.5
2
1.5
1
0.5
0
250
450
650
Wavelength (nm)
B
Absorbance
0.8
0.6
0.4
0.2
0
250
450
650
Wavelength (nm)
C
Absorbance
2
1
0
250
450
650
Wavelength (nm)

Figure 4

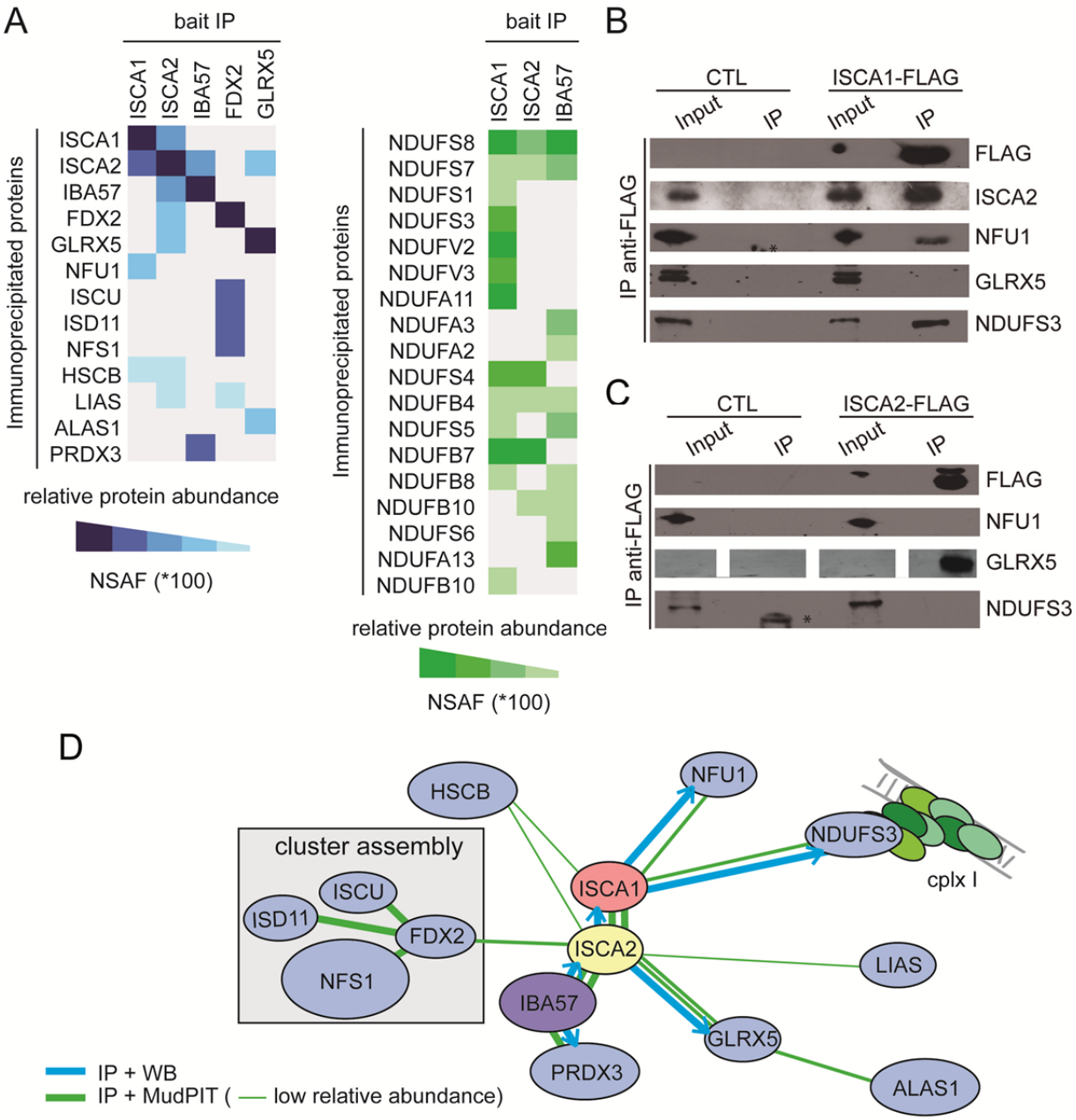
A
bait IP
ISCA1
ISCA2
IBA57
FDX2
GLRX5
Immunoprecipitated proteins
ISCA1
ISCA2
IBA57
FDX2
GLRX5
NFU1
ISCU
ISD11
NFS1
HSCB
LIAS
ALAS1
PRDX3
relative protein abundance
NSAF (*100)
bait IP
ISCA1
ISCA2
IBA57
Immunoprecipitated proteins
NDUFS8
NDUFS7
NDUFS1
NDUFS3
NDUFV2
NDUFV3
NDUFA11
NDUFA3
NDUFA2
NDUFS4
NDUFB4
NDUFS5
NDUFB7
NDUFB8
NDUFB10
NDUFS6
NDUFA13
NDUFB10
relative protein abundance
NSAF (*100)
B
CTL
ISCA1-FLAG
Input
IP
Input
IP
IP anti-FLAG
FLAG
ISCA2
NFU1
GLRX5
NDUFS3
C
CTL
ISCA2-FLAG
Input
IP
Input
IP
IP anti-FLAG
FLAG
NFU1
GLRX5
NDUFS3
D
HSCB
NFU1
NDUFS3
cplx I
cluster assembly
ISCU
ISD11
FDX2
NFS1
ISCA1
ISCA2
LIAS
IBA57
GLRX5
PRDX3
ALAS1
IP + WB
IP + MudPIT (— low relative abundance)

Figure 5

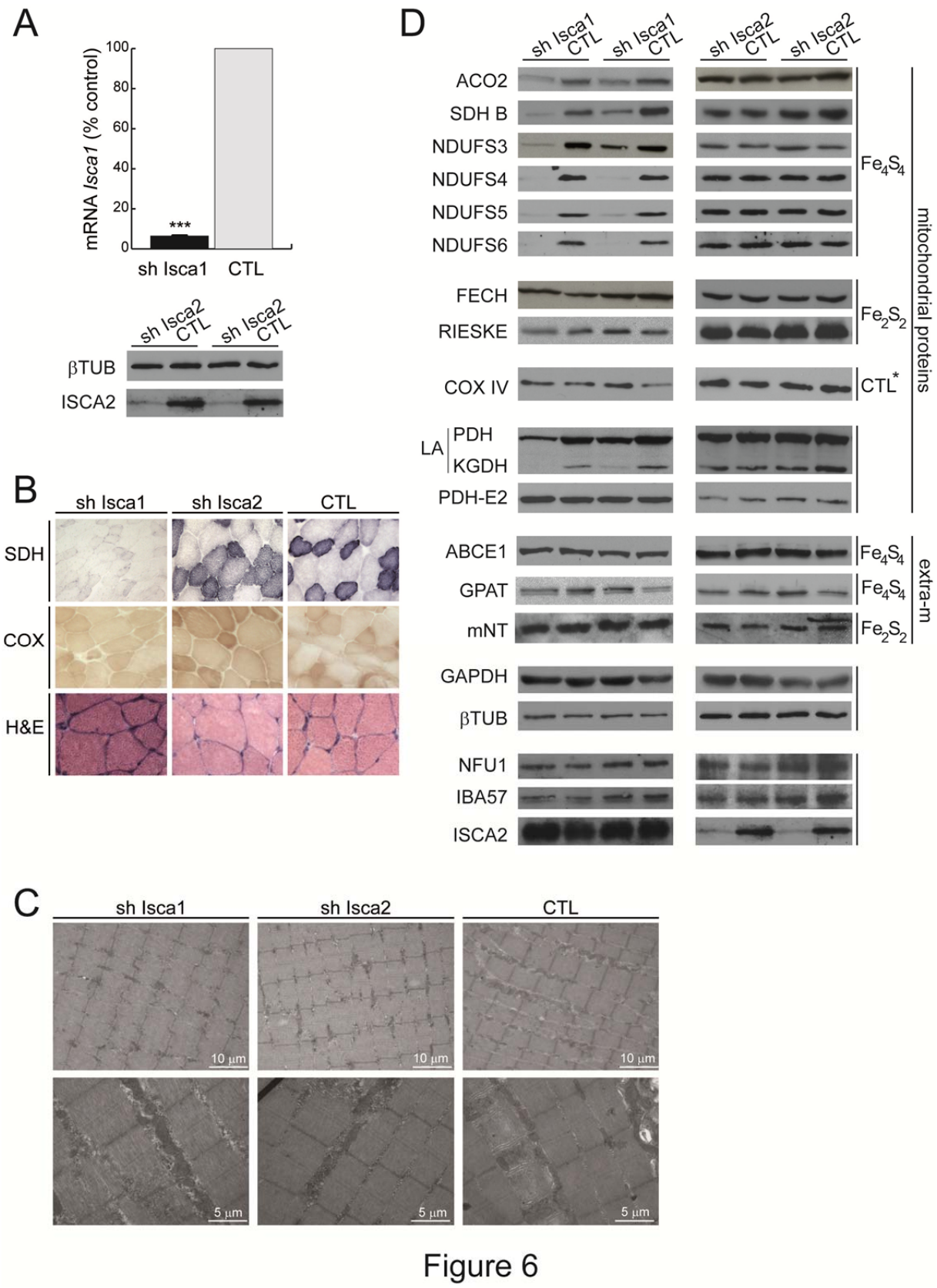
A
mRNA Isca1 (% control)
100
80
60
40
20
0
***
sh Isca1
CTL
sh Isca2 CTL
sh Isca2 CTL
βTUB
ISCA2
B
sh Isca1
sh Isca2
CTL
SDH
COX
H&E
C
sh Isca1
sh Isca2
CTL
10 μm
5 μm
D
sh Isca1 CTL
sh Isca1 CTL
sh Isca2 CTL
sh Isca2 CTL
ACO2
SDH B
NDUFS3
NDUFS4
NDUFS5
NDUFS6
Fe4S4
FECH
RIESKE
Fe2S2
COX IV
CTL*
LA
PDH
KGDH
PDH-E2
mitochondrial proteins
ABCE1
GPAT
mNT
Fe4S4
Fe4S4
Fe2S2
extra-m
GAPDH
βTUB
NFU1
IBA57
ISCA2

Figure 6

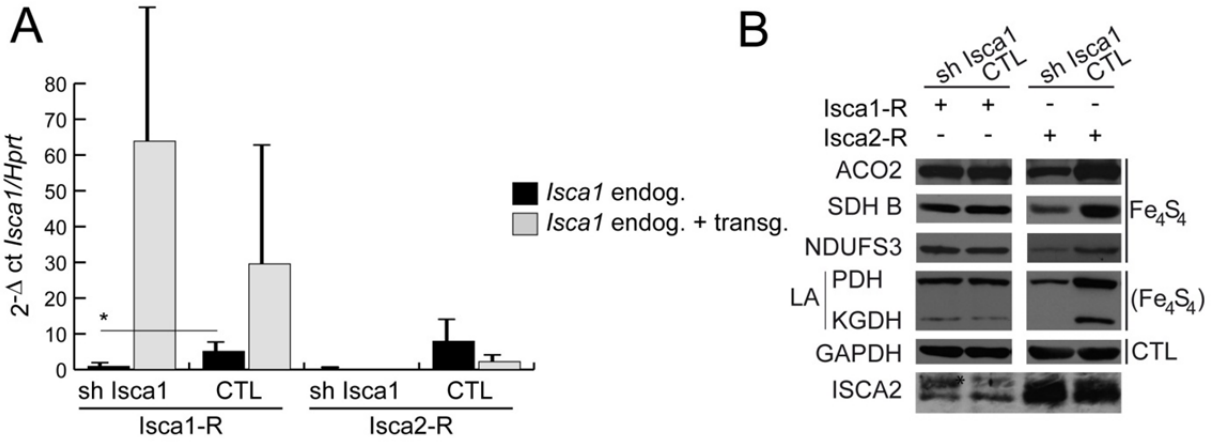
A
2^-Δ ct Isca1/Hprt
80
70
60
50
40
30
20
10
0
*
sh Isca1
CTL
sh Isca1
CTL
Isca1-R
Isca2-R
Isca1 endog.
Isca1 endog. + transg.
B
sh Isca1
CTL
sh Isca1
CTL
Isca1-R + + - -
Isca2-R - - + +
ACO2
SDH B
NDUFS3
Fe4S4
LA
PDH
KGDH
(Fe4S4)
GAPDH
CTL
ISCA2

Figure 7

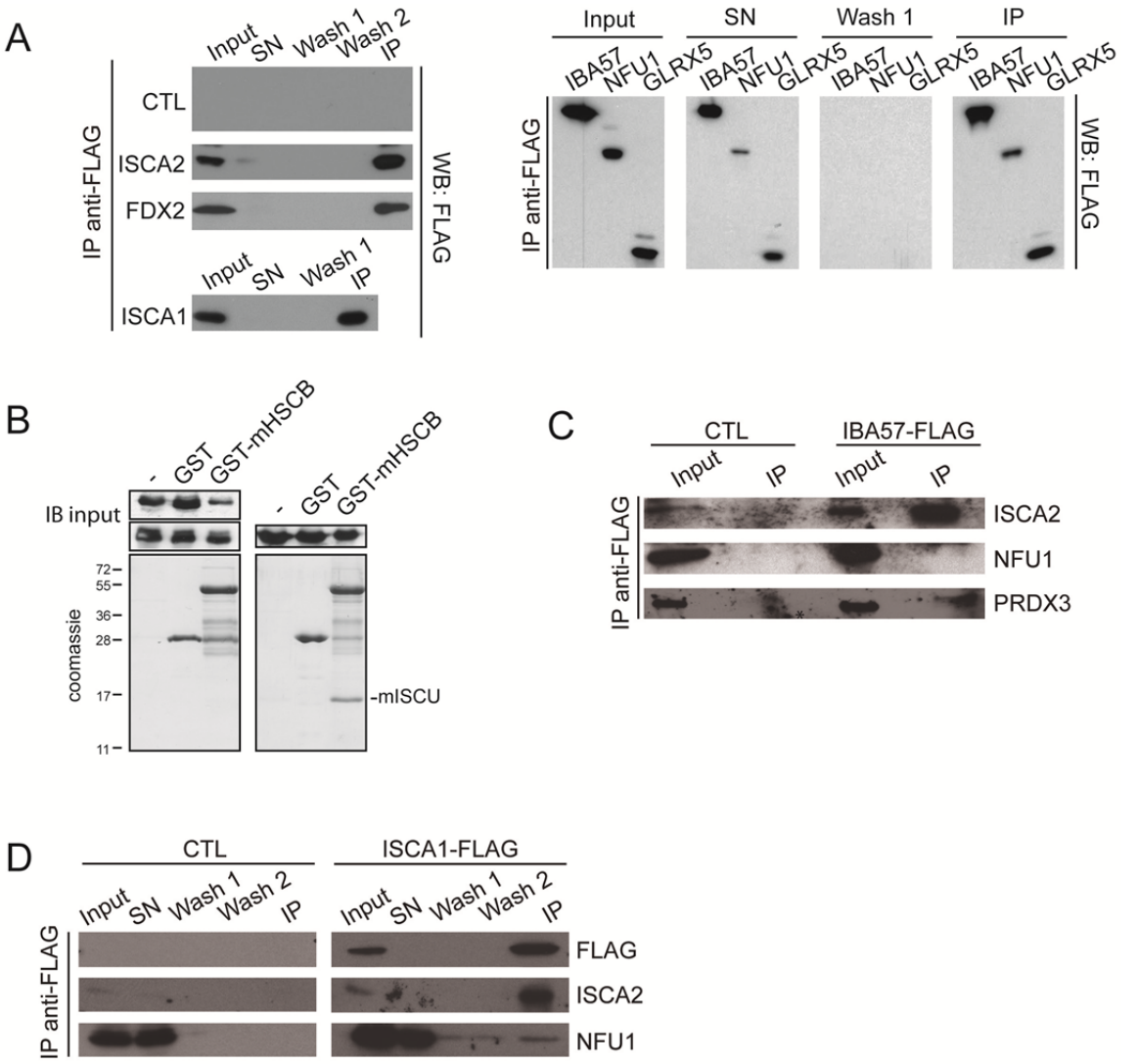
A
Input
SN
Wash 1
Wash 2
IP
CTL
ISCA2
FDX2
IP anti-FLAG
WB: FLAG
ISCA1
Input
SN
Wash 1
IP
Input
SN
Wash 1
IP
IBA57
NFU1
GLRX5
IP anti-FLAG
WB: FLAG
B
-
GST
GST-mHSCB
IB input
coomassie
72
55
36
28
17
11
-mISCU
C
CTL
IBA57-FLAG
Input
IP
IP anti-FLAG
ISCA2
NFU1
PRDX3
D
CTL
ISCA1-FLAG
Input
SN
Wash 1
Wash 2
IP
IP anti-FLAG
FLAG
ISCA2
NFU1

Figure S1

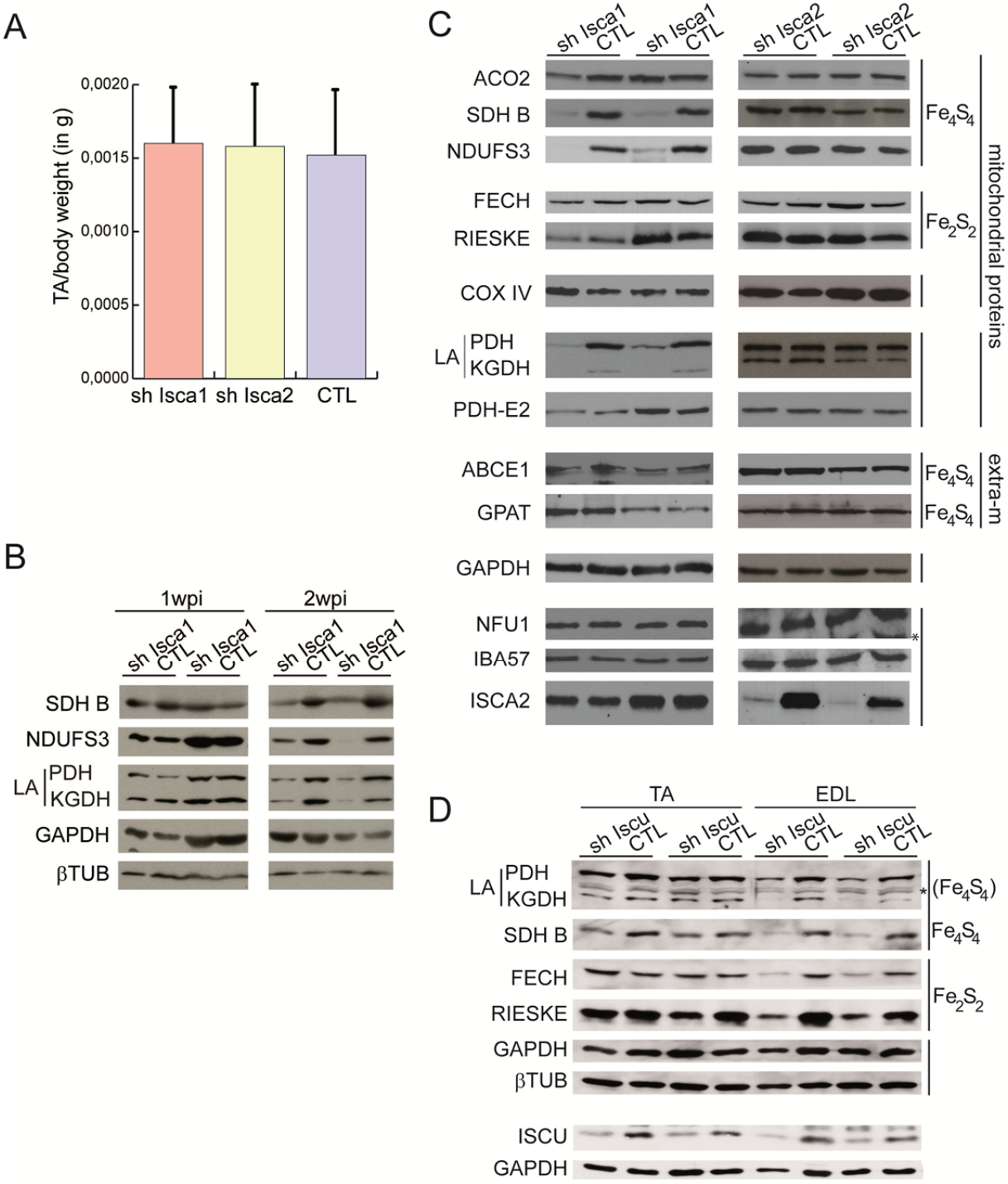
A
TA/body weight (in g)
0,0020
0,0015
0,0010
0,0005
0,0000
sh Isca1
sh Isca2
CTL
B
1wpi
2wpi
sh Isca1
CTL
SDH B
NDUFS3
LA
PDH
KGDH
GAPDH
βTUB
C
sh Isca1
sh Isca2
ACO2
SDH B
NDUFS3
FECH
RIESKE
COX IV
PDH-E2
ABCE1
GPAT
GAPDH
NFU1
IBA57
ISCA2
Fe4S4
Fe2S2
mitochondrial proteins
extra-m
D
TA
EDL
sh Iscu
CTL
(Fe4S4)
ISCU

Figure S2

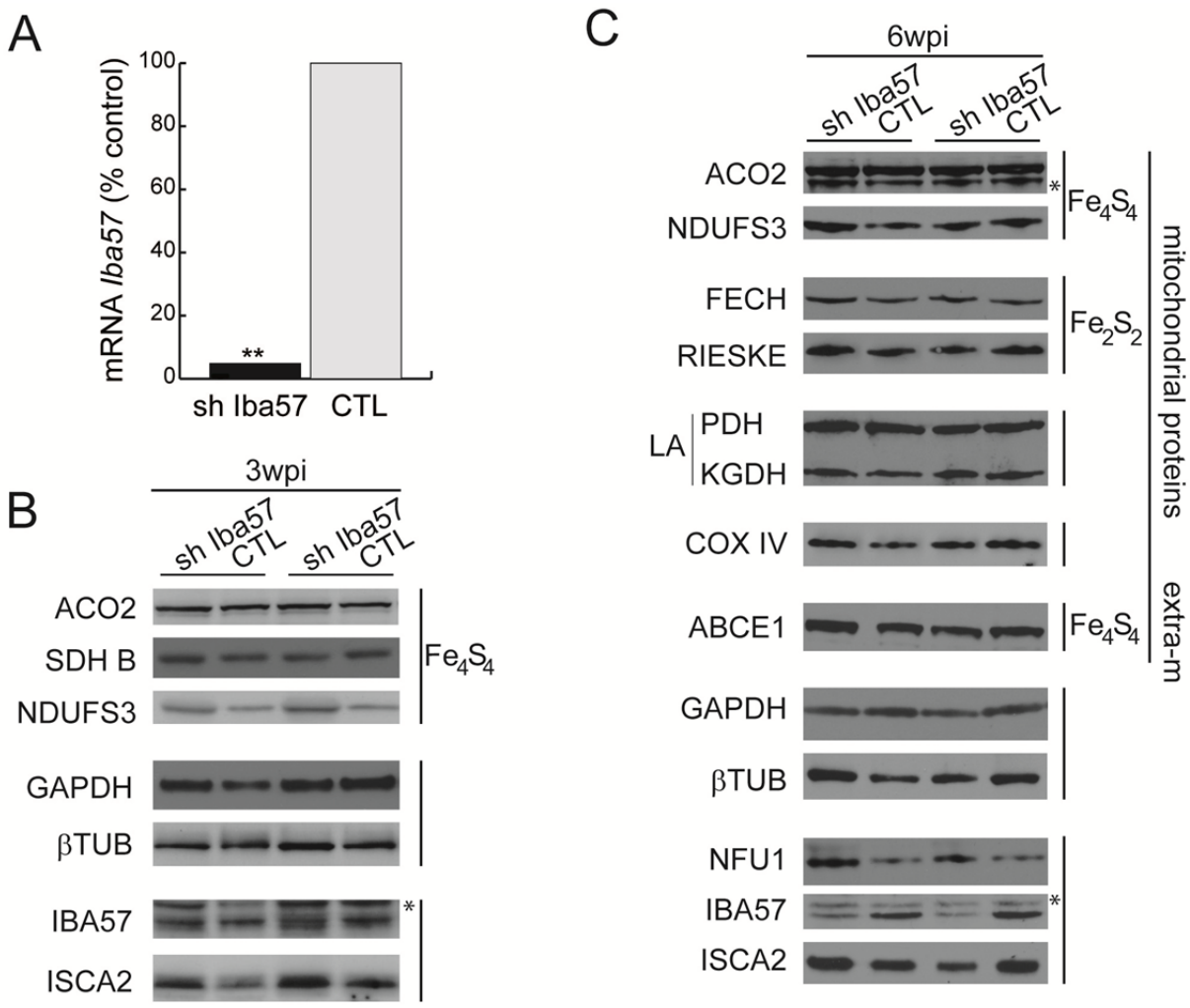
A
mRNA Iba57 (% control)
100
80
60
40
20
0
**
sh Iba57
CTL
B
3wpi
sh Iba57
CTL
sh Iba57
CTL
ACO2
SDH B
NDUFS3
Fe4S4
GAPDH
βTUB
IBA57
*
ISCA2
C
6wpi
sh Iba57
CTL
sh Iba57
CTL
ACO2
*
NDUFS3
Fe4S4
FECH
RIESKE
Fe2S2
LA
PDH
KGDH
COX IV
mitochondrial proteins
ABCE1
Fe4S4
extra-m
GAPDH
βTUB
NFU1
IBA57
*
ISCA2

Figure S3

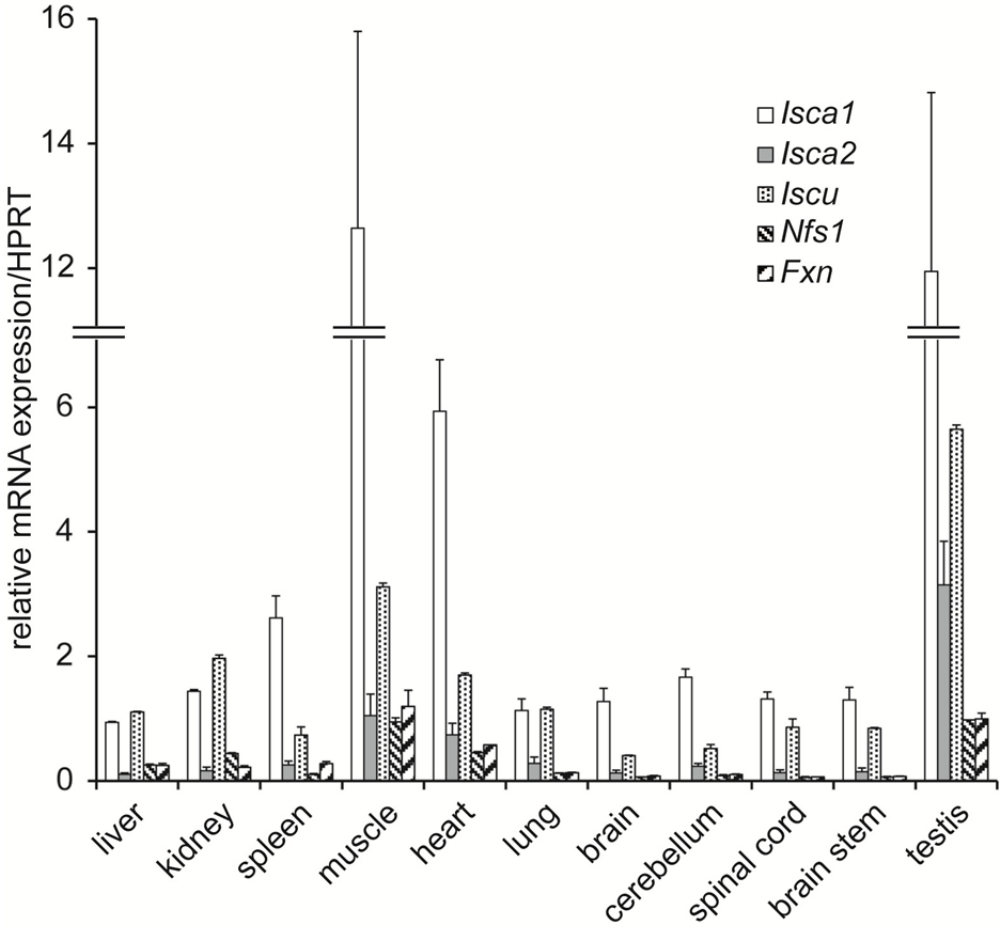
16
14
12
6
4
2
0
relative mRNA expression/HPRT
Isca1
Isca2
Iscu
Nfs1
Fxn
liver
kidney
spleen
muscle
heart
lung
brain
cerebellum
spinal cord
brain stem
testis

Figure S4

Supplementary Tables:

Table S 1: rAAV vectors

rAAV	batch	titer	sh RNA sequence
rAAV2/1- CMV-eGFP-mU6-sh Isca1 208	193 423	1.2×10^{13} 1.4×10^{12}	GGAGATTCTGATGAAGAAG
rAAV2/1-CMV-eGFP-mU6-scrambled shRNA 208	194 422	4.7×10^{12} 1.1×10^{12}	GGAGGGTACGATAAATTGA
rAAV2/1- CMV-eGFP-mU6-sh Isca2 471	427	7.1×10^{11}	GGTCATCCTTCTCTGTCAAAG
rAAV2/1-CMV-eGFP-mU6-scrambled shRNA 471	367	1.2×10^{12}	GAGTCCCTTCCGCAGTTATAT
rAAV2/1-CMV-eGFP-mU6-sh Iba57 334	379	1.7×10^{12}	GCGTATGCCCATTTCCTGAAT
rAAV2/1-CMV-eGFP-mU6-sh Iscu 111	383	8.3×10^{11}	GGCTCTACCACAAGAAGGTTG
rAAV2/9-CMV-eGFP-mU6-scrambled sh (universal)	324	4.9×10^{12}	GCGCTTAGCTGTAGGATTC
rAAV2/1- CMV-Isca1^{R}	300	1.2×10^{12}	
rAAV2/1- CMV-Isca2^{R}	366	1.3×10^{12}	

Table S 2: Mutagenesis primers

Mutagenesis	Forward primer	Reverse primer
Isca1R	gtacacaaagacaaaaggagacagtgatgaagaagttattcaag	cttgaataacttcttcatcactgtctccttttgtctttgtgtac
Isca2 R	agcaaggctgctcctgtgggtctagcttctctgtcaaagtctga	tcagactttgacagagaagctgctcccacaggagcagccttgct

Table S 3: Antibodies

Antibody against	Clone (monoclonal, (c)) or antigen/epitope (polyclonal, (e)); Reference Number (R)	Producer	Concentration WB
ISCA1	GLEYTKTKGDSDEEV (e) , 3671 (R)	IGBMC	1: 1.000
ISCA1	His-mISCA1 (e), 2778 (R)	IGBMC	
ISCA2	GST-mISCA2 (e), 2883 (R)	IGBMC	1: 2.000
IBA57	CLGDLQDYHKYRYQQG (e), 3230/3229 (R)	IGBMC	1: 1.000
NFU1	GST-NFU1 (e)	Kindly provided by T. Rouault	1: 5.000
GLRX5	YLDDPELRQGIKDYS (e)	Kindly provided by C. Bouton	1: 1.000

ISCU	CKLQIQVDEKGIVDARFK (e), 2385 PH233 (R) CADYKLKQESKKEEPEKQ (e), 2386 (R)	IGBMC	1: 1.000
FLAG	M2 (c), F3165 (R)	SIGMA	1: 5.000
Lipoic acid (LA)	LA-KLH (e), 437695 (R)	Calbiochem	1: 5.000
SDHB (complex II)	459230 (c), 21A11AE7 (R)	Invitrogen	1: 5.000
NDUFS3 (complex I)	17D950C9H11 (c), 439200 (R)	Invitrogen	1: 5.000
Rieske, UQCRFS1 (complex III)	5A5 (c) , MS305 (R)	abcam/ MitoSciences	1: 5.000
COX IV (complex IV)	20E8C12 (c), ab14744 (R)	abcam/ MitoSciences	1: 1.000
GPAT	CLTGQYPVELEW (e), 2374 (R)	IGBMC	1: 1.000
FECH	CRKTKSFFTSQQL (e), 2381 (R)	IGBMC	1: 1.000
ACO2	CYDLLEKNINIVRKRLNR (e), 2377 (R)	IGBMC	1: 1.000-1: 10.000
GAPDH	6c5 (c), MAB374 (R)	Millipore	1: 40.000
β-Tubulin	2A2 (c) 1TUB-2A2 (R)	IGBMC	1: 10.000-1.20.000
GFP	2A5 (c), 1GFP-2A5 (R)	IGBMC	<1: 1.000
PRDX3	12B (c), ab16751 (R)	abcam	1: 1.000
ABCE1	KLH-aa 550-C-terminus (human ABCE1) (e), ab32270 (R)	abcam	1: 1.000
NDUFS4 (complex I)	2C7CD4AG3 (c), ab87399/ MS 104 (R)	abcam/ MitoSciences	1: 1.000
NDUFS5 (complex I)	aa1-106 (human NDUFS5) (e), ab188510 (R)	abcam	1: 1.000
NDUFS6 (complex I)	KLH-aa28-56 (human NDUFS6) (e), ab156099 (R)	abcam	1: 500
mitoNEET/mNT	H2N- CDGAHTKHNEETGDNV–CONH2	Kindly provided by C. Bouton	1: 1.000

Table S 4: Oligonucleaotides for qRT-PCR

Gene	5'-3'
Isca1 ORF Fd	CTGAGCATGTGGGTCTGAAA
Isca1 ORF Rv	TTCCCTTGATGTTGGGGTTA
Isca1 UTR Fd	CAAGCCAATGTGGGAAGAGT
Isca1 UTR Rv	CAAAGCAGGCTACAGCACAA
Isca2 ORF Fd	GCTGCAAGTAGAGGGAGGTG
Isca2 ORF Rv	GAGAAGGATGACCCACAGGA
Isca2 UTR Fd	TCTGATAGCTTGGCCTTCGT

Isca2 UTR Rv	GGTTGTTCACACTGGTGCAG
Iba57 Fd	AAGGCACCACCATGCTTATC
Iba57 Rv	TGGGGGAAGATCACAGACTC
Hprt Fd	GTA ATG ATC AGT CAA CGG GGG AC
Hprt Rv	CCA GCA AGC TTG CAA CCT TAA CCA

4. Additional results

4.1 Interactions

In this section additional result and further explanations particularly about the data mining process will be provided. The results concern different aspects of the approach to determine ISCA1 and ISCA2 interacting proteins and will be presented following the outline of the introduction to the paper (see 2.1).

4.1.1 Mitochondrial localization and toxicity effect of over-expressed IP bait proteins

Prior of performing mitochondrial-enrichments of over-expressed Flag-tagged proteins for IPs, it was tested, if the C-terminal tagged proteins localize to mitochondria upon over-expression (Sheftel, Stehling et al. 2010; Ye, Jeong et al. 2010; Sheftel, Wilbrecht et al. 2012). Confocal microscopy on immunofluorescences showed that all tagged bait proteins localize exclusively to mitochondria upon over-expression in cultured cells (performed for all proteins in HeLA and Cos-1 cells) (Figure 15**Figure 15**). Notably, upon exceeding 24-36 h post transfection over-expression of any of the bait proteins except IBA57, cell death was observed to different extend and was particularly apparent for ISCA2. This suggests that expression of different Fe-S biogenesis proteins is toxic and was previously observed (unpublished previous observation i.e. for NFS1 over-expression). This was problematic to obtain large enough quantities of cells expressing the respective bait protein sufficient amounts and therefore sample size was increased for ISCA1, ISCA2 and FDX2.

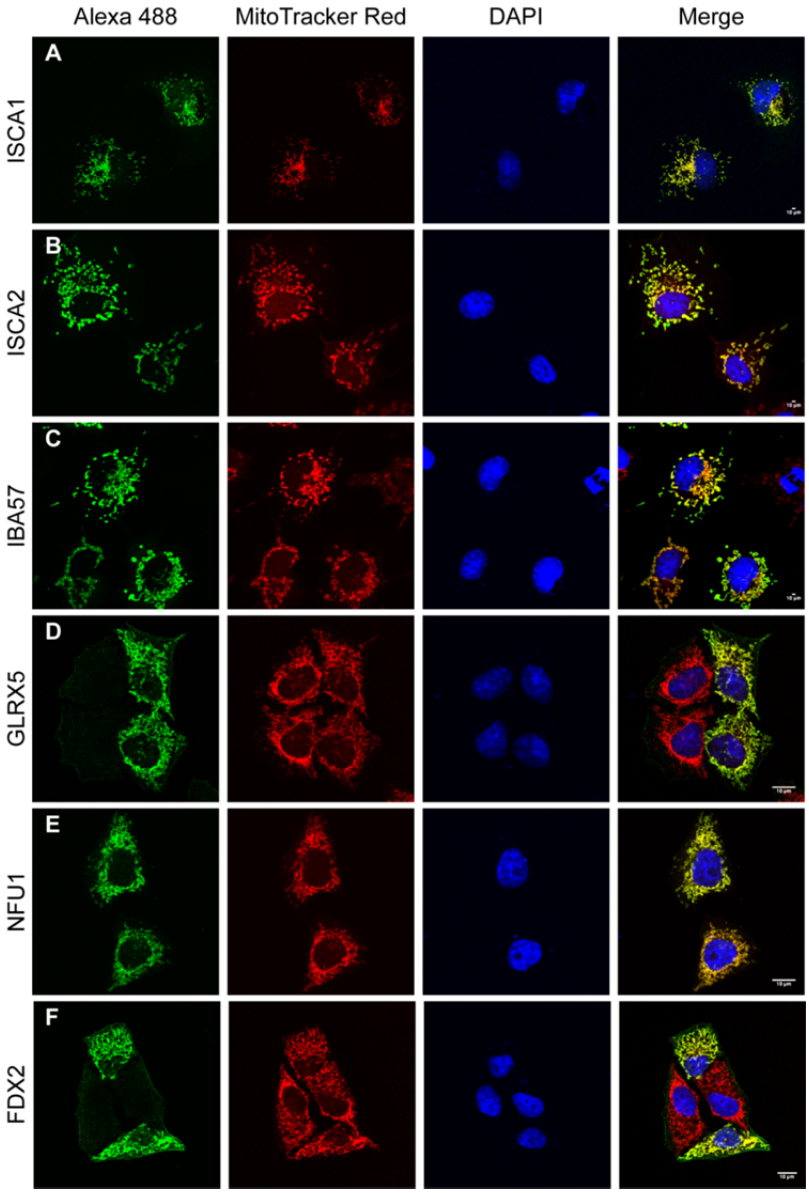

Figure 15: Overexpressed Fe-S biogenesis proteins localize to mitochondria of cultured cells.

Confocal microscopy on immunofluorescence on cultured cells overexpressing Fe-S biogenesis proteins as follows; ISCA1 (a), ISCA2 (b), IBA57 (c), GLRX5 (d), NFU1 (e) and FDX2 (f). Transiently transfected Cos-1 (a-c) and HeLa (d-f) cells were fixed with 4% PFA and permeabilized with PBS-Triton X-100 0.1%. Cells were treated with DAPI, Mito Tracker Red CMXRos, primary antibodies and Alexa 488-coupled secondary antibody as indicated. Combinations of expression constructs and primary antibodies as follows: ISCA1-MYC with anti-ISCA1, ISCA2-MYC with anti-ISCA2, IBA57-MYC with anti-MYC, GLRX5-FLAG with anti-FLAG, NFU1-FLAG with anti-NFU1, and FDX2-FLAG with anti-FLAG.

Overexpression of any of the bait proteins except IBA57 lead to a different extent to toxicity effects like cell death, but was particularly apparent for ISCA2.

4.1.2 Abundance of proteins in the Mass Spectrometry analysis of control samples and the effectiveness of filtering

For MudPIT analysis IP datasets were filtered against two types of negative controls (first the control-IP and second two mitochondria-enriched input-controls). The decision of including a second filtering step against the non-transfected input (mitochondria-enriched input) was based on several observations. First, it was noticed that bait-IP datasets after the first normalization against control-IP still contained a relatively high number of cytosolic and nuclear proteins (data not shown), which are due to the mitochondrial-localization of the bait (Figure 15) likely to be false-positive binding partners. Second, by comparing the total number of PSM counts among controls (Table 2), it was noted that the total PSM counts show the following differences between the two types of controls. As expected for crude protein extracts the total PSM counts were much higher in the mitochondria-enriched inputs. Although this also showed that the extent of unspecific binding to the Flag antibody coupled beads in control-IPs and bait-IPs was rather low, normalization against the control-IPs decreased the stringency of analysis. Therefore, including the mitochondrial-enriched inputs as controls filtered particularly against high-abundance proteins, which were likely non-specific and therefore, the precision and stringency of the whole analysis was highly increased.

Table 2: Total PSM counts in the negative controls reveals quality differences between mass spectrometry runs.

Negative controls were compared based on the total PSM counts as well as on abundance of several high and low abundance proteins (data for the latter not shown).

run	PSM total
CTL IP Replicate 1	2301
CTL IP Replicate 2	4272
CTL IP Replicate 3	7530
CTL IP Replicate 4	807
Mito-enriched input Replicate 1	95931
Mito-enriched input Replicate 2	92386

An increase of the total PSM counts for control-IP replicates numbers 1 to 3 was noted (Table 2), probably due to gradually increased sample sizes based on expression difficulties (see 4.1.1) as well as an update of the machine (LTQ Velos to LTQ Velos Pro). Control-IP replicate 4 was excluded from further analysis, since the total number of counts of low and the distribution of high and low

abundance proteins was not homogeneous to the other controls (for Fe-S biogenesis proteins shown in Table 2).

4.1.2.1 Abundance of Fe-S biogenesis proteins among controls

The assessment of PSM counts for proteins of the Fe-S biogenesis showed that although most of them were detected in the mitochondria-enriched input, they were of low abundance (Table 3), suggesting low expression levels compared to other mitochondrial proteins (i.e. SDH A in Table 3). Furthermore, proteins of the Fe-S biogenesis rarely appeared in the control-IP replicates, both directly implying that if a protein is enriched over controls may indicate a specific protein interaction.

Table 3: Abundance of Fe-S biogenesis proteins and selected candidates amongst controls.

Negative controls were compared for PSM counts of Fe-S biogenesis proteins and selected candidate proteins.

PSM	CTL-IP Replicate 1	CTL-IP Replicate 2	CTL-IP Replicate 3	Mito-enriched input Replicate 1	Mito-enriched input Replicate 1
ISCA1					1
ISCA2					
IBA57				2	4
NFU1				1	
GLRX5					2
FDX2				1	
FXN				2	2
NFS1					1
ISCU			1	2	
ISD11		1			1
BOLA3			2	2	5
NUBPL				4	1
FDXR				3	1
ABCB7				1	1
FDX1					
HSCA					
HSCB					
SDH A		17	5	87	113
SDH B	10	7	2	2	4
SDHAF2				7	3
LIAS					
ALAS1			1	1	1
PRDX3	8	27	1	41	31

4.1.2.2 Abundance of subunits of respiratory chain complex I in controls

To validate the interaction of ISCA1 and to a lesser extent ISCA2 with complex I subunits (manuscript Figure 5), the abundance of complex I subunits in control samples was carefully analyzed. Although complex I is an abundant and important component of the mitochondrial respiratory chain, the spectral counts detected for the different subunits appeared rather low in control samples (Table 4), suggesting a specific enrichment, and thus a specific interaction with ISCA1 (and potentially ISCA2).

Notably, out of the core subunits in the membrane arm of complex I only ND5 is detected in one of the controls, which argues against an unspecific enrichment of membrane proteins in our approach.

Table 4: Detection of respiratory chain complex I's subunit amongst controls.

Negative controls were compared for PSM counts of subunits of complex I.

PSM	CTL-IP Replicate 1	CTL-IP Replicate 2	CTL-IP Replicate 3	Mito-enriched input Replicate 1	Mito-enriched input Replicate 1
NDUFAF6					1
NDUFAF3		2		1	
NDUFAF4	1			2	1
NDUFAF5					1
NDUFA1					1
NDUFA10		1		1	4
NDUFA12		2		1	
NDUFA2		3			
NDUFA4				1	
NDUFA4L2				1	1
NDUFA5	2	3	2	8	6
NDUFA6		1		1	
NDUFA7		3	6	1	
NDUFA8		5	4	3	4
NDUFA9				4	
NDUFB10		3	2		
NDUFB11					1
NDUFB3				1	
NDUFB5				1	
NDUFB9					1
NDUFC1				1	
NDUFC2			1	1	1
NDUFV1				4	
NDUFV2	2	9	3		
NDUFV3		4	1		
NDUFS2		3		1	1
NDUFS3		1	1	1	3
NDUFS5		1			
NDUFS6		6	2		
NDUFS1		13	4	1	2
ND5				1	

4.1.2.3 Testing different stringency criteria for data analysis

Two different stringencies (2x or 10x enriched over controls) were tested to filter for specific binding partners. Since in the low stringency 2x enrichment I observed increased total numbers of potential binding proteins that had in average rather low NSAF values, the 2x enrichment was excluded from further analysis. I had further tested to select for candidate binding proteins, by selecting for proteins that appeared at least in two out of the three independent bait-IP replicates. This approach appeared

too stringent, since the total number of potential interactions decreased substantially, but the candidates seemed non-specific, since membrane-associated proteins or proteins involved in cell stress regulation got highly enriched; these likely to be present from the general abundance of membrane proteins and toxic effects of the over-expression (see 4.1.1).

4.1.2.4 Comparison between bait-IP datasets

The bait-IP datasets were compared to determine how abundant the over-expressed bait protein itself is before and after normalization (Table 4). (For instance for ISCA1 IPs: sum PSM 61.689 before and 18.524 after normalization showed effective filtering of non-specific proteins. The sum PSM for ISCA1-Flag (9268), showed high presence of ISCA1 in the data, consisting of 15% of the bait itself in the whole dataset and it got to 50% with the normalization.) Notably, the total counts of PSM for each bait show big differences before and after normalization in between the bait-IP datasets (Table 4). This is likely due to the differences in sample size, different extend of toxicity during overexpression, the stability of the bait-protein and detection sensitivity between the LTQ Velos and LTQ Velos Pro. This is illustrated by the FDX2 dataset. FDX2-Flag over-expression was thought to be rather high (SUM PSM FDX2 bait is the second highest with 8586 counts), but the percentage of the bait PSM to sum of PSM is rather low. In this dataset a high number of binding proteins is identified with low detection values. The negative charge of FDX2 could potentially account for rather high unspecific binding to other proteins.

Table 5: Comparison PSM in different bait-merges before and after normalization.

Total PSM counts were compared before and after normalization (here shown for the lower stringency/ 2x) and percentages of the respective bait detection calculated.

	ISCA1	ISCA2	IBA57	FDX2	GLRX5	NFU1
SUM PSM	61689	27789	9112	89688	5243	2816
SUM PSM normalized	18524	6934	6478	36050	2012	1103
SUM PSM bait	9268	5792	5324	8586	1816	943
% bait	15,0	20,8	58,4	9,6	34,6	33,5
% bait normalized	50,0	83,5	82,2	23,8	90,3	85,5

Although the differences between GLRX5 IP and NFU1 IP analysis do not show big differences while roughly compared (Table 5), a closer look at the NFU1 MudPIT results did not reveal any interesting interaction candidates. Most proteins in the 2x and 10x analysis seemed to be unspecific, either as a result of the cytosolic or membrane localization of the hit or because they were not described as Fe-S-containing proteins (data not shown). In the filtered NFU1 datasets, no candidate protein involved in Fe-S biogenesis or suggested to harbor a cluster could be identified. Hence, NFU1 IPs were not included in the analysis.

4.1.3 Candidate selection and abundance or strength of an interaction

During analysis, different sets of proteins were analyzed in depth and compared among IPs. According to the focus of the study, these were (1) only the bait proteins compared to each other, (2) mitochondrial Fe-S biogenesis proteins only, (3) mitochondrial Fe-S biogenesis and known Fe-S proteins (including or excluding complex I subunits) and (4) all mitochondrial proteins. In addition, it has to be noted that although the normalization steps were extensive, many proteins remained that are probably unspecific. These are usually of low abundance in the normalized IP datasets and include for example components of the respiratory chain complex IV, which does not contain an Fe-S cluster.

Notably, since generally rather extensive detection of low-binding of FDX2 to different proteins was observed (Table 5), FDX2 was excluded from detailed analysis on complex I. (GLRX5 was also not considered for subunits of complex I, since only few subunits were detected in the GLRX5 IP and only with low abundance.) By further looking at the abundance for interactions of FDX2 it occurred that compared to the abundance of FDX2 with NFS1 (NSAF*100: 8,009), ISCU (NSAF*100: 3,648) and ISD11 (NSAF*100: 3,018) specific interactions observed for ISCA1 and ISCA2 in Fe-S biogenesis do not appear with similar high abundance; the highest being ISCA2 (NSAF*100: 2,57) in the ISCA1 IP. The ISCA-interactions are thus likely to be either less strong or frequent and transient. The FDX2 dataset thus strongly suggests the existence of a complex between FDX2-NFS1-ISD11-ISCU, refining previous suggestions from bacterial data (Chandramouli, Unciuleac et al. 2007; Kim, Frederick et al. 2013; Yan, Konarev et al. 2013). Interestingly, FXN was not detected along with FDX2, suggesting exclusive binding of FXN or FDX2 on the Fe-S assembly complex.

4.1.4 Clustering and Gene Ontology (GO) search

Large scale protein data sets generated by mass spectrometry approaches are a big challenge to interpretation. It is not recommended to just browse through long list of identified proteins, since this is inefficient, time consuming and rarely informative (Gramolini and Emili 2005; Kislinger and Emili 2005; Kislinger, Gramolini et al. 2005). It is rather advised to use or develop automated data analysis strategies for “streamlined filtering and facile pattern recognition” to reveal biologically interesting features.

Data clustering is used to identify biologically meaning full patterns in large-scale datasets. Hierarchical clustering builds tree of relationships to identify pairs of results that are most similar. Further, it is generally suggested to apply several clustering techniques to the data, since different clustering metrics use a variety of algorithms and obtain distinct patterns for grouping of proteins

(Quackenbush 2001; Kislinger and Emili 2005). The composition of proteins linked to a cluster is then evaluated if a biologically meaningful pattern or classification is behind. Such results may serve to validate or strengthen the results of the proteomic study (Kislinger and Emili 2005; Meunier, Dumas et al. 2007). We have applied two different hierarchical clustering methods here, Euclidean distance and Pearson correlation. The Euclidean distance represents the similarity of the patterns as a distance. The closer they are in the Euclidean distance the more similar are the binding partners and their abundance in between the datasets. The Pearson correlation is a measure of a linear correlation or dependence between datasets. The different subsets (see (1)-(4) in 4.1.3) were analyzed for hierarchical clustering. None of the interaction patterns cluster together, suggesting that the overlap between the datasets is low.

Three online softwares were tested for the analysis of the present MudPIT results; Gene Ontology, Manteia and DAVID. The Gene Ontology (GO) summarizes biologic roles, molecular functions and biochemical properties ((Ashburner, Ball et al. 2000) and geneontology.org). Manteia is a data mining system that was developed in the igbmc to allow researchers to address complex biological question for a variety of data (http://manteia.igbmc.fr/) (Tassy and Pourquie 2014). DAVID is a bioinformatics database for "annotation, visualization and integrated discovery (http://david.abcc.ncifcrf.gov/). The terms being enriched with all the softwares were "mitochondria", "respiratory chain", "metabolism" and "apoptosis", which was expected when selecting for mitochondrial proteins with toxic effect of over-expression.

4.2 The role of ISCA1 and ISCA2 *in vivo*

4.2.1 Muscle inflammation upon rAAV injections

During analysis of the skeletal muscle, signs of inflammation were observed in virus injected muscles. These were mainly seen within the tissue structure by histology and ultrastructural analysis using electron microscopy (Figure 16). Of note, the extent of inflammation did not differ between injections with specific shRNAs and injections with the scrambled control shRNAs. Although inflammation was present in roughly less than 5% of the analyzed areas (Figure 16A) a few samples displayed stronger signs of inflammation (Figure 16B). By EM, fibers adjacent to infiltration were mostly not structurally affected (Figure 16C). Even in the few regions were the muscle fiber was strongly structurally disturbed, mitochondrial ultrastructure was preserved (Figure 16D). No signs of inflammation were observed upon saline injection. Taken together, this shows that the inflammation observed is originating from the injected virus and not a consequence of the knockdown of ISCA1 or ISCA2.

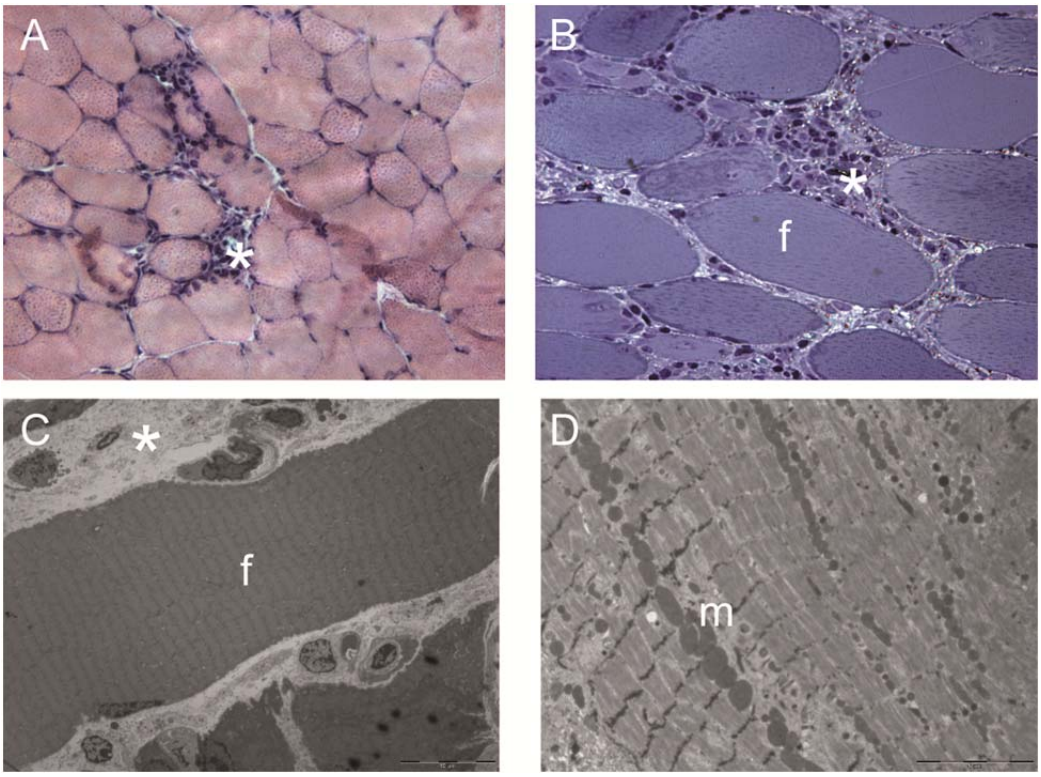

Figure 16: Different extend of inflammation observed in rAAV injected muscle.

Selected images of histological and ultrastructural analysis to illustrate signs of inflammation detected in rAAV injected muscle. H&E staining (A) and toluidine blue staining (B) show inflammatory infiltrations (*) between muscle fibers (f). Electron microscopy (C, D) shows unaffected fibers in between infiltrations (C) and mitochondria (m) of normal shape and size in degenerating fibers (D). Note that these images are not representative of the overall characterized phenotype. (Images are taken with 10x magnification (A), 20x magnification (B) and the scale bars correspond to 10μm (C) and 5μm (D).

4.2.2 Finding the role for ISCA2 in Fe-S biogenesis *in vivo*

We show that ISCA1 and ISCA2 display different function, but the conditions to define ISCA2 function remain to be determined. Therefore, I addressed this specific aspect by testing the following: First, the role of ISCA2 in different tissues by performing systemic knockdown of ISCA2 in the mouse. Second, I analyzed the immediate-upstream genomic regions of mammalian ISCA2 for prediction of transcription factor binding sites. We further tested Isca2 expression under different stress conditions. Third, knockdown of ISCA-proteins in cultured muscle cells was tested, since an effect on mitochondrial Fe_4S_4 proteins was previously observed by knocking down ISCA1, ISCA2 and IBA57 in HeLa cells (Sheftel, Wilbrecht et al. 2012).

4.2.2.1 Systemic knockdown of A-type proteins in mice

The use of rAAVs to deliver shRNA in mice has proven efficient when locally injected. However, rAAVs are also used for systemic gene delivery in a variety of scientific purposed (for instance: (Asokan,

Schaffer et al. 2012; Perdomini, Belbellaa et al. 2014). To uncover a potential tissue specific requirement of ISCA2, systemic injection of rAAV-shRNA was tested. Recombinant AAV2/9 produced in house was shown to successfully deliver a GFP-transgene to different tissues in the lab (Belbellaa and Perdomini unpublished results) (as shown in the literature i.e. in (Bostick, Ghosh et al. 2007; Zincarelli, Soltys et al. 2008). Expression from rAAV2/9 to rAAV2/1 in skeletal muscle was confirmed and TA transduction of comparable levels obtained based on the knockdown efficiency and the intensity of GFP expression (data not shown).

Retro-orbital injections were performed in 3 weeks old wild type mice. First, three different doses of injected rAAV were tested. The three doses chosen were 1x 10^{13}vg/kg, 2.5x 10^{13} vg/kg and x 10^{13} vg/kg (vg: vector genome) (termed the low, the medium and the high dose, respectively). As for the local knockdown study, dissection was carried out 3 wpi. All results for the systemic rAAV knockdown trial are preliminary, since the number of animals per group is below 3 (n=2) and only the lowest and medium doses were tested.

Mice were checked each day and the weight was measured every 3 days (Figure 17). All mice developed in a similar manner during the first 7 days post-injection (dpi) for both the lowest and the medium dose. Mice injected with rAAV encoding for shRNA against ISCA1 started to develop phenotypic changes within the second wpi (for low dose at 14 dpi and medium dose at 10 dpi). These mice started to lose weight compared to littermates, showed reduced activity in the cage and different signs of pain such as nose retraction, miscurvature of the back and signs of anxiety. Mice injected with shRNA against ISCA2 at the medium dose seemed to stop developing around 10 dpi when compared to control littermates.

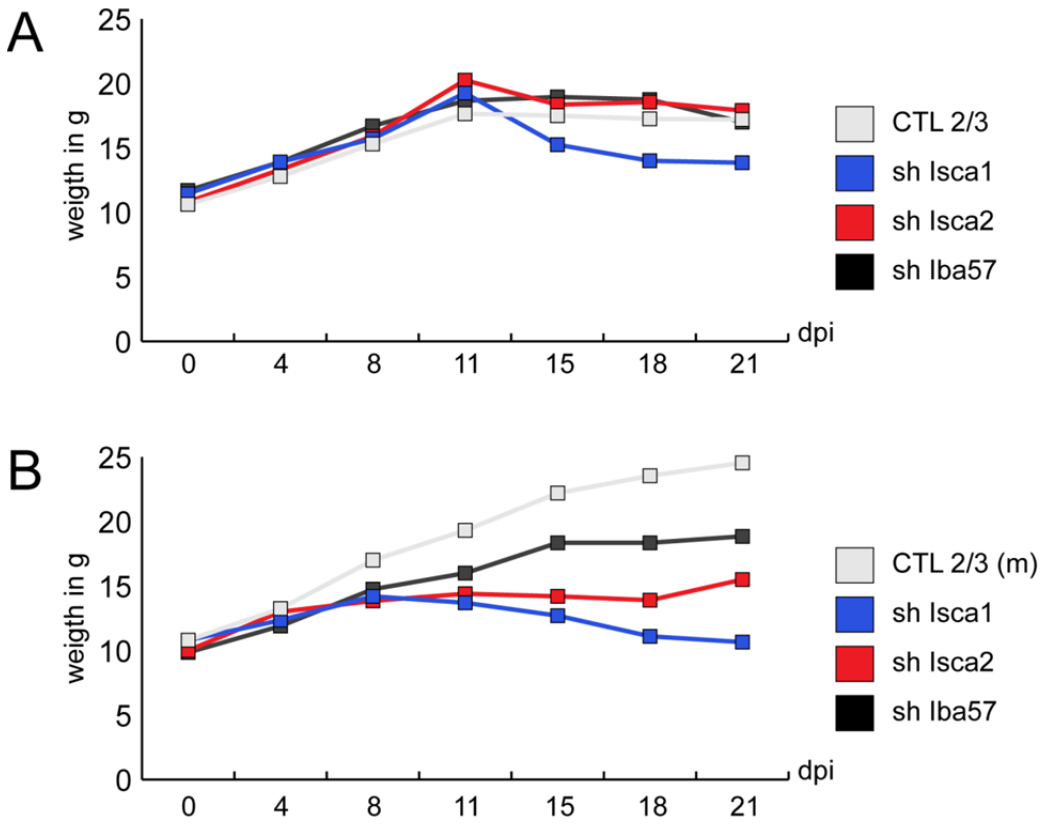

Figure 17: Weight development of mice after retro-orbital delivery of rAAV encoding for shRNA and eGFP.

rAAV encoding for shRNA and eGFP were injected with 1x 10^{13}vg/kg (A) and 2.5x 10^{13} vg/kg (B) in 3 weeks old mice. Weight was checked every 3 days. Mice were sacrified 3 wpi (21 dpi) at 6 weeks of age. Note that error bars are missing, since the number of mice per group is 2 (n=2).

At dissection (3 wpi), shISCA1-mice were strongly affected. No overt morphological changes of the organs were however observed during dissection, with the exception of a consistent paler liver compared to saline injected controls.

Knockdown was determined on mRNA expression levels in the respective tissues (here shown for the medium dose) (Figure 18), showing clear knockdown only for *Isca1* expression in heart and TA.

Different tissues were tested for their levels of cellular Fe-S proteins by western blot shown for the low dose (Figure 19). In contrast to the clear effect of local ISCA1 knockdown in cells, upon systemic injection, if at all only minimal decrease levels of mitochondrial Fe_4S_4 proteins and Fe_4S_4-dependent proteins observed in animals injected with AAV encoding for shRNA against *Isca1*: NDUFS3 in liver; NDUFS3 and SDH in TA; and SDH and LA-PDH/LA-KGDH in heart (Figure 19). No decrease of any of the tested Fe-S proteins was detected upon administration of rAAV-shIsca2. (Please note that SDH B levels in heart need to be compared to GAPDH' loading control and thus are not decreased compared

to control.) GFP protein levels in different tissues showed strong variability between mice. (Please also note that the first control (CTL) was injected with saline solution.) Knockdown for *Isca2* on the protein level was not obtained (shown for TA) (Figure 19) and IBA57 protein was found to be decreased in livers injected with rAAVs encoding shRNA against Iba57.

Preliminary western blot analysis of mice injected with the medium dose showed only minor decreased levels of mitochondrial Fe_4S_4 proteins and Fe_4S_4-dependent proteins in mice with knockdown of *Isca1* (data not shown). Due to the insufficient knockdown of ISCA2, and the lack of higher titers for injections at the highest dose, this approached was not further pursued to find the role for ISCA2 *in vivo*.

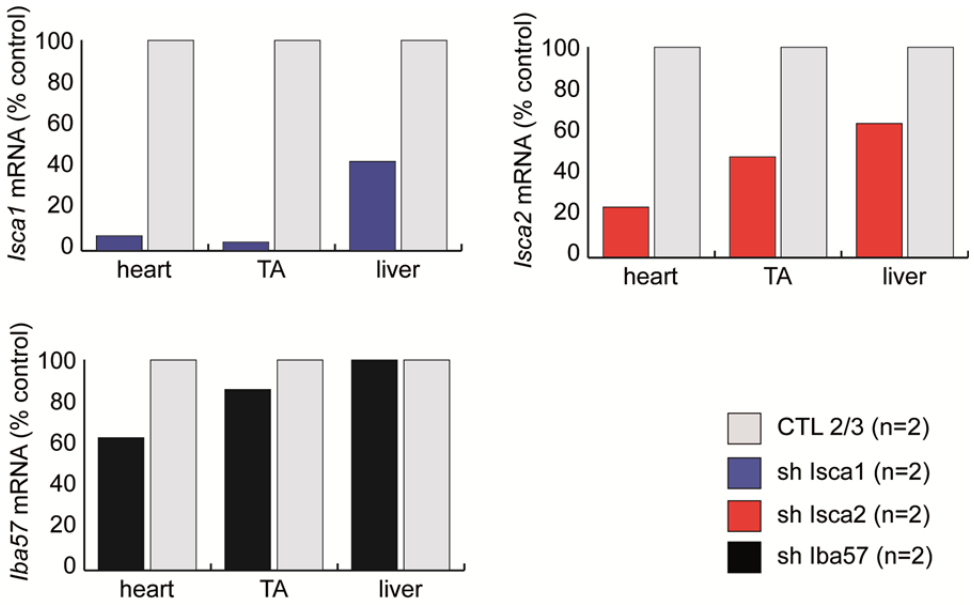

Figure 18: mRNA expression in tissues upon systemic delivery of rAAV.

Mice were treated at 3 weeks of age with 2.5x 10^{13} vg/kg rAAV-shRNA-eGFP as indicated and sacrifieced at 6weeks of age. mRNA expression of the gene of interest was determined for the heart, TA and liver. CTL: control vector encoding for scrambled shRNA, sh Isca1/sh Isca2/ Is Iba57: vector encoding for shRNA against Isca1 (blue), against Isca2 (red) or against Iba57 (black).

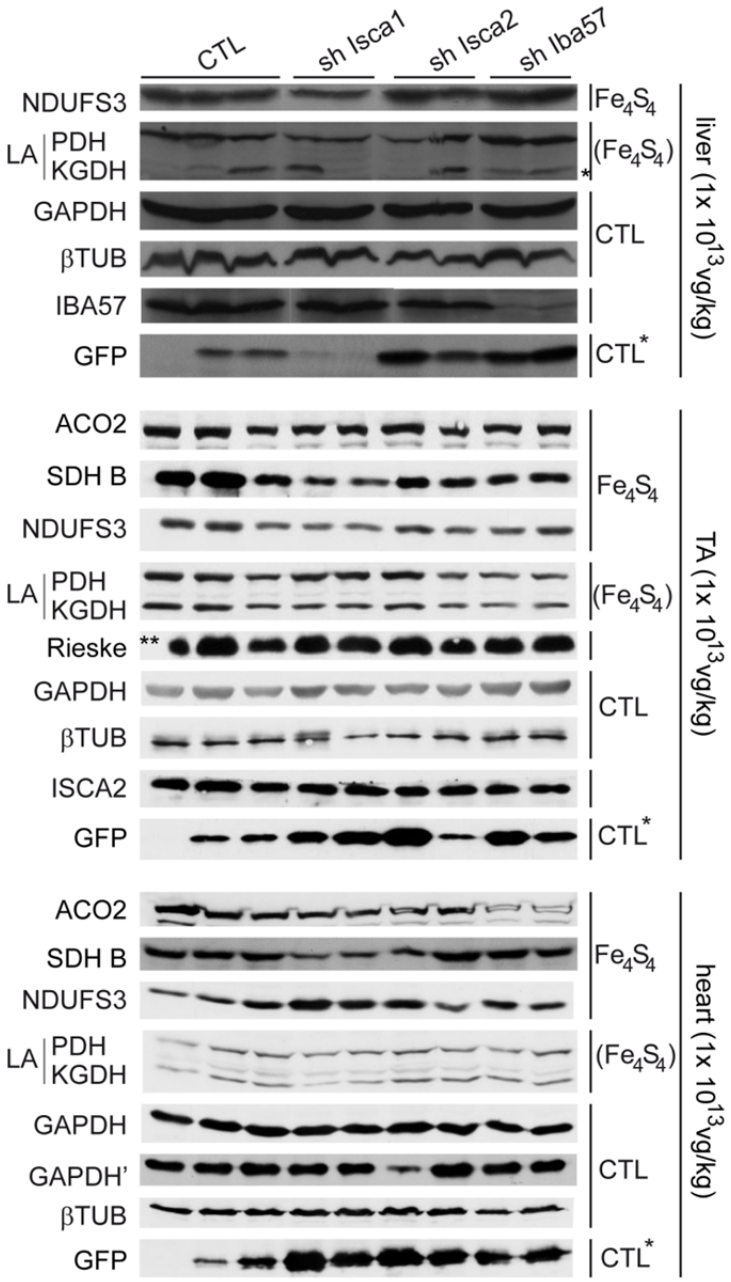

Figure 19: Western blot analysis of Fe-S proteins in samples of mice injected with the indicated rAVV.

Mice were treated at 3 weeks of age with 1x 10^{13} vg/kg rAAV-shRNA-eGFP as indicated and sacrificed at 6weeks of age. Protein levels were determined for the liver (top), TA (middle) and heart (bottom). CTL: saline injected (1st row) and control vector encoding for scrambled shRNA injected (2nd and 3rd row), sh Isca1: vector encoding shRNA against Isca1 and eGFP, sh Isca2: vector encoding shRNA against Isca2 and eGFP, sh Iba57: vector encoding shRNA against Iba57 and eGFP. n=1 for saline injection, n=2 for CTL, sh Isca1, sh Isca2 and sh Iba57. * Band corresponding to the size of LA-KGDH appeared non-conclusive. ** Band corresponding to the RIESKE protein in the saline CTL was not entirely revealed.

4.2.2.2 Expression studies and promoter analysis

To test for a potential role or differential requirement for ISCA2, mRNA expression of *Isca1* and *Isca2* was assessed under different stress or physiological conditions. These included expression at different time points during muscle regeneration upon injection of the snake-toxin notexin; expression in the liver upon different durations of fasting; expression in muscle (TA) during systemic inflammation upon LPS treatment; and expression during differentiation of the muscle myoblast cell line C2C12. The expression of *Isca1* and *Isca2* was further analyzed in a published dataset of RNA expression upon treatment of the muscle myoblast cell line C2C12 with PGC1α, a transcriptional co-activator of genes involved in energy metabolism and mitochondrial biogenesis and function (Rensvold, Ong et al. 2013). None of these conditions revealed a differential regulation of *Isca2* compared to *Isca1*. Either both expressions changed in a similar way, not at all or results were non-conclusive (data not shown).

Upstream genomic regions of *Isca1* and *Isca2* genes were analyzed to assess whether it contains promoter elements that could give a hint about potential differential expression or requirements. For this purpose, upstream genomic regions of the mouse, rat and human genes were aligned. These were then analyzed for the presence of highly conserved regions and the presence of typical transcription factor binding sites using MEME suite motif based sequence analysis tools (http://meme.nbcr.net/meme/) and transcriptional element search system TESS (http://www.cbil.upenn.edu/tess). While the adjacent area to the transcription start site of *Isca1* and *Isca2* genes were rather conserved, no other elements were found to be conserved and potentially containing a high probability of transcription factor binding site (data not shown). In addition, non-conserved regions were analyzed using UCSC genome browser (https://genome.ucsc.edu/). Specific peaks for transcription elements (like Pol II) were not observed in the relatively short genomic-intergenic region. Thus, it is probable that a promoter further upstream or at a separate genomic region is regulating *Isca1* and *Isca2* expression.

4.2.2.3 ISCA-protein knockdown in cells

I tested knockdown of ISCA-proteins in cultured muscle cells, to test whether I can reproduce and confirm the role for ISCA2 (and IBA57) in the maturation of mitochondrial Fe_4S_4 clusters (Sheftel, Wilbrecht et al. 2012).

First, I decided to work with two different mouse cell lines initially: C2C12 and NIH 3T3. C2C12 cells are murine myoblasts, and NIH3T3 are mouse embryonic fibroblasts. First, different transfection methods were tested. Based on previous experiments in the lab and what is reported for knockdown of Fe-S biogenesis proteins (Biederbick, Stehling et al. 2006; Sheftel, Wilbrecht et al. 2012; Rensvold, Ong et al. 2013), serial transfections were performed to obtain protein knockdown. pAAV-vectors,

which were previously used for AAV production and encoding for the respective shRNA and eGFP, were used for transfections. Transfection efficiencies were assessed by observing GFP expression in fluorescence microscopy. Different transfection efficiencies were observed for different reagents tested, with the highest rates for lipofectamin 2000 (Invitrogen) in C2C12 (max. 20%) and Fugene 6 (Promega) for NIH 3T3 (max. 60%) (data not shown). Three serial transfections every 3 days were performed for C2C12 and NIH3T3. Cell growth and transfection rates were accessed by microscopy on a daily basis. To select for transfected cells, fluorescence-activated cell sorting (FACS) for eGFP-positive cells was performed the day before re-transfection and for final cell collection. The effect on the mitochondrial Fe_4S_4 proteins was accessed by western blot for SDH and LA-bound PDH and KGDH using GAPDH as a loading control.

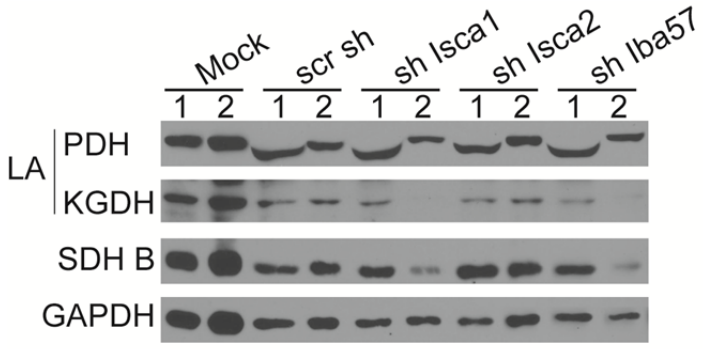

Figure 20: Knockdown experiment in C2C12 cells show requirement of ISCA1 and IBA57 for mitochondrial Fe4S4 cluster proteins.

C2C12 murine myoblasts cells were transiently transfected twice with pAAV plasminds encoding for the indicated shRNA and GFP. GFP-positive cells were sorted 2 dpt, transfected the day after and sorted again 2 dpt. Maturation of Fe-S proteins was tested by western blot for SDH and LA. Samples were taken after the respective FACS (1, 2).

Overall, slow cell growth was observed for all cells transfected with shRNA. Cells transfected with scrambled shRNA grew slower than Mock-cells, but considerably faster all shRNA transfected cells. Although transfection rates were much higher for NIH3T3 cells, no impairment of Fe-S maturation by western blot was detected for neither of the shRNA constructs (data not shown). Preliminary results on C2C12 cells show impaired SDH B and LA-bound KGDH levels upon transfection with shRNA against ISCA1 and IBA57 (Figure 20). So far, knockdown efficiency was only tested for ISCA2 by western blot, but not obtained (data not shown).

5. Discussion

5.1 Understanding the role of ISCA2

Our investigation on the A-type proteins eventually raises the question of the actual role of ISCA2. Herein, we provided several lines of evidence that it is different from ISCA1. This is shown by the absence of a phenotype upon ISCA2 knockdown in skeletal muscle, and by the fact that ISCA2 is unable to compensate for ISCA1 knockdown. We have further seen that ISCA1 and ISCA2 proteins interact, but both have a specific interaction network, which will be discussed below.

5.1.1 Using local AAV injection

Simultaneous knockdown of ISCA1 and ISCA2 in skeletal muscle may either show a similar phenotype to single ISCA1 knockdown or provoke a stronger or different phenotype. A similar phenotype would further suggest that ISCA2 is not required in mature skeletal muscle and the roles of ISCA1 and ISCA2 do not overlap. If the double knockdown phenotype appears different, it would suggest that ISCA2 functions along with ISCA1 but is not necessarily required for ISCA1 function in skeletal muscle.

I addressed whether ISCA2 expression can compensate for the ISCA1 knockdown, since mRNA expression levels for ISCA1 were higher than those for ISCA2 in all tissues and the endogenous (and not up-regulated) ISCA2 levels may not be enough to compensate for ISCA1 knockdown. Although transgenic expression of ISCA2 does not compensate for the ISCA1 knockdown (see manuscript Figure 7), the following aspects are required to prove that they are functionally non-redundant proteins. It needs to be shown that the transgenic expression of ISCA2 reaches at least the endogenous levels of ISCA1 and that it is efficiently targeted to the mitochondria. Since we don't have an antibody to detect endogenous ISCA1, determining mRNA expression will show whether the over-expressed ISCA2 the reaches levels of endogenous ISCA1. Fractionation experiments or immunofluorescence for ISCA2 on muscle will show whether or not transgenic ISCA2 is targeted to the mitochondria.

5.1.2 Testing other approaches for ISCA-protein knockdown

Considering that no phenotype was observed upon ISCA2 knockdown *in vivo*, but that ISCA2 knockdown in cells showed a phenotype in a previous publication (Sheftel, Wilbrecht et al. 2012), different approaches were tested to try to uncover a role for ISCA2. An attempt to define ISCA2 role was addressed by systemic injection of rAAVs for knockdown, but preliminary results suggest that the knockdown of ISCA2 was inefficient. This did not enable to conclude on a potential tissue specific role for ISCA2 yet. Notably, these experiments have confirmed the important role of ISCA1 in

mammalian physiology. The following technical aspects may be considered to be improved to achieve efficient knockdown of ISCA2 using first, the efficiency of transduction of the targeted tissue which is determined by the serotype, the dose and the route of injection and second, the transgene itself and the respective promoter. The serotype rAAV2/9 has previously been shown to efficiently transduce mouse tissues upon systemic delivery (Zincarelli 2008, Bostick 2007) and rAAV9 expressing eGFP produced in the IGBMC was shown to efficiently transduce several tissues including the heart upon retro-orbital injection (personal communication with Brahim Belbellaa). The transgene itself has proven efficient for ISCA2 knockdown upon local injection of rAAV into the TA. However, considerable differences in knockdown efficiency and eGFP expression were observed: variations were observed between mice, but to a bigger extend between viruses (different virus productions for the same transgene, but stronger differences even for the different transgenes). This strongly suggests a major influence of the respective virus production and will have to improve (and improving virus production accounts similarly for decreasing inflammation observed in certain injected muscles). Testing the systemic delivery with the high dose was not possible due to the lack of high titers, however this may potentially result in efficient knockdown of ISCA2, further suggesting to improve virus production. It can also be envisaged to inject at a different (likely earlier) stages of development to see whether ISCA2 function is required particularly during early developmental stages (for instance in dividing cells, see next paragraph).

I further tested whether the phenotype obtained upon knockdown in HeLa cells (Sheftel, Wilbrecht et al. 2012) is reproducible, based on the hypothesis that ISCA2 may be required in dividing cells. If knockdown of ISCA2 in cells recapitulates what was published previously, thiswould argue towards a differential requirement of ISCA1 and ISCA2 potentially depending on the cellular state. Therefore, knockdown in the murine myoblast cell line C2C12 was tested to relate to the knockdown in mature skeletal muscle *in vivo*. Preliminary experiments have shown that transfection of the respective pAAV plasmids encoding shRNA against *Isca1* or *Iba57* leads to decreased levels of SDH B and LA. All cells transfected with a pAAV encoding an shRNA (against *Isca1, Isca2* or *Iba57*) showed reduces growth compared to control (pAAV endocing scrambled shRNA), suggesting a specific effect of the knockdown. However, to compensate for low transfection rates, enrichment for GFP-positive cells by FACS (as GFP is encoded by all transfected pAAV) was performed, but appeared to reduce cell growth drastically. These preliminary experiments suggest that in addition to ISCA1, IBA57 is also required for mitochondrial Fe_4S_4 cluster in cultured cells. Therefore, it would be interesting to follow this approach to test for a potential role for ISCA2. To avoid the potentially harmful FACS, I will test transfection of C2C12 using electroporation of pAAV plasmids. Recent ongoing work in the department points to electroporation as a method of choice for transfection C2C12 with a much higher efficiency (>60 %) that could make FACS dispensable.

If the approach to knockdown ISCA-proteins in cells proves technically feasible, several methods can be further used to study their respective phenotypes. Fe-S protein maturation by western blot is one of the first to be performed to investigate the so-called secondary effects on non-Fe-S proteins or Fe_2S_2 cluster proteins in detail (as previously stated by (Sheftel, Wilbrecht et al. 2012)) in addition to the potential effect of ISCA2 on the maturation of mitochondrial Fe_4S_4 proteins, also. Ultrastructural study of the mitochondria by electron microscopy would allow concluding further on the mitochondrial state. If ISCA2 knockdown in C2C12 cells impairs maturation of the same set of mitochondrial proteins as ISCA1, it strongly supports our hypothesis on a differential requirement for ISCA1 and ISCA2 potentially depending on the cellular state (for instance in dividing versus non-dividing cells). Importantly, over-expression of ISCA1 or ISCA2 in the respective other knockdown in cells, would eventually support or negate the question of functional redundancy.

5.1.3 Targeting early effects of the ISCA-protein knockdown

The reasoning of characterizing the knockdown phenotype in muscle as early as possible was justified by the fact that I wanted to target early phenotypic consequences and potentially separate them from the long term effects of the knockdown. As ISCA1 knockdown results in decreased levels of key enzymes in metabolism and respiration, the succession of events is likely to provoke a fatal phenotype with time. I did not address how the present mitochondrial state is influencing muscle function in terms of respiratory capacity, metabolism and actual muscle force because the mechanistic insights I aimed to gain were not on secondary consequences of a mitochondrial phenotype. Moreover, it has to be considered that first shut down of AAV expression has been previously observed in long term studies and second that satellite cells which are responsible for muscle regeneration under normal conditions are usually not targeted by rAAVs. While long term knockdown will likely disrupt mitochondrial function and structure completely (as observed in the cellular knockdown in (Sheftel, Wilbrecht et al. 2012)), also further consequences on heme biosynthesis would probably appear. ISCA1 knockdown affects four different enzymes of the Krebs cycle: Aconitase and SDH as well as the LA-bound PDH and KGDH (Figure 8). The efficiency of the Krebs cycle is thus likely to be diminished, and in turn lower levels of the porphyrin and heme precursor succinyl CoA are expected (Ye and Rouault 2010). Although succinyl CoA can also be generated from isoleucine and valine, this is a LA-dependent process via the BCDH (which is presumably affected as well). Conversion of propionyl CoA would instead be a Krebs cycle and LA-independent pathway of generating heme, and it may be enough for normal heme biogenesis but likely not in erytropoetic tissues (Nilsson, Schultz et al. 2009). This could further explain why upon use of morpholinos against ISCA1 (and IBA57), heme biogenesis is diminished (Wingert, Galloway et al. 2005). Moreover, this should be considered in case of systemic rAAV delivery in mice.

5.2 Understanding the differences and the interaction of ISCA1 and ISCA2

It is possible that the labile cluster on ISCA2 is either targeted to other Fe-S biogenesis proteins or directly to acceptor proteins. Contrary to the cluster on ISCA2, the rather stable Fe_2S_2-cluster on ISCA1 can potentially be converted by reductive coupling prior to transfer to Fe_4S_4 acceptor proteins.

Several features are known to control the state of the cluster in Fe-S proteins including the cellular environment like “oxygen-state” and the pH, the clusters accessibility to the solvent and the electrostatics or local charges (Liu, Chakraborty et al. 2014). Previous studies showed that charged residues close to the cluster ligation can have significant influence on the reduction potential of the cluster (Shen, Jollie et al. 1994; Liu, Chakraborty et al. 2014). Indeed, close to the potentially cluster ligating cysteine in the ISCA-amino acid sequence, ISCA1 and ISCA2 possess residues with differences in the local charge (see 87.1). Therefore, it would be interesting to test whether mutation of these particular residues would change the properties of the Fe-S cluster on ISCA1 and ISCA2.

5.2.1 Uncovering the role of ISCA1 and ISCA2 interaction

ISCA1 and ISCA2 could interact to enable cluster transfer between these two proteins. Due to the different stability of the cluster (in the presence of oxygen), a transfer from ISCA2 to ISCA1 is more likely than the reverse direction. To demonstrate such a possibility, holo-ISCA2 would have to be incubated with apo-ISCA1 *in vitro* and measurements of the presence or absence of cluster on the proteins by biophysical techniques such as UV-visible spectra chould be done. Possible cluster transfer would have to be assessed also by a reciprocal transfer experiment. Due to the observation that the vast majority of apo-ISCA1 is unstable under anaerobic conditions, the corresponding transfer reaction is possibly not easily assessed. The direction of cluster transfer would be an important parameter to define to allow conclusion about uni- or bidirectional possibility of transfer and thus about potential upstream or downstream function (see below).

The second possibility is that interaction between holo-ISCA1 and holo-ISCA2 facilitates formation of Fe_4S_4 cluster out of the two Fe_2S_2 cluster. It was previously suggested that Fe_2S_2 to Fe_4S_4 cluster conversion takes place on the A-type proteins (Stehling 2013 coldSpring Habor). This suggestion was previously based on characterization of a Fe_4S_4 cluster after detection of a Fe_2S_2 intermediate on bacterial IscA proteins (Krebs, Agar et al. 2001), thus suggesting that a homo-dimer alone can fulfill this function. Recent studies on bacterial IscA (^{Nif}IscA) showed a reversible cycle between Fe_2S_2-containing and Fe_4S_4 cluster containing forms. For Fe_2S_2 to Fe_4S_4 cluster conversion, reductive coupling was induced by DTT providing two electrons (Mapolelo 2012 Biochem). The reverse effect (Fe_4S_4 to Fe_2S_2 cluster conversion) was induced by oxygen. Interestingly, in the experiments described

herein (see manuscript) characterized a rather oxygen-stable Fe_2S_2 cluster on ISCA1. It would be worth to test, whether this cluster can be further converted by reductive coupling to a Fe_4S_4 cluster (in the presence of DTT) and whether the labile cluster on ISCA2, can be used for reductive coupling on ISCA1. This would then point to a role of ISCA2 rather as cluster storage for cluster conversion on ISCA1, which is due to the specific effect of the ISCA1 knockdown in muscle not required in all conditions. Of note, since IBA57-homologues were suggested to potentially function as electron donor, due to folate binding reported on *E. coli* IBA57 homologue YgfZ, the experiment could be performed in presence and absence of IBA57 to test, whether it could provide electrons for reductive coupling (see 5.2.3).

5.2.2 Defining the sites of interaction

Determining the sites of interaction between ISCA1 and ISCA2 would show whether the site binding site between the two proteins lies within conserved regions of each protein, which could suggest also interaction of different A-type proteins in other phyla. Moreover, to defining whether different interacting proteins of A-type proteins (the respective other ISCA-protein, IBA57 and GLRX5 for ISCA2, NFU1 for ISCA1) bind at the same or different sites of interaction may allow conclusion on the potential existence of smaller or bigger complexes. For instance this could show if IBA57 can bind ISCA2 during ISCA1-ISCA2 binding.

During the characterization of ISCA1 and ISCA2 binding using heterologous co-expression in bacteria, Alain Martelli had performed mutational studies on residues that are adjacent to the potentially coordinating cysteines and highly conserved residues between ISCA1-type and ISCA2-type proteins (see 1.5, 87.1). First, mutations were introduced to change the positively charged residues of ISCA1 to negatively ISCA2-like charged residues ($ISCA1^{R53E/R53G}$ and $ISCA1^{R55G}$). A similar approach was applied for a highly conserved negatively charged residue two positions downstream of the third cysteine in ISCA1, mutating ISCA1 to ISCA2-like $ISCA1^{E125S}$. Mutating these residues did not influence direct binding of ISCA1 to ISCA2 indicating that these residues close to the cluster ligating cysteine are not of importance for direct ISCA1- ISCA2 binding.

Investigating the binding site between ISCA1 and ISCA2 may further determine whether or not a hetero-dimer between two different ISCA-monomers can physically exist. Although rather unlikely, since it was not described in the literature before that any A-type protein forms a heterodimer with another A-type protein, the possibility has to be considered and assessed, because homologues of other cluster binding proteins (GLRX5 and BOLA3) were shown to form heterodimers and coordinate Fe-S cluster (Roret, Tsan et al. 2014). Heterodimer formation between different A-type proteins would drastically change the idea of their function, because throughout phyla so far they are only

reported to act as homo-dimers (or homo-tetramers) (Wada, Hasegawa et al. 2005; Morimoto, Yamashita et al. 2006; Gupta, Sendra et al. 2009). If heterodimer formation is possible, it would be interesting to evaluate whether it can ligate an Fe-S cluster and what the properties of this latter are.

To go further into perspectives, subsequent resolution of the structure of mammalian A-type proteins would help to conclude on the possibility whether the interaction sites of a hetero-dimer would overlap with interaction sites of the homo-dimers.

5.2.3 Understanding the role of ISCA2 by understanding IBA57?

Several lines of evidence were found for a role of IBA57 to function together with ISCA2 and not ISCA1. IBA57 is found to bind ISCA2 *in vivo* and single knockdown of each, ISCA2 or IBA57, in skeletal muscle showed no phenotype. However, the molecular function of IBA57 can only be speculated for now. Based on the reported folate binding to the *E. coli* IBA57-homologue YgfZ it would be interested to test, whether mammalian IBA57-homologues also bind folate. In case of folate binding, the potential function as an electron donor could be assessed (as discussed above for instance in the case of testing reductive coupling on the ISCA-proteins, see 5.2.1). In addition, in the MudPIT analysis IBA57 was found to co-immunoprecipitate PRDX3, the thioredoxin-dependent peroxide reductase that is mainly studied in the context of cancer and suggested to be involved in the redox regulation of the cell (Angeles, Gan et al. 2011; Whitaker, Patel et al. 2013). Since this interaction was of relatively high abundance and solely found for IBA57, this could point to either an additional role for IBA57 or to a link between PRDX3 and Fe-S biogenesis.

5.3 Determine ISCA-protein cluster transfer direction

Herein, we provide data on cluster transfer from holo-ISCU to apo-ISCA2 as well as from both holo-ISCA proteins to the classical acceptor proteins ferredoxin and ACO2, suggesting that ISCA-proteins are involved in Fe-S transfer. Still, many open questions remain as to how the cluster is transferred and if other proteins are further involved. Since we detected NFU1 and GLRX5 as specific binding partners for ISCA1 or ISCA2 *in vivo* it may suggest specific transfer pathways for ISCA1 and ISCA2, respectively.

Using co-immunoprecipitations I identified a potential transient interaction between ISCA1 and NFU1. Since both proteins were shown to possess an Fe-S cluster (Tong 2003, (Krebs, Agar et al. 2001; Ollagnier-de-Choudens, Mattioli et al. 2001; Ollagnier-de Choudens, Nachin et al. 2003; Wollenberg, Berndt et al. 2003; Ollagnier-de-Choudens, Sanakis et al. 2004)), it suggests a linked function for ISCA1 and NFU1 in Fe-S biogenesis potentially by cluster transfer between them. The phenotype in patients with *NFU1* mutations and NFU1 knockdown in HeLa cells affected a subset of

mitochondrial Fe4S4 proteins and partially overlapped with the protein affected by ISCA1 knockdown (Cameron, Janer et al. 2011; Navarro-Sastre, Tort et al. 2011; Sheftel, Wilbrecht et al. 2012). This partial overlap may propose NFU1 to function downstream of ISCA1; however, potential cluster transfer as well as its direction will have to be shown.

Our interaction data for GLRX5 along with the clinical and biochemical phenotype described for the recently reported patients exhibiting a defect in LA synthesis, (Baker, Friederich et al. 2014), strongly suggested revising the idea that GLRX5 acts as a link between the nascent cluster transport from ISCU via the chaperones but rather in the late-acting mitochondrial Fe-S biogenesis. Interestingly, GLRX5 was seen to interact with ISCA2, but not with the chaperone/co-chaperone as previously shown (Uzarska, Dutkiewicz et al. 2013). Moreover, also direct cluster targeting to complex II from ISCU via the chaperone co-chaperone system was described recently without the involvement of GLRX5 (Maio, Singh et al. 2014). The most urging question is probably, whether a cluster can be transferred between ISCA-proteins and GLRX5, as suggested from previous studies (Vilella, Alves et al. 2004; Kim, Chung et al. 2010; Mapolelo, Zhang et al. 2013), and whether this transfer takes place in an uni-directional or bi-directional manner. Uni-directional cluster transfer could point to a sequential action of the proteins and would contribute to the sequence of events during Fe-S biogenesis. Potentially, that could place GLRX5 upstream of ISCA-proteins and downstream of the chaperones. However, previous studies suggested that cluster transfer from bacterial ^{Nif}IscA only takes place in case Grx-nif forms a hetero-dimer with the BOLA-protein Fra2 (Mapolelo, Zhang et al. 2013). If this is also the case for the mammalian GLRX5, the binding partner would have to be defined. The first candidate to be tested for hetero-dimer formation with GLRX5 would be BOLA3, since in addition to be a homologue of Fra2, phenotypes of mutations in BOLA3 overlap with the new GLRX5 mutations (Cameron, Janer et al. 2011; Baker, Friederich et al. 2014). Notably, BOLA3, although detected in the mitochondrial input samples (see Table 3), did not co-immunoprecipitate in any of the bait-IPs. Recently, uni-directional cluster transfer from human GLRX5 to ISCA-proteins was shown *in vitro* (Banci, Brancaccio et al. 2014), thus proposing GLRX5 to function potentially upstream of the ISCA-proteins.

5.3.1 ISCA1 is likely directly involved in Fe_4S_4 protein maturation

We suggested ISCA1 to participate directly in complex I assembly, since in the MudPIT analysis several subunits of the hydrophilic arm of complex I were detected to co-immunoprecipitate with ISCA1. Detection of several different subunits of the Fe-S containing hydrophilic arm made complex I emerging as a potential direct acceptor of Fe-S clusters from ISCA1, and co-immunoprecipitation of NDUFS3 with ISCA1 was confirmed by western blot. Moreover, ISCA1 knockdown in muscle and in cells (Sheftel, Wilbrecht et al. 2012) had shown a specific effect on the maturation of complex I.

However, complex I assembly is a rather complex process and although several assembly factors, like the Fe-S protein IND1/NUBPL, are known, it is not known when and how it acquires the Fe-S cluster (see 1.3.2). Therefore, experimental validation of a direct participation may be difficult due to the following reasons. It is not known at which point of the assembly process the Fe-S clusters are transferred to complex I. It may require correct stoichiometric ratios and sequential assembly of certain subunits prior to cluster transfer, which would be difficult to be recapitulated *in vitro*. On the other hand, it was recently suggested for complex II that cluster transfer to the Fe-S subunit SDH B takes place prior to the assembly with SDH A (Maio, Singh et al. 2014), suggesting that cluster transfer takes place rather early during the assembly process. Moreover, Maio and colleagues had identified sequence motifs in SDH B that were necessary to guide binding to Fe-S biogenesis proteins. A similar approach could be followed to clarify on that aspect; however the process likely to be more complicated for complex I assembly, because of the number of clusters, subunits and the complicated assembly procedure.

5.3.2 GLRX5 is potentially directly involved in heme biogenesis

We have further uncovered an interesting link of GLRX5 to heme biogenesis. GLRX5 was long suggested to play a role in heme biogenesis, due to a patient with a mutation in *Glrx5* exhibiting sideroblastic-like microcytic anemia (Camaschella, Campanella et al. 2007). Herein, we uncovered co-immunoprecipitation of ALAS1 with GLRX5, ALAS1 being the first enzyme in the heme biogenesis pathway. GLRX5 was previously described to be highly expressed in murine bone marrow, spleen and liver (Wingert, Galloway et al. 2005) and studies from cell models and lower model organisms had drawn a link between loss of GLRX5 function and activation of the cytosolic iron regulatory protein (IRP1) (Wingert, Galloway et al. 2005; Camaschella, Campanella et al. 2007; Ye, Jeong et al. 2010; Uzarska, Dutkiewicz et al. 2013). Since the erythroid-specific ALAS2 contains an iron-responsive element (IRE) in its 5'UTR, activation and binding of IRP1 would block its translation. However, the direct binding of GLRX5 to ALAS1 in HeLa cells could open up another and potentially more direct link between GLRX5 and heme biogenesis.

5.4 The MudPIT analysis and technical aspects

The interaction study performed during my thesis was chosen to have an unbiased approach that would address ISCA1 and ISCA2 interactions *in vivo*. The detailed rational behind the choice of performing MudPIT on IPs of over-expressed tagged-bait proteins is provided above along with minor conclusions (see manuscript and 4.1).

5.4.1 Cell line and transfection

We have shown that mitochondria-rich tissues also show higher expression of mitochondrial Fe-S biogenesis proteins including Isca1 and Isca2 (see manuscript Figure S4). Since HeLa cells are human cervical cancer cells, and mitochondrial Fe-S biogenesis proteins are detected in low levels only (see Table 3), this cell line may not be the optimal system. Selection of a cell line of tissue origin with higher content of mitochondrial Fe-S biogenesis proteins would thus be preferable. However, these may be difficult to transfect for protein over-expression and therefore not suitable. A screen to select for cell lines with higher content of mitochondrial Fe-S biogenesis proteins as well as different strategies for overexpression should be compared. The C2C12 murine myoblast cell line is an interesting candidate. Although not as easily transfectable as HeLa cells, the species and tissue origin as well as the concordant tissue as used for the knockdown study potentially increases data significance of the present study.

5.4.2 Transient binding and potential saturation

Although I detect abundant and reproducible binding of ISCA1 and ISCA2 as well as ISCA2 and IBA57, the relative abundance of these interactions appears relatively low in the MudPIT analysis. This is easily seen when compared to the binding of FDX2 to the known nascent Fe-S biogenesis proteins NFS1, ISD11 and ISCU. Although FDX2 is likely not directly binding all three NFS1, ISCU and ISD11, all three proteins are detected with rather high NSAF values, suggesting existence of a rather stable complex between FDX2, NFS1, ISD11 and ISCU. Therefore, I hypothesize that the ISCA-protein complexes are less stable than the one for Fe-S assembly. Although studies in our and in other labs have previously been shown for FXN to bind to the complex of NFS1, ISD11 and ISCU as well, the core complex of NFS1, ISD11 and ISCU seems very stable compared to the ISCA-protein interactions. It is thus probable that transfer of Fe-S cluster between carrier proteins does not need very stable interactions to enable the cluster to get carrier from ISCU to the acceptor protein(s).

Further I cannot exclude that the strong over-expression of bait proteins is saturating the detection capacity of our approach and thus potentially masking what can be observed with regards to binding to other proteins due to predominant presence of the ISCA-protein homo-dimers (see manuscript**Erreur ! Source du renvoi introuvable.**). A lesser strong expression of bait proteins could potentially increase detection of other binding proteins. Stable expression in cell lines is usually less strong than transient overexpression. Attempts for stable expression of mitochondrial Fe-S biogenesis proteins in the laboratory have previously shown to be difficult to achieve (i.e. for NFS1, ISCA1 and ISCA2). This is potentially caused by toxicity resulting from over-expression of the proteins in questions, which was also observed for the ISCA-proteins (see 4.1.1) (and previous unpublished results). Generation of an inducible over-expression cell line could presumably assist to address these

and other research questions concerning ISCA1 and ISCA2. In addition, potential gene expression or metabolic changes in the respective cells due to extensive expression of one of the other Fe-S cluster biogenesis bait protein were not accessed. Notably, these effects likely influenced the global state of the cells and thus the proteins in the proteomic analysis. This effect was however minimized by the normalization steps used. The relative abundance of an interaction in "that system" as a measure of abundance, strength or stability seems thus to be valid for data interpretation.

5.4.3 Data analysis and strength or abundance of interactions

Large scale protein data sets generated by mass spectromery approaches are a big challenge to interpret. It is not recommended to just browse through long list of identified proteins, since this is inefficient, time consuming and rarely informative (Kislinger, Gramolini et al. 2005). It is rather advised to use or develop automated data analysis strategies for "streamlined filtering and facile pattern recognition" to reveal biologically interesting features. Three online softwares were tested for the analysis of the present MudPIT results; Gene Ontology, Manteia and DAVID. The Gene Ontology (GO) summarizes biologic roles, molecular functions and biochemical properties. Manteia is a data mining system that was developed in the IGBMC to allow researchers to address complex biological question for a variety of data. DAVID is a bioinformatics database for "annotation, visualization and integrated discovery. The output of these three databases proved to be non-informative for the present study presumably due to the following causes: the low abundance of ISCA-protein complexes as discussed before and the presence of a still large number of probably false positive proteins, the big difference in abundance between overexpressed bait proteins and immunoprecipitated proteins and the observation that even the strongest or most abundant protein-protein interaction of ISCA1 and ISCA2 seem to be rather low. In addition, none of these softwares annotats the known Fe-S proteins or Fe-S biogenesis proteins correctly, thereby falsifying data analysis. As a result, the terms being enriched are "mitochondria", "respiratory chain" and "metabolism", which is expected when selecting for mitochondrial proteins. An example for incorrect annotation is once more the respiratory chain complex I (see 1.3.1). Subunits carrying the Fe-S in their ID (like NFUFS1 and NDUFS3) are not all proven to contain an Fe-S cluster, therefore influencing the outcome. Accordingly, data mining through one of these strategies was not included in the analysis.

5.4.4 Stringency of MudPIT analysis

I have tested two different stringencies for filtering against the control datasets. It appears that the 2x enrichment over negative controls represents even more interactions with low abundance that seem nonspecific. The 2x stringency was therefore not considered for the representation of results.

5.4.5 Other mass spectrometry approaches

The proteomic approach chosen in the present study has shown valuable to approach ISCA1 and ISCA2 interactions in cells. MudPIT was chosen to decrease procedure complexity and outperforms other approaches that include potentially degrading steps like separation of protein mixtures on gel.

MudPIT is a sensitive and semi-quantitative technique since it relies on the absolute numbers of spectral counts. To increase quantitative output of the approach, other proteomic methods could be applied, for instance labeling methods. An example could be stable isotope labeling by amino acids in cell culture (SILAC) (Hoedt and Neubert, 2014 Adv Exp Med Biol). On the one hand, theis would allow direct comparison of the spectral counts between bait-IP and control-IP. On the other hand, the number of required controls would be increased extensively since each bait-IP would need its own control-IP. Moreover, normalization over mitochondria-enriched input samples has proven valid in the approach undertaken in the present study.

6. Long term perspectives

6.1 Characterization of Fe-S clusters on ISCA-proteins *in vivo*

An emerging challenge in the field working with Fe-S cluster proteins like the ISCA-proteins is to characterize the cluster on the respective protein *in vivo*. *In vitro* characterization of Fe-S cluster properties is determining the general possible properties as seen for the characterization of the cluster on ISCA1 and ISCA2 and showed substantial differences, which opens up many scientific questions as discussed above. To characterize the Fe-S cluster under physiological relevant conditions as for instance in intact organelles, cells or even tissues could contribute to provide answers to these questions. However, characterization of cluster on one single protein within these seems improbable due to the number of different Fe-S proteins within on cell or organelle.

We have shown herein to purify ISCA1 and ISCA2 directly as Fe-S proteins without the necessity of reconstitution upon expression in bacteria. Since the heterologous expression in bacteria is very strong, biophysical characterization on the bacterial cluster may allow defining cluster properties of a single Fe-S cluster protein under conditions closer to the *in vivo* state. Methodologies are developed to get closer to achieving these goals and it was shown that different classes of iron-containing proteins could be quantitatively characterized *in vivo* (Holmes-Hampton, Chakrabarti et al. 2012; Holmes-Hampton, Jhurry et al. 2013).

6.2 Deciphering cluster targeting processes and following an Fe-S cluster from formatting to targeting

The role for ISCA1 and ISCA2 during Fe-S biogenesis can only be seen in the context of the whole pathway. Several different proteins were shown to participate in targeting Fe-S cluster towards acceptor proteins and, as discussed, several lines of evidence are given that suggest that there is not one single possible way of Fe-S biogenesis. Our present results revealed that the ISCA-proteins, which were previously thought to fulfill a similar role in cluster targeting, show in fact different functions. Also the other proteins thought to function during late-acting mitochondrial Fe-S biogenesis (i.e. NFU1, BOLA3, GLRX5, IBA57 and NUBPL) and shown partly overlapping roles upon characterization of patient phenotypes and knockdown studies in cells. What does that mean generally for our understanding of targeting Fe-S cluster to acceptor proteins? It will be important to determine, if *in vivo* several different transfer proteins directly provide Fe-S cluster to acceptor proteins or if the

acceptor protein targeting is specific. Deciphering molecular mechanisms of interactions and cluster transfer could therefore allow conclusion on the decision process how and where a cluster is further targeted. To define, whether different proteins transfer the cluster in a specific succession may allow conclusion on parallel or subsequent targeting events.

In a similar manner we provide characterization here for ISCA1 and ISCA2, the role and molecular function of each and every Fe-S biogenesis protein needs to be defines in details in a way. However, of even higher value would be the technical possibility to experimentally follow an Fe-S cluster from its formation to the insertion into the acceptor protein (*in vivo*).

6.3 Generation of other mouse models to study ISCA gene/protein function

New and powerful tools to develop knockout models arose during the last decade and were proven to speed up the process of model generation. These genome editing tools include transcription activator-like effector nucleases (TALENs), zinc finger nucleases (ZNFs) and clustered regularly interspaced short palindromic repeats/CRISPR-associated (CRIPSR/Cas). They base on either designed DNA binding protein fused to (in case of TALENs and ZNFs) or RNA sequence co-expressed with (in case of CRISPR/CAs) a non-specific endonuclease, which is thus specifically guided and induces DNA double-strand breaks. They have been shown to have increased efficiency in gene editing and reduce the generation time of mutant mice. It is further possible to mutagenize several genes at the same time. However, concerns about off-target effects have to be considered (Gaj, Gersbach et al. 2013; Wijshake, Baker et al. 2014). Since different cell types can be targeted, ranging from embryonic stem cells to conventional cultured cells, the number of possibilities to assess a gene's function is enormous. Thus, in the future these techniques may be applied to study ISCA1 and ISCA2 and other mammalian Fe-S biogenesis proteins, for which knockout models don't exist yet. Due to the possibility that conditional ISCA-protein knockout may be lethal, using the recent achievement of inducing knockout at specific developmental stages should be considered (Gonzalez, Zhu et al. 2014).

7. Annex

7.1 Alignment of ISCA1 and ISCA2

ISCA1 and ISCA2 share highly similar protein sequences and harbor conserved cysteine residues that were suggested to coordinate Fe-S (Jensen and Culotta 2000; Kaut, Lange et al. 2000; Krebs, Agar et al. 2001) (**Erreur ! Source du renvoi introuvable.**). Some differences between ISCA1 and ISCA2 can however be highlighted. For instance, close to the highly conserved N-terminal cysteine, ISCA1 possesses two positively charged amino acids whereas ISCA2 displays two negatively charged amino acids at the same positions (Figure 1). Similarly, a highly conserved negatively charged residue downstream of the most C-terminal cysteine is found in ISCA1, which is not present in ISCA2 (Figure 21).

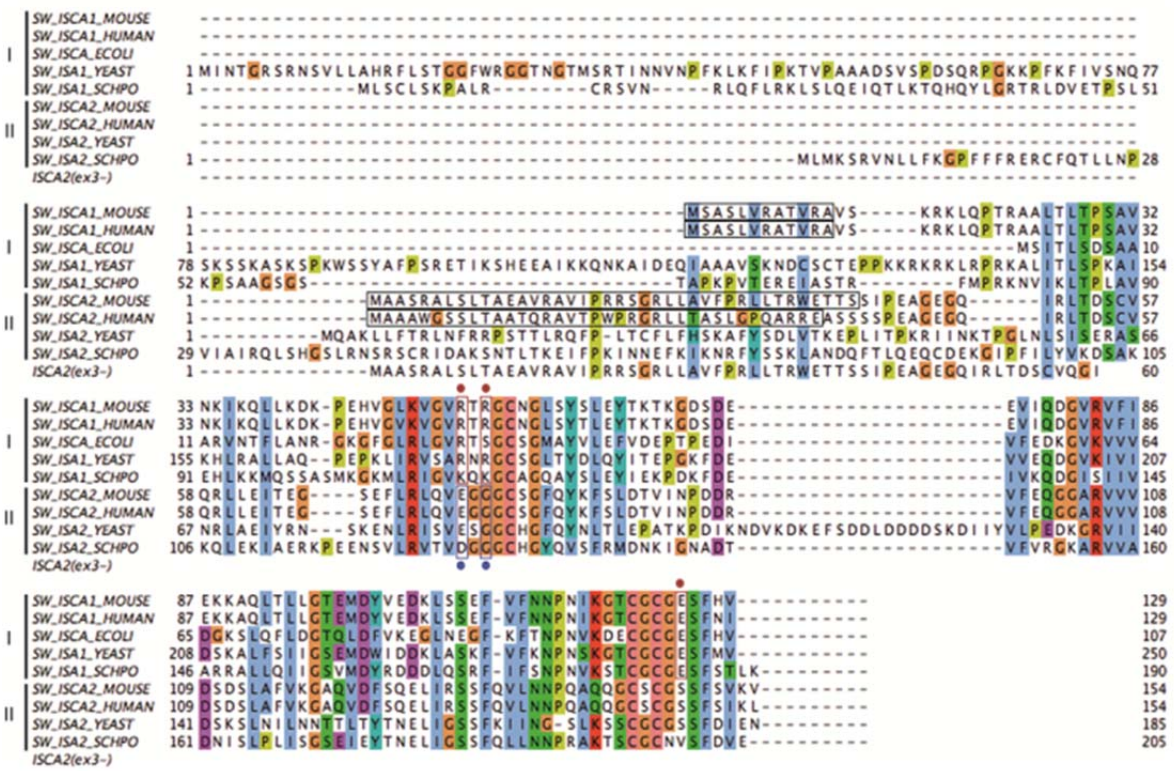

Figure 21: Alignment of ISCA1 and ISCA2 with their homologues in bacteria and yeast.

High sequence conservation can be seen upon alignment of the ISCA1 and ISCA2 homologous. Also high sequences similarity between ISCA1-homologues and ISCA2-homologues can be seen. Both possess three conserved cysteine residues that were previously shown to be essential for function (Jensen and Culotta 2000; Kaut, Lange et al. 2000). Notably, certain residues close to these cysteines differ in the properties between ISCA1-homologues and ISCA2-homologous (marked by dots above and below the residues in question). Alignment performed with PipeAlign and kindly provided by A. Martelli.

7.2 Material and Methods

Statistics: All data represent mean ± SD. The statistical analysis was performed by standard Student T-test. Statistical significance was considered at $p<0.05$ (*). Inclusion criteria for further analysis were knockdown levels >75%.

Cell culture and transfections for Cos-1 and HeLa cells: Cells were grown at 37°C, 5% CO2 in Dulbeccos modified Eagle's medium (Invitrogen) with 1 g/l glucose supplemented with 5 % fetal calf serum (FCS). Cells were transiently transfected using Fugene Reagent 6 (Roche Diagnostics) as recommended by the manufacturer.

Immunofluorescence: Immunofluorescence staining was performed 24 h post transfection of HeLa or Cos-1 cells tagged-proteins as indicated. Mitotracker Red CMXRos (Invitrogen) was used for mitochondria counterstaining following instructor manual. Briefly, 30 min to 1 h before fixation, Mitotracker was added to culture medium at a final concentration of 12.5 μl/ml. Cells were fixed using 4 % PFA and permeabilized with PBS Triton X-100 0.1 %. Normal goat serum was used for clocking (Jackson ImmunoResearch). Primary antibodies were used as indicated. Secondary fluorophore-coupled to Alexa 488 (AB28172; Molecular Probes) antibodies were used at a dilution of 1: 1.000. Nucleus counterstaining was achieved using 1 μg/ml DAPI (Sigma). Slides were mounted with Aqua PolyMount (Polysciences).

Fluorescence microscopy analysis: Images were acquired with DM 4000 B (Leica) light microscope with CoolSNAP (Ropert Scientific-Photometrics) software and confocal analysis was performed on a Leica TCS SP2 upright confocal microsystem with a Plan Apo CS (numerical aperture 1.4) 63× objective.

Cell knockdown study: Murine myoblasts C2C12 at 37°C, 5 % CO2 in Dulbeccos modified Eagle's medium (Invitrogen) with 1 g/l glucose supplemented with 20 % fetal calf serum (FCS). Cells were transiently transfected using Lipofectamine 2000 (Life Technologies) following instructor's manual in OptiMEM and a change of medium 3 hours post transfection. Two days post transfection GFP-positive cells were selected by Flow cytometry activated cell sorting using FACS Calibur cell sorting (BECTON DICKINSON) and the process of transfection and sorting repeated twice.

Systemic AAV injection: For the systemic trial, 3 weeks old C57BL/6J wild-type mice were anesthetized by intraperitoneal injection of ketamine-xylazine (75 and 10 mg per kg body weight, respectively) to allow systemic virus administration by retroorbital injection of rAAV at the doses of 1× 1012 vg /kg or 2.5 × 1012 vg/kg. Animal were checked on a daily basis and weight checked every

three days. Mice were anesthetized by intraperitoneal injection of ketamine-xylazine, dissected and killed 3 weeks after injection as indicated.

8. References

Abdel-Ghany, S. E., H. Ye, et al. (2005). "Iron-sulfur cluster biogenesis in chloroplasts. Involvement of the scaffold protein CpIscA." Plant Physiol 138(1): 161-172.

Adam, A. C., C. Bornhovd, et al. (2006). "The Nfs1 interacting protein Isd11 has an essential role in Fe/S cluster biogenesis in mitochondria." EMBO J 25(1): 174-183.

Adinolfi, S., C. Iannuzzi, et al. (2009). "Bacterial frataxin CyaY is the gatekeeper of iron-sulfur cluster formation catalyzed by IscS." Nat Struct Mol Biol 16(4): 390-396.

Ajit Bolar, N., A. V. Vanlander, et al. (2013). "Mutation of the iron-sulfur cluster assembly gene IBA57 causes severe myopathy and encephalopathy." Hum Mol Genet 22(13): 2590-2602.

Allikmets, R., W. H. Raskind, et al. (1999). "Mutation of a putative mitochondrial iron transporter gene (ABC7) in X-linked sideroblastic anemia and ataxia (XLSA/A)." Hum Mol Genet 8(5): 743-749.

Amoasii, L., D. L. Bertazzi, et al. (2012). "Phosphatase-dead myotubularin ameliorates X-linked centronuclear myopathy phenotypes in mice." PLoS Genet 8(10): e1002965.

Anderson, C. P., M. Shen, et al. (2012). "Mammalian iron metabolism and its control by iron regulatory proteins." Biochim Biophys Acta 1823(9): 1468-1483.

Angeles, D. C., B. H. Gan, et al. (2011). "Mutations in LRRK2 increase phosphorylation of peroxiredoxin 3 exacerbating oxidative stress-induced neuronal death." Hum Mutat 32(12): 1390-1397.

Angelini, S., C. Gerez, et al. (2008). "NfuA, a new factor required for maturing Fe/S proteins in Escherichia coli under oxidative stress and iron starvation conditions." J Biol Chem 283(20): 14084-14091.

Angerer, H., M. Radermacher, et al. (2014). "The LYR protein subunit NB4M/NDUFA6 of mitochondrial complex I anchors an acyl carrier protein and is essential for catalytic activity." Proc Natl Acad Sci U S A 111(14): 5207-5212.

Applegarth, D. A. and J. R. Toone (2006). "Glycine encephalopathy (nonketotic hyperglycinemia): comments and speculations." Am J Med Genet A 140(2): 186-188.

Ashburner, M., C. A. Ball, et al. (2000). "Gene ontology: tool for the unification of biology. The Gene Ontology Consortium." Nat Genet 25(1): 25-29.

Asokan, A., D. V. Schaffer, et al. (2012). "The AAV vector toolkit: poised at the clinical crossroads." Mol Ther 20(4): 699-708.

Bailey, S. (2012). "Nuclear replication: Hidden iron-sulfur clusters." Nat Chem Biol 8(1): 24-25.

Baker, P. R., 2nd, M. W. Friederich, et al. (2014). "Variant non ketotic hyperglycinemia is caused by mutations in LIAS, BOLA3 and the novel gene GLRX5." Brain 137(Pt 2): 366-379.

Banci, L., D. Brancaccio, et al. (2014). "[2Fe-2S] cluster transfer in iron-sulfur protein biogenesis." Proc Natl Acad Sci U S A 111(17): 6203-6208.

Bandyopadhyay, S., K. Chandramouli, et al. (2008). "Iron-sulfur cluster biosynthesis." Biochem Soc Trans 36(Pt 6): 1112-1119.

Beilschmidt, L. K. and H. M. Puccio (2014). "Mammalian Fe-S cluster biogenesis and its implication in disease." Biochimie 100: 48-60.

Beinert, H. (2000). "Iron-sulfur proteins: ancient structures, still full of surprises." J Biol Inorg Chem 5(1): 2-15.

Beinert, H., R. H. Holm, et al. (1997). "Iron-sulfur clusters: nature's modular, multipurpose structures." Science 277(5326): 653-659.

Beinert, H. and W. Lee (1961). "Evidence for a new type of iron containing electron carrier in mitochondria." Biochem Biophys Res Commun 5: 40-45.

Bekri, S., G. Kispal, et al. (2000). "Human ABC7 transporter: gene structure and mutation causing X-linked sideroblastic anemia with ataxia with disruption of cytosolic iron-sulfur protein maturation." Blood 96(9): 3256-3264.

Berns, K. I. (1990). "Parvovirus replication." Microbiol Rev 54(3): 316-329.

Biederbick, A., O. Stehling, et al. (2006). "Role of human mitochondrial Nfs1 in cytosolic iron-sulfur protein biogenesis and iron regulation." Mol Cell Biol 26(15): 5675-5687.

Bilder, P. W., H. Ding, et al. (2004). "Crystal structure of the ancient, Fe-S scaffold IscA reveals a novel protein fold." Biochemistry 43(1): 133-139.

Bostick, B., A. Ghosh, et al. (2007). "Systemic AAV-9 transduction in mice is influenced by animal age but not by the route of administration." Gene Ther 14(22): 1605-1609.

Bridwell-Rabb, J., C. Iannuzzi, et al. (2012). "Effector role reversal during evolution: the case of frataxin in Fe-S cluster biosynthesis." Biochemistry 51(12): 2506-2514.

Buning, H., L. Perabo, et al. (2008). "Recent developments in adeno-associated virus vector technology." J Gene Med 10(7): 717-733.

Bych, K., S. Kerscher, et al. (2008). "The iron-sulphur protein Ind1 is required for effective complex I assembly." EMBO J 27(12): 1736-1746.

Camaschella, C., A. Campanella, et al. (2007). "The human counterpart of zebrafish shiraz shows sideroblastic-like microcytic anemia and iron overload." Blood 110(4): 1353-1358.

Cameron, J. M., A. Janer, et al. (2011). "Mutations in iron-sulfur cluster scaffold genes NFU1 and BOLA3 cause a fatal deficiency of multiple respiratory chain and 2-oxoacid dehydrogenase enzymes." Am J Hum Genet 89(4): 486-495.

Cavadini, P., G. Biasiotto, et al. (2007). "RNA silencing of the mitochondrial ABCB7 transporter in HeLa cells causes an iron-deficient phenotype with mitochondrial iron overload." Blood 109(8): 3552-3559.

Chacinska, A., C. M. Koehler, et al. (2009). "Importing mitochondrial proteins: machineries and mechanisms." Cell 138(4): 628-644.

Chahal, H. K., Y. Dai, et al. (2009). "The SufBCD Fe-S scaffold complex interacts with SufA for Fe-S cluster transfer." Biochemistry 48(44): 10644-10653.

Chandramouli, K., M. C. Unciuleac, et al. (2007). "Formation and properties of [4Fe-4S] clusters on the IscU scaffold protein." Biochemistry 46(23): 6804-6811.

Cicchillo, R. M. and S. J. Booker (2005). "Mechanistic investigations of lipoic acid biosynthesis in Escherichia coli: both sulfur atoms in lipoic acid are contributed by the same lipoyl synthase polypeptide." J Am Chem Soc 127(9): 2860-2861.

Colin, F., A. Martelli, et al. (2013). "Mammalian frataxin controls sulfur production and iron entry during de novo Fe4S4 cluster assembly." J Am Chem Soc 135(2): 733-740.

Cozar-Castellano, I., M. del Valle Machargo, et al. (2004). "hIscA: a protein implicated in the biogenesis of iron-sulfur clusters." Biochim Biophys Acta 1700(2): 179-188.

Craig, E. A. and J. Marszalek (2002). "A specialized mitochondrial molecular chaperone system: a role in formation of Fe/S centers." Cell Mol Life Sci 59(10): 1658-1665.

Crouse, B. R., V. M. Sellers, et al. (1996). "Site-directed mutagenesis and spectroscopic characterization of human ferrochelatase: identification of residues coordinating the [2Fe-2S] cluster." Biochemistry 35(50): 16222-16229.

Cupp-Vickery, J. R., J. J. Silberg, et al. (2004). "Crystal structure of IscA, an iron-sulfur cluster assembly protein from Escherichia coli." J Mol Biol 338(1): 127-137.

D'Hooghe, M., D. Selleslag, et al. (2012). "X-linked sideroblastic anemia and ataxia: a new family with identification of a fourth ABCB7 gene mutation." Eur J Paediatr Neurol 16(6): 730-735.

Dean, D. R. and K. E. Brigle (1985). "Azotobacter vinelandii nifD- and nifE-encoded polypeptides share structural homology." Proc Natl Acad Sci U S A 82(17): 5720-5723.

Ding, B., E. S. Smith, et al. (2005). "Mobilization of the iron centre in IscA for the iron-sulphur cluster assembly in IscU." Biochem J 389(Pt 3): 797-802.

Ding, H. and R. J. Clark (2004). "Characterization of iron binding in IscA, an ancient iron-sulphur cluster assembly protein." Biochem J 379(Pt 2): 433-440.

Ding, H., R. J. Clark, et al. (2004). "IscA mediates iron delivery for assembly of iron-sulfur clusters in IscU under the limited accessible free iron conditions." J Biol Chem 279(36): 37499-37504.

Ding, H., K. Harrison, et al. (2005). "Thioredoxin reductase system mediates iron binding in IscA and iron delivery for the iron-sulfur cluster assembly in IscU." J Biol Chem 280(34): 30432-30437.

Ding, H., J. Yang, et al. (2007). "Distinct iron binding property of two putative iron donors for the iron-sulfur cluster assembly: IscA and the bacterial frataxin ortholog CyaY under physiological and oxidative stress conditions." J Biol Chem 282(11): 7997-8004.

Dutkiewicz, R., B. Schilke, et al. (2004). "Sequence-specific interaction between mitochondrial Fe-S scaffold protein Isu and Hsp70 Ssq1 is essential for their in vivo function." J Biol Chem 279(28): 29167-29174.

Estellon, J., S. Ollagnier de Choudens, et al. (2014). "An integrative computational model for large-scale identification of metalloproteins in microbial genomes: a focus on iron-sulfur cluster proteins." Metallomics 6(10): 1913-1930.

Farhan, S. M., J. Wang, et al. (2014). "Exome sequencing identifies NFS1 deficiency in a novel Fe-S cluster disease, infantile mitochondrial complex II/III deficiency." Mol Genet Genomic Med 2(1): 73-80.

Ferrari, F. K., X. Xiao, et al. (1997). "New developments in the generation of Ad-free, high-titer rAAV gene therapy vectors." Nat Med 3(11): 1295-1297.

Ferrer-Cortes, X., A. Font, et al. (2012). "Protein expression profiles in patients carrying NFU1 mutations. Contribution to the pathophysiology of the disease." J Inherit Metab Dis.

Fontecave, M. (2006). "Iron-sulfur clusters: ever-expanding roles." Nat Chem Biol 2(4): 171-174.

Frazzon, J., J. R. Fick, et al. (2002). "Biosynthesis of iron-sulphur clusters is a complex and highly conserved process." Biochem Soc Trans 30(4): 680-685.

Fregoso, M., J. P. Laine, et al. (2007). "DNA repair and transcriptional deficiencies caused by mutations in the Drosophila p52 subunit of TFIIH generate developmental defects and chromosome fragility." Mol Cell Biol 27(10): 3640-3650.

Friedrich, T. (2014). "On the mechanism of respiratory complex I." J Bioenerg Biomembr 46(4): 255-268.

Fujisawa, H. and H. Nakata (1987). "Phenylalanine 4-monooxygenase from Chromobacterium violaceum." Methods Enzymol 142: 44-49.

Gaj, T., C. A. Gersbach, et al. (2013). "ZFN, TALEN, and CRISPR/Cas-based methods for genome engineering." Trends Biotechnol 31(7): 397-405.

Gari, K., A. M. Leon Ortiz, et al. (2012). "MMS19 links cytoplasmic iron-sulfur cluster assembly to DNA metabolism." Science 337(6091): 243-245.

Garland, S. A., K. Hoff, et al. (1999). "Saccharomyces cerevisiae ISU1 and ISU2: members of a well-conserved gene family for iron-sulfur cluster assembly." J Mol Biol 294(4): 897-907.

Gelling, C., I. W. Dawes, et al. (2008). "Mitochondrial Iba57p is required for Fe/S cluster formation on aconitase and activation of radical SAM enzymes." Mol Cell Biol 28(5): 1851-1861.

Goldberg, A. V., S. Molik, et al. (2008). "Localization and functionality of microsporidian iron-sulphur cluster assembly proteins." Nature 452(7187): 624-628.

Gonzalez, F., Z. Zhu, et al. (2014). "An iCRISPR platform for rapid, multiplexable, and inducible genome editing in human pluripotent stem cells." Cell Stem Cell 15(2): 215-226.

Goraca, A., H. Huk-Kolega, et al. (2011). "Lipoic acid - biological activity and therapeutic potential." Pharmacol Rep 63(4): 849-858.

Gramolini, A. O. and A. Emili (2005). "Uncovering early markers of cardiac disease by proteomics: avoiding (heart) failure!" Expert Rev Proteomics 2(5): 631-634.

Grieger, J. C. and R. J. Samulski (2012). "Adeno-associated virus vectorology, manufacturing, and clinical applications." Methods Enzymol 507: 229-254.

Gupta, V., M. Sendra, et al. (2009). "Native Escherichia coli SufA, coexpressed with SufBCDSE, purifies as a [2Fe-2S] protein and acts as an Fe-S transporter to Fe-S target enzymes." J Am Chem Soc 131(17): 6149-6153.

Haack, T. B., B. Rolinski, et al. (2013). "Homozygous missense mutation in BOLA3 causes multiple mitochondrial dysfunctions syndrome in two siblings." J Inherit Metab Dis 36(1): 55-62.

Hashiguchi, K. and Q. M. Zhang-Akiyama (2009). "Establishment of human cell lines lacking mitochondrial DNA." Methods Mol Biol 554: 383-391.

Hentze, M. W., M. U. Muckenthaler, et al. (2010). "Two to tango: regulation of Mammalian iron metabolism." Cell 142(1): 24-38.

Herrero, E. and M. A. de la Torre-Ruiz (2007). "Monothiol glutaredoxins: a common domain for multiple functions." Cell Mol Life Sci 64(12): 1518-1530.

Hiltunen, J. K., K. J. Autio, et al. (2010). "Mitochondrial fatty acid synthesis and respiration." Biochim Biophys Acta 1797(6-7): 1195-1202.

Hoff, K. G., J. R. Cupp-Vickery, et al. (2003). "Contributions of the LPPVK motif of the iron-sulfur template protein IscU to interactions with the Hsc66-Hsc20 chaperone system." J Biol Chem 278(39): 37582-37589.

Holmes-Hampton, G. P., M. Chakrabarti, et al. (2012). "Changing iron content of the mouse brain during development." Metallomics 4(8): 761-770.

Holmes-Hampton, G. P., N. D. Jhurry, et al. (2013). "Iron content of Saccharomyces cerevisiae cells grown under iron-deficient and iron-overload conditions." Biochemistry 52(1): 105-114.

Imlay, J. A. (2006). "Iron-sulphur clusters and the problem with oxygen." Mol Microbiol 59(4): 1073-1082.

Jacobson, M. R., V. L. Cash, et al. (1989). "Biochemical and genetic analysis of the nifUSVWZM cluster from Azotobacter vinelandii." Mol Gen Genet 219(1-2): 49-57.

Jain, R., E. S. Vanamee, et al. (2014). "An iron-sulfur cluster in the polymerase domain of yeast DNA polymerase epsilon." J Mol Biol 426(2): 301-308.

Jensen, L. T. and V. C. Culotta (2000). "Role of Saccharomyces cerevisiae ISA1 and ISA2 in iron homeostasis." Mol Cell Biol 20(11): 3918-3927.

Johansson, C., A. K. Roos, et al. (2011). "The crystal structure of human GLRX5: iron-sulfur cluster co-ordination, tetrameric assembly and monomer activity." Biochem J 433(2): 303-311.

Johnson, D. C., D. R. Dean, et al. (2005). "Structure, function, and formation of biological iron-sulfur clusters." Annu Rev Biochem 74: 247-281.

Johnson, D. C., M. C. Unciuleac, et al. (2006). "Controlled expression and functional analysis of iron-sulfur cluster biosynthetic components within Azotobacter vinelandii." J Bacteriol 188(21): 7551-7561.

Kaut, A., H. Lange, et al. (2000). "Isa1p is a component of the mitochondrial machinery for maturation of cellular iron-sulfur proteins and requires conserved cysteine residues for function." J Biol Chem 275(21): 15955-15961.

Kiley, P. J. and H. Beinert (2003). "The role of Fe-S proteins in sensing and regulation in bacteria." Curr Opin Microbiol 6(2): 181-185.

Kilkenny, M. L., M. A. Longo, et al. (2013). "Structures of human primase reveal design of nucleotide elongation site and mode of Pol alpha tethering." Proc Natl Acad Sci U S A 110(40): 15961-15966.

Kim, J. H., R. O. Frederick, et al. (2013). "[2Fe-2S]-Ferredoxin binds directly to cysteine desulfurase and supplies an electron for iron-sulfur cluster assembly but is displaced by the scaffold protein or bacterial frataxin." J Am Chem Soc.

Kim, K. D., W. H. Chung, et al. (2010). "Monothiol glutaredoxin Grx5 interacts with Fe-S scaffold proteins Isa1 and Isa2 and supports Fe-S assembly and DNA integrity in mitochondria of fission yeast." Biochem Biophys Res Commun 392(3): 467-472.

Kislinger, T. and A. Emili (2005). "Multidimensional protein identification technology: current status and future prospects." Expert Rev Proteomics 2(1): 27-39.

Kislinger, T., A. O. Gramolini, et al. (2005). "Multidimensional protein identification technology (MudPIT): technical overview of a profiling method optimized for the comprehensive proteomic investigation of normal and diseased heart tissue." J Am Soc Mass Spectrom 16(8): 1207-1220.

Kispal, G., P. Csere, et al. (1999). "The mitochondrial proteins Atm1p and Nfs1p are essential for biogenesis of cytosolic Fe/S proteins." EMBO J 18(14): 3981-3989.

Komarnisky, L. A., R. J. Christopherson, et al. (2003). "Sulfur: its clinical and toxicologic aspects." Nutrition 19(1): 54-61.

Krebs, C., J. N. Agar, et al. (2001). "IscA, an alternate scaffold for Fe-S cluster biosynthesis." Biochemistry 40(46): 14069-14080.

Lange, H., T. Lisowsky, et al. (2001). "An essential function of the mitochondrial sulfhydryl oxidase Erv1p/ALR in the maturation of cytosolic Fe/S proteins." EMBO Rep 2(8): 715-720.

Lauble, H., M. C. Kennedy, et al. (1992). "Crystal structures of aconitase with isocitrate and nitroisocitrate bound." Biochemistry 31(10): 2735-2748.

Li, H., D. T. Mapolelo, et al. (2009). "The yeast iron regulatory proteins Grx3/4 and Fra2 form heterodimeric complexes containing a [2Fe-2S] cluster with cysteinyl and histidyl ligation." Biochemistry 48(40): 9569-9581.

Lill, R. (2009). "Function and biogenesis of iron-sulphur proteins." Nature 460(7257): 831-838.

Lill, R. and U. Muhlenhoff (2006). "Iron-sulfur protein biogenesis in eukaryotes: components and mechanisms." Annu Rev Cell Dev Biol 22: 457-486.

Lill, R. and U. Muhlenhoff (2008). "Maturation of iron-sulfur proteins in eukaryotes: mechanisms, connected processes, and diseases." Annu Rev Biochem 77: 669-700.

Liu, J., S. Chakraborty, et al. (2014). "Metalloproteins containing cytochrome, iron-sulfur, or copper redox centers." Chem Rev 114(8): 4366-4469.

Liu, T., W. J. Qian, et al. (2004). "High-throughput comparative proteome analysis using a quantitative cysteinyl-peptide enrichment technology." Anal Chem 76(18): 5345-5353.

Liu, Y. and J. A. Cowan (2007). "Iron sulfur cluster biosynthesis. Human NFU mediates sulfide delivery to ISU in the final step of [2Fe-2S] cluster assembly." Chem Commun (Camb)(30): 3192-3194.

Liu, Y. and J. A. Cowan (2009). "Iron-sulfur cluster biosynthesis: characterization of a molten globule domain in human NFU." Biochemistry 48(31): 7512-7518.

Liu, Y., W. Qi, et al. (2009). "Iron-sulfur cluster biosynthesis: functional characterization of the N- and C-terminal domains of human NFU." Biochemistry 48(5): 973-980.

Loiseau, L., C. Gerez, et al. (2007). "ErpA, an iron sulfur (Fe S) protein of the A-type essential for respiratory metabolism in Escherichia coli." Proc Natl Acad Sci U S A 104(34): 13626-13631.

Loiseau, L., S. Ollagnier-de-Choudens, et al. (2003). "Biogenesis of Fe-S cluster by the bacterial Suf system: SufS and SufE form a new type of cysteine desulfurase." J Biol Chem 278(40): 38352-38359.

Long, S., M. Jirku, et al. (2008). "Mitochondrial localization of human frataxin is necessary but processing is not for rescuing frataxin deficiency in Trypanosoma brucei." Proc Natl Acad Sci U S A 105(36): 13468-13473.

Long, S., M. Jirku, et al. (2008). "Ancestral roles of eukaryotic frataxin: mitochondrial frataxin function and heterologous expression of hydrogenosomal Trichomonas homologues in trypanosomes." Mol Microbiol 69(1): 94-109.

Long, S., Z. Vavrova, et al. (2008). "The import and function of diatom and plant frataxins in the mitochondrion of Trypanosoma brucei." Mol Biochem Parasitol 162(1): 100-104.

Lu, J., J. P. Bitoun, et al. (2010). "Iron-binding activity of human iron-sulfur cluster assembly protein hIscA1." Biochem J 428(1): 125-131.

Lu, J., J. Yang, et al. (2008). "Complementary roles of SufA and IscA in the biogenesis of iron-sulfur clusters in Escherichia coli." Biochem J 409(2): 535-543.

Lukes, J., H. Hashimi, et al. (2005). "Unexplained complexity of the mitochondrial genome and transcriptome in kinetoplastid flagellates." Curr Genet 48(5): 277-299.

Maio, N., A. Singh, et al. (2014). "Cochaperone binding to LYR motifs confers specificity of iron sulfur cluster delivery." Cell Metab 19(3): 445-457.

Mapolelo, D. T., B. Zhang, et al. (2012). "Spectroscopic and functional characterization of iron-bound forms of Azotobacter vinelandii (Nif)IscA." Biochemistry 51(41): 8056-8070.

Mapolelo, D. T., B. Zhang, et al. (2012). "Spectroscopic and functional characterization of iron-sulfur cluster-bound forms of Azotobacter vinelandii (Nif)IscA." Biochemistry 51(41): 8071-8084.

Mapolelo, D. T., B. Zhang, et al. (2013). "Monothiol glutaredoxins and A-type proteins: partners in Fe-S cluster trafficking." Dalton Trans 42(9): 3107-3115.

Marquet, A., B. T. Bui, et al. (2001). "Biosynthesis of biotin and lipoic acid." Vitam Horm 61: 51-101.

Martelli, A., M. Wattenhofer-Donze, et al. (2007). "Frataxin is essential for extramitochondrial Fe-S cluster proteins in mammalian tissues." Hum Mol Genet 16(22): 2651-2658.

Matthews, R. G. (1982). "Are the redox properties of tetrahydrofolate cofactors utilized in folate-dependent reactions?" Fed Proc 41(9): 2600-2604.

Mayr, J. A., F. A. Zimmermann, et al. (2011). "Lipoic acid synthetase deficiency causes neonatal-onset epilepsy, defective mitochondrial energy metabolism, and glycine elevation." Am J Hum Genet 89(6): 792-797.

Mays, L. E. and J. M. Wilson (2011). "The complex and evolving story of T cell activation to AAV vector-encoded transgene products." Mol Ther 19(1): 16-27.

Merten, O. W., C. Geny-Fiamma, et al. (2005). "Current issues in adeno-associated viral vector production." Gene Ther 12 Suppl 1: S51-61.

Meunier, B., E. Dumas, et al. (2007). "Assessment of hierarchical clustering methodologies for proteomic data mining." J Proteome Res 6(1): 358-366.

Miller, J. R., R. W. Busby, et al. (2000). "Escherichia coli LipA is a lipoyl synthase: in vitro biosynthesis of lipoylated pyruvate dehydrogenase complex from octanoyl-acyl carrier protein." Biochemistry 39(49): 15166-15178.

Mimaki, M., X. Wang, et al. (2012). "Understanding mitochondrial complex I assembly in health and disease." Biochim Biophys Acta 1817(6): 851-862.

Miyabe, I., T. A. Kunkel, et al. (2011). "The major roles of DNA polymerases epsilon and delta at the eukaryotic replication fork are evolutionarily conserved." PLoS Genet 7(12): e1002407.

Morais, R. (1980). "On the effect of inhibitors of mitochondrial macromolecular-synthesizing systems and respiration on the growth of cultured chick embryo cells." J Cell Physiol 103(3): 455-466.

Morimoto, K., E. Yamashita, et al. (2006). "The asymmetric IscA homodimer with an exposed [2Fe-2S] cluster suggests the structural basis of the Fe-S cluster biosynthetic scaffold." J Mol Biol 360(1): 117-132.

Muhlenhoff, U., M. J. Gerl, et al. (2007). "The ISC [corrected] proteins Isa1 and Isa2 are required for the function but not for the de novo synthesis of the Fe/S clusters of biotin synthase in Saccharomyces cerevisiae." Eukaryot Cell 6(3): 495-504.

Muhlenhoff, U., N. Richter, et al. (2011). "Specialized function of yeast Isa1 and Isa2 proteins in the maturation of mitochondrial [4Fe-4S] proteins." J Biol Chem 286(48): 41205-41216.

Navarro-Sastre, A., F. Tort, et al. (2011). "A fatal mitochondrial disease is associated with defective NFU1 function in the maturation of a subset of mitochondrial Fe-S proteins." Am J Hum Genet 89(5): 656-667.

Netz, D. J., J. Mascarenhas, et al. (2014). "Maturation of cytosolic and nuclear iron-sulfur proteins." Trends Cell Biol 24(5): 303-312.

Netz, D. J., A. J. Pierik, et al. (2012). "A bridging [4Fe-4S] cluster and nucleotide binding are essential for function of the Cfd1-Nbp35 complex as a scaffold in iron-sulfur protein maturation." J Biol Chem 287(15): 12365-12378.

Netz, D. J., C. M. Stith, et al. (2012). "Eukaryotic DNA polymerases require an iron-sulfur cluster for the formation of active complexes." Nat Chem Biol 8(1): 125-132.

Nilsson, R., I. J. Schultz, et al. (2009). "Discovery of genes essential for heme biosynthesis through large-scale gene expression analysis." Cell Metab 10(2): 119-130.

Ollagnier-de-Choudens, S., T. Mattioli, et al. (2001). "Iron-sulfur cluster assembly: characterization of IscA and evidence for a specific and functional complex with ferredoxin." J Biol Chem 276(25): 22604-22607.

Ollagnier-de-Choudens, S., Y. Sanakis, et al. (2004). "SufA/IscA: reactivity studies of a class of scaffold proteins involved in [Fe-S] cluster assembly." J Biol Inorg Chem 9(7): 828-838.

Ollagnier-de Choudens, S., L. Nachin, et al. (2003). "SufA from Erwinia chrysanthemi. Characterization of a scaffold protein required for iron-sulfur cluster assembly." J Biol Chem 278(20): 17993-18001.

Ollagnier-De Choudens, S., Y. Sanakis, et al. (2000). "Iron-sulfur center of biotin synthase and lipoate synthase." Biochemistry 39(14): 4165-4173.

Ortolano, S., C. Spuch, et al. (2012). "Present and future of adeno associated virus based gene therapy approaches." Recent Pat Endocr Metab Immune Drug Discov 6(1): 47-66.

Pandey, A., H. Yoon, et al. (2011). "Isd11p protein activates the mitochondrial cysteine desulfurase Nfs1p protein." J Biol Chem 286(44): 38242-38252.

Paris, Z., P. Changmai, et al. (2010). "The Fe/S cluster assembly protein Isd11 is essential for tRNA thiolation in Trypanosoma brucei." J Biol Chem 285(29): 22394-22402.

Patel, M. S. and R. A. Harris (1995). "Mammalian alpha-keto acid dehydrogenase complexes: gene regulation and genetic defects." FASEB J 9(12): 1164-1172.

Paul, V. D. and R. Lill (2014). "SnapShot: Eukaryotic Fe-S Protein Biogenesis." Cell Metab 20(2): 384-384 e381.

Pelzer, W., U. Muhlenhoff, et al. (2000). "Mitochondrial Isa2p plays a crucial role in the maturation of cellular iron-sulfur proteins." FEBS Lett 476(3): 134-139.

Perdomini, M., B. Belbellaa, et al. (2014). "Prevention and reversal of severe mitochondrial cardiomyopathy by gene therapy in a mouse model of Friedreich's ataxia." Nat Med 20(5): 542-547.

Picciocchi, A., C. Saguez, et al. (2007). "CGFS-type monothiol glutaredoxins from the cyanobacterium Synechocystis PCC6803 and other evolutionary distant model organisms possess a glutathione-ligated [2Fe-2S] cluster." Biochemistry 46(51): 15018-15026.

Pinske, C. and R. G. Sawers (2012). "A-type carrier protein ErpA is essential for formation of an active formate-nitrate respiratory pathway in Escherichia coli K-12." J Bacteriol 194(2): 346-353.

Pondarre, C., B. B. Antiochos, et al. (2006). "The mitochondrial ATP-binding cassette transporter Abcb7 is essential in mice and participates in cytosolic iron-sulfur cluster biogenesis." Hum Mol Genet 15(6): 953-964.

Pondarre, C., D. R. Campagna, et al. (2007). "Abcb7, the gene responsible for X-linked sideroblastic anemia with ataxia, is essential for hematopoiesis." Blood 109(8): 3567-3569.

Prakash, S. and L. Prakash (2002). "Translesion DNA synthesis in eukaryotes: a one- or two-polymerase affair." Genes Dev 16(15): 1872-1883.

Puccio, H., D. Simon, et al. (2001). "Mouse models for Friedreich ataxia exhibit cardiomyopathy, sensory nerve defect and Fe-S enzyme deficiency followed by intramitochondrial iron deposits." Nat Genet 27(2): 181-186.

Py, B. and F. Barras (2010). "Building Fe-S proteins: bacterial strategies." Nat Rev Microbiol 8(6): 436-446.

Py, B., C. Gerez, et al. (2012). "Molecular organization, biochemical function, cellular role and evolution of NfuA, an atypical Fe-S carrier." Mol Microbiol 86(1): 155-171.

Qian, L., C. Zheng, et al. (2013). "Characterization of iron-sulfur cluster assembly protein IscA from Acidithiobacillus ferrooxidans." Biochemistry (Mosc) 78(3): 244-251.

Quackenbush, J. (2001). "Computational analysis of microarray data." Nat Rev Genet 2(6): 418-427.

Rabinowitz, J. E., F. Rolling, et al. (2002). "Cross-packaging of a single adeno-associated virus (AAV) type 2 vector genome into multiple AAV serotypes enables transduction with broad specificity." J Virol 76(2): 791-801.

Raulfs, E. C., I. P. O'Carroll, et al. (2008). "In vivo iron-sulfur cluster formation." Proc Natl Acad Sci U S A 105(25): 8591-8596.

Rensvold, J. W., S. E. Ong, et al. (2013). "Complementary RNA and protein profiling identifies iron as a key regulator of mitochondrial biogenesis." Cell Rep 3(1): 237-245.

Robbins, A. H. and C. D. Stout (1989). "The structure of aconitase." Proteins 5(4): 289-312.

Robbins, A. H. and C. D. Stout (1989). "Structure of activated aconitase: formation of the [4Fe-4S] cluster in the crystal." Proc Natl Acad Sci U S A 86(10): 3639-3643.

Rodriguez-Manzaneque, M. T., J. Ros, et al. (1999). "Grx5 glutaredoxin plays a central role in protection against protein oxidative damage in Saccharomyces cerevisiae." Mol Cell Biol 19(12): 8180-8190.

Rodriguez-Manzaneque, M. T., J. Tamarit, et al. (2002). "Grx5 is a mitochondrial glutaredoxin required for the activity of iron/sulfur enzymes." Mol Biol Cell 13(4): 1109-1121.

Roret, T., P. Tsan, et al. (2014). "Structural and spectroscopic insights into BolA-glutaredoxin complexes." J Biol Chem 289(35): 24588-24598.

Rouault, T. A. (2012). "Biogenesis of iron-sulfur clusters in mammalian cells: new insights and relevance to human disease." Dis Model Mech 5(2): 155-164.

Rouault, T. A., D. J. Haile, et al. (1992). "An iron-sulfur cluster plays a novel regulatory role in the iron-responsive element binding protein." Biometals 5(3): 131-140.

Samulski, R. J., K. I. Berns, et al. (1982). "Cloning of adeno-associated virus into pBR322: rescue of intact virus from the recombinant plasmid in human cells." Proc Natl Acad Sci U S A 79(6): 2077-2081.

Sazanov, L. A., R. Baradaran, et al. (2013). "A long road towards the structure of respiratory complex I, a giant molecular proton pump." Biochem Soc Trans 41(5): 1265-1271.

Sazanov, L. A. and P. Hinchliffe (2006). "Structure of the hydrophilic domain of respiratory complex I from Thermus thermophilus." Science 311(5766): 1430-1436.

Schaedler, T. A., J. D. Thornton, et al. (2014). "A conserved mitochondrial ATP-binding cassette transporter exports glutathione polysulfide for cytosolic metal cofactor assembly." J Biol Chem 289(34): 23264-23274.

Schilke, B., C. Voisine, et al. (1999). "Evidence for a conserved system for iron metabolism in the mitochondria of Saccharomyces cerevisiae." Proc Natl Acad Sci U S A 96(18): 10206-10211.

Schmucker, S., A. Martelli, et al. (2011). "Mammalian frataxin: an essential function for cellular viability through an interaction with a preformed ISCU/NFS1/ISD11 iron-sulfur assembly complex." PLoS One 6(1): e16199.

Schultz, B. R. and J. S. Chamberlain (2008). "Recombinant adeno-associated virus transduction and integration." Mol Ther 16(7): 1189-1199.

Schumacher, S. B., M. Stucki, et al. (2000). "The N-terminal region of DNA polymerase delta catalytic subunit is necessary for holoenzyme function." Nucleic Acids Res 28(2): 620-625.

Sellers, V. M., M. K. Johnson, et al. (1996). "Function of the [2FE-2S] cluster in mammalian ferrochelatase: a possible role as a nitric oxide sensor." Biochemistry 35(8): 2699-2704.

Sellers, V. M., K. F. Wang, et al. (1998). "Evidence that the fourth ligand to the [2Fe-2S] cluster in animal ferrochelatase is a cysteine. Characterization of the enzyme from Drosophila melanogaster." J Biol Chem 273(35): 22311-22316.

Sharma, A. K., L. J. Pallesen, et al. (2010). "Cytosolic iron-sulfur cluster assembly (CIA) system: factors, mechanism, and relevance to cellular iron regulation." J Biol Chem 285(35): 26745-26751.

Sheftel, A., O. Stehling, et al. (2010). "Iron-sulfur proteins in health and disease." Trends Endocrinol Metab 21(5): 302-314.

Sheftel, A. D., O. Stehling, et al. (2010). "Humans possess two mitochondrial ferredoxins, Fdx1 and Fdx2, with distinct roles in steroidogenesis, heme, and Fe/S cluster biosynthesis." Proc Natl Acad Sci U S A 107(26): 11775-11780.

Sheftel, A. D., O. Stehling, et al. (2009). "Human ind1, an iron-sulfur cluster assembly factor for respiratory complex I." Mol Cell Biol 29(22): 6059-6073.

Sheftel, A. D., C. Wilbrecht, et al. (2012). "The human mitochondrial ISCA1, ISCA2, and IBA57 proteins are required for [4Fe-4S] protein maturation." Mol Biol Cell 23(7): 1157-1166.

Shen, B., D. R. Jollie, et al. (1994). "Azotobacter vinelandii ferredoxin I. Alteration of individual surface charges and the [4FE-4S]2+/+ cluster reduction potential." J Biol Chem 269(11): 8564-8575.

Shi, Y., M. Ghosh, et al. (2012). "Both human ferredoxins 1 and 2 and ferredoxin reductase are important for iron-sulfur cluster biogenesis." Biochim Biophys Acta 1823(2): 484-492.

Smid, O., E. Horakova, et al. (2006). "Knock-downs of iron-sulfur cluster assembly proteins IscS and IscU down-regulate the active mitochondrion of procyclic Trypanosoma brucei." J Biol Chem 281(39): 28679-28686.

Song, D., Z. Tu, et al. (2009). "Human ISCA1 interacts with IOP1/NARFL and functions in both cytosolic and mitochondrial iron-sulfur protein biogenesis." J Biol Chem 284(51): 35297-35307.

Stehling, O. and R. Lill (2013). "The role of mitochondria in cellular iron-sulfur protein biogenesis: mechanisms, connected processes, and diseases." Cold Spring Harb Perspect Med 3(7): 1-17.

Stehling, O., A. A. Vashisht, et al. (2012). "MMS19 assembles iron-sulfur proteins required for DNA metabolism and genomic integrity." Science 337(6091): 195-199.

Stehling, O., C. Wilbrecht, et al. (2014). "Mitochondrial iron-sulfur protein biogenesis and human disease." Biochimie 100: 61-77.

Suhasini, A. N. and R. M. Brosh, Jr. (2013). "Disease-causing missense mutations in human DNA helicase disorders." Mutat Res 752(2): 138-152.

Suhasini, A. N. and R. M. Brosh, Jr. (2013). "DNA helicases associated with genetic instability, cancer, and aging." Adv Exp Med Biol 767: 123-144.

Sulo, P. and N. C. Martin (1993). "Isolation and characterization of LIP5. A lipoate biosynthetic locus of Saccharomyces cerevisiae." J Biol Chem 268(23): 17634-17639.

Tan, G., J. Lu, et al. (2009). "IscA/SufA paralogues are required for the [4Fe-4S] cluster assembly in enzymes of multiple physiological pathways in Escherichia coli under aerobic growth conditions." Biochem J 420(3): 463-472.

Tassy, O. and O. Pourquie (2014). "Manteia, a predictive data mining system for vertebrate genes and its applications to human genetic diseases." Nucleic Acids Res 42(Database issue): D882-891.

Teplyakov, A., G. Obmolova, et al. (2004). "Crystal structure of the YgfZ protein from Escherichia coli suggests a folate-dependent regulatory role in one-carbon metabolism." J Bacteriol 186(21): 7134-7140.

Tong, W. H., G. N. Jameson, et al. (2003). "Subcellular compartmentalization of human Nfu, an iron-sulfur cluster scaffold protein, and its ability to assemble a [4Fe-4S] cluster." Proc Natl Acad Sci U S A 100(17): 9762-9767.

Tovar, J., G. Leon-Avila, et al. (2003). "Mitochondrial remnant organelles of Giardia function in iron-sulphur protein maturation." Nature 426(6963): 172-176.

Tsai, C. L. and D. P. Barondeau (2010). "Human frataxin is an allosteric switch that activates the Fe-S cluster biosynthetic complex." Biochemistry 49(43): 9132-9139.

Uhrigshardt, H., A. Singh, et al. (2010). "Characterization of the human HSC20, an unusual DnaJ type III protein, involved in iron-sulfur cluster biogenesis." Hum Mol Genet 19(19): 3816-3834.

Uzarska, M. A., R. Dutkiewicz, et al. (2013). "The mitochondrial Hsp70 chaperone Ssq1 facilitates Fe/S cluster transfer from Isu1 to Grx5 by complex formation." Mol Biol Cell 24(12): 1830-1841.

Vickery, L. E. and J. R. Cupp-Vickery (2007). "Molecular chaperones HscA/Ssq1 and HscB/Jac1 and their roles in iron-sulfur protein maturation." Crit Rev Biochem Mol Biol 42(2): 95-111.

Vilella, F., R. Alves, et al. (2004). "Evolution and cellular function of monothiol glutaredoxins: involvement in iron-sulphur cluster assembly." Comp Funct Genomics 5(4): 328-341.

Vinella, D., C. Brochier-Armanet, et al. (2009). "Iron-sulfur (Fe/S) protein biogenesis: phylogenomic and genetic studies of A-type carriers." PLoS Genet 5(5): e1000497.

Vinothkumar, K. R., J. Zhu, et al. (2014). "Architecture of mammalian respiratory complex I." Nature.

Wada, K., Y. Hasegawa, et al. (2005). "Crystal structure of Escherichia coli SufA involved in biosynthesis of iron-sulfur clusters: implications for a functional dimer." FEBS Lett 579(29): 6543-6548.

Waller, J. C., S. Alvarez, et al. (2010). "A role for tetrahydrofolates in the metabolism of iron-sulfur clusters in all domains of life." Proc Natl Acad Sci U S A 107(23): 10412-10417.

Wang, W., H. Huang, et al. (2010). "In vivo evidence for the iron-binding activity of an iron-sulfur cluster assembly protein IscA in Escherichia coli." Biochem J 432(3): 429-436.

Wang, Z., H. I. Ma, et al. (2003). "Rapid and highly efficient transduction by double-stranded adeno-associated virus vectors in vitro and in vivo." Gene Ther 10(26): 2105-2111.

Weinberg, M. S., R. J. Samulski, et al. (2013). "Adeno-associated virus (AAV) gene therapy for neurological disease." Neuropharmacology 69: 82-88.

Whitaker, H. C., D. Patel, et al. (2013). "Peroxiredoxin-3 is overexpressed in prostate cancer and promotes cancer cell survival by protecting cells from oxidative stress." Br J Cancer 109(4): 983-993.

White, M. F. and M. S. Dillingham (2012). "Iron-sulphur clusters in nucleic acid processing enzymes." Curr Opin Struct Biol 22(1): 94-100.

Wiedemann, N., E. Urzica, et al. (2006). "Essential role of Isd11 in mitochondrial iron-sulfur cluster synthesis on Isu scaffold proteins." EMBO J 25(1): 184-195.

Wijshake, T., D. J. Baker, et al. (2014). "Endonucleases: new tools to edit the mouse genome." Biochim Biophys Acta 1842(10): 1942-1950.

Wingert, R. A., J. L. Galloway, et al. (2005). "Deficiency of glutaredoxin 5 reveals Fe-S clusters are required for vertebrate haem synthesis." Nature 436(7053): 1035-1039.

Wollenberg, M., C. Berndt, et al. (2003). "A dimer of the FeS cluster biosynthesis protein IscA from cyanobacteria binds a [2Fe2S] cluster between two protomers and transfers it to [2Fe2S] and [4Fe4S] apo proteins." Eur J Biochem 270(8): 1662-1671.

Wu, G., S. S. Mansy, et al. (2002). "Iron-sulfur cluster biosynthesis: characterization of Schizosaccharomyces pombe Isa1." J Biol Inorg Chem 7(4-5): 526-532.

Wydro, M. M., P. Sharma, et al. (2013). "The evolutionarily conserved iron-sulfur protein INDH is required for complex I assembly and mitochondrial translation in Arabidopsis [corrected]." Plant Cell 25(10): 4014-4027.

Xiao, P. J., T. B. Lentz, et al. (2012). "Recombinant adeno-associated virus: clinical application and development as a gene-therapy vector." Ther Deliv 3(7): 835-856.

Yan, R., P. V. Konarev, et al. (2013). "Ferredoxin competes with bacterial frataxin in binding to the desulfurase IscS." J Biol Chem.

Yankovskaya, V., R. Horsefield, et al. (2003). "Architecture of succinate dehydrogenase and reactive oxygen species generation." Science 299(5607): 700-704.

Ye, H., S. Y. Jeong, et al. (2010). "Glutaredoxin 5 deficiency causes sideroblastic anemia by specifically impairing heme biosynthesis and depleting cytosolic iron in human erythroblasts." J Clin Invest 120(5): 1749-1761.

Ye, H. and T. A. Rouault (2010). "Erythropoiesis and iron sulfur cluster biogenesis." Adv Hematol 2010.

Yi, X. and N. Maeda (2005). "Endogenous production of lipoic acid is essential for mouse development." Mol Cell Biol 25(18): 8387-8392.

Yoshida, T. and G. Kikuchi (1969). "Physiological significance of glycine cleavage system in human liver as revealed by the study of a case of hyperglycinemia." Biochem Biophys Res Commun 35(4): 577-583.

Zeng, J., M. Geng, et al. (2007). "The IscA from Acidithiobacillus ferrooxidans is an iron-sulfur protein which assemble the [Fe4S4] cluster with intracellular iron and sulfur." Arch Biochem Biophys 463(2): 237-244.

Zheng, L., V. L. Cash, et al. (1998). "Assembly of iron-sulfur clusters. Identification of an iscSUA-hscBA-fdx gene cluster from Azotobacter vinelandii." J Biol Chem 273(21): 13264-13272.

Zincarelli, C., S. Soltys, et al. (2008). "Analysis of AAV serotypes 1-9 mediated gene expression and tropism in mice after systemic injection." Mol Ther 16(6): 1073-1080.

Zybailov, B., A. L. Mosley, et al. (2006). "Statistical analysis of membrane proteome expression changes in Saccharomyces cerevisiae." J Proteome Res 5(9): 2339-2347.

9. French summary

Mise en évidence de la non-redondance des protéines de type A, ISCA1 et ISCA2, dans la biosynthèse des centres fer-soufre

Les centres fer-soufre (Fe-S) (Figure 22) sont des cofacteurs protéiques essentiels qui participent à un nombre important de fonctions cellulaires allant du métabolisme de l'ADN à la respiration mitochondriale. Malgré la caractérisation d'un nombre croissant de maladies associées à un défaut dans la biosynthèse des Fe-S, la compréhension des mécanismes impliqués dans la voie de biosynthèse chez les mammifères est encore limitée (Beilschmidt and Puccio 2014; Paul and Lill 2014).

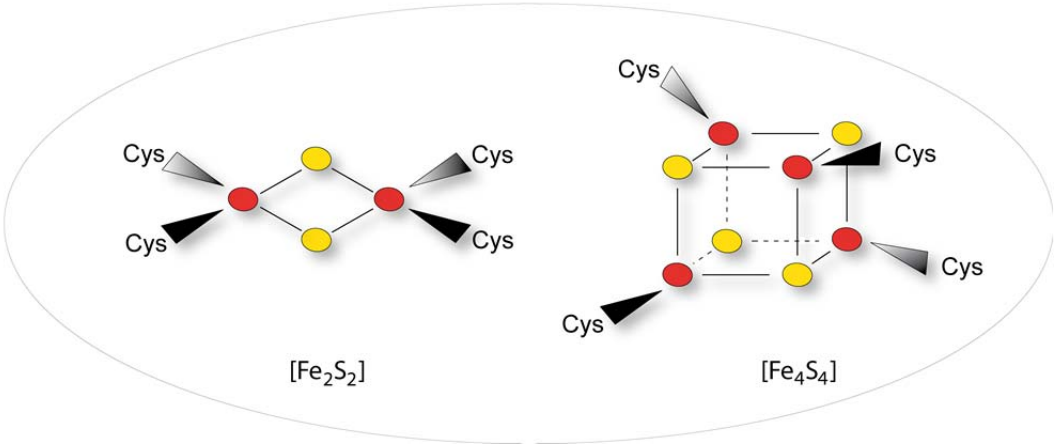

Figure 22: Structures des centres fer-soufre (Fe-S) les plus frequants: centre Fe2S2 (gauche) et centre Fe4S4 (droit).

Chez les eucaryotes, les mitochondries jouent un rôle central dans la formation des Fe-S de toute la cellule. Différentes protéines sont requises pour les différentes étapes du processus et la plupart sont conservées au cours de l'évolution (Figure 23). La biosynthèse des Fe-S peut être décomposées en plusieurs étapes : 1) le fer et le soufre sont assemblés pour former un cluster sur une protéine d'échafaudage, appelée ISCU. Le soufre est fourni par une cystéine désulfurase formé par le complexe NFS1/ISD11 ; 2) Le Fe-S est ensuite transféré à des protéines acceptrices dans la matrice mitochondriale ; 3) en parallèle, un composé dérivé de la glutathione et issu de la machinerie mitochondriale est exporté vers le cytosol où il est utilisé par une machinerie dédiée afin de générer

des Fe-S pour les protéines cytosoliques et nucléaires (Beinert, Holm et al. 1997; Lill 2009; Sheftel, Stehling et al. 2010).

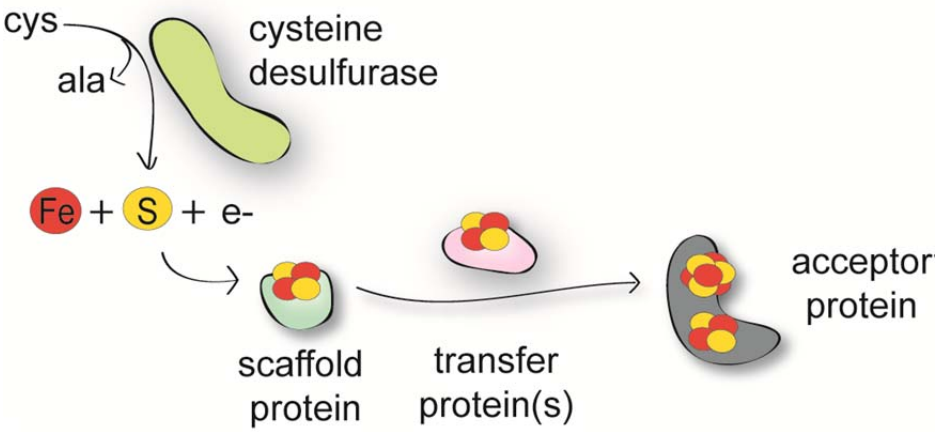

Figure 23: Principe de base de la biosynthèse de clusters Fe-S

Les protéines mammifères ISCA1 et ISCA2 sont des protéines conservées et exprimées de façon ubiquitaire. Ces deux protéines sont impliquées dans la biosynthèse mitochondriales des Fe-S. Cependant, plusieurs fonctions ont été proposées : 1) donneur de fer lors de l'assemblage initiale du Fe-S (Ding and Clark 2004; Ding, Clark et al. 2004; Lu, Bitoun et al. 2010; Mapolelo, Zhang et al. 2012; Mapolelo, Zhang et al. 2012); 2) protéine d'échafaudage des Fe-S alternative à ISCU (Krebs, Agar et al. 2001); 3) protéine de transport du Fe-S entre ISCU et les protéines acceptrices (Ollagnier-de-Choudens, Sanakis et al. 2004; Gupta, Sendra et al. 2009; Vinella, Brochier-Armanet et al. 2009) (Figure 24).

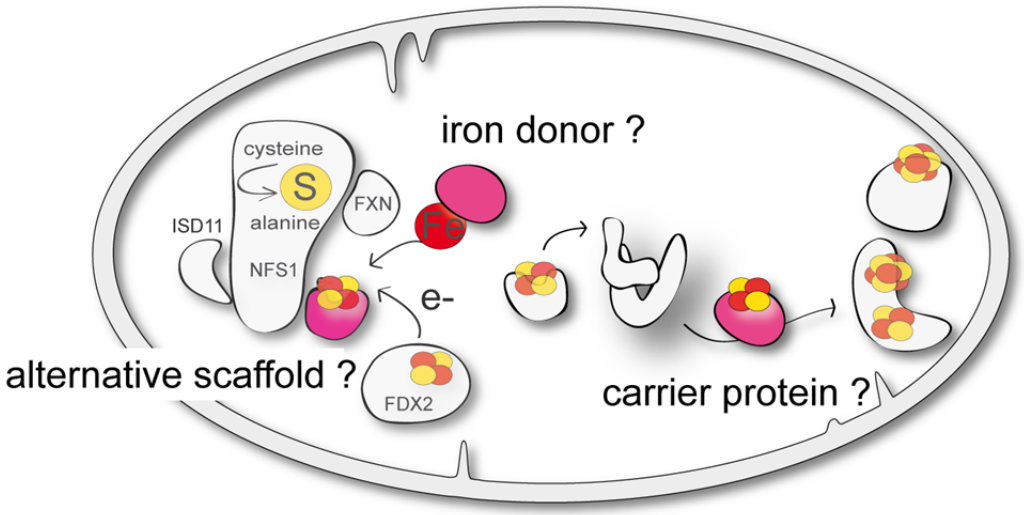

Figure 24: Fonctionnes proposées pour les protéines de type A

Des fonctionnes différentes ont été proposée pour les protéines de type A.

Comme beaucoup de protéines dans la biosynthèse des Fe-S, la plupart des données obtenues sur ISCA1 et ISCA2 proviennent d'études dans la bactérie et la levure. Des données récentes obtenues par ARN interférence sur des cellules HeLa suggèrent cependant qu'ISCA1 et ISCA2 ont des fonctions redondantes pour la distribution de Fe_4-S_4 à une sous-population de protéines mitochondriales chez les mammifères (Sheftel, Wilbrecht et al. 2012). Cette étude a néanmoins été effectuée dans des conditions de déficience mitochondriale avancée pouvant entraîner une analyse de phénomènes non-spécifiques qui pourraient empêcher la caractérisation précise de la fonction d'ISCA1 et ISCA2.

Des expériences préliminaires effectuées au laboratoire ont permis la première caractérisation biochimique des protéines ISCA1 et ISCA2 murines. Elles montrent notamment qu'ISCA1 et ISCA2 sont purifiés directement en tant qu'homodimère portant un Fe-S lorsqu'elles sont exprimées dans la bactérie. Bien que les deux protéines ont de fortes homologies de séquence et peuvent coordonner un centre Fe_2S_2, les Fe-S respectifs présentent une sensibilité différente à l'oxydation.

Pour compléter cette étude préliminaire, mon travail de thèse a consisté à caractériser l'interaction et le rôle d'ISCA1 et ISCA2 *in vivo*. Pour cela, j'ai combiné des approches d'immunoprécipitation couplée à une étude protéomique par spectrométrie de masse avec un knockdown dans la souris utilisant des AAV (virus adéno-associés) exprimant un shRNA spécifique.

Chez les eucaryotes, ISCA1 et ISCA2 sont des protéines mitochondriales (Sheftel, Wilbrecht et al. 2012). Cependant, certaines données de la littérature suggèrent également une localisation cytosolique (Song, Tu et al. 2009). Grâce à des expériences d'immunofluorescence, j'ai confirmé la localisation prépondérante dans la mitochondrie d'ISCA1 et ISCA2.

Pour mieux comprendre le réseau d'interaction et identifier de potentiels interacteurs protéiques d'ISCA1 et ISCA2, j'ai réalisé des expériences de MudPIT (Multidimensional protein identification technology) sur des immuprécipitats obtenus à partir de plusieurs protéines de la machinerie Fe-S mitochondriales, dont ISCA1 et ISCA2. L'approche par MudPIT a été initialement développée pour identifier des protéines dans des complexes protéiques, sans préalablement séparer les composants par électrophorèse sur gel (Kislinger and Emili 2005). Lors de l'analyse par MudPIT, les

immunoprécipitats sont digérés en solution et séparés par chromatographie 2D avant l'analyse par spectrométrie de masse.

La localisation mitochondriale des protéines utilisées comme cible lors de l'immunoprécipitation a été vérifiée au préalable par immunofluorescence. L'analyse MudPIT a été réalisée en collaboration avec Majorie Fournier au sein de l'IGBMC. Les données ont été normalisées pour réduire le nombre de faux positifs en utilisant différents niveaux de stringence lors de l'analyse. Par la suite, les candidats identifiés ont été testés par western blot pour vérifier l'interaction (Figure 25).

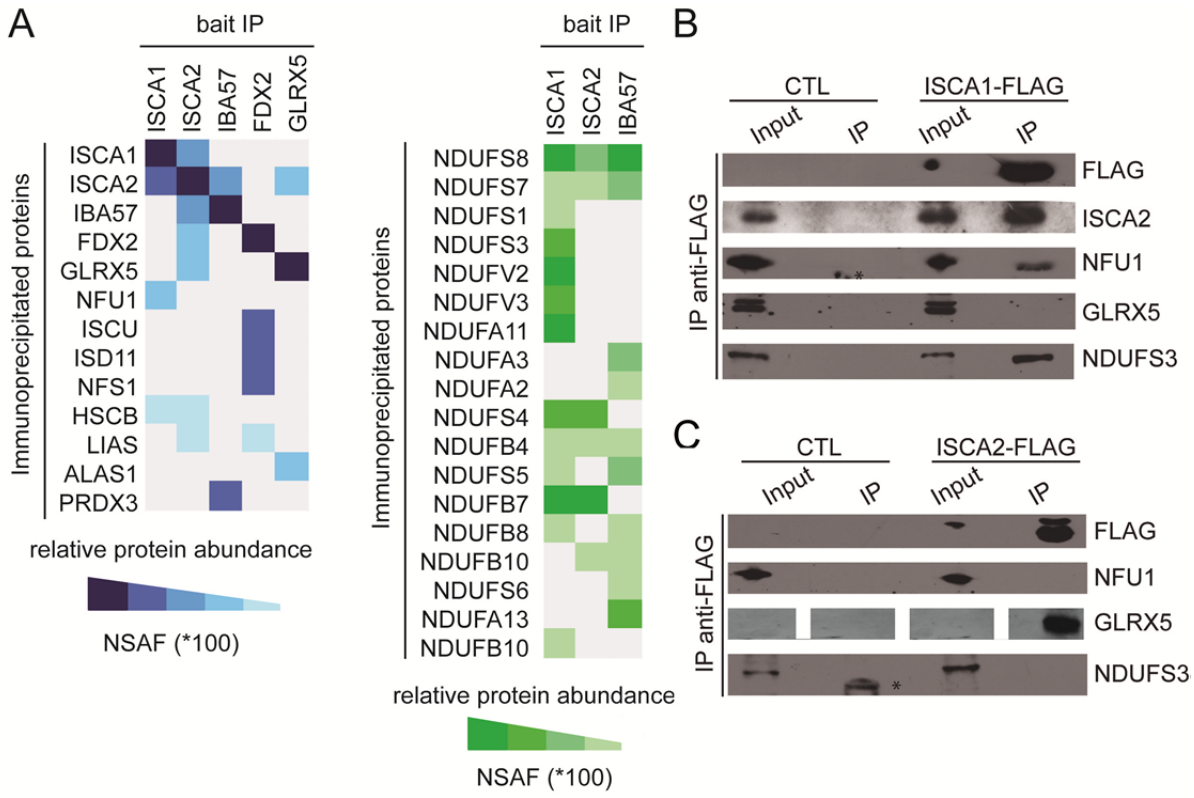

Figure 25: Un screening des interactions par immunoprécipitation.

(A) des protéines co - immunoprécipitées et leur abondance relative (NSAF) déterminée par analyse MudPIT. Les données représentent des protéines enrichies 10x par rapport aux contrôles. L'intensité de la couleur reflète les valeurs NSAF multipliées par 100. Le panneau de gauche représente les valeurs NSAF obtenues pour les sous-unités du complexe I de la chaîne respiratoire en IP de ISCA1, ISCA2 et IBA57. (B) Analyse par Western blot de l'IP ISCA1 par rapport à une IP-contrôle (CTL) en utilisant des anticorps différents, comme indiqué. (C) Analyse par Western blot de l'IP ISCA2 par rapport à une IP-contrôle (CTL) en utilisant des anticorps différents, comme indiqué.

Les données montrent qu'ISCA1 et ISCA2 interagissent l'un avec l'autre. Cependant, des différences d'interaction avec d'autres protéines de la machinerie Fe-S ou des protéines acceptrices ont été observées. L'analyse a ainsi permis de placer ISCA1 et ISCA2 dans le contexte de la biosynthèse des Fe-S. Aucune interaction entre les deux ISCA et la cystéine désulfurase NFS1/ISD11 n'a été observée,

excluant ainsi un rôle en tant que protéine d'échafaudage alternative à ISCU (Figure 26). De façon intéressante, les résultats suggèrent que seulement ISCA2 interagit avec IBA57, une protéine de fonction encore inconnue mais qui a précédemment été montré comme agissant de concert avec ISCA1 et ISCA2 dans la levure et les cellules HeLa (Muhlenhoff, Richter et al. 2011; Sheftel, Wilbrecht et al. 2012). Une interaction faible ou transitoire entre ISCA1 et NFU1 a pu être mise en évidence, NFU1 étant une protéine impliquée dans la distribution des Fe-S (Cameron, Janer et al. 2011; Navarro-Sastre, Tort et al. 2011). Enfin, une interaction avec la glutaredoxin 5 (GLRX5) a été observée avec ISCA2. GLRX5 a été proposé comme agissant dans la distribution des Fe-S (Wingert, Galloway et al. 2005; Camaschella, Campanella et al. 2007; Ye, Jeong et al. 2010). Des interactions spécifiques entre les ISCA et plusieurs sous-unités du complexe I de la chaîne respiratoire ont été mises en évidence. En particulier, l'interaction entre ISCA1 et NDUFS3 a été confirmée par western blot, suggérant ainsi qu'il y a un transfert direct du cluster d'ISCA1 vers cette sous unité du complexe I.

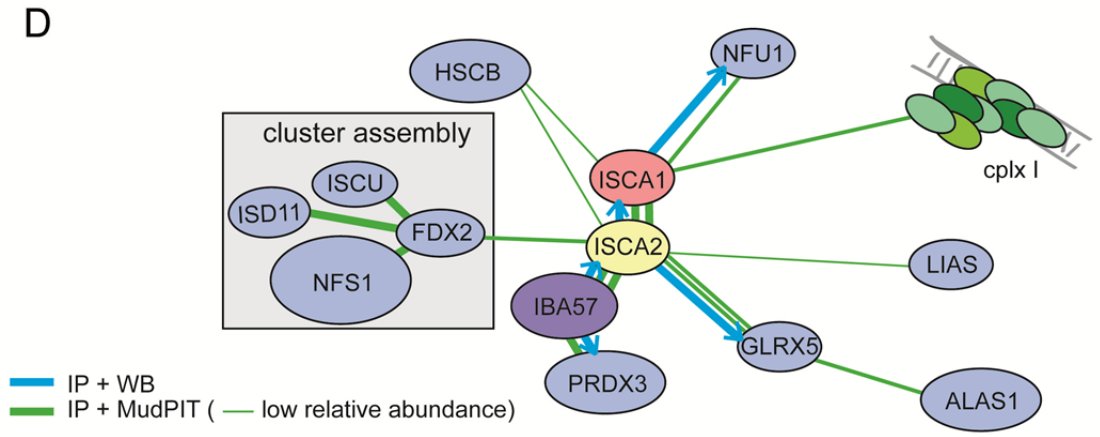

Figure 26: Représentation schématique d' interactiones protéines des type A dans la biogenèse des centres Fe-S

(D) Le réseau d'interaction pour ISCA1 et ISCA2 sur la base des Western blots (ligne bleue) ou le MudPIT (ligne verte) des IPs. L'épaisseur des lignes et les distances spatiales représentent une abondance relative élevée, moyenne et faible, respectivement. cplx I: complexe I.

Pour étudier la fonction d'ISCA1 et ISCA2 *in vivo*, j'ai utilisé une approche d'ARN interférence utilisant des virus AAV exprimant un shRNA. Les AAV sont des virus simple brin d'ADN ne présentant pas d'enveloppe et qui sont non-pathogènes et non-integratifs (Berns 1990). Le sérotype du virus détermine le tropisme, c'est à dire l'affinité tissulaire de l'infection. Le génome du virus s'exprime sous forme d'épisome dans les noyaux du tissu infecté (Merten, Geny-Fiamma et al. 2005).

Comme ISCA1 et ISCA2 sont fortement exprimés dans le muscle squelettique, nous avons choisi d'injecter les AAV recombinants dans ce tissu (Figure 27). En particulier, les injections ont été effectuées dans le tibialis antérieur (TA), un muscle facilement accessible. Le choix du muscle permet

également de travailler sur un tissu post-mitotique et d'adresser ainsi la fonction première des protéines en évitant les effets dus à la division cellulaire, comme dans le cas de l'étude sur les cellules HeLa citée plus haut (Sheftel, Wilbrecht et al. 2012)

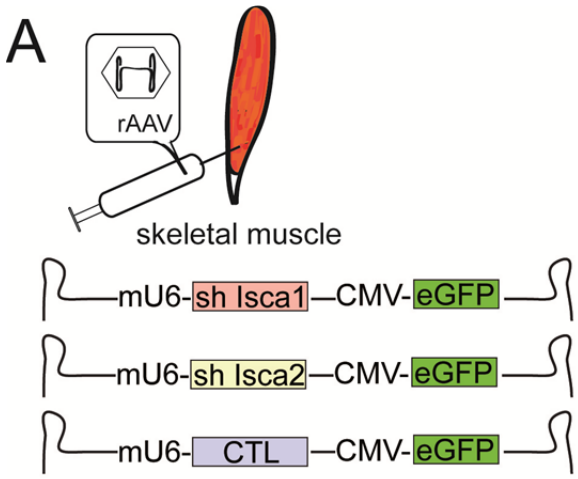

Figure 27: Représentation schématique d'injection des virus adeno-associée recombinantes (rAAV) dans le muscles squelettique de la souri

Les capacités de production et de manipulation du virus AAV sont présentes au sein de l'institut. Des séquences de shRNA pour cibler ISCA1 ou ISCA2 ont été sélectionnées et des AAV de sérotype 2/1 ont été produits par Pascale Koeble. Les expériences ont été réalisées en injectant 25uL d'une suspension à $1x10^{12}$ vg/mL dans le TA d'une souris âgée de 4 semaines, c'est à dire à un âge où le muscle est jeune mais déjà mature. Comme contrôle, un AAV codant pour un shRNA *scrambled* a été injecté dans le TA de la patte opposée. Comme les AAV ont un maximum d'expression 3 semaines après l'injection, les souris ont été sacrifiées et analysées 3 semaines après l'injection. Le phénotype a été caractérisé par histologie et analyses moléculaires, en particulier par western blot. Les protéines contenant un Fe-S sont sensibles à la perte du Fe-S et beaucoup d'entre elles sont dégradées. L'étude du niveau des protéines Fe-S par western blot est ainsi un moyen indirect d'évaluer l'efficacité de distribution des Fe-S.

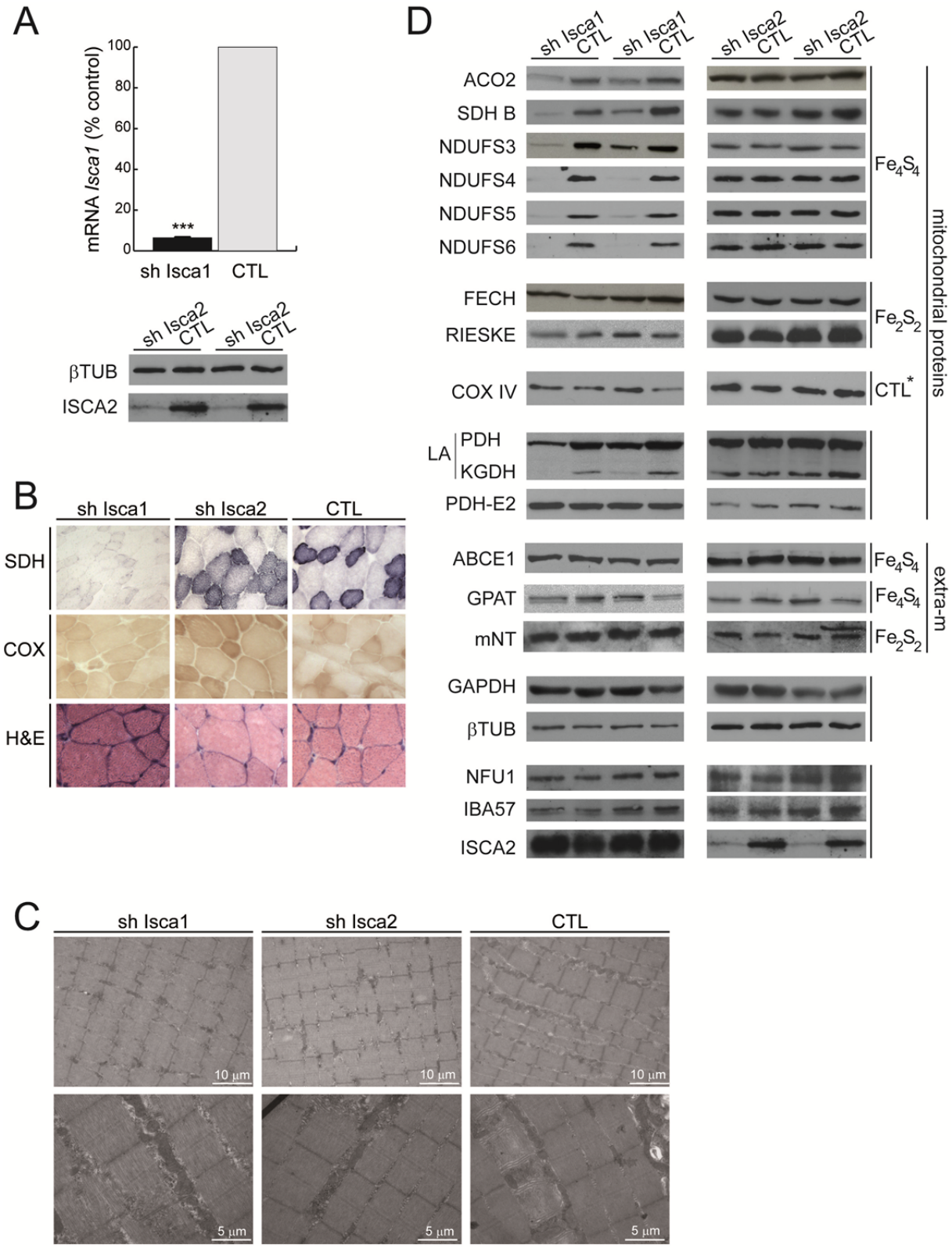

Figure 28: Charactérisation phénotypique par des analyses moléculaires et histologie.

Knockdown d'ISCA1 et d'ISCA2 dans le muscle squelettique. (A) Expression de l'ARN messager d'Isca1 dans le muscle TA injecté avec un rAAV-shISCA1 ou un rAAV-scramble shRNA (CTL). Résultats donnés sous forme de moyennes (n=9) ± SD. ***p<0.0001. (B) Analyse histologique de cryosections de muscle TA injectés avec un rAAV-shISCA1 ou un rAAV-shISCA2 et leurs contrôles respectifs (CTL). (C)

Structure observée en ME du muscle TA injecté avec un rAAV-shISCA1 ou un rAAV-shISCA2 et leurs contrôles respectifs (CTL). Echelle: 10 μm (ligne du haut) et 5 μm (ligne du bas). (D) Western blots représentatifs des protéines indiquées en utilisant des extraits de muscle TA à 3 semaines post-injection, injectés avec un rAAV-shISCA1 ou un rAAV-shISCA2 et leurs contrôles respectifs (CTL).

Les résultats obtenus par cette approche montrent que les diminutions de l'expression d'ISCA1 et ISCA2 conduisent à différents phénotypes (Figure 28). En particulier, seul ISCA1 est nécessaire dans le muscle squelettique pour le transfert de centres Fe_4S_4 aux protéines mitochondriales qui en ont besoin. Les résultats sont similaires 6 semaines après l'injection. Malgré une forte diminution de l'expression d'ISCA2 grâce à cette méthode 3 ou 6 semaines après l'injection, aucun effet n'a été observé sur aucune des protéines Fe-S testées.

Ces résultats sont en partie en contradiction avec ceux obtenus lors des expériences de knockdown sur les cellules HeLa (Sheftel, Wilbrecht et al. 2012). Nos résultats suggèrent plutôt qu'ISCA1 et ISCA2 ont des fonctions différentes *in vivo* lors de la synthèse et distribution des Fe-S.

Néanmoins, les niveaux d'expression ARN d'ISCA1 sont plus élevés que ceux d'ISCA2 dans le muscle squelettique. Il est donc probable que l'absence de phénotype dans les knockdowns d'ISCA2 soit due à une compensation par ISCA1, alors que l'inverse ne serait pas possible.

Pour tester cette possibilité et déterminer clairement la redondance fonctionnelle d'ISCA1 et ISCA2, la capacité de compensation de chacune des protéines a été évaluée en exprimant une forme résistante au shRNA d'ISCA1 et ISCA2 dans des souris avec un knockdown pour ISCA1 (Figure 29). Alors que la forme résistante au shRNA d'ISCA1 peut compenser le knockdown d'ISCA1, la surexpression d'ISCA2 n'a eu aucun effet sur le phénotype induit par la diminution d'ISCA1, démontrant ainsi la non-redondance fonctionnelle des deux protéines.

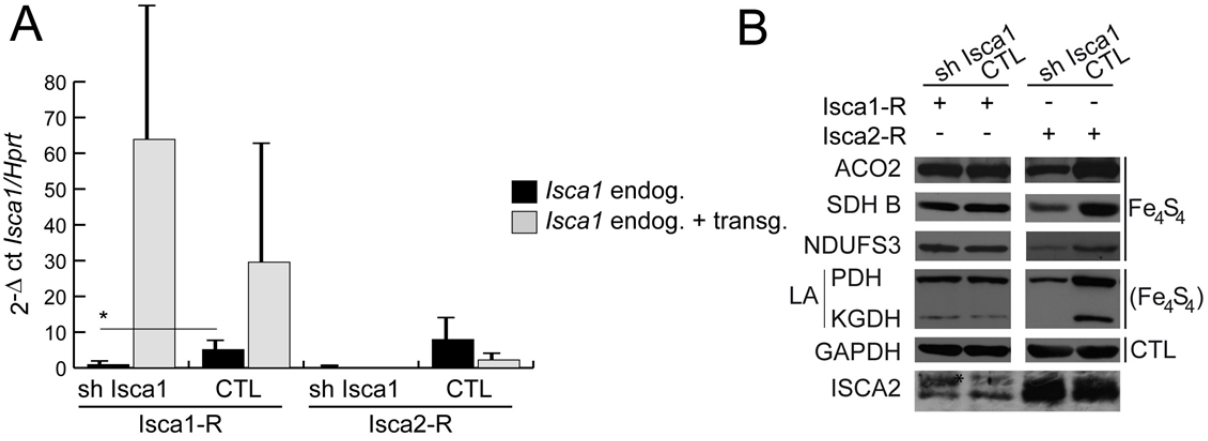

Figure 29: Non-redondance fonctionelle d'ISCA1 et ISCA2.

Analyse de la compensation du knockdown d'ISCA1. (A) Expression relative d'ARN messager endogène d'Isca1 et d'Isca1 total dans le muscle TA, simultanément injecté avec un rAAV-shISCA1 ou un rAAV-scramble shRNA (CTL) et un rAAV-ISCA1R ou un rAAV-ISCA2R. Résultats donnés sous forme de moyennes (n=3) ± SD.* $p<0.05$. (B) Western blots représentatifs des protéines indiquées en utilisant des extraits de muscle TA à 3 semaines post-injection, simultanément injectés avec un rAAV-shISCA1 ou un rAAV-scramble shRNA (CTL) et un rAAV-ISCA1R ou rAAV-ISCA2R. GAPDH utilisé comme témoin de charge.

En conclusion, cette étude montre qu'ISCA1 et ISCA2 sont deux protéines homologues pouvant coordonner un Fe-S mais effectuant des fonctions différentes dans la distribution des Fe-S chez les mammifères.

UNIVERSITÉ DE STRASBOURG

Lena Kristina BEILSCHMIDT

igbmc institut de génétique et de biologie moléculaire et cellulaire

Evidences for the non-redundant function of A-type proteins ISCA1 and ISCA2 in iron-sulfur cluster biogenesis

Résumé

Les centres fer-soufre (Fe-S) sont des cofacteurs protéiques essentiels qui participent à un nombre important de fonctions cellulaires allant du métabolisme de l'ADN à la respiration mitochondriale. L'assemblage des centres Fe-S et leur insertion dans des protéines acceptrices requièrent l'activité d'une machinerie protéique dédiée. Bien que les protéines de la biogenèse des centres Fe-S soient conservées, plusieurs aspects fonctionnels et mécanistiques restent inconnus. Notre travail de thèse a consisté à caractériser les protéines mammifères de type A, ISCA1 et ISCA2, qui sont impliquées dans la biogenèse mitochondriales des centres Fe-S. En utilisant une approche couplant l'immunoprécipitation avec une analyse protéomique par spectrométrie de masse, plusieurs interactions protéiques d'ISCA1 et ISCA2 ont pu être identifiées. En plus d'une interaction entre ISCA1 et ISCA2, nous avons ainsi montré l'existence d'interactions spécifiques à chacune de ces protéines. Une approche de *knockdown* dans la souris via l'injection de virus adéno-associés, a permis de montrer l'absence de redondance fonctionnelle entre ISCA1 et ISCA2 puisque seul ISCA1 se trouve être nécessaire dans la maturation d'une catégorie de protéines à centre Fe-S.

Biogenèse de centre Fe-S, ISCA1, ISCA2

Summary in English

Iron-sulfur clusters (Fe-S) are essential cofactors involved in different cellular processes ranging from DNA metabolism to respiration. Assembly of Fe-S clusters and their insertion into acceptor proteins is performed by dedicated protein machineries. Despite the high conservation from bacteria to man, different functional and mechanistic aspects of the Fe-S biogenesis remain elusive. In the present work, the function of the two mammalian A-type proteins ISCA1 and ISCA2 that are implicated in Fe-S biogenesis was investigated *in vivo.* First, an extensive analysis coupling immunoprecipitations and mass spectrometry led to the identification of a direct binding between ISCA1 and ISCA2 as well as specific protein partners of each protein. Furthermore, knockdown experiments in the mouse using adeno-associated virus provided clear evidence of the non-redundant function of ISCA1 and ISCA2, since only ISCA1 was shown to be required for a specific subset of mitochondrial Fe-S proteins.

Fe-S cluster biogenesis, ISCA1, ISCA2